THE UNIVERSITY OF HULL

Decentralized Sliding Mode Control and Estimation for Large-Scale Systems

Being a Thesis submitted for the Degree of PhD

in the University of Hull

by

ZHENG HUANG

BSc in Engineering (China)

February 2013

Acknowledgements

Abstract

This thesis concerns the development of an approach of decentralised robust control and estimation for large scale systems (LSSs) using robust sliding mode control (SMC) and sliding mode observers (SMO) theory based on a linear matrix inequality (LMI) approach. A complete theory of decentralized first order sliding mode theory is developed. The main developments proposed in this thesis are:

- The novel development of an LMI approach to decentralized state feedback SMC. The proposed strategy has good ability in combination with other robust methods to fulfill specific performance and robustness requirements.

- The development of output based SMC for large scale systems (LSSs). Three types of novel decentralized output feedback SMC methods have been developed using LMI design tools. In contrast to more conventional approaches to SMC design the use of some complicated transformations have been obviated.

- A decentralized approach to SMO theory has been developed focused on the Walcott-Żak SMO combined with LMI tools. A derivation for bounds applicable to the estimation error for decentralized systems has been given that involves unknown subsystem interactions and modeling uncertainty. Strategies for both actuator and sensor fault estimation using decentralized SMO are discussed.

The thesis also provides a case study of the SMC and SMO concepts applied to a non-linear annealing furnace system modelderived from a distributed parameter (partial differential equation) thermal system. The study commences with a lumped system decentralised representation of the furnace derived from the partial differential equations. The SMO and SMC methods derived in the thesis are applied to this lumped parameter furnace model. Results are given demonstrating the validity of the methods proposed and showing a good potential for a valuable practical implementation of fault tolerant control based on furnace temperature sensor faults.

Table of Contents

List of Figures

List of Tables

List of Symbols and Abbreviation

Symbols

$\|\cdot\|$	Euclidean norm (vectors) or induced spectral norm (matrices)
$|a|$	The absolute value of the real number a
$\lambda_{\min}, \lambda_{\max}$	Smallest and largest eigenvalues
$\mathbb{R}, \mathbb{R}_+$	Field of real numbers and the set of strictly positive real numbers
$\mathbb{C}_-$	The set of complex number with negative real part
$\widetilde{A}$	The matrix orthogonal to the matrix A
$\otimes$	Matrix Kronecker product

Abbreviations

AFTC	Active fault tolerant control
CS	Cubic Spline
DM	Decision maker
FDI	Fault detection and isolation
FTC	Fault tolerant control
ISM	Integral sliding mode
LIP	Lagrangian Interpolation Polynomial
LMI	Linear matrix inequality
LQR	Linear-quadratic regulator
LSS	Large scale system
ODE	Ordinary differential equation
OISMC	Output feedback ISM control
PDE	Partial differential equation
PFTC	Passive fault tolerant control
PI-OSMC	Proportional integral control and output feedback sliding mode control
SMC	Sliding mode control
SMO	Sliding mode observer
SOF	Static output feedback
VSC	Variable structure control
VSS	Variable structure system
s.p.d.	Symmetric positive definite

List of Publications

Within the period of this research the following works were published:

Huang, Z. & Patton, R. J. 2012a. An adaptive sliding mode approach to decentralized control of uncertain systems. *UKACC International Conference Control on Control*, Cardiff, UK, 70-75, 3-5 Sep.

Huang, Z. & Patton, R. J. 2012b. Decentralized Control of Uncertain Systems Via Adaptive Sliding and Overlapping Decomposition. *7th IFAC Symposium on Robust Control Design*, Aalborg, Denmark, 784-789, 20-23 June.

Chapter 1

Introduction

1.1   Introduction

With the fast developments of modern technologies, the complexity of industrial systems keeps increasing and as a consequence system applications become more interconnected and distributed. These systems are often referred to as "Large Scale Systems" since potentially a significant number of variables can be involved with non-linear inter-relationships. As a consequence of complexity, mathematical models of their dynamics may be hard to define precisely and hence modelling uncertainty is a significant challenge if model-based methods of control or estimation are to be used.

In fact the term *Large scale systems*(LSSs) does not represent a single type of system having special structure (e.g. distributed) but systems which cannot be solved by one-shot approaches (Bakule, 2008). As a consequence of increased complexity, resulting in an ever increasing range of applications, the research interest in LSS does not decrease, even after three decades. However, it can be noted that the terminology has changed over the years. In the early years the term LSS was frequently used (Singh and Titli, 1978; Sandell *et al*, 1978; Ikeda, 1989; Šiljak, 1996). In subsequent years the terminology and emphasis have changed with the recent literature focussing more on decentralized control and control of inter-connected systems, driven very much by the needs of ever changing applications. (Stanković Stanojevic and Šiljak, 2000; Akar and Özgüner, 2002; Yan, Spurgeon and Edwards, 2003; Pagilla and Zhu, 2004; Shyu, Liu and Hsu, 2005; Kalsi Lian and Żak, 2009; Lu, Lin and Beteman, 2009; Stanković and Šiljak, 2009; Tlili and Braiek, 2009; Yau and Yan, 2009; Kalsi Lian and Żak, 2010; Parutka, 2010; Zhu and Li, 2010; Liu, 2011; Mahmoud, 2011; Mukaidani, 2011, Wei and Jin, 2012; Wu, 2012, etc.).

The IFAC Large Scale Systems symposium in France 2010 states the applications using LSS theory, including: aerospace engineering, environment systems, power systems, transportation systems, medical systems, business systems engineering, etc

(<u>lss2010.ulbsibiu.ro</u>, 2010). These are typical application areas of LSS that present significant challenges to control systems theory and to control system designers.

The practical physical LSSs are often characterized by geographical separation or large dimensionality so that issues such as the inter-connection expense and reliability (e.g. possibility and frequency of interconnection failure, delays, information constraints for each subsystem, etc.) have to be taken into account. (Šiljak, 1991) concluded that the complexity of real systems may not be well organized, whilst for control to be effective good structural organization of a system is required. Hence, "well-organized complexity" is the main challenge of large scale interconnected system design, including the notions of subsystems, interactions, neural networks, parallel processing, etc. It should be noted that these complexities bring in some confusing (and sometimes over-lapping) terminology , e.g. the words "*Large scale systems*", "*Distributed systems*", "*Decentralized systems*" and "*Interconnected systems*", which can have similar meaning.

To develop this subject properly, these terms need to be carefully defined. A "*Distributed system*" is a system containing a collection of autonomous subsystems whose components and resources may not be shared by all local decision makers. It is often used in computer science. The word *distributed* originally referred to computer networks where individual computers were physically distributed within some geographical area. However, the term is nowadays used in a much wider sense. The common defining properties of distributed system are: 1). There are several individual subsystems, each of which has its own local decision maker and 2). They communicate with each other. On the other hand a "*Decentralized system*" is more concerned with the subject of taking the control action(s) from a central function to control actions at decentralized locations of the system. A system that is decentralized lacks a controller nucleus as it is usually composed of many subsystems which are working in unison to form a stable structure. That means that the emphasis of this notion is that the system lacks centralized decision makers or coordinators. The notion "*Interconnected system*" is concerned more with interactions. In this case, if there are interconnections between subsystems, the overall system can be referred to as an "Interconnected System". Some literature use the notion "Large scale interconnected system" (e.g. Kalsi Lian and Żak, 2010) only to state that the subsystems of the LSS are interconnected. These three notions have their own emphasis and should not be mixed up. They all belong to the

concept of a LSS but each in turn has a different classification. And no matter what kind of classification the system is in, the challenges described in the next Section are what LSS control system designers need to deal with.

1.2   Main Difficulties and faults in LSSs

Some researchers state that the complexity and difficulties of LSSs arise mainly from the dimensionality, uncertainty, delay and information constraints (Šiljak, 1991; Bakule, 2008). These are defined as follows:

- **Dimensionality.** The dimension (dynamical order) of a system can be very large. For a single LSS system, there are a large number of states and inputs that cannot be handled easily by using a one-shot control method. Some LSSs that are already decomposed consist of many subsystems that require structure and robustness analysis before effective control systems (at hierarchical and/or local levels) can be designed.

- **Uncertainty.** The overall system cannot be precisely described by a linear mathematical model. Uncertainties come from incomplete identification of the system and some unknown disturbances/control signals. Moreover, model aggregation or simplification which is deliberately designed to make the system manageable may also lead to uncertainties.

- **Information Constraints.** Because of the dimensionality problem, it is necessary to design many decision makers (DMs) to manage the subsystems. None of these DMs knows the system completely. A controller is an example of a DM for a subsystem that can only use the local information, i.e. states/outputs of this subsystem, to stabilize the subsystem.

As a consequence of these difficulties, the analysis and synthesis tasks cannot be solved efficiently in a single step controller. Many control experts take the pragmatic view of LSS as a system that cannot be managed by "conventional" methods (Bakule, 2008). The development of LSS decomposition theory is devoted to the problems arising from the dimensionality problem. The theory answers the question of how to decompose the given control problem into manageable sub-problems. In this case, the system is no longer controlled by a single controller but several independent local controllers which together perform the control function of the overall system.

A significant number of publications focus on approaches to the remaining challenges of handling modelling uncertainty and information constraints. Various control methods have been used to address these challenges, for example, variable structure control (Yan, Tsai and Kung, 1997; Hu and Zhang , 2002; Yan, Edwards and Spurgeon, 2003, 2004a, 2004b, 2009; Shyu, Liu and Hsu, 2003), eigenstructure assignment (Labibi *et al*, 2003), vector Lyapunov function (Lunze, 1989; Martynyuk, 1998; Nersesov and Haddad, 2006), adaptive control (Jain, Khorrami and Fardanesh, 1994; Hansheng, 2002;), Riccati-type control (Bakule and Rodellar, 1996), model predictive control (Lavaei, Momeni and Aghdam, 2008; Ocampo-Martinez *et al*, 2012); etc.

In LSSs, the performance of subsystems after decomposition may be affected by: *interactions* from other subsystems, *external disturbances* and *modelling uncertainty* arising from structure uncertainty or parameter variations.

The difference between *external disturbance* (or *exogenous disturbance*) and *modelling uncertainty* is that the former perturbation does not vary with the system parameter (states, input or output, etc.). However, it should be noted that in regulation problems (the goal of the system is to drive the system error to zero), with proper control design, the effect of the modelling uncertainty maybe significantly reduced when the control objective has been reached.

Unlike external disturbance and uncertainty, traditionally interactions have been treated as a part of the system and are taken care of in system design at a centralized level (Aoki, 1972; Tilti Lefevre and Richetin, 1973; Smith and Sage, 1973; Singh and Tamura, 1974; Singh, Hassan and Titli, 1976, Ikeda, 1981; Ikeda, 1983). With the development of the complexity of a dynamic system attempts were made to deal with LSS designs using decentralized control (Bakule and Lunze, 1988; Gavel and Siljak, 1989, Feng and Jiang, 1995; Hsu, 1997; Chou and Cheng, 2000; Hu and Zhang, 2002; Šiljak, and Zečević, 2005; Tilili and Braiek, 2009; etc.). However, it should be clear that the book of (Singh and Titli, 1978) makes a clear definition of the differences between hierarchical and de-centralized control, the concepts were around a long time before being fully taken up in the literature.

It became apparent that the control of an LSS with decentralized control requires that the interactions be treated as special signals. As the interactions involve coupling

between other subsystems, it is seldom possible to have complete information about them when designing local controllers. In other words the interactions may have uncertain structure/parameters. It is clearly desirable to attempt to reduce the effect of the interactions between the subsystems. From this it follows that the designs of individual control systems can be made without assuming knowledge of the interactions but taking account of their uncertain effects, as a robustness problem.

If all the subsystems are combined into an aggregate system, the interactions are affected by variations of the combined set of all system parameters. However, using the robustness statement above, it can be assumed that for a single subsystem point of view, the interactions from other subsystems can be treated as external disturbances. This is still an open problem (Rosinová and Veselý, 2012)

The notion of "*uncertainty*" described above does not fully represent the unwanted changes in the LSS. Faults also affect the dynamic behaviour of the system in uncertain ways. Various publications provide alternative definitions for the term "fault". For example, Isermann (1984) defines a fault as '*… a non-permitted deviation of a characteristic property, which leads to the inability to fulfil the intended purpose…*' (Blanke *et al*, 2006) defined a fault as '*…a deviation in the system structure or the system parameters from the nominal situation…*'. Moreover, if faults are not taken care of carefully, they might become *failures* (Patton, Frank and Clark, 1989). A failure describes the condition when the system is no longer performing the required function and cannot be corrected by a controller. (Iserman, 2006) defines failure as '*… a permanent interruption of a system's ability to perform a required function under specified operating conditions …*'. That is exactly what is to be avoided.

(Chen and Patton, 1999) classifies clearly different faults by the location of a fault (where it acts in the system). According to this classification, the fault can be recognized as i). *Actuator faults*, ii). *Sensor faults*, and iii). *Component faults*. An actuator fault and a sensor fault appear in an actuator and a sensor of the system, respectively and are normally considered as additive effects whilst the component fault shows up through structural and/or parameter variations of the system, i.e. as multiplicative or parameter-varying effects. However, in LSS decentralized control, from a subsystem point of view, one additional fault should be considered as an abnormal behaviour in the interaction between two subsystems. One can thus think of

an *interaction fault* (Figure 1-1). The local controller design that seeks to take account of interaction faults must do so by attempting to minimize the sensitivity of the local control to these faults. This is an extension of the idea of the concept of robustness to parameter variations and modelling uncertainty. In this respect a fault can be considered as a form of uncertainty (Chen and Patton, 1999). However, the reverse is not true, the uncertainty is not a form of fault!
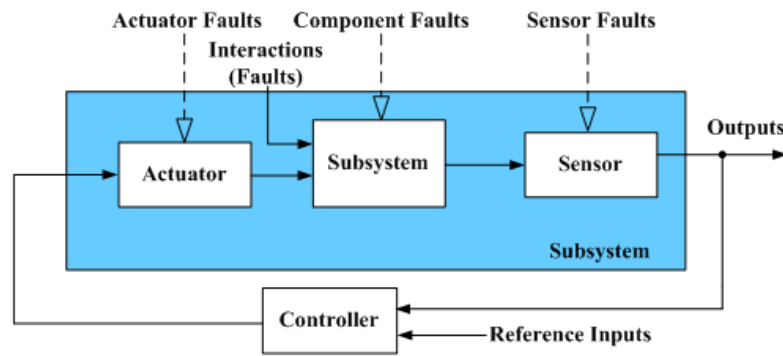
Figure 1-1. Fault classification with respect to their location in LSS

1.3   Fault tolerant control and sliding mode theory in LSS

Several investigators have considered minimization of the local control function to system faults as a so-called fault tolerant control (FTC) problem (Patton et al, 2007). Compared with the number of publications on robust control of LSS, the number of publications that include FTC aspects of LSS is much lower (especially before 21 century). Fifteen years' ago robust control was not widely considered as a part of the FTC problem. (Patton, 1997; Chen and Patton, 1999; Blanke et al, 2006) have pointed out that FTC includes three major research fields, i.e. Fault Detection and Isolation (FDI)/Fault Detection and Identification (Estimation), Robust control and Reconfigurable control. (Figure 1-2)
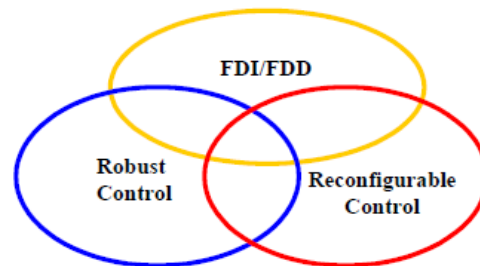
Figure 1-2. The three disciplines of FTC (Patton, 1997)

Generally, two main approaches to FTC are known: i). Passive fault tolerant control (PFTC) and ii). Active fault tolerant control (AFTC). (Beard, 1971; Patton, 1997; Chen and Patton, 1999)
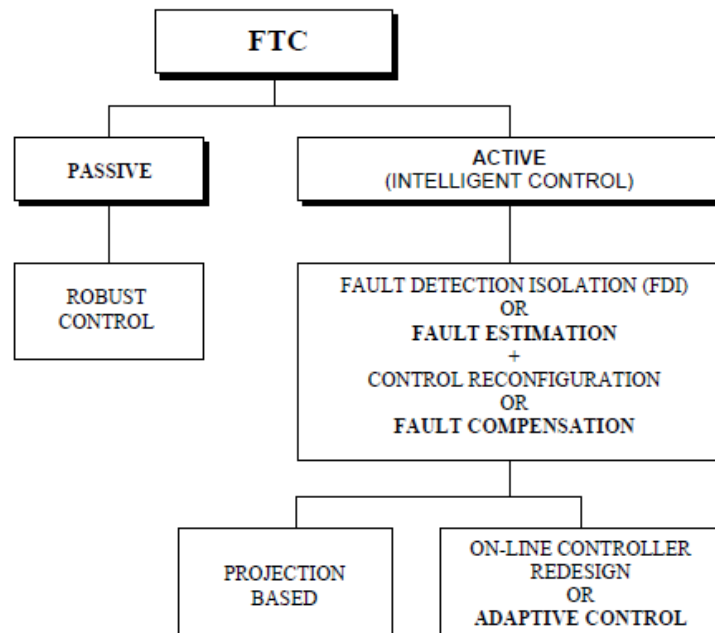
Figure 1-3. Fault tolerant control methods (adapted from Patton, 1997)

Figure 1-3 shows the generally accepted taxonomy of active and passive FTC methods. The main difference between these two methods is whether or not a reconfiguration/adaption procedure is required. In the passive approach, robust control methods are used to ensure that small and bounded faults are tolerated in a fixed gain controller design, however this approach is limited to minor fault effects. On the other hand, active FTC requires online fault information to reconfigure/re construct the controller. Active FTC methods are further classified according to whether or not they make direct use of FDI residual signals to provide fault information. A special type of active FTC system use fault estimation and compensation to "hide" the effect of a fault in a controller, however this approach is mainly applicable to FTC for sensor fault effects.

A special case of FTC classification is the use of sliding mode theory. Sliding mode control (SMC) is a type of control that provides inherent robustness properties of sliding modes to a certain class of faults. It has the ability to directly handle actuator faults without requiring the fault to be detected and without requiring controller

reconfiguration. Classical SMC is actually a form of PFTC with fixed structure that can de-couple the effects of the faults in the feedback control (during sliding motion) as long as the faults are bounded and satisfy a so-called matching condition. Several studies have considered applying SMC to LSS problems. However, most of these studies assume that the interactions satisfy the matching condition constraints. Unfortunately, this assumption does not hold for most practical system applications.. However, SMC has good compatibility with other methods. For example, adaptive SMC can be categorized as an AFTC method (Patton, Putra and Klinkhieo, 2010) which combines a sliding mode observer to estimate the fault with an SMC; the fault estimate causes the SMC non-linear gain to switch according to the magnitude of the fault estimate.

This thesis is concerned with the challenges of applying SMC and sliding mode observer (SMO) theory to handle the joint problem of local controller design and uncertainty compensation in LSS. Whilst the thesis does not focus on approaches to FTC as such the work contains an application example of a thermal annealing furnace system which is shown to be fault tolerant to temperature sensor faults using SMC and a simple concept of fault estimation.

1.4   Thesis Structure and Contributions

The remainder of the thesis is arranged in the following manner:

Chapter 2 provides an introductory motivation for the thesis by reviewing the various known approaches to control and estimation methods for LSSs. After describing the generalized multilevel structure of the LSS problem a further specialization to the single level case is given in which various approaches to system decomposition for LSS control are described, focussing on attempts to minimize the effects of the subsystem interactions. The LSS properties presented lead to a discussion of methods for robust stabilization of LSS. Furthermore, decentralized estimation approaches are also reviewed and different types of observer based estimation methods are briefly introduced based on the LSS concept.

Chapter 3 introduces a steel annealing furnace model taken from a New Zealand Steel project. The furnace model is set up as an example of a LSS to which the methods developed in Chapters 4, 5 and 6 can be applied and described more fully as a robust

control example in Chapter 7. This is an original study using a little known but very powerful way of transforming the thermal model into a suitable framework for decentralized control and estimation.

A mathematical model of the furnace system is derived starting from the non-linear partial differential equation thermal system taken from the project report by (McGuinness and Taylor, 2004). The idea is to transform the "infinite dimensional" thermal system into a lumped representation of a system with interconnected thermal subsystems. A strategy called "differential quadrature" is used to derive the corresponding non-linear ordinary differential equation system using two different interpolation methods, which takes the required boundary conditions into account as well. Several simplifications to the non-linear system are proposed to prepare a model system that is suitable for the decentralized control design. Then the thermal properties of the model are discussed based on a zero-input response of the nonlinear model to qualitatively validate the simplified model. To discuss the modelling accuracy the steady state solutions to the partial differential equations (PDEs) (i.e. considering heat balance) are compared with the results of the nonlinear ordinary differential equation (ODE) system using PID control.

Chapter 4 starts with an introduction to sliding mode theory. For the sliding surface design, two approaches are described for partitioning the system into different regular form structures (Zinober, 1990; Choi, 1997). These regular form decompositions lead to two clearly different approaches to the SMC problem. Following this, the SMC reachability problem is then presented. Several approaches used to reduce or remove the reaching phase are also discussed. At the end of the introduction, typical methods for bound constraint relaxation and chattering reduction are also discussed and proved.

A novel decentralized SMC approach based on linear matrix inequality (LMI) theory is then proposed in Chapter 4. With this approach, the unmatched interactions (uncertainties) are considered in the sliding surface design procedure and the stability of the overall system is guaranteed. The pole assignment, H_∞ theory and quadratic minimization are then combined with this method to provide improved robustness to uncertainty and interactions. A tutorial example of a non-linear interconnected system is used to illustrate the method at the end of this Chapter.

Chapter 5 focuses on the output feedback approach to the decentralized SMC as an extension to the state feedback approaches described in Chapter 4. As contributions, to formulate a systematic LMI-based decentralized SMC theory, novel decentralized static output feedback as well as dynamic output feedback are presented and compared based on a common SMC representation. An output feedback integral SMC design method is also introduced in this Chapter as a new contribution to this research. With this method, the SMC reaching phase can be eliminated.

At the end of this Chapter, a multi-machine problem is introduced to illustrate the proposed methods. The system interactions are adapted to satisfy the so called "quadratic constraint". It is shown that both static output feedback and observer-based integral sliding mode give good robust regulation performance.

Chapter 6 focuses on the design decentralized observer systems using sliding mode observer (SMO) theory. Both the Walcott-Żak observer and the Edwards & Spurgeon observer are reviewed. To achieve decentralized system state estimation an LMI-based decentralized Walcott-Żak observer is developed from the theory used for single or centralized systems. The chosen SMO approach is an extension of the Walcott-Żak observer using a novel improvement to the control law in which the output errors are guaranteed to be zero when the sliding surfaces are reached in the presence of bounded unmatched uncertainties and bounded uncertain interactions (arising from non-linearity). The SMO methods developed in this Chapter are applied to both actuator and sensor fault estimation. The influence from interactions/uncertainties to the actuator fault estimation is discussed with this decentralized SMO design.

A tutorial example of an interconnected non-linear system is used at the end of this Chapter to illustrate the proposed SMO approach, providing robust state and fault estimation.

Chapter 7 further discusses the furnace problem proposed in Chapter 3 to illustrate the SMC and SMO methods described in Chapters 4, 5 and 6. The Chapter starts with a simulation of the furnace model developed in Chapter 3. Then a linearization strategy is applied to linearized the nonlinear furnace model. Three types of faults are chosen to test the robustness of the SMC strategy proposed in Chapters 4 and 5. In comparison with the PID controller, state feedback SMC is first proposed. However, since not all

the states are measurable, static output SMC is then used to control the system. Moreover, to simplify the implementation of the SMC, a PID-OSMC algorithm is proposed, which gives more design freedom and makes the system insensitive to the matched faults.

In this Chapter, sensor faults due to the thermocouple deterioration are also considered. If the thermocouples give lower measurements, PID-OSMC cannot control the furnace temperature appropriately. After using a state augmentation filter in the SMO it is shown that the deterioration of the thermocouple fault can be estimated precisely, even if the fault is of the multiplicative type. The fault estimation signal is then used to compensate the effect of the thermocouple in the PID-OSMC controllers for each heating zone subsystem. The result demonstrates the robustness of the fault estimation and compensation and enhances the value of the proposed PID-OSMC method.

Chapter 8 summarizes and concludes the overall work described by the thesis and makes suggestions and recommendations as to how the research can be further developed in the future.

Chapter 2
Review of Large Scale System Control

2.1   Introduction

The development of control for LSSs can be recognized from publications (Sandell, 1978; Ikeda, 1989; Šiljak, 1991; Šiljak, 1996; Šiljak and Zečević, 2005; Bakule, 2008). Noting that the concept of driving an LSS by a centralized controller is no longer attractive, it is better to design a decentralized system (Šiljak, 1996).

The advantages of using decentralized control can be found from either economy or reliability standpoints. When the system is too large to be dealt with by centralized control, it is computationally efficient to use only local information, i.e. local states or outputs, to make the control decision. This method is also economical since it is easier to implement and it can effectively reduce the communication cost (Šiljak, 1996). Decentralized control also facilitates the development of good robustness. It makes the stability of the closed-loop system tolerant to a broad range of uncertainties regardless of the uncertainties in the subsystems or in the interconnections (Šiljak and Zečević, 2005). Following (Šiljak, 1996). *"decentralized control strategies are inherently robust with respect to a wide variety of structured and unstructured uncertainties in the interconnections. The strategies can be made reliable to both interactions and control failure involving individual subsystems."* As described in Chapter 1, there are several difficulties in designing control strategies for LSSs. Different control structures and different decomposition methods are reviewed in this Chapter to overcome these difficulties.

2.2   Multilevel control structure

The research about multilevel control started in the 1960s and attracted significantly more attention from the 1970s (Mahmoud, 1977, Singh and Tilli, 1978). After a further 4 decades of research investigators still work with this control structure. Now it has become quite a mature control strategy with application studies on several practical systems (Meisel, 1980; Van Cutsem, Howard and Ribbens-Pavella, 1981; Rubaai, 1991; Okou, 2005; Gómez-Expósito and Villa Jaén, 2009; Chen 2012). Some interesting

research about FTC using SMC concepts and two-level structures have been published (Lin, Patton and Zong, 2009; Larbah and Patton, 2010).

The central idea of the multilevel strategy is to form a control structure in a pyramid-like form (Figure 2-1) (Mahmoud, 1977). The problems at the base of the pyramid are simpler though numerous. Each of the problems can be solved according to some decision rules (local decision maker) which should be manipulated by problems located higher in the pyramid. In a three or more level structure, this model of parameterized sub-problems repeats itself over many levels within the organization. It can be referred to as a "*level*" comprising a group of decision problems performing similar kinds of problems in the structure. There is one decision problem, upon which the overall objective of the system depends, standing at the top of the pyramid. In this sense, a multilevel system is a hierarchy of goal-seeking subsystems or decision problems.

As we can see, the more levels the control structure has, the more complicated the strategies become. The complexity of the structure which limits the implementation of hierarchical control is one of the main disadvantages. On the other hand, the pyramid structure implies centralization. It has the disadvantages of centralized control, i.e. communication delay etc.
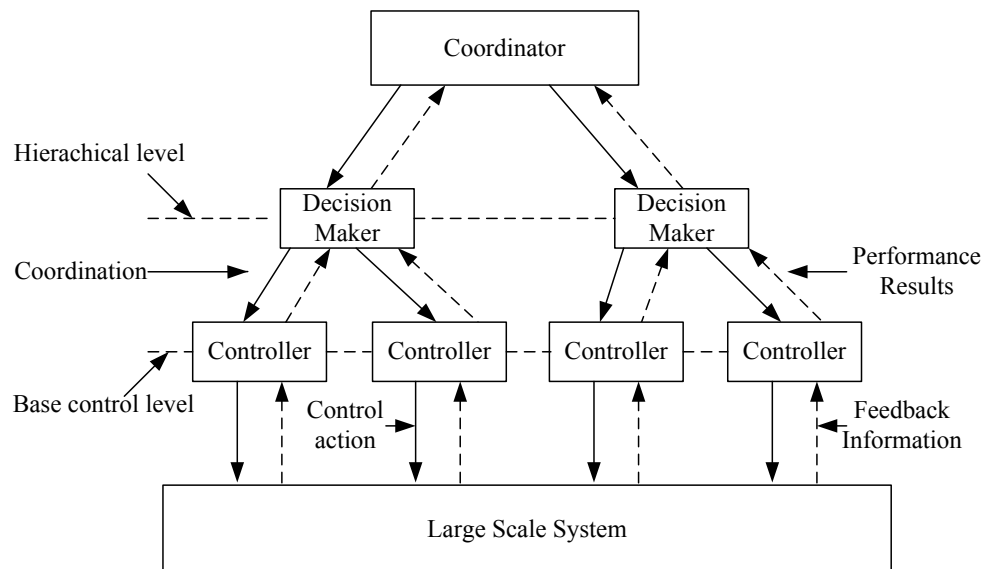
Figure 2-1. Multilevel control structure for LSSs (adapted from Mahmoud, 1977)

In the structure of the two-level LSS control strategy, the base level is a group of local controllers dealing with local information, whilst the second level is a coordinator dealing with interactions. The algorithm of quadratic optimization two-level control is proposed in (Singh, Hassan and Titli, 1976), this is the so called "interaction prediction" method.

Assuming that after proper decomposition, the i-th subsystems of the LSS are in the form of:

$$\dot{x}_i(t) = A_i x_i(t) + B_i u_i(t) + C_i z_i(t), \quad i = 1, \dots, N$$

$$\dot{z}_i(t) = \sum_{j=1}^{N} L_{ij} x_j(t), \quad i = 1, \dots, N$$

where $x_i \in \mathbb{R}^{n_i}$, $u_i \in \mathbb{R}^{m_i}$ are the states and inputs of the i-th subsystem respectively, $z_i \in \mathbb{R}^{q_i}$ represents the interactions from other subsystems. It can be noted that z_i is a linear combination of the states of the overall system.

Local control design

The local controller is designed following the LQR theory. The subsystem control performances are measured via the $J_i(x_i, t, u_i)$ subject to the isolated subsystem, i.e. neglecting the interactions:

$$J_i(x_i, t, u_i) = \frac{1}{2} \int_0^{\infty} (x_i^T Q_i x_i + u_i^T R_i u_i) dt, \quad i = 1, \dots, N \tag{2-1}$$

where $Q_i \in \mathbb{R}^{n_i \times n_i}$, $R_i \in \mathbb{R}^{m_i \times m_i}$ are positive semi-definite and positive definite weighting matrices, respectively.

The local controllers can be obtained by solving the Riccati equation:

$$\dot{K}_i + K_i A_i + A_i^T K_i - K_i B_i R_i B_i^T K_i = -Q_i$$

Using the MATLAB Robust control toolbox, the control low for the base level is given by setting $\dot{K}_i = 0$:

$$u_{i,local} = -R_i^{-1} B_i^T K_i x_i \tag{2-2}$$

Global control

The objective of using global control is to compensate the influence from the interaction terms $C_i z_i, i = 1, \ldots, N$. The global control performance is measured by the quadratic performance index:

$$J(x, t, u) = \frac{1}{2} \int_0^\infty (x^T Q x + u^T R u) dt$$

The analysis gives the following Lagrangian $\mathcal{L}(x_i, u_i, \lambda_i, \rho_i, z_i)$ which must be minimized in order to determine the system control inputs:

$$\min_{x,u,\lambda,\rho,z} \mathcal{L}(x_i, u_i, \lambda_i, \rho_i, z_i)$$

$$= \sum_{i=1}^N \frac{1}{2} \int_0^\infty \left[x_i^T Q_i x_i + u_i^T R_i u_i + \lambda_i^T \left(z_i - \sum_{\substack{j=1 \\ j \neq i}}^N L_{ij} x_j \right) \right.$$

$$\left. + \rho_i^T (A_i x_i + B_i u_i + C_i z_i - \dot{x}_i) \right]$$

where $\lambda_i \in \mathbb{R}^{n_i}$ are the Lagrange multipliers, $\rho_i \in \mathbb{R}^{n_i}$ are the co-states. The Hamiltonian for each subsystem can be written as:

$$H_i = \frac{1}{2} (x_i^T Q_i x_i + u_i^T R_i u_i) + \frac{1}{2} \lambda_i^T \left(z_i - \sum_{\substack{j=1 \\ j \neq i}}^N L_{ij} x_j \right) + \rho_i^T (A_i x_i + B_i u_i + C_i z_i - \dot{x}_i)$$

The the corresponding necessary conditions for optimality are:

$$\frac{\partial H_i}{\partial x_i} = \dot{\rho}_i = 0, \quad \frac{\partial H_i}{\partial u_i} = 0, \quad \frac{\partial H_i}{\partial z_i} = 0, \quad \frac{\partial H_i}{\partial \lambda_i} = 0$$

Define $\rho_i = K_i x_i + s_i$ and the global control $u_{i,global} = -R_i^{-1} B_i^T s_i$. Following the algorithm in (Singh, Hassan and Titli, 1976), the control gain can be obtained by solving:

$$\dot{s}_i = [K_i B_i R_i^{-1} B_i^T - A_i] s_i - K_i C_i \sum_{\substack{j=1 \\ j \neq i}}^N L_{ij} x_j + \sum_{j=1}^N [\lambda_j^T L_{ji}]^T \qquad (2\text{-}3)$$

with $s_i(\infty) = 0$. The control law for each subsystem is thus given in terms of the local control $u_{i,local}$ and $u_{i,global}$ as:

$$u_i = u_{i,local} + u_{i,global} = -R_i^{-1}B_i^T K_i x_i - R_i^{-1}B_i^T s_i \qquad (2\text{-}4)$$

The structure of this two level control strategy is shown in Figure 2-2.

Since the centralized coordinator requires information from every controller, it might have the same problem as we have in centralized control. However, it might provide better results than the total decentralized single level control strategy since it has a coordinator to deal with the interactions. In the single level strategies, it is more like designing local controllers which are robust to the interactions (as perturbations) coming from other subsystems.
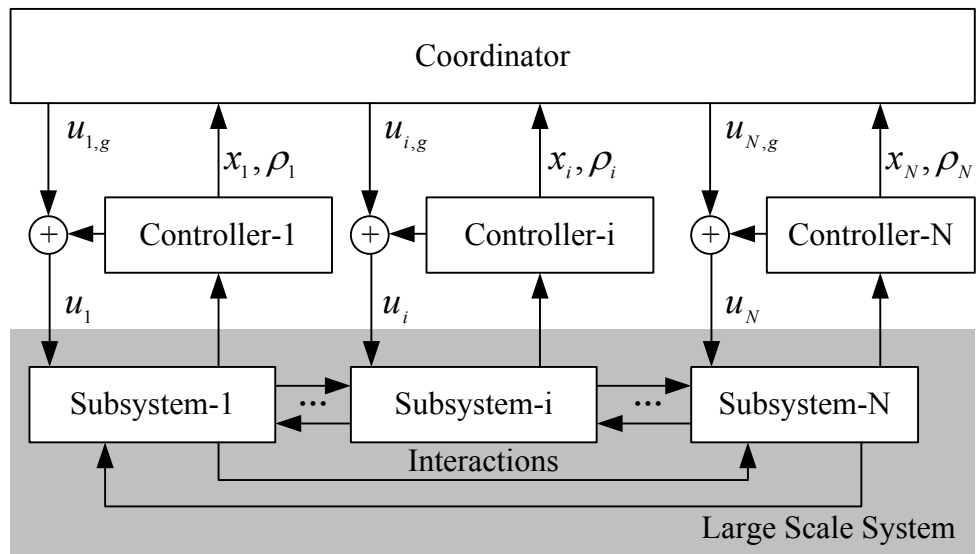
Figure 2-2. Two-level interaction prediction control structure

2.3 Single Level decentralized control

The single-level decentralized control system has a much simpler structure than the multi-level strategy. The control structure only contains the base control level (see Figure 2-1). The interactions are taken care of by the local controllers. The more robust the local controllers the better the performance the LSSs will have. As described in Chapter 1, dimensionality, uncertainty, information constraints are the three main difficulties in designing LSSs control. Several general methodologies have been and are being researched during 3 decades of development of for the single level structure. Most of them belong to one or more of the following three groups (Šiljak, 1978; Šiljak, 1991; Bakule, 2008):

- Decentralization;
- Decomposition;
- Robustness and model simplification.

Decentralization concerns the information structure inherent to the given problem. The desired goal is to achieve as closely as possible completely independent implementation of the LSS control in each subsystem. There are various motivations of decentralization of the design process, such as weak coupling between subsystems, contradictory goals of different subsystems or high dimensionality of the overall system. (Bakule, 2008)

Decomposition is another part of the control design. It concerns the simplifications of the analysis and synthesis tasks for LSS by decomposing the problem into several sub-problems. The goals of decomposition are the reduction of computational complexity and weakening the interaction influence. Different decomposition methods give different base control level structures.

Robustness concerns the robust property of a control design when dealing with uncertainties on the bases of the stability analysis of coupled systems. Robustness analysis becomes more serious in LSS since the interactions might act as uncertainties and they are unavoidable. *Model simplification* mainly includes model reduction methods and approximations (Šiljak and Zečević, 2005).

For robust feedback control strategies, (Šiljak, 1996) introduce a bordered block-diagonal form for the gain matrix and extended this idea in (Šiljak and Zečević, 2005). In their work, *"such a structure can significantly improve the decentralized stabilization of LSSs, at the expense of only minimal communication overhead."* (Šiljak and Zečević, 2005). (Chen, Ikeda and Gui, 2005; Chen Gui and Zhai. 2006) used a homotopy method to design an H_∞ decentralized dynamic control and interconnected descriptor system. (Rosinová and Veselý, 2007) proposed an LMI based decentralized PID control. The adaptive stabilized decentralized control strategy was first proposed by (Gavel and Šiljak, 1989). (Shi and Singh, 1992) then provided an adaptive algorithm for strong nonlinear interactions with single input $u_i \in \mathbb{R}$. (Wu 2002, 2003) further proposed adaptive strategies for uncertain interconnections. Then Perutka (Perutka, 2010) gave a good survey of decentralized adaptive control, stating that that it can be useful to combine the robust and adaptive control together.

Another big impact to single-level LSS is the quick development of variable structure theory (sliding mode theory). (Richter and Lefebvre, 1982) first combined the decentralized control with variable structure theory and apply it in a two-pendulum system example. Following this, many researchers paid attention to a particular type of variable structure — the sliding mode (Furuta, 1990; Drakunov, 1992; Young, 1996; Utkin, 1993; Levant, 1998 etc.). In the sliding mode theory, there are two parts in the control law. The first part is used to stabilize the system and the second discontinuous part is used to drive the system to the so called "sliding surface". Once the system operates on the sliding manifold, the system is insensitive to the matched perturbations (the perturbations coming from input channel), with the concept of matching first defined by (Draženović, 1969) It becomes obvious that if the interactions satisfying the "matching condition", they can be compensated completely by the SMC. Later (Edwards and Spurgeon, 1998) systematically extended the sliding mode concepts to include control and estimation. Meanwhile, the decentralized sliding mode control started being popular (Xu, 1990; Wang, 1993; Feng, 1995; Hsu, 1997; Yan, 1997; Koan-Yuh, 1997). However, some certain restrictive conditions, such as the matching condition for interactions and known upper bounds, were always assumed in a simplistic way in these research studies. From about 2000, the sliding mode, as a powerful disturbance rejection method, has been considered more and more often in studies on decentralized systems (Hu, 2002; Yan, Spurgeon and Edwards, 2003; Yan, Edwards and Spurgeon, 2004; Shyu, 2005; Cheng and Chang, 2008; Kalsi, 2009; Yan, Spurgeon and Edwards, 2009; Kalsi, 2010; Zhu and Li, 2010).

However, no systematic way of using sliding mode theory in LSS has as yet been proposed. Some studies in the literature even further complicate the problem! Hence, a need to build up a systematic concept of interaction minimization SMC theory and to further extend this method in LSSs have been the main motivations for this current PhD research. This thesis also provides some new, less restrictive and easier to implement concepts in robust control and estimation for LSSs.

In the single-level control structure, decomposition plays a significant part of the control design process. Proper decomposition not only simplifies the computation process but also weakens the influence from interconnections and at the same time provides an opportunity for improving the system performance. It is well known that some LSSs

have natural spatial decompositions. Spatial decomposition here means that the subsystems are defined according to their different locations/distributions. For example, power distribution networks and traffic regulation. However, at least on a theoretical basis or as a system plan some of the LSSs can be decomposed by control system designers. The decomposition methods can be classified by whether or not the subsystems shared state variable information according to: 1). Disjoint decomposition or 2). Overlapping decomposition.

2.3.1 Disjoint decomposition

The disjoint *tearing* of the system may be performed for either physical or numerical reasons. The physical reason is mainly because of the spatial separation of the subsystems. Numerical conditioning reasons require the development of a universal control technique for application to LSSs (Bakule, 2008). This section is only concerned about the numerical reasons since the decomposition method cannot be made if the system is already spatially separated.

A typical disjoint decomposition is described by (Šiljak, 1991; Šiljak, 1996), the so called "Nested epsilon decomposition". The idea of this type of decomposition can be illustrated by a simple linear example: $\dot{x} = (A_D + \epsilon A_C)x$, where the matrix A_D is in the form of a block diagonal, and the matrix A_C has all elements < 1 and ϵ is a prescribed small number representing the strength of the interactions. Then: "*The algorithm gives freedom to conveniently choose the strength of coupling between the subsystems and control the size and dominance of the subsystems.*" (Šiljak, 1996).

As the most used decomposition method, the algorithm of disjoint control design is illustrated by a linear LSS in Figure 2-3.

The control strategies for disjoint decentralized systems mainly focus on the reduction of the influence from interactions and uncertainties. Many of the researchers keep seeking the possibility of treating the interactions among the subsystems as perturbations (Jiang, 2000; Šiljak and Stipanović and Zečević, 2002; Castaños and Fridman, 2005, Hung, 2007; Zhu and Pagilla, 2007; Shyu, Liu and Hsu, 2005; Yan, Spurgeon and Edwards, 2009). Some investigators do not clarify this idea in their work, but they treat the interactions and perturbations in the same way. This idea means that the system designers can reject or at least minimize the disturbance coming from

interactions as well as the faults acting in each subsystem by disconnecting or reconnecting subsystems. This is the so-called "plug and play" problem of LSS (Patton et al, 2007).

(a)

x1 | x2 | x3

$$\dot{x}_D = A_D x_D + B_D u_D$$

(b)

x1 ⇄ x2 ⇄ x3

$$\dot{x}_i = A_i x_i + B_i u_i + \sum_{\substack{i=1 \\ j \neq i}}^{3} A_{ij} x_j$$

$$i = 1,2,3$$

(c)

C1   C2   C3

x1 ⇄ x2 ⇄ x3

$$u_i = K_i x_i, \quad i = 1,2,3$$
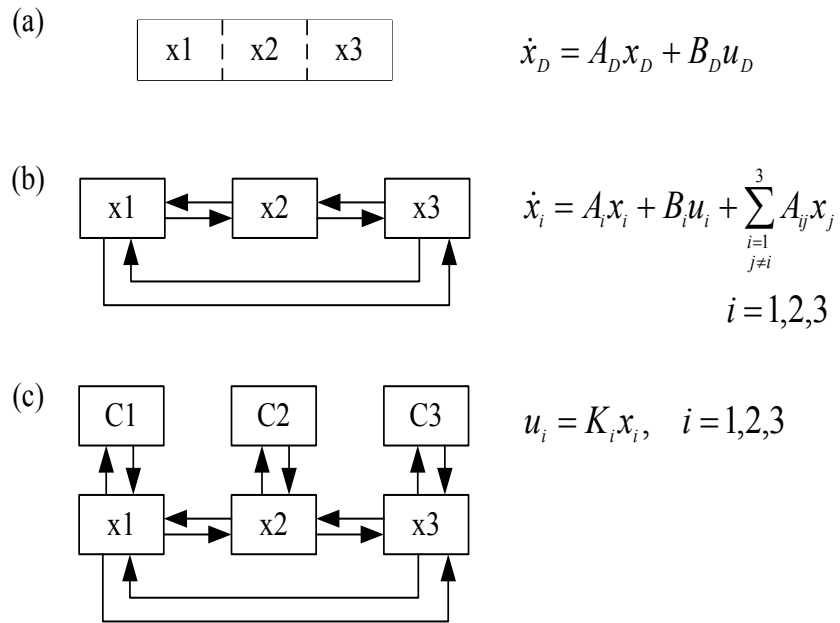
Figure 2-3. Disjoint linear system control design: (a) overall system; (b) decompose into interconnected subsystem; (c) decentralized control design.

In most publications about decentralized control, the subsystem state equation is described in the form:

$$\dot{x}_i(t) = A_i x_i(t) + B_i u_i(t) + h_i(x,t), \quad i = 1, \dots, N \tag{2-5}$$

where $x_i(t) \in \mathbb{R}^{n_i}$, $u_i(t) \in \mathbb{R}^{m_i}$ are the states and inputs of the i-th subsystem respectively. N is the number of the subsystems. The term $h_i(x,t)$ represents the interactions from other subsystems. In linear LSS, $h_i(x,t) = \sum_{\substack{i=1 \\ j \neq i}}^{N} A_{ij} x_j$.

The advantage of using $h_i(x,t)$ is that it can represent not only the linear interactions but also nonlinear interactions and the uncertainty of the subsystem itself. (Šiljak and Stipanović, 2000) gives a quadratic constraint for these interactions as follows:

$$h_i^T(x,t) h_i(x,t) \leq \alpha_i^2 x^T H_i^T H_i x$$

where α is the bounding parameter and H_i is a constant $n_i \times n$, $n = n_1 + \cdots + n_N$ matrix. This assumption also offers a possibility to apply a variety of strategies available in the LMI framework. Some of the research based on this assumption has been done (Šiljak and Stipanović and Zečević, 2002; Zhu and Pagilla, 2007; Tlili and Braiek, 2009; Kalsi, 2010), as well as some work of this thesis. More details are given in Chapter 4.

2.3.2 Overlapping decomposition

Different from Disjoint decomposition, overlapping decomposition of an LSS allows the decomposed subsystems to share some common parts and gives more flexibility in the choices of the subsystems. The motivation of this type of decomposition is the necessity of building decentralized control and estimation schemes using overlapping information sets on realistic applications such as power systems, large space structures etc. Moreover, many large scale systems (e.g. see Özgüner Khorrami and İftar, 1988) may consist of subsystems which are strongly connected through certain dynamics (the overlapping part), but weakly connected otherwise (İftar, 1993). For those systems, disjoint decentralized control may easily fail whilst overlapping decomposition may produce feasible solutions.

The control design strategy is illustrated in Figure 2-4. There are four steps in designing overlapping controller:

a) Decide which parts of the system are the overlapping parts;
b) Expand the system by using the Inclusion Principle (Ikeda, 1980);
c) Design the decentralized controller based on the expanded system;
d) Contract the controller to form the decentralized controller for the original system.

The research about overlapping structures started inthe 1980s. (Ikeda, 1980) proposed the Inclusion Principle as the basic theory underlying the strategy of overlapping decomposition, which justifies the transformation of a lower dimensional original system to a higher dimensional expanded system. (Šiljak, 1991) gives a very clear statement of overlapping decomposition. Two different design methods have been brought out in the 1980s and 1990s. (İftar, 1991; İftar 1993) designs the controller based on the expanded system and contracted to the smaller spaces for implementation on the

original system. (Ikeda and Šiljak, 1986), on the other hand, they define the control law in the original space and obtain the input structure in the expanded space. Later, the structure of the expansion-contraction relations including the contractibility of controllers is analyzed in (Šiljak ana and Stipanović, 2000; Stankovi Stanković and Šiljak, 2001; Chu and Šiljak, 2005) for LTI systems and (Bakule, Rodellar and Rossell, 2001; Stanković and Šiljak, 2003) for LTV system.
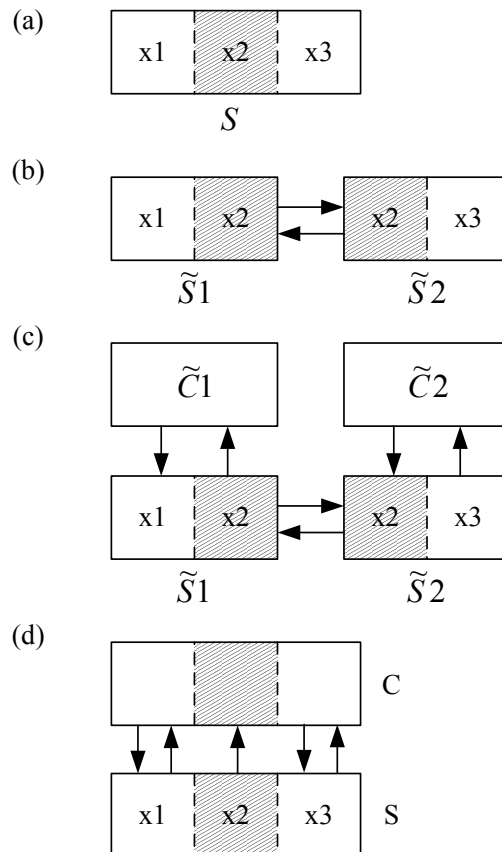
Figure 2-4. Overlapping control design: (a) overall system; (b) expanded system; (c) control design; (d) contracted closed loop system. (Bakule, 2008)

However, the complexity of expansion and contraction is quite high. The expansion and contraction operation must be performed with non-square transformation matrices and the controller design must be performed carefully. Later in 2005, (Zečević and Šiljak, 2005) proposed a convenient LMI approach to design the overlapping control on the original system directly. In this approach, a symmetric positive definite (s.p.d.) Lyapunov matrix P should be pre-structured in block-diagonal form, according to the structure of the system. The control gain matrix is also pre-determined according to a procedure defined in (Zečević and Šiljak, 2005; Šiljak and Zečević, 2005):

$$K = \begin{bmatrix} \begin{array}{c|c} K_{11} & K_{12} \\ \hline 0 & K_{22} \end{array} & \begin{array}{cc} 0 & 0 \\ K_{23} & 0 \end{array} \\ 0 & 0 \quad K_{33} \end{bmatrix}$$

$$(2\text{-}6)$$

The idea proposed by (Zečević and Šiljak, 2005) is different from the idea in (İftar, 1993). The system model in (Zečević and Šiljak, 2005) considers that the overlapping parts do not have their own controllers. In this way the approach can constrain the overlapping parts to be stable. In (İftar, 1993), the overlapping parts have their own controllers.

Thus, the gain matrix for the İftar's method is in the form:

$$K = \begin{bmatrix} K_{11} & K_{12} & 0 \\ K_{13} & K_{14}+K_{21} & K_{22} \\ 0 & K_{23} & K_{24} \end{bmatrix}$$

$$(2\text{-}7)$$

Quite a number of studies have been done to apply the overlapping decomposition methods to realistic systems, for example, power systems by (Šiljak, 1991; Chen and Stanković, 2005, 2007), a platoon of vehicles by (Stanković, Stanojevic and Šiljak, 2000), formation of aerial vehicles by (Stipanović *et al*, 2004) etc. Also, the more complex multi-overlapping decomposition structure is discussed by (Chen and Stanković, 2005).

To combine with other robust methods, (Bakule *et al*, 2005) consider the H_∞ approach to minimize the interactions in the overlapping structure. A quadratic optimization approach has been represented by (Bakule and Rossell, 2008). (Akar and Özgüner 2002) proposed a sliding mode method based on the overlapping structure. (Huang and Patton, 2012b) used integral sliding mode combined with İftar's structure to reduce the influence from interactions.

There are still a lot of problems left in this overlapping structure area such as robust fault tolerant control, uncertainty in the interactions or output based overlapping decomposition using LMI approach etc.

2.4   Decentralized estimation for LSSs

Very few publications focused only on the state estimation problem using decentralized estimation methods until the presence of modern robust estimation methods (Šiljak and Vukcevic, 1976; Edwards and Menon, 2008). The difficulty of state reconstruction for LSSs is obvious when it can be seen that the unavoidable interactions prevent the estimation error from reaching zero value. The decentralized estimation strategies for LSSs mainly focus on: two aspects:

- Decentralized observer based control
- Fault detection/estimation

In the first aspect, the disturbance from interactions can be handled by both control and observer. The objective is to achieve some control goal. For the fault detection/estimation, interactions act as uncertainties which can be tolerated or compensated in the fault estimation.

2.4.1 Decentralized observer based control

A strong research effort has been made in the literature towards the development of decentralized control schemes based on output feedback via construction of decentralized observers. Assume that the i-th ($i = 1, ..., N$) subsystem is in the form:

$$\dot{x}_i(t) = A_i x_i(t) + B_i u_i(t) + h_i(x,t)$$

$$y_i(t) = C_i x_i(t) \tag{2-8}$$

where $x_i \in \mathbb{R}^{n_i}$, $u_i \in \mathbb{R}^{m_i}$, $y_i \in \mathbb{R}^{p_i}$ are the states and inputs of the i-th subsystem, respectively. N is the number of the subsystems. The term $h_i(x,t)$ represents the interactions from other subsystems. Three broad methods are then used to design observer-based decentralized output feedback controllers for LSSs as follows:

(1) Design a local observer and controller for each subsystem independently and check the stability of the overall closed-loop system. In this method, the interconnection terms acting in each subsystem are regarded as an unknown input (faults). A typical example of this is given by (Kalsi, 2009) an SMO to make the observer insensitive to the interactions. With this method, the interactions have to satisfy certain conditions. For subsystem (2-8), assuming that the interactions $h_i(x,t) = G_i \bar{h}_i(x,t)$, the conditions are $rank(C_i G_i) =$

$rank(G_i)$ and any invariant zeros of the triple (A_i, G_i, C_i) are in the open left-hand complex plane. In this case, the observer can estimate the states precisely without any other uncertainties. The control structure of the system is illustrated by in Figure 2-5 with two interconnected subsystems.
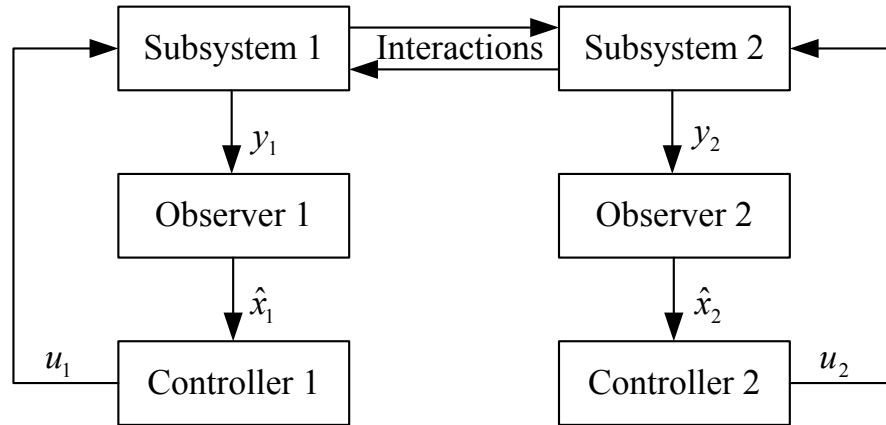
Figure 2-5. Observer based decentralized control without interactions between observers

(2) Design local observer and controller for each subsystem independently and check the stability of the overall closed-loop system. Compared with (1), in this method, the interaction information is assumed known. For example, if the interaction term in subsystem (2-8) is linear and in the form of $h_i(x,t) = \sum_{j=1, j \neq i}^{N} A_{ij} x_j$, then the gain matrices A_{ij} are known. Thus, the observer for the i-th subsystem is in the form of:

$$\dot{\hat{x}}_i(t) = A_i \hat{x}_i(t) + B_i u_i(t) + \sum_{j=1, j \neq i}^{N} A_{ij} \hat{x}_j(t) + L[y(t) - \hat{y}(t)]$$

$$\hat{y}_i(t) = C_i \hat{x}_i(t)$$

Or if the interaction is nonlinear, it should satisfy the Lipschitz condition $\|h_i(x,t) - h_i(\hat{x},t)\| \leq \mathcal{L}_i \|x - \hat{x}\|$ and the observer is in the form of:

$$\dot{\hat{x}}_i(t) = A_i \hat{x}_i(t) + B_i u_i(t) + h_i(\hat{x},t) + L[y(t) - \hat{y}(t)]$$

$$\hat{y}_i(t) = C_i \hat{x}_i(t)$$

A number of publications use this method since it considers the interactions in the design of the observer (Šiljak and Vukcevic, 1976; Looze *et al*, 1978; Sandareshan and Huang, 1984; Date and Chow, 1989; Hu, 1994; Uang and Chen,

2000; Zhang and Polycarpou and Parasini, 2010). The structure of this method is shown in Figure 2-6.
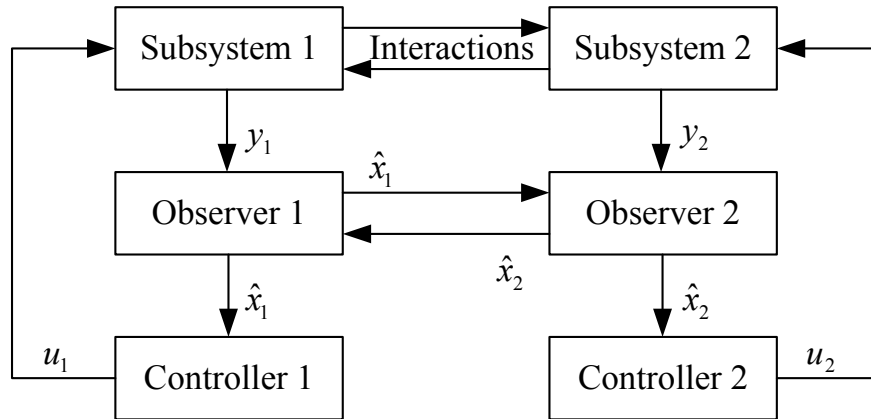
Figure 2-6. Observer based decentralized control with interactions between observers

(3) Design the observer and controller by posing the output feedback stabilization problem as an optimization problem based on the overall system. The framework of the optimization approach using LMIs can be found in (Šiljak and Stipanović, 2001). The idea of the decentralized controller and observer design problems were formulated in the LMI framework for LSSs with non-linear interconnections satisfying quadratic constraints described in Section 2.3.1. The existence of a stabilizing controller and observer depends on the feasibility of solving a series of LMIs. The optimization problem will result in the selection of controller and observer gains that will not only stabilize the overall LSSs but also maximize the interconnection bounds (Zhu and Pagilla, 2007). The control structure is in the same form of Figure 2-5. The interactions are treated as uncertainties and can be tolerated by proper choice of control and observer gain matrices. The recent research can be found in (Šiljak and and Stipanović, 2001; Pagilla and Zhu, 2005; Zhu and Pagilla, 2007; Swarnakar and Marquez, 2008; Kalsi Lian and Żak, 2009, 2010; Shafai Ghadami and Saif, 2011). This method is also the basic idea behind the output feedback methods proposed in Chapter 5.

2.4.2 Fault estimation in LSS

The history of fault detection and isolation (FDI) can be traced back to the 1970s. From both theoretical and application-based perspectives, FDI has attracted considerable attention (Clark, 1978; Himmelblau, 1978; Chow and Willsky, 1984; Isermann, 1984;

Gertler, 1988; Patton, Frank and Clark, 1989; Chen and Patton, 1999; Patton, Frank and Clark, 2000; Isermann, 2006; Ding, 2008).

The main idea of the model-based approach to FDI is to generate signals that reflect inconsistencies between nominal and faulty system operation. Such signals, termed "residuals", are usually generated using analytical approaches, such as observers (Chen and Patton, 1999; Patton, Frank and Clark, 2000), parameter estimation (Isermann, 1994) or parity equations (Gertler, 1998) based on analytical (or functional) redundancy. Among all of the FDI approaches, observer-based methods are the most popular method to be researched and applied (Edwards Spurgeon and Patton, 2000b), for example, see (Chen and Patton, 1999; Shields and Du, 2003; Xu and Zhang, 2004).

All the literature outlined above focus on centralized systems. When considering the FDI of LSSs, rather less research has been done (Yan and Edwards, 2008). The reason is the interactions act as an extra disturbance/uncertainty for the fault estimation. The influence from interactions leads to inaccurate estimation of faults while most research on FDI method can only deal with single types of faults (without uncertainties or with very small uncertainties). Early work on FDI for LSSs can be traced back to (Hassan, Sultan and Attia, 1992) who used a Kalman filter based on overlapping decomposition to detect and isolate the fault in discrete time. In (Chung and Speyer, 1998), a game theoretic fault detection filter combining with decentralized filter approach is proposed. (Shankar, Darbha and Datta, 2002) discusses the decentralized observer based fault detection for interconnected LTI subsystems. More recently, (Farrari, 2009) detects faults with a decentralized adaptive estimator based on overlapping structure. (Zhang and Polycarpou and Parasini, 2010) represent the decentralized fault detection under canonical form and using an adaptive threshold for robust fault detection.

With the development of sliding mode theory, the idea of utilizing sliding mode theory in an observer has proved to be very effective in the field of FDI. However, compared with the residual generation approach, the sliding mode observer (SMO) forces the estimation of the outputs to be identical to the outputs of the plant with the so called "switching function". Thus, the conventional residual generated by the output estimation error would be zero. The actuator and sensor fault estimation problems have been proposed in (Edwards and Spurgeon, 1998) and extended in (Tan and Edwards, 2002, 2003). Later in (Yan and Edwards, 2008), the fault estimation sliding mode

approach for LSS is proposed. In this important research, the Edwards & Spurgeon SMO is used to estimate the actuator fault. Information about the situations under which the influence from interactions and uncertainties are minimized in the fault estimation is also included. However, Yan and Edwards assumed that the structure of the interactions is known (the second situation in section 2.4.1) and the uncertainties satisfy certain conditions. There seems to be no other literature on the application of decentralized SMO theory for nonlinear-interconnected systems to obtain a decentralized and precise fault reconstruction. This motivated the method proposed in Chapter 6.

2.5   Conclusion

This Chapter gives a review of decentralized control and estimation methods for LSSs. According to the control structure, the control strategies can be classified as multi-level and single-level structures. Multi-level control constructs a pyramid structure, using local control level to deal with the independent information of subsystems whilst using higher level to give the decision rules to the lower lever. The Two-level control strategy, as a typical multi-level, is reviewed in this Chapter. This structure gives a clear vision of the multi-level structure. However, the higher level of multi-level control still requires centralization (i.e. a requirement for a coordinator). This condition increases the complexity of this method.

The rapid increase in computer technology in the last decade means that the single-level control structure is much simpler and more widely used than multi-level LSS structures. As this Chapter describes, the interactions are taken care of by robust local controllers. There are numerous decentralized methods for LSSs. Most of them can be classified by their decomposition methods. This Chapter reviews two main decomposition methods when using single-level control structure: disjoint decomposition and overlapping decomposition.

To concentrate on the main topic of this thesis, the "quadratic constraint" assumption for interactions is introduced for disjoint state space structures. Also a brief idea about decentralized sliding mode theory is given. The treatment of these topics is useful in Chapters 4 and 5.

Although this thesis mainly focuses on the disjoint decomposition, some work on overlapping decomposition (Huang and Patton, 2012b) has also been done. For the

future work, there are still a lot of open problems to be addressed based on the overlapping structure.

For the estimation applied to LSSs, the decentralized observers are often in the role of observer based control or fault estimation. In this Chapter, three observer based control methods are reviewed which give a good basis for Chapters 5 and 6. Decentralized fault estimation methods based on the use of decentralized observers are also discussed.

Chapter 3

Annealing Furnace Modelling: A Differential Quadrature Approach

3.1 Introduction

Furnaces have been widely used in industrial applications as heating devices to raise the temperature of particular system processes, such as for power systems or in the annealing process used for preparation of a metal for rolling in the metal industry. This Chapter proposes the development of a model of a steel annealing furnace system as an example of a LSS application.

The work is based on a well-known model formulation included in the McGuinness and Taylor's report of the MISG project. *"New Zealand Steel use a unique process to convert New Zealand iron-sand into steel sheet products at its Glenbrook mill near Auckland. Traditional galvanised steel and the new product Zincalume are produced in a range of dimensions, grades and coating weights."* (McGuinness and Taylor, 2004).

The steel strip is annealed before being coated. The furnace heats the steel strip to a pre-determined temperature in well defined time, producing desirable changes in the crystalline structure of the steel strip to tailor its strength and ductility.

The Cross-section of the furnace is shown in Figure 3-1. The steel strips pass through the furnace to get heated up. The furnace length is denoted by l m. The velocity of the strip v m/s is constant. Thus, if the steel achieves the desired temperature at the end of the heating zone, the time of heating up can be calculated by $t_h = l/v$. The temperature of the furnace is controlled by several heating elements fixed in the wall. In this Chapter, the cooling part of the furnace is not considered although it exists in the real system (McGuinness and Taylor, 2004). It's important that the steel exits the furnace with the correct temperature because the coating process is applied at the exit point.
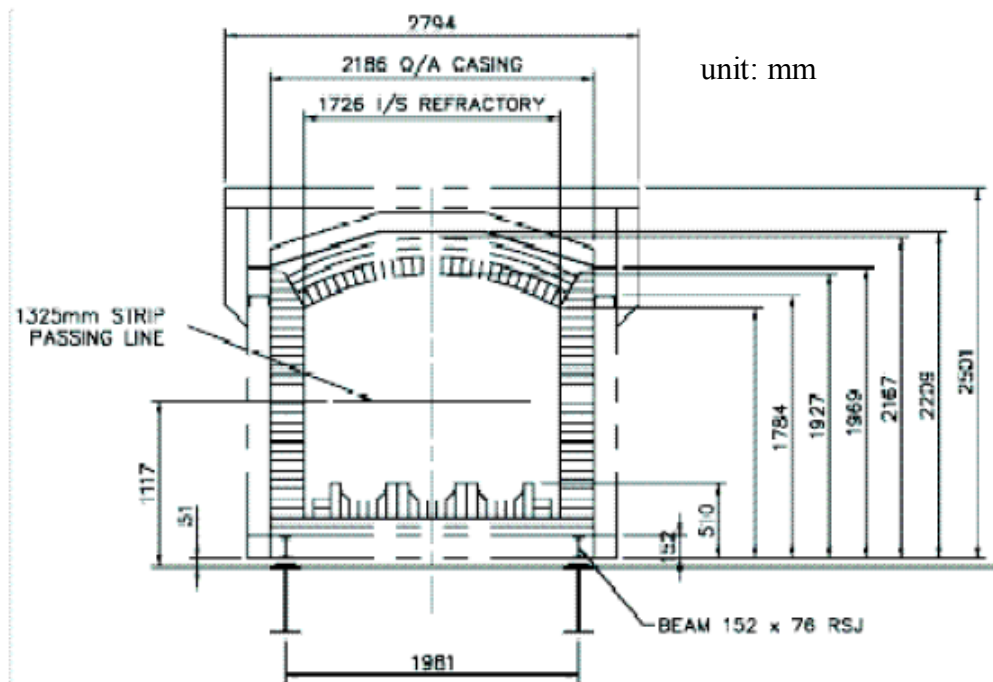
Figure 3-1. Cross-section of the furnace (McGuinness and Taylor, 2004)

Assume that the line speed and the thickness of the steel are constants (might be varied as a form of parametric uncertainty), and the width of the steel strip is a constant so that the heating process is continuous. It is also assumed that the whole strip achieves the required temperature (as either a single temperature or as a defined variation of temperatures).

The temperature measurements of the furnace are made using thermocouples and non-contacting pyrometers. The thermocouples used to measure the furnace temperature are fixed to the furnace wall and the non-contact pyrometers are used to measure the temperature at three distinct strip locations

If there is no variation in strip dimensions and annealing settings then the system will run in a steady state (McGuinness and Taylor, 2004). The furnace temperature will remain steady at the desired thermocouple settings. However, parameter variations can be considered as uncertainties. The appropriate control method is then chosen to attenuate or compensate the influence of the uncertainty.

The Chapter has the following structure: Section 3.2 describes the main equations of the furnace model in two parts, the strip temperature and furnace wall temperature models,

respectively. In order to fully develop the model several further assumptions must be made. Section 3.3 introduces two alternative methods for discretising the PDEs into ODE format. These methods are known as differential quadrature methods following the work introduced by Bellman (Bellman Kashef and Casti, 1972): One quadrature approach uses cubic spline interpolation in which the partial derivatives are represented over one data interval using a separate cubic spline. In contrast the differential quadrature using orthogonal interpolation polynomials are chosen as Lagrangian Interpolation polynomials spanning the whole range of the quadrature. These two approaches are applied separately to the strip and furnace wall models, respectively. Section 3.4 then describes an organization and simplification of the structure of the equations leading to a non-linear state space system, where the non-linearity comes mainly from considering Stefan's radiation law applied to the furnace system. The two boundary conditions of the original partial differential system are handled via a simple trick in the use of the Lagrange interpolation. The modelling procedure produces a nonlinear furnace model for simulation which is shown in Chapter 7.

3.2   Furnace System Mathematical Modelling

As outline in Section 3.1, the furnace model contains two heat transfer components: the strip model and the furnace wall model, respectively, together making up the strip-furnace model. This Chapter describes the development of an appropriate non-linear state space model to illustrate the main dynamic properties of the strip-furnace system. Several assumptions are made for the identification of this system (McGuinness and Taylor, 2004):

Assumption 1: The temperature of the strip over each cross-section is considered constant.

With this assumption, the temperature variation in the cross-section area can be ignored.

Assumption 2: It is assumed that the metal is conveyed only in the longitudinal direction.

Consider that the furnace is perfectly straight with rectangular cross section as shown in the 3-dimensional model of Figure 3-2 Consider the longitudinal direction via the axis x, the latitudinal direction with axis y, and the vertical direction via axis z. Then assuming

all strip motion is only in the longitudinal direction, the temperature variations orthogonal to the conveyor direction will be negligible i.e. $v\frac{\partial T}{\partial y} \approx 0$ and $\frac{\partial T}{\partial z} \approx 0$.
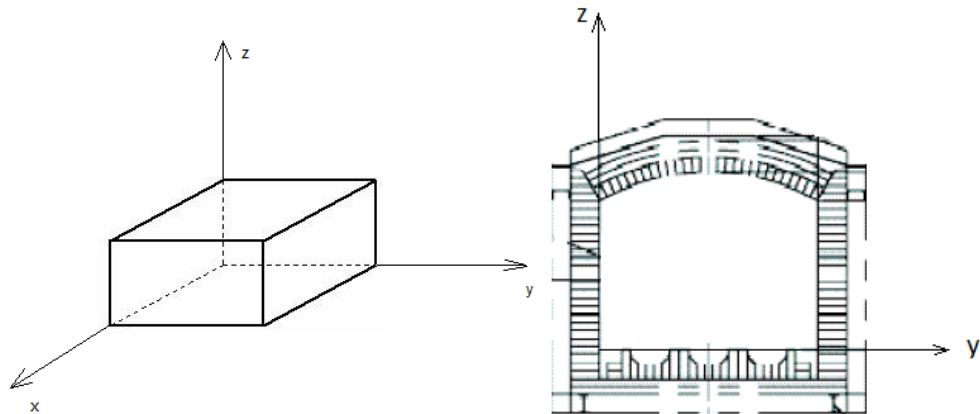
Figure 3-2. Furnace dimensions

Assumption 3: The inner surface temperature of the furnace walls depends on time t and distance x along the furnace measured from the entry point of the strip.

Assumption 4: The temperature of a heating element is the same as the temperature of the inner surface of the wall adjacent to the element.

Assumptions 3 and 4 contributing to the simplification of the thermal equations of the furnace model are described in the Section 3.4.

Assumption 5: Temperature changes within the furnace are so gradual that the radiative or convective heat transfer components along the length of the furnace can be ignored.

This assumption leads to a reduction in complexity since there is no not net radiation heat transfer as the strip travels from one zone into another, i.e. there is no interactions between the furnace wall models.

Assumption 6: This model only concerns the heating zone of the furnace.

Normally, the furnace contains cooling tubes after the heating zone. However, this work is only concerned with the heating function of the furnace. Between the heating and cooling zones, Assumption 5 is not valid.

3.2.1 Strip Thermal Model

Firstly, set up a region of space:

$$S = \{(x, y, z) : 0 < x < l, 0 < y < w, 0 < z < h\}$$

where, l is the length of the furnace, h, w are typical values of the thickness and width of the strip, all dimensions in m.

For the strip, the heat conduction equation of the conveyed material is given by the classical heat conduction equation modified by a convective term and a term which accounts for the heat source

$$\rho_s C_s \left(\frac{\partial T}{\partial t} + v \frac{\partial T}{\partial x} \right) = \lambda_s \left(\frac{\partial^2 T}{\partial x^2} + \frac{\partial^2 T}{\partial y^2} + \frac{\partial^2 T}{\partial z^2} \right) + \frac{q}{wh} \tag{3-1}$$

T is the strip temperature, ρ_s, λ_s, c_s, are the strip density, thermal conductivity and specific heat capacity , respectively. q is the radiative heat transfer between the furnace wall and the strip. v is the conveyor speed in $m \cdot s^{-1}$.

Assumption 1 implies that the temperature variation in the cross section of the strip can be ignored. This means that the heat conduction in the lateral and vertical directions $(\frac{\partial^2 T}{\partial y^2}, \frac{\partial^2 T}{\partial z^2})$ can be removed from the strip model. And following Assumption 2, there is no conveyor movement in the lateral and vertical directions. According to this Assumption the term $v \frac{\partial T}{\partial x}$ describes the temperature variation in the longitudinal direction influenced by the conveyor speed v.

In this case, the heat equation can be further simplified to reduce the computation burden, as follows:

$$\frac{\partial T}{\partial t} = \frac{\lambda_s}{\rho_s C_s} \frac{\partial^2 T}{\partial x^2} - v \frac{\partial T}{\partial x} + \frac{q}{wh \rho_s C_s} \tag{3-2}$$

The thermal properties of steel (λ_s, c_s) change with temperature are shown in Table 3-1. Taken from (McGuinness and Taylor, 2004):

Table 3-1. Properties of steel in different temperature

$T(K)$	300	400	600	800	1000
$\lambda_s\ (W/m \cdot K)$	60.5	56.7	48.0	39.2	30.0
$c_s\ (J/Kg \cdot K)$	434	487	559	685	1169

According to this table, two suitable polynomial interpolations can be achieved for (λ_s, c_s) as:

$$\lambda_s = -5e-6T^2 - 0.0374T + 72.245 \tag{3-3}$$

$$c_s = 345 - 0.5043333T + 0.004895T^2 - 9.0667e-6T^3 + 5.5e-9T^4 \tag{3-4}$$

Because the annealing process has a large range of temperature variation, the properties of steel cannot be ignored in the system. Hence, Eqs. (3-3) and (3-4) should be considered during the linearization in Chapter 7.

By considering the thermal combination of the strip and furnace wall, McGuinness and Taylor gives the equation for the radiation per unit length of the heat source q of the furnace walls to the strip as:

$$q = \frac{2w\varepsilon_s\sigma}{1 + \dfrac{\varepsilon_s(1-\varepsilon_w)}{\varepsilon_w}\dfrac{w}{p}}\left(T_w^4 - T^4\right) \tag{3-5}$$

w is the strip width, p is the approximately the sum of the vertical length and width of the inside of the furnace. $\varepsilon_s, \varepsilon_w$ are the thermal emissivity of the strip and furnace wall, respectively. σ is the Stefan-Boltzmann constant which is $\sigma = 5.67 \times 10^{-8}\ W/(m^2 \cdot K^4)$.

By assuming $\varepsilon_w \approx 1$, the Eq. (3-5) is finally simplified to:

$$q \approx 2w\varepsilon_s\sigma(T_w^4 - T^4) \tag{3-6}$$

3.2.2 Furnace wall thermal model

Now consider the energy balance for a single unit of the heating elements and inner wall surface to construct the thermal model for the furnace walls. Assume that the unit length is Δx, the specific heat capacity of the unit is c_u and the mass of the unit is m. By

considering the combined inner wall surface and heating elements as a single lumped isothermal object, the appropriate energy balance can be expressed as (McGuinness and Taylor, 2004):

$$mc_u \frac{dT_w}{dt} \Delta x = P\Delta x - \Phi 2p\Delta x - q\Delta x \qquad (3\text{-}7)$$

Where, Φ is the heat flux into the walls, P is the energy supplied to the unit, p is the width and height of the inner surface of the furnace so that $2p\Delta x$ denotes the total area of the inner surface. The terms in Eq. (3-7) are illustrated in Figure 3-3:
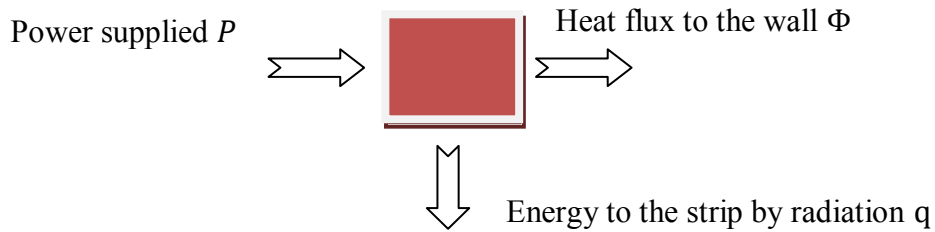
Figure 3-3. Energy balance in a single unit of furnace

Assuming that the heating elements have little thermal inertia (no energy storage), Eq. (3-7) can be further simplified to:

$$mc_u \frac{dT_w}{dt} \Delta x = P\Delta x - \Phi 2p\Delta x - q\Delta x = 0$$

$$\Phi = \frac{(P-q)}{2p} \qquad (3\text{-}8)$$

A further simplification can be made by treating each heating element and furnace wall as a separate one dimensional brick thermal model, considering only heat conduction (i.e. no convection or radiation). (McGuinness and Taylor, 2004):

$$\rho_w c_w \frac{\partial T_B}{\partial t} = \lambda_w \frac{\partial^2 T_B}{\partial r^2} \quad 0 < r < d \qquad (3\text{-}9)$$

This is combined with the following boundary conditions:

$$T_B(x,0,t) = T_w(x,t) \qquad (3\text{-}10)$$

$$\lambda_w \left. \frac{\partial T_B}{\partial r} \right|_{r=0} = -\Phi \tag{3-11}$$

$$\lambda_w \left. \frac{\partial T_B}{\partial r} \right|_{r=d} = H\big(T_\infty - T_B(x,d,t)\big) \tag{3-12}$$

Where, ρ_w, c_w, λ_w are the density $(kg \cdot m^{-3})$, specific heat capacity $(J \cdot kg^{-1} \cdot K^{-1})$ and thermal conductivity of the walls $(W \cdot m^{-1} \cdot K^{-1})$, respectively. $T_B(x,r,t)$ (K) is the temperature of the internal wall (brick) of the furnace (at a distance x (m) and a depth r (m) into the wall. $T_w(x,t)$ (K) is the temperature of the inner surface of the furnace. d (m) is the thickness of the wall. T_∞ is the external ambient temperature. H is a convection coefficient. The structure of furnace wall is shown in Figure 3-4.
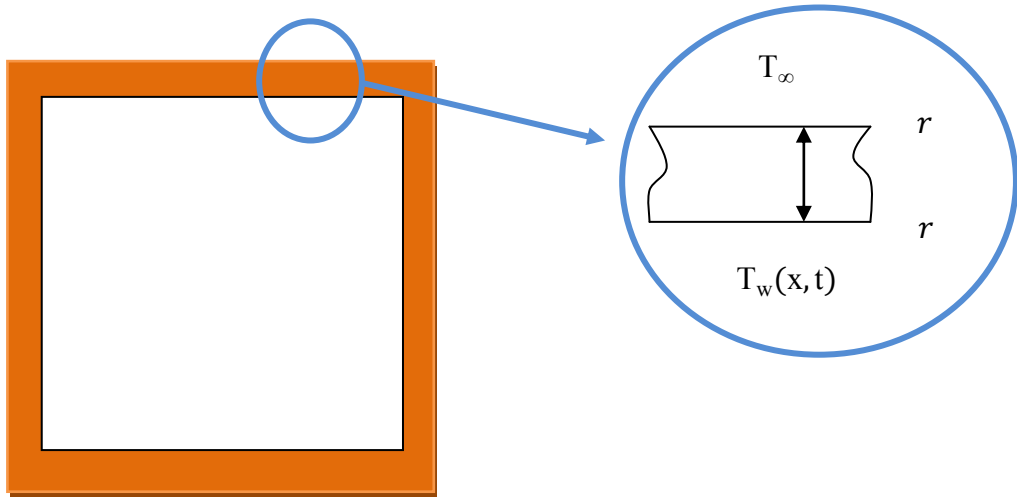
Figure 3-4. Cross section of furnace and wall temperature model

Moreover, the thermal properties of the wall as given in (McGuinness and Taylor, 2004), are shown in Table 3-2

Table 3-2. Properties of brick of the furnace wall

$T(K)$	478	1145
λ_w $(W/m \cdot K)$	0.25	0.30
c_w $(J/Kg \cdot K)$	≈ 900	≈ 900
ρ_w (Kg/m)	≈ 2000	≈ 2000

It can be seen that the variation of the thermal properties with temperature are small, which means that it can be assumed that these brick properties are constant.

$$\lambda_w = 0.28(W \cdot m^{-1} \cdot K^{-1}), c_w = 900(J \cdot kg^{-1} \cdot K^{-1}), \rho_w = 2000(kg \cdot m^{-3})$$

To conclude, the nonlinear model of the whole system can be written as:

$$\frac{\partial T}{\partial t} = \frac{\lambda_s}{\rho_s C_s} \frac{\partial^2 T}{\partial x^2} - v \frac{\partial T}{\partial x} + \frac{q}{wh\rho_s C_s} \tag{3-2}$$

$$q \approx 2w\varepsilon_s\sigma(T_w^4 - T^4) \tag{3-6}$$

$$\Phi = \frac{(P-q)}{2p} \tag{3-8}$$

$$\rho_w c_w \frac{\partial T_B}{\partial t} = \lambda_w \frac{\partial^2 T_B}{\partial r^2} \quad 0 < r < d \tag{3-9}$$

$$T_B(x,0,t) = T_w(x,t) \tag{3-10}$$

$$\lambda_w \frac{\partial T_B}{\partial r}\bigg|_{r=0} = -\Phi \tag{3-11}$$

$$\lambda_w \frac{\partial T_B}{\partial r}\bigg|_{r=d} = H\big(T_\infty - T_B(x,d,t)\big) \tag{3-12}$$

3.3   Two methods of differential quadrature

The method of differential quadrature developed by Richard Bellman in the 1970s (Bellman Kashef and Casti, 1972) is a numerical solution technique for differential systems by means of a polynomial-collocation approach at a finite number of points. Two differential quadrature approaches have been adopted in this work. Firstly, the continuous derivative function (partial derivative) is approximated using an orthogonal polynomial (over a finite number of collocation points – the roots of the polynomial). This method has a disadvantage that the node spacing in the lumped parameter system (spacing in the x direction) is non-uniform. The approach is compared with the use of Bellman's second quadrature which uses a set of cubic spline polynomials with each spline function effective over a collocation interval.

It can be seen that both strip and furnace wall dynamical models contain PDEs, which make these models hard to be controlled. This Section introduces two differential quadrature methods: Lagrangian Interpolation Polynomial (LIP) method (Hsu, 2009)

and Cubic Spline (CS) Interpolation (Bellman, 1972 Shampine and Allen, 1973). With these two methods, the approximate models which are in the form of ODE can be obtained. However, once the model is cast in the state space form, it becomes possible to develop suitable robust control and estimation designs to achieve the required furnace performance objectives.

The concept of differential quadrature starts with the notion of applying m-dimensional differential operator to a continuous and differentiable function where $x \in \mathbb{R}^n$. The m-dimensional vector differentiation can be written in the following form:

$$\frac{\partial^m}{\partial x^m} \begin{Bmatrix} f(x_1,t) \\ f(x_2,t) \\ \vdots \\ f(x_n,t) \end{Bmatrix} = D^{(m)} \begin{Bmatrix} f(x_1,t) \\ f(x_2,t) \\ \vdots \\ f(x_n,t) \end{Bmatrix} \tag{3-13}$$

where $f(x_i,t)$ is the functional value at grid point x_i, and $D_m \in \mathbb{R}^{n \times n}$ is a matrix defining the operations required to achieve *differential quadrature.*

In the following subsections, LIP and CS are introduced, respectively. The further application of both these methods in furnace system is proposed in Section 3.4.

3.3.1 Lagrangian Interpolation Polynomial

This subsection describes a Lagrangian Interpolation Polynomial approach for the discretization of PDE systems into ODE system form. This interpolation is valid over a range of the space variable x, for which the range is divided into "collocation points" that match the roots of the orthogonal polynomial used. For example, the Chebyshev-Gauss-Lobatto polynomial roots are distributed according to (Hsu, 2009) .

$$x_i = \frac{1}{2}\left(1 - \cos\frac{(i-1)\pi}{N_w - 1}\right) \qquad for\ i = 1,2,\ldots,N_w \tag{3-14}$$

where N_w is the order of the polynomial, for example for $N_w = 10$, the roots are distributed as shown in Figure 3-5:
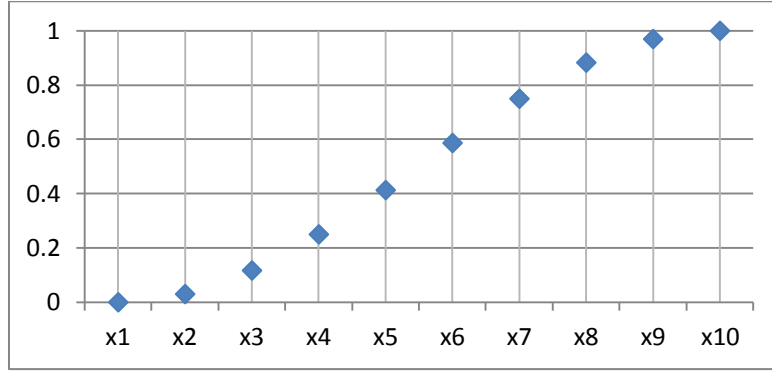
Figure 3-5. Chebyshev-Gauss-Lobatto distribution

The concept of the Lagrangian Interpolation is given as follows:

$$f(x,t) \cong \sum_{i=1}^{N_w} \frac{M(x)}{(x-x_i)M_l(x_i)} f(x_i,t) \tag{3-15}$$

where

$$M(x) = \prod_{j=1}^{N_w} (x-x_j)$$

$$M_l(x_i) = \prod_{\substack{j=1 \\ j \neq i}}^{N_w} (x_i - x_j) \qquad for \ i = 1,2,...,N_w$$

In this case, the matrix D in (3-13) can be expressed as:

$$D_{ij}^{(1)} = \frac{M_l(x_i)}{(x_i - x_j)M_l(x_j)} \qquad for \ i = 1,2,...,N_w, i \neq j \tag{3-16}$$

also:

$$D_{ii}^{(1)} = -\sum_{\substack{j=1 \\ j \neq i}}^{N} D_{ij}^{(1)} \qquad for \ i = 1,2,...,N_w \tag{3-17}$$

Once the grid points are selected, the coefficients of the weighted matrix can be acquired using equations (3-16) and (3-17).

According to (3-13) quadrature matrices representing second-order derivative operations on a function $f(x)$ can also be acquired using matrix multiplication:

$$D_{ij}^{(2)} = \sum_{k=1}^{N} D_{ik} D_{kj} \qquad (3\text{-}18)$$

3.3.2 Cubic spline differential quadrature

It is sometimes the case that equally spaced collocation points are desirable or actually required, or freedom to choose the spacing is necessary. CS provides a convenient interpolation approach for which the spacing of the collocation pints can be chosen arbitrarily within the domain of the space variable.

The Lagrangian approach to interpolate the continuous and differentiable function $f(x)$ requires a single polynomial for which the polynomial order is increased according to the required number of collocation points. In the CS interpolation individual CS functions are applied to each interval of the interpolation with special properties as follows.

Suppose the functional values $f(x_0), f(x_1), \ldots, f(x_n)$ are known at each grid point of interest over the interval $[a, b]$ with a $= x_0 < x_1 < \cdots < x_n = b$. The CS function $S(x)$ must satisfy the following conditions:

(i). $S(x)$ is continuous along with its first and second derivatives on $[a, b]$

(ii). $S(x_i) = f_i, \quad i = 0, 1, \ldots, n$

(iii). $S(x)$ is a cubic polynomial on each interval $[x_i, x_{i+1}], i = 0, 1, \ldots, n - 1$.

(iv). $\ddot{S}(x_0) = 0, \quad \ddot{S}(x_n) = 0$.

For convenience, use the same interval in the strip model, hence let:

$$h_{i+1} = h_i = x_{i+1} - x_i = \text{constant}$$

$$S_i(x) = S(x) \quad x \in [x_i, x_{i+1}]$$

$$s_i = \ddot{S}(x_i)$$

Note the difference between $S(x_i)$ and $S_i(x)$: $S(x_i)$ is the overall interpolatory spline function at the collocation point x_i whilst $S_i(x)$ is the sub-function in the interval $x \in [x_i, x_{i+1}]$.

From condition (iii), since $S(x)$ is a cubic polynomial, $\ddot{S}_i(x)$ is a linear polynomial that can be expressed in the form:

$$\ddot{S}_i(x) = s_i \frac{x_{i+1} - x}{h} + s_{i+1} \frac{x - x_i}{h} \quad i = 0,1,...,n-1 \tag{3-19}$$

To obtain the expression of $S_i(x)$, integrating (3-19) twice:

$$S_i(x) = \frac{s_i}{6h}(x_{i+1} - x)^3 + \frac{s_{i+1}}{6h}(x - x_i)^3 + c_1(x - x_i) + c_2(x_{i+1} - x) \tag{3-20}$$

The integration constants c_1 and c_2 are determined according to the property (ii): $S_i(x_i) = f_i$, $S_i(x_{i+1}) = f_{i+1}$. It follows that:

$$S_i(x_i) = f_i = \frac{s_i}{6}h^2 + c_2 h$$

$$S_i(x_{i+1}) = f_{i+1} = \frac{s_{i+1}}{6}h^2 + c_1 h$$

The constants c_1 and c_2 can thus be represented by two functions:

$$c_1 = \frac{f_{i+1}}{h} - \frac{s_{i+1}h}{6}, \quad c_2 = \frac{f_i}{h} - \frac{s_i h}{6}$$

Then Eq. (3-20) can be rewritten as:

$$S_i(x) = \frac{s_i}{6h}(x_{i+1} - x)^3 + \frac{s_{i+1}}{6h}(x - x_i)^3 + \left(\frac{f_{i+1}}{h} - \frac{s_{i+1}h}{6}\right)(x - x_i) + \left(\frac{f_i}{h} - \frac{s_i h}{6}\right)(x_{i+1} - x)$$

$$for \quad i = 0,1,...,n-1 \tag{3-21}$$

Differentiating (3-22) with respect to time, it follows that:

$$\dot{S}_i(x) = -\frac{s_i}{2h}(x_{i+1} - x)^2 + \frac{s_{i+1}}{2h}(x - x_i)^2 + \frac{f_{i+1} - f_i}{h} - \frac{h}{6}(s_{i+1} - s_i) \tag{3-22}$$

Using condition (i), $S(x)$ and its first derivative are continuous functions, i.e.:

$$\dot{S}_{i-1}(x_i) = \dot{S}_i(x_i) \tag{3-23}$$

Eqs. (3-22) and (3-23) can be combined and thus a new condition is given by:

$$s_{i+1} + 4s_i + s_{i-1} = \frac{6}{h}\left(\frac{f_{i+1} - 2f_i + f_{i-1}}{h}\right), \quad i = 1,...,n-1 \qquad (3\text{-}24)$$

The set of Eq. (3-24) is a system of $(n-1)$ linear equations with $(n+1)$ unknown variables $s_0, s_1, ..., s_n$. Two additional conditions should be added to solve this equation set. Normally, these two conditions are the boundary conditions of the PDEs. For some PDE problems, (e.g. furnace temperature problem), the second derivatives of the first and last points might be considered constant. i.e.

$$s_0 = 0, \quad s_n = 0 \qquad (3\text{-}25)$$

The method used to solve (3-24) and (3-25) is taken from (Shampine and Allen, 1973). This mathematical procedure is applied here to the discretization of the PDE system into a set of non-linear ODEs. It is important to note that the linearization operation is applied to the non-linear ODE system and this is described in Chapter 7.

By further defining:

$$d_i = \frac{6}{h^2}\left(f_{i+1} - 2f_i + f_{i-1}\right) \qquad (3\text{-}26)$$

From (3-24), it follows that:

$$s_{i+1} + 4s_i + s_{i-1} = d_i, \quad i = 1,...,n-1 \qquad (3\text{-}27)$$

Recalling that the spline is always of order 3, it then follows without loss of generality that the second derivative s_i has the form:

$$s_i = \rho_{i+1}s_{i+1} + \tau_{i+1} \qquad (3\text{-}28)$$

On substituting (3-28) into (3-27) and after some manipulation it follows that:

$$s_i = -\frac{1}{\rho_i + 4}s_{i+1} + \frac{d_i - \tau_i}{\rho_i + 4} = \frac{1}{\rho_i + 4}\left(d_i - \tau_i - s_{i+1}\right) \qquad (3\text{-}29)$$

Eq. (3-29) has the same form as Eq. (3-28), thus the following definitions can be derived:

$$\rho_{i+1} = -\frac{1}{\rho_i + 4}, \qquad \tau_{i+1} = \frac{d_i - \tau_i}{\rho_i + 4} \qquad\qquad (3\text{-}30)$$

Since $s_0 = 0$, $\rho_1 = 0$ and $\tau_1 = 0$. Note that the scalar multiplier ρ_{i+1} only depends on ρ_i, and hence as $\rho_1 = 0$, ρ_i can be calculated by recursive iteration. Furthermore, to compute the τ_i, the following procedure is considered:

Rewriting (3-26) as:

$$d_i = \frac{6}{h^2}\left(f_{i+1} - 2f_i + f_{i-1}\right) = \begin{bmatrix} 0_{1\times(i-2)} & \dfrac{6}{h^2} & -\dfrac{12}{h^2} & \dfrac{6}{h^2} & 0_{1\times(n-i-1)} \end{bmatrix} \begin{bmatrix} f_1 \\ \vdots \\ f_n \end{bmatrix} = \Theta_i F \quad (3\text{-}31)$$

where, $\Theta_i = \begin{bmatrix} 0_{1\times(i-2)} & \dfrac{6}{h^2} & -\dfrac{12}{h^2} & \dfrac{6}{h^2} & 0_{1\times(n-i-1)} \end{bmatrix} \in \mathbb{R}^{1\times n}$, $F = \begin{bmatrix} f_1 \\ \vdots \\ f_n \end{bmatrix} \in \mathbb{R}^n$.

By further iteration, τ_i is calculated as:

$$\tau_1 = 0 = [0]F = \Pi_1 F$$

$$\tau_2 = \frac{1}{\rho_1 + 4}d_1 = \frac{1}{\rho_1 + 4}\Theta_1 F = \Pi_2 F$$

$$\tau_3 = \frac{1}{\rho_2 + 4}d_2 - \frac{1}{\rho_2 + 4}\tau_2 = \frac{1}{\rho_2 + 4}\left(\Theta_2 - \frac{1}{\rho_1 + 4}\Theta_1\right)F = \Pi_3 F$$

$$\vdots$$

$$\tau_i = \frac{1}{\rho_{i-1} + 4}d_{i-1} - \frac{1}{\rho_{i-1} + 4}\tau_{i-1} = \frac{1}{\rho_{i-1} + 4}\left\{\Theta_{i-1} - \sum_{j=1}^{i-2}\left[(-1)^{(i-j+1)}\left(\prod_{k=j}^{i-2}\frac{1}{\rho_k + 4}\right)\Theta_j\right]\right\}F = \Pi_i F$$

Hence, τ_i is given by:

$$\tau_i = \Pi_i F$$

where,

$$\Pi_i = \frac{1}{\rho_{i-1}+4}\left\{\Theta_{i-1} - \sum_{j=1}^{i-2}\left[(-1)^{(i-j)}\left(\prod_{k=j}^{i-2}\frac{1}{\rho_k+4}\right)\Theta_j\right]\right\} \in \mathbb{R}^{1\times n}$$

Since $s_n = 0 = [0]F$, by combining all the τ_i and using a similar iteration to the one given in (3-29) can be rewritten as:

$$s_i = D_{s,i}F$$

where $D_{s,i} \in \mathbb{R}^{1\times n}$ has a similar form to the Π_i and can be calculated simply by iteration. In this case, the second derivative can be written as:

$$s = \begin{bmatrix} s_1 \\ \vdots \\ s_n \end{bmatrix} = \begin{bmatrix} D_{s,1} \\ \vdots \\ D_{s,n} \end{bmatrix} F = D_s F \tag{3-32}$$

Substituting (3-32) into (3-22), the first derivatives of the spline functions have the form:

$$\begin{bmatrix} \dot{S}_1 \\ \vdots \\ \dot{S}_n \end{bmatrix} = D_f F \tag{3-33}$$

3.4 System model identification

Recalling the furnace wall model (3-9)-(3-12) and the strip model (3-2), with the differential quadrature methods described in Section 3.3, these PDEs could be transferred into ODEs. However, the methods should be chosen carefully for different models.

Furnace wall model

For the furnace wall model, only two spacial grids are of interest, (a) the inner wall surface temperature T_w and (b) the outer surface temperature $T_B(x,d,t)$ both of which are assumed measured. The grid points inside the furnace wall do not need to be equally spaced in the grid and hence, LIP is suitable for generating the required differential quadrature. Another advantage of applying this method in the furnace wall model is that the boundary conditions could be easily handled.

Using differential quadrature, the heating equations (3-9)-(3-12) are transferred to:

$$\rho_w c_w \frac{d}{dt} T_{B,i}(t) = \lambda_w D_w^{(2)} T_{B,i}(t) \tag{3-34}$$

$$T_{B,i,1}(t) = T_{w,i}(x,t) \tag{3-35}$$

$$\lambda_w \frac{\partial T_{B,i}}{\partial r}\bigg|_{r=0} = -\Phi_i \tag{3-36}$$

$$\lambda_w \frac{\partial T_{B,i}}{\partial r}\bigg|_{r=d} = H\big(T_\infty - T_{B,i,N_w}(t)\big) \tag{3-37}$$

where, $T_{B,i}(t) \in \mathbb{R}^{N_w}$ is the temperature vector for grids in the furnace wall of the i-th furnace model. Since there is no need to specify a different number of grids for the furnace model in different zones, N_w is a constant and it represents the number of grids for the furnace model of all subsystems. Moreover, the interval between the nodes in the furnace wall satisfies Chebyshev-Gauss-Lobatto distribution:

$$x_{B,i} = \frac{1}{2} d \left(1 - \cos \frac{(i-1)\pi}{N_w - 1} \right) \qquad for \; i = 1, 2, \ldots, N_w \tag{3-38}$$

where d is the thickness of the furnace wall. It should be noted that (3-35), (3-36) and (3-37) are the boundary conditions for the furnace model. They are handled later in this Section.

Strip model

The reason for choosing CS as the interpolation method for this strip model is that in the strip the same interval distance between two nodes is adopted. In the CS method, splines between two nearby points are designed separately. The distribution of the collocation points does not much affect the accuracy of the methods. This is different from LIP method introduced in Section 3.3.1. Moreover, with the CS method, the larger the interval between two grids, the smaller the interactions they have. This is much closer to the real situation than LIP method which might have very large interactions between two long-distance points.

According to Section 3.3.2, the PDE (3-2) of the strip model can be transferred to:

$$\frac{d}{dt}T_s(t) = \left(\frac{\lambda_s}{\rho_s C_s} D_s - vD_f \right) T_s(t) + \frac{1}{wh\rho_s C_s} q_s(t) \qquad (3\text{-}39)$$

where $T_s(t) \in \mathbb{R}^n$ is the temperature of the strip, $q_s(t) \in \mathbb{R}^n$ is the vector of heating source. It should be noted that (3-39) is the model for the overall system. The interval between the nodes is constant.

Interactions between furnace wall model and strip Model

The interconnection between the furnace wall model and strip model is radiative heat transfer from the furnace wall to the strip. It is represented by Φ_i of Eq. (3-36) and $q_s(t)$ of Eq. (3-39). They can be expressed by:

$$\Phi_i = \frac{(P_i - q_i)}{2p} \qquad (3\text{-}8)$$

$$q_i(t) \approx 2w\varepsilon_s \sigma(T_{w,i}^4(t) - T_{s,i}^4(t)) \qquad (3\text{-}40)$$

where, P is the input heating power for the system. $T_{w,i}(t)$ is the inner furnace wall temperature which $T_{w,i}(t) = T_{B,i,1}(t)$.

It can be seen that the strip model and the furnace wall model have different coordinates. The distribution of nodes in the strip is in the direction x, and the distribution of nodes in the wall model is in the direction z. Thus, in the x direction, the strip model is seperated into N zones with n_i nodes ($i = 1,2,...,N$) and each zone has its own heater (furnace heating model). The interactions between the subsystems (heating zones) are heat conductive and the movement of the strip is given by the decomposition of the matrix $\left(\frac{\lambda}{\rho c} D_s - vD_f \right)$.

To briefly illustrate the procedure of modelling, using a single zone, the state vector for each subsystem is chosen as:

$$x = \begin{bmatrix} T_s \\ T_B \end{bmatrix}$$

Since LIP is used in the furnace wall model, Eqs. (3-36) and (3-37) could be rewritten as:

$$\lambda_w \left. \frac{\partial T_B}{\partial r} \right|_{r=0} = \sum_{k=1}^{N_w} D_{w,1k} T_{B,k} = -\frac{1}{\lambda_w} \Phi \tag{3-41}$$

$$\lambda_w \left. \frac{\partial T_B}{\partial r} \right|_{r=d} = \sum_{k=1}^{N_w} D_{w,N_w k} T_{B,k} = \frac{1}{\lambda_w} H\left(T_\infty - T_{B,N_w}(t)\right) \tag{3-42}$$

And the state equation (3-34) for the furnace model can be written as:

$$\dot{T}_B(t) = \frac{\lambda_w}{\rho_w c_w} D_w \left[D_w T_B(t) \right] \tag{3-43}$$

The idea of dealing with the boundary conditions is to substitute the right side of (3-41) and (3-42) into (3-43). Thus, first defining two matrices:

$$Q_1 = \begin{bmatrix} 1 & 0 & & & 0 \\ 0 & 0 & \cdots & & \\ \vdots & & \ddots & & \vdots \\ & & & 0 & 0 \\ 0 & & \cdots & & \\ & & & 0 & 1 \end{bmatrix} \in \mathbb{R}^{N_w \times N_w}, \quad Q_2 = \begin{bmatrix} 0 & & \cdots & & 0 \\ \vdots & & \ddots & & \vdots \\ & & & 0 & 0 \\ 0 & & \cdots & & \\ & & & 0 & 1 \end{bmatrix} \in \mathbb{R}^{N_w \times N_w}$$

and rewriting (3-43) as:

$$\dot{T}_B(t) = \frac{1}{\rho_w c_w} D_w \left[\lambda_w D_w T_B(t) - \lambda_w Q_1 D_w T_B(t) + \begin{bmatrix} -\Phi \\ 0 \\ \vdots \\ 0 \end{bmatrix} + \begin{bmatrix} 0 \\ \vdots \\ 0 \\ HT_\infty \end{bmatrix} - H Q_2 T_B \right]$$

By further defining:

$$A_w = \frac{1}{\rho_w c_w} \left(D_w \lambda_w D_w - D_w \lambda_w Q_1 D_w - D_w H Q_2 \right)$$

$$B_w = \frac{1}{\rho_w c_w} D_w \begin{bmatrix} -1 \\ 0 \\ \vdots \\ 0 \end{bmatrix}, \quad E_w = \frac{1}{\rho_w c_w} D_w \begin{bmatrix} 0 \\ \vdots \\ 0 \\ HT_\infty \end{bmatrix}$$

it gives the furnace wall model in the state space:

$$\dot{T}_B(t) = A_w T_B + B_w \Phi + E_w \tag{3-44}$$

48

On the other hand, the strip model can be simplified as:

$$\dot{T}_s(t) = A_s T_s(t) + B_s q_s(t) \tag{3-45}$$

where $A_s = \frac{\lambda}{\rho c} D_s - v D_f$ and $B_s = \frac{1}{wh}$.

Since the input is the power P in (3-8), Combining Eqs. (3-44) and (3-45), gives the system equation is in the form of:

$$\dot{x} = \begin{bmatrix} \dot{T}_s \\ \dot{T}_B \end{bmatrix} = \begin{bmatrix} A_s & 0 \\ 0 & A_w \end{bmatrix} \begin{bmatrix} T_s \\ T_B \end{bmatrix} + \begin{bmatrix} 0 \\ \frac{1}{2p} B_w \end{bmatrix} u + \begin{bmatrix} B_s \\ -\frac{1}{2p} B_w \end{bmatrix} q + \begin{bmatrix} 0 \\ E_w \end{bmatrix} \tag{3-46}$$

Now that the partial differential equations are transferred to ordinary differential equations and combined with the boundary conditions in the model equations, the problem remaining is the nonlinear part q.

The nonlinear part q in Eq. (3-46) is not easy to be handled. As it can be seen, in the strip model, every strip grid point (with its temperature represented by $T_{s,i}$) receives the heating energy from the furnace wall. In this case, the term q of Eq. (3-46) should be a vector. However, in the furnace wall model, q is a scalar which can only be used in the boundary condition (3-11). Ideally, q is a vector, $q = [q_1 \quad \cdots \quad q_n]^T \in \mathbb{R}^n \ with \ q_1 = \cdots = q_n = q_w$, where $q_i, i = 1, ..., n$ are the heat sources received in the strip model and q_w is the scalar hidden in the boundary condition (3-11) of the furnace wall model. As a matter of fact, temperatures at different points of the strip are different. Thus, it is necessary to make q a vector with different elements $q_i, i = 1, ..., n$. There are 3 different ways to deal with the scale q_w in the wall model.

1) Using

$$q_w = 2w\varepsilon_s \sigma(T_w^4 - T_{s,m}^4)$$

Where, $T_{s,m}$ is the temperature of the middle point of the strip grids.

2) Using

$$q_w = 2w\varepsilon_s \sigma(T_w^4 - T_{s,aver}^4)$$

Where, $T_{s,aver}$ is the average temperature of the strip grids. $T_{s,aver} = \frac{1}{n}\sum_{i=1}^{n} T_{s,i}$.

3)   Using

$$q_w = 2w\varepsilon_s\sigma\frac{1}{n}\sum_{i=1}^{n}(T_w^4 - T_{s,i}^4)$$

to get the average energy to the wall.

Intuitively, the 1st method seems the easiest approach to use. However, it can be seen that with the 3rd method, the only information needed is the states (temperatures of grid points) of the strip model instead of grid selection or more computation. Thus, the heating model can be written as:

$$q = 2w\varepsilon_s\sigma\begin{bmatrix} I_n \\ \frac{1}{n} & \cdots & \frac{1}{n} \end{bmatrix}\begin{bmatrix} T_{B,1}^4 - T_{s,1}^4 \\ \vdots \\ T_{B,1}^4 - T_{s,n}^4 \end{bmatrix} \tag{3-47}$$

Substitute (3-47) into the system equations (3-46), the new system equation is given by:

$$\dot{x} = \overline{A}x + Bu + \overline{B}\begin{bmatrix} T_{B,1}^4 - T_{s,1}^4 \\ \vdots \\ T_{B,1}^4 - T_{s,n}^4 \end{bmatrix} + \overline{E} \tag{3-48}$$

where, $x \in \mathbb{R}^{n+N_w}$, $u \in \mathbb{R}$,

$$\overline{A} = \begin{bmatrix} A_s & 0 \\ 0 & A_w \end{bmatrix}, \quad B = \begin{bmatrix} 0 \\ \frac{1}{2p}B_w \end{bmatrix}, \quad \overline{B} = 2w\varepsilon_s\sigma\begin{bmatrix} B_s I_n & 0 \\ 0 & -\frac{1}{2p}B_w \end{bmatrix}\begin{bmatrix} I_n \\ \frac{1}{n} & \cdots & \frac{1}{n} \end{bmatrix}$$

$$\overline{E} = \begin{bmatrix} 0 \\ E_w \end{bmatrix}$$

Assume that the temperature of the input point of the furnace is fixed. Thus, if the initial conditions for the strip are known. The strip model can be further simplified and the order of it can be reduced to $(n-1)$. Since the first state of the strip model is fixed, i.e. the derivative of this temperature is zero, the system matrix A of the strip model can be modified by:

$$A_s = \begin{bmatrix} 0 & 0 \\ A_{2:n,1} & A_s^* \end{bmatrix}$$

Thus, the new system matrix becomes:

$$A = \begin{bmatrix} A_s^* & 0 \\ 0 & A_w \end{bmatrix} \in \mathbb{R}^{(n+N_W-1)\times n+N_W-1}$$

Meanwhile, the influence from the input point should not be ignored. the constant E of the system should be modified as:

$$E = \begin{bmatrix} E_s \\ E_w \end{bmatrix} \in \mathbb{R}^{n+N_W-1}$$

where, $E_s = A_{2:n,1}T_{s,1}$.

Note that if the nonlinearities of the properties of steel are neglected, the system contains three linear parts Ax, Bu, E, and one nonlinear part $\overline{B}\begin{bmatrix} T_{B,1}^4 - T_{s,1}^4 \\ \vdots \\ T_{B,1}^4 - T_{s,n}^4 \end{bmatrix}$.

The above description illustrates the modelling procedure of the furnace system with only one heater. To model a large scale furnace system which has several heaters, assuming that the large scale furnace system has N zones, the states of the overall system should be in the form of:

$$x = \begin{Bmatrix} T_{1,s} \\ T_{1,B} \\ \vdots \\ T_{N,s} \\ T_{N,B} \end{Bmatrix} \in \mathbb{R}^{(N*N_W)+(n_1-1+n_2+\cdots+n_N)} \tag{3-49}$$

where n_i $(i = 1,2,\dots,N)$ is the number of points in the i-th strip model. $T_{i,s} = \begin{bmatrix} T_{i,s,1}^T & \cdots & T_{i,s,n_i}^T \end{bmatrix}^T$ is the strip temperatures of the i-th strip model. $T_{i,B} = \begin{bmatrix} T_{i,B,1}^T & \cdots & T_{i,B,N_W}^T \end{bmatrix}^T$ is the furnace wall temperatures of the i-th furnace heating model. It should be noted that the first zone contains the input point, thus the dimension of it is

$n_1 - 1$. Normally, choose $n_1 = n_2 = \cdots = n_N = n$. The system matrix of the overall system is in the form of (3-48) but with different structure:

$$A = \begin{bmatrix} A_{s,11} & 0 & A_{s,12} & 0 & & & A_{s,1N} & 0 \\ 0 & A_w & 0 & 0 & \cdots & & 0 & 0 \\ A_{s,21} & 0 & & \ddots & & & & \vdots \\ 0 & 0 & & & & & & \\ \vdots & & & & \ddots & A_{s,(N-1)N} & 0 \\ & & & & & 0 & 0 \\ A_{s,1N} & 0 & & A_{s,N(N-1)} & 0 & A_{s,NN} & 0 \\ 0 & 0 & \cdots & 0 & 0 & 0 & A_w \end{bmatrix} \tag{3-50}$$

where, $A \in \mathbb{R}^{(N*(N_w+n)-1)\times(N*(N_w+n)-1)}$. $A_{s,ij} \in \mathbb{R}^{n_i \times n_j}$ is the submatrices of the overall strip model matrix A_s in (3-45). Thus, the interactions between different zones are the heat conduction and the temperature movement in the strip model (3-45). Other matrices should be modified in order to satisfy the state structure (3-49).

3.5   Model Validation

According to the description in Section 3.4, the state space model of the large scale furnace model has been established. To verify the modelling procedure, this section first describes the simulation of the furnace model with MATLAB using the parameters given in (McGuinness and Taylor, 2004). Following this, the model properties can be validated by using the zero input response, i.e. by inspecting the furnace system's natural "open-loop" thermal behaviour without temperature regulation. Then the steady state solution of the PDE system can be calculated by giving some of the reference temperatures of the strip model. A PID control for the nonlinear system model is then designed to provide good tracking performance of the same references. By comparing the results of the steady state solution of the PDEs and the nonlinear model with control, the modelling accuracy can be discussed.

3.5.1   System simulation

To simulate the furnace system, with the number of zones chosen to be $N = 3$, the number of grid points for each strip model is $n_i = 6, i = 2, \dots, N$ ($n_1 = 5$ according to Section 3.4) and the number of grid points for the furnace wall model is $N_w = 4$. These parameters are appropriate for the furnace model system derived in Chapter 3.

According to Chapter 3, the aggregate model system structure has the following form:

$$\dot{x} = Ax + Bu + f + E \tag{3-51}$$

where:

$$
A = \begin{bmatrix}
A_{s,11} & 0 & A_{s,12} & 0 & A_{s,13} & 0 \\
0 & A_w & 0 & 0 & 0 & 0 \\
A_{s,21} & 0 & A_{s,22} & 0 & A_{s,23} & 0 \\
0 & 0 & 0 & A_w & 0 & 0 \\
A_{s,1N} & 0 & A_{s,32} & 0 & A_{s,33} & 0 \\
0 & 0 & 0 & 0 & 0 & A_w
\end{bmatrix}, B = \begin{bmatrix}
0 & 0 & 0 \\
\dfrac{1}{2p}B_w & 0 & 0 \\
0 & 0 & 0 \\
0 & \dfrac{1}{2p}B_w & 0 \\
0 & 0 & 0 \\
0 & 0 & \dfrac{1}{2p}B_w
\end{bmatrix}
$$

$$
f = \begin{bmatrix} f_1 \\ f_2 \\ f_3 \end{bmatrix},\ f_i = \overline{B}_i q_i = 2w\varepsilon_s\sigma \begin{bmatrix} B_s I_{n_i} & 0 \\ 0 & -\dfrac{1}{2p}B_w \end{bmatrix} \begin{bmatrix} I_{n_i} \\ \dfrac{1}{n_i} & \cdots & \dfrac{1}{n_i} \end{bmatrix} \begin{bmatrix} T_{i,B,1}^4 - T_{i,s,1}^4 \\ \vdots \\ T_{i,B,1}^4 - T_{i,s,n_i}^4 \end{bmatrix}
$$

$$
E = \begin{bmatrix} E_{1,s}^T & E_w^T & \cdots & E_{N,s}^T & E_w^T \end{bmatrix}
$$

In the first strip model, by considering the input point temperature as constant, the dimension of the first strip model is reduced to 5. Thus, the dimension of the overall system is 29. The system parameters are taking from (McGuinness and Taylor, 2004) and they are shown in Table 3-3.

Table 3-3. Furnace System parameters

Strip			
Density ρ_s	7854 [Kg·m^{-3}]	Thickness h	0.5 [mm]
Width w	0.94 [m]	Velocity v	2 [m·s^{-1}]
Emissivity ε_s	0.2	Interval of the strip model h_s	1.5 [m]
Furnace			
Width+height p	3.4 [m]	Density ρ_w	2000 [Kg·m^{-3}]
Heat capacity c_w	900 [J·(Kg·K)$^{-1}$]	Thermal conductivity λ_w	0.28 [W·(m·K)$^{-1}$]
Thickness of the wall d	0.4 [m]	Heat convection coefficient H	14.7 [W·(m^2·K)$^{-1}$]

3.5.2 Zero input response

The furnace system is assumed to stable. Without any input, when the temperature of the inner wall is higher than the strip, the temperatures of the strip grids are (1). increased because the inner wall temperature is higher, then (2). decreased slowly because there is no power supply and the temperature of the wall is decreasing. Meanwhile the temperature of the furnace wall should keep decreasing. Bearing these in mind, by setting the initial conditions of the system: $T_s = 300K$, $T_{i,B} = [600\ 525\ 375\ 300]^T(K)$, the strip temperature response with zero input can be given:
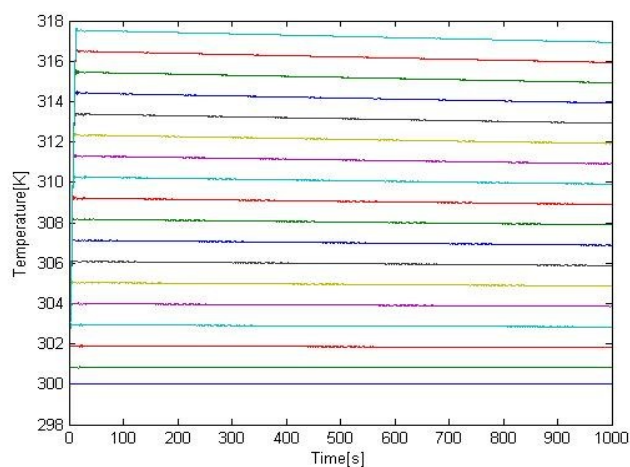
Figure 3-6. Strip temperature response without power input

Figure 3-6 shows the system response of the strip temperature with zero input. As discussed above, the strip temperature first increases as the inner wall heats up. As the strip moves further, the further the grid is away from the input, the more heat it gets from the wall.

From Figure 3-7, the temperature of the furnace wall is decreasing during the operating since there is no power supply. Thus, the inner wall is cooled by the radiation from the strip and the outer wall is heated by the heat conduction from the inner wall. But one can expect that after a long time, the inner and outer wall temperatures (as well as the strip temperature) will converge to the ambient temperature which is $297K$ in this model.
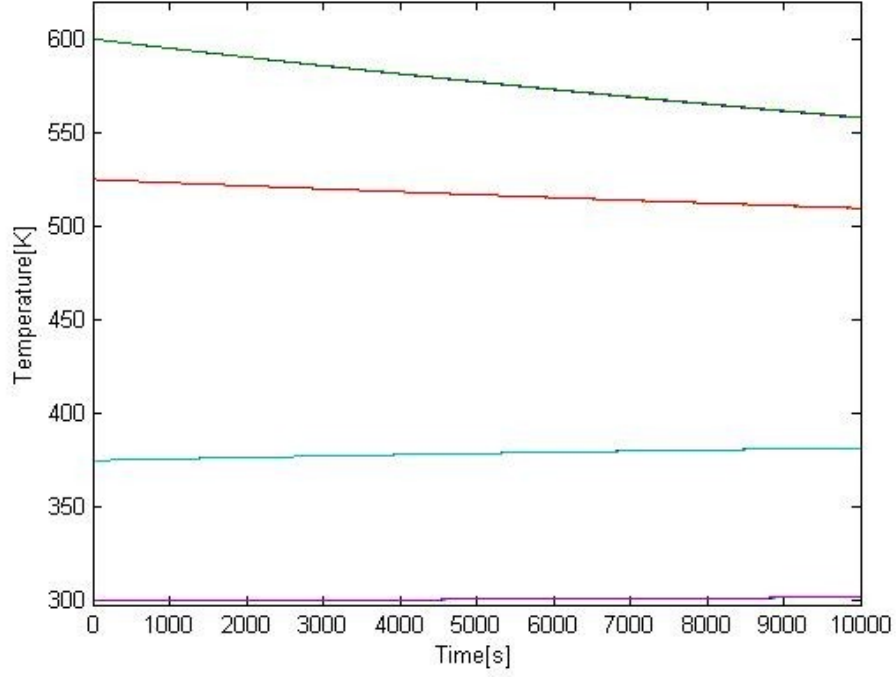
Figure 3-7. Furnace wall temperature response without power input

Since only the inner and outer wall temperatures are concerned, the order of the furnace wall temperature model can be reduced by a model reduction function using MATLAB. The final furnace model for each zone can be represented by a simple second order system.

3.5.3 Steady state solution

Consider all the temperatures are invariant with time, i.e. $\frac{\partial T}{\partial t} = 0$, it follows that the steady state solution from the system Eqs. (3-2), (3-6), (3-9)-(3-12) are (McGuinness and Taylor, 2004):

$$\frac{\partial T}{\partial t} = \frac{\lambda_s}{\rho_s C_s} \frac{\partial^2 T}{\partial x^2} - v\frac{\partial T}{\partial x} + \frac{q}{wh\rho_s C_s} \qquad \rightarrow \qquad \frac{dT_s}{dx} = -\frac{q}{vwh\rho_s C_s} \qquad (3\text{-}52)$$

$$\rho_w c_w \frac{\partial T_B}{\partial t} = \lambda_w \frac{\partial^2 T_B}{\partial r^2} \quad 0 < r < d \qquad \rightarrow \qquad \frac{d^2 T_B}{dr^2} = 0 \qquad (3\text{-}53)$$

$$T_B(x,0,t) = T_w(x,t) \qquad \rightarrow \qquad T_B(x,0) = T_w(x) \qquad (3\text{-}54)$$

55

$$\lambda_w \frac{\partial T_B}{\partial r}\bigg|_{r=d} = H\big(T_\infty - T_B(x,d,t)\big) \qquad \rightarrow \qquad \lambda_w \frac{\partial T_B}{\partial r}\bigg|_{r=d} = H\big(T_\infty - T_B(x,d)\big) \quad (3\text{-}55)$$

The reason that the term $\dfrac{\lambda_s}{\rho_s C_s}\dfrac{\partial^2 T}{\partial x^2}$ is neglected in (3-52) is that the influence from this second order partial differential term is so small in steady states. Hence, the steady state furnace wall temperature can be calculated as follows:

$$\frac{dT_B}{dr} = \frac{\big(T_w - T_B(x,d)\big)}{d} = \frac{\big(T_w - T_B\big)}{r} = \frac{H}{\gamma_w}\big(T_\infty - T_B(x,d)\big)$$

Then the wall temperature is given by:

$$T_B = T_w - \frac{(T_w - T_\infty)}{d + \lambda_w/H}\, r \tag{3-56}$$

where $\dfrac{(T_w - T_\infty)}{d + \lambda_w/H}$ is the gradient of the wall temperature. Now consider (3-11) which is:

$$\lambda_w \frac{\partial T_B}{\partial r}\bigg|_{r=0} = -\Phi \tag{3-11}$$

it gives:

$$\Phi = \frac{\lambda_w}{d + \lambda_w/H}(T_w - T_\infty)$$

Considering (3-6) and (3-8):

$$q \approx 2w\varepsilon_s \sigma(T_w^4 - T^4) \tag{3-6}$$

$$\Phi = \frac{(P - q)}{2p} \tag{3-8}$$

the steady-state power input of the i-th zone is given as:

$$P_i = \frac{2p\lambda_w}{d + \lambda_w/H}(T_{i,w} - T_\infty) + 2w\varepsilon_s \sigma(T_{i,w}^4 - T_{i,s}^4) \tag{3-57}$$

Compared with what is assumed in Section 3.4, by substituting the temperature of the input point of the i-th zone into (3-6), an approximation solution of (3-52) is obtained:

$$T_{i,s}(x) = T_{i,s,0} + \frac{2\varepsilon_s \sigma}{vh\rho_s C_s}(T_{i,w}^4 - T_{i,s,0}^4)(x - x_{i,0}) \tag{3-58}$$

The wall temperature can be written as:

$$T_{i,w} = \sqrt[4]{\left(T_{i+1,s,0} - T_{i,s,0}\right)\frac{vh\rho_s C_s}{2\varepsilon_s \sigma(n_i - 1)h} + T_{i,s,0}^4} \tag{3-59}$$

3.5.4 PID furnace control

PID control is the most common control structure used for process systems and it is easy to implement in the furnace system. It is known that the integral controller can remove the static output error. Thus, it can be applied as a good inner-loop controller or a controller for linearization. The model outputs are the end points of the zones. Thus, considering the furnace model (3-51), the controller (power input) can be designed in the form of:

$$u_i = P_i = K_{i,P}(T_{i,ref} - T_{i,s,end}) + K_{i,I}\int_0^t (T_{i,ref} - T_{i,s,end})d\mu + K_{i,D}(T_{i,ref} - T_{i,s,end})' \quad i = 1,2,3$$

$$\tag{3-60}$$

Setting the desired temperatures of each zones as $T_{ref} = [480°C \quad 580°C \quad 680°C]^T$. Table 3-4 shows the choices of the gains of the controller.

Table 3-4. PID controller gains

$K_{1,P}$	10	$K_{2,P}$	5	$K_{3,P}$	5
$K_{1,I}$	0.0001	$K_{2,I}$	0.0003	$K_{3,I}$	0.0003
$K_{1,D}$	1	$K_{2,D}$	1	$K_{3,D}$	1
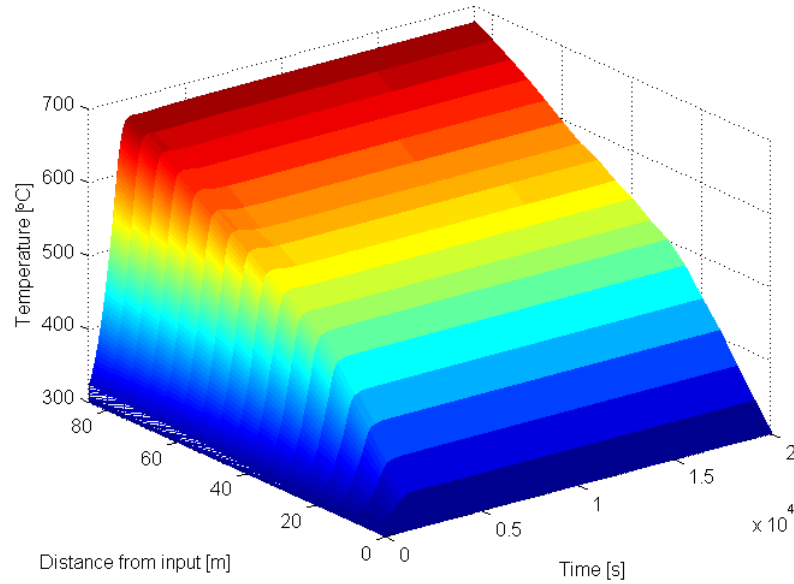
Figure 3-8. Strip temperature with PID control

Figure 3-8 shows the strip temperatures of the furnace model.

Assume that the input temperature is 300°C and the zone exit strip exit temperatures for heating zones are $T_{ref} = [480°C \quad 580°C \quad 680°C]^T$. The grid interval of the strip model is chosen as $h = 2.8m$. Using (3-58) and (3-59), the temperatures of the inner wall surface and the strips in the steady state can be calculated. Then by driving the nonlinear model to the required reference temperatures, the temperature of each state can be obtained. Comparing the temperatures calculated from the PDEs ((3-58) and (3-59)) and from simulation, the errors are shown in Table 3-5.

Table 3-5. Modeling error at steady states with interval $h = 2.8m$

Position	Heating Zone 1 Temperature [°C]			Heating Zone 2 Temperature [°C]			Heating Zone 3 Temperature [°C]		
	PDE	Model	Error	PDE	Model	Error	PDE	Model	Error
Strip-1	300	300	0	497.8	504.8	-7	599.3	598	1.3
Strip-2	337.9	335.8	2.1	515.6	519.7	-4.1	618.6	616.9	1.7
Strip-3	375.8	372.7	3.1	533.4	537.3	-3.9	637.8	634.7	3.1
Strip-4	413.7	411.7	2	551.2	551.4	-0.2	657.1	651	6.1
Strip-5	451.5	449.5	2	568.9	568.6	0.3	676.4	670.3	6.1

58

Strip-6	480	480	0	580	580	0	680	680	0
Inner wall	977.2	972.9	4.3	851.5	842.7	8.8	900.1	894.1	6

It can be seen that the modelling error is acceptable. Because of the strong numerical accuracy of the Bellman differential quadrature interpolation methods used to derive the approximate ODE (state space) model system it can be deduced that if one reduces the gird interval, the error is also reduced. The results are given by setting $h = 2.8m$, $h = 2m$ and $h = 1m$.

Table 3-6. Error between PDE and Simulation under different interval distance

Position	Heating Zone 1 Temperature [°C]			Heating Zone 2 Temperature [°C]			Heating Zone 3 Temperature [°C]		
	Error $h = 2.8m$	Error $h = 2m$	Error $h = 1m$	Error $h = 2.8m$	Error $h = 2m$	Error $h = 1m$	Error $h = 2.8m$	Error $h = 2m$	Error $h = 1m$
Strip-1	0.0	0.0	0.0	-7	-6.2	-5.5	1.3	1.1	0.1
Strip-2	2.1	0.3	-0.8	-4.1	-4	-3.5	1.7	1.6	-0.3
Strip-3	3.1	3	2.2	-3.9	-3.5	-3.0	3.1	2.6	-0.4
Strip-4	2.0	1.0	0.6	-0.2	-1.4	-2.0	6.1	4.4	0.0
Strip-5	2.0	1.5	1	0.3	-0.8	-1.4	6.1	5.9	0.7
Strip-6	0.0	0.0	0.0	0.0	0.0	0.0	0	0	0
Inner wall	4.3	3.4	2.5	8.8	6.4	2.2	6	1.6	1
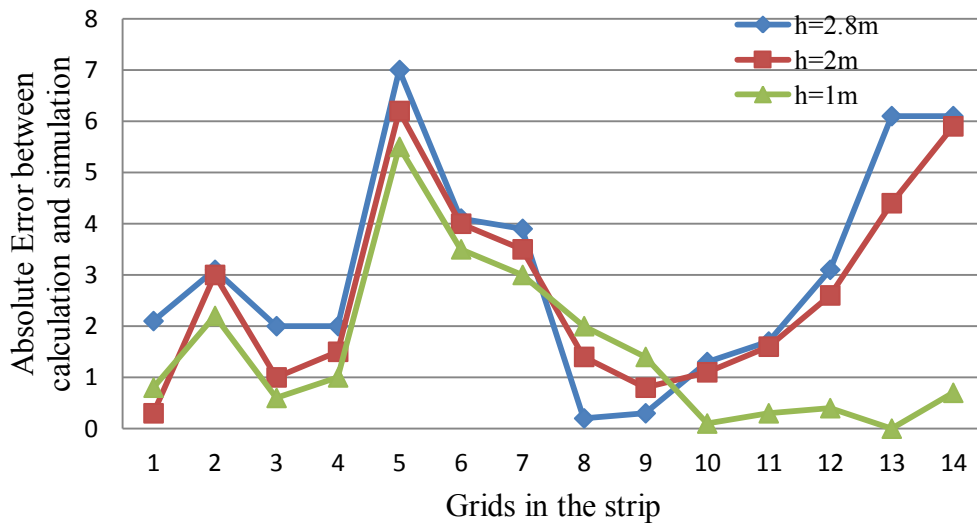
Figure 3-9. Absolute value of the errors between the PDE solution and the system simulation results under different grid spacing

From Table 3-6 and Figure 3-9, it can be seen that reducing the strip model grid spacing improves the approximation accuracy of the PDE solution, as expected.

However, there are still residual errors even with a small enough choice of the interval. These errors are introduced as a consequence of some restrictions used in the computation of the cubic spline coefficients and hence in the coefficients of the differential quadrature matrices. Further errors may be due to the approximation of heat source q used in Section 3.4). This may be the subject of further work on this example.

3.6   Conclusion

In this Chapter, the concept of a steel annealing furnace, the model equations and the identification of this furnace model are presented.

Generally speaking, the aim of this furnace is to heat the steel up to a certain temperature at the end this heating zone. Several heating elements are set in the wall to control the temperature of the furnace wall. And heat up the steel by heat radiation. Several PDEs are introduced to represent the heating procedure.

However, in order to apply modern control in this furnace, PDEs model should be approximated by ODEs first. In this Chapter, two interpolation methods for differential

quadrature are proposed to convert the PDE problem to ODE problem. The infinite nodes of PDEs (distributed parameter system) which can be approximated by finite nodes ODEs make this furnace system large scaled. Some simplification and assumptions are further made to identify the nonlinear model. In this case, the state space model for this large scale furnace model is proposed.

In the final part of this Chapter, the nonlinear model is simulated and validated qualitatively compared using zero-input response. Then the steady state solutions to the partial differential equations (i.e. considering heat balance) are compared with the results of the nonlinear ODE system using PID control to discuss the modelling accuracy. This model is controlled and further discussed in Chapter 7.

Chapter 4
Sliding Mode Control for Large Scale Systems

4.1   Introduction

The so called "*sliding mode control*" (SMC) emphasizes the important role of "sliding" when designing "*variable structure control*" (VSC). VSC can be considered as a set of control laws driven by a decision rule. The control law for the system switches from one control law to another if the system satisfies a certain decision rule. Normally using the switching function, the decision rule considers some properties or behaviour of the current system and helped change the control law instantly. The system with this specific structure is so called "*variable structure system*" (VSS) (Hung, 1993). It is easy to find that the benefit of using VSC is to combine useful properties of each of the composite structures of the system and the system may contain new properties (Edwards and Spurgeon, 1998).

Variable structure control with a sliding mode was first described in Russian in the early 1930s. It did not appear outside of Russia until the mid-1970s. In the late 70s, (Itkis, 1976) and (Utkin, 1977) introduced this methodology in English. During 1970-1980, VSC did not attract much attention since (1) people prefer other simpler linear control design techniques and (2) the robustness properties of VSC were not yet fully recognized. In 1980s, engineers started to pay attention to this very robust method with the development of general VSC design methods (Hung, 1993). By 1993, general application areas included: robotic control, motor control, flexible structure control and power systems (Hung, 1993). Today, research and development continue to apply VSC to a wide variety of engineering systems. During the 1990s and the beginning of 21 century, VSC theory for linear systems became a rather complete subject. Some other types of VSC, such as integral sliding mode, high-order sliding mode etc., also received considerable attention. Current applications also include: Three-Axis Optical Pickup (Chao and Shen, 2009), Permanent-Magnet Synchronous Motor Control System (Feng and Jiang, 2009), Satellite system (Lee and Kim, 2010), Spacecraft system (Pukdeboon, Zinober and Thein, 2010) etc.

Section 4.3 contains material that has been presented as "An adaptive sliding mode approach to decentralized control of uncertain systems." *UKACC International Conference on Control*, Cardiff, UK, 70-75, 3-5 Sep.

The concept of "*sliding mode*" can be traced back to 1934, Nikolski first used the term "*sliding mode motion*" in Russian (Hung, 1993). During the development of VSC theory in 90s and 00s, the term "*sliding mode control*" was quickly accepted by most of researchers because of its visual description to VSC. One of the most attractive aspects of sliding mode theory is the discontinuous property of the control action whose primary function of each of the feedback channels is to switch between two distinctively different system structures such that a new type of system motion, called "*sliding motion*", exists in a manifold. This special system characteristic is claimed to result in superb system performance which includes insensitivity to parameter variations, and complete rejection of the matched disturbances (Young, Utkin and Özgüner, 1999). This robust property makes the sliding mode attractive from a design perspective.

Within two decades, SMC has become more like a branch of VSC. It has a well-defined design procedure containing two components. The first is the sliding surface design in which some desired design specifications should be considered. Some other robust control idea can be integrated into this design framework. The second component is concerned with the selection of a control law which drives the system to the sliding surface. Survey and tutorial papers have been written on sliding mode in (Utkin, 1977; Hung, 1993; DeCarlo, Żak and Matthews, 1988; Edwards and Spurgeon, 1998; Young, Utkin and Özgüner, 1999; Castaños and Fridman, 2006; etc.)

Although there are many publications discussing sliding mode principles, the literatures contain much less information to describe sliding mode methods applicable to LSSs. As a consequence of the insensitivity property after reaching the sliding surface, sliding mode theory is mostly combined with disjoint and decentralized control. One can note this through the publications in 20 years (Feng and Jiang, 1995; Hsu, 1997; Chou and Cheng, 2003; Shyu, Liu and Hsu, 2005; Yau and Yan, 2009; Zhu and Li, 2010). However, most of these literatures are based on the assumption that the interactions satisfy an appropriate so-called *matching condition*. (Yan, Spurgeon and Edwards, 2003, 2004, 2009) propose several papers discussing decentralized sliding mode using the Edwards & Spurgeon canonical form. However, in this approach the rather complicated use of state transformations and calculation procedure are the main problem.

In this Chapter, the developments of sliding mode theory are proposed, including regular form, reachability and control law design. Systematic sliding mode control

methods for LSS are introduced as well. Combined with the properties of LSS, typical decentralized state feedback and output based SMC methods are represented. A numerical example is also used to illustrate the methodology.

4.2 Review of typical sliding mode control theory

The sliding mode has proved to be a very powerful tool for disturbance rejection. In this Section, the sliding mode control is introduced and the properties of it are outlined based on the two steps of (1) sliding surface design and (2) control law design. The regular form of decomposition is first discussed.

4.2.1 Regular form and matched perturbations rejection

Consider the following linear time invariant (LTI) system:

$$\dot{x}(t) = Ax(t) + Bu(t) \tag{4-1}$$

$x \in \mathbb{R}^n$ is the system state vector, $u \in \mathbb{R}^m$ are the system inputs, and the system matrices are $A \in \mathbb{R}^{n \times n}$, $B \in \mathbb{R}^{n \times m}$. The input matrix B is assumed to have full rank and the pair (A, B) is stabilizable.

Normally, the classical sliding surface function is design as:

$$\sigma(t) = Sx(t) \tag{4-2}$$

Each sliding surface function describes a linear surface $\sigma(x) = 0$, the so called "*sliding surface*". Other terms like "*sliding (switching) manifold*", "*switching hyperplane*" are also used. The classical sliding mode surface designing algorithms are mostly based on the so called "regular form". The main idea of this form is to decompose the system states equations into two part: (1) the states controlled by inputs directly and (2) the states controlled by inputs indirectly. i.e.

$$\dot{z}_1(t) = A_{11}z_1(t) + A_{12}z_2(t) \tag{4-3}$$

$$\dot{z}_2(t) = A_{21}z_1(t) + A_{22}z_2(t) + B_2u(t) \tag{4-4}$$

where,

$$z = Tx, \quad T = \begin{bmatrix} B^{\perp T} \\ M \end{bmatrix}, \quad TB = \begin{bmatrix} 0 \\ B_2 \end{bmatrix}, \quad TAT^{-1} = \begin{bmatrix} A_{11} & A_{12} \\ A_{21} & A_{22} \end{bmatrix} \tag{4-5}$$

The main advantage of this regular form is that disturbances or faults are decomposed into matched (appear in Eq. (4-4)) and unmatched parts (appear in Eq. (4-3)). The matched part can be compensated by the control input $B_2 u$. Hence the problem remaining is how to attenuate the unmatched part of disturbances appearing in Eq. (4-3).

To make the transformation matrix T invertible, the matrix M should be designed properly such that T is full rank. The simplest way to design M is by setting $M = B^T$. The following describes *two* other approaches that appear in the literature.

The method used in (Zinober, 1990; Edwards and Spurgeon, 1998) is QR decomposition, the advantage of using this decomposition is that there is no longer a need to consider the design of a matrix M. After using QR Orthogonal-triangular decomposition, the matrix B is decomposed into an upper-triangular matrix and the transformation matrix T is an orthogonal matrix, i.e. full rank and invertible. By modifying this transformation matrix, the structure (4-5) can be shown to be satisfied.

In the new coordinates, the sliding surface function becomes:

$$\sigma(t) = S_1 z_1(t) + S_2 z_2(t) \tag{4-6}$$

where $ST^{-1} = [S_1 \quad S_2]$.

Once the sliding surface is reached, i.e. $\sigma = S_1 z_1 + S_2 z_2 = 0$, it follows that:

$$z_2(t) = -S_2^{-1} S_1 z_1(t) = -N z_1(t) \tag{4-7}$$

Moreover,

$$\dot{z}_1(t) = (A_{11} - A_{12}N)z_1(t) \tag{4-8}$$

So the problem becomes designing the matrix N so that $(A_{11} - A_{12}N)$ is stable. Note that this problem is similar to the state feedback control problem: that of designing the matrix K to make $(A + BK)$ stable. For this problem, several methods are available based on this regular form, e.g. pole-placement, H∞, Linear-quadratic regulator (LQR),

etc. Three sliding surface function design approaches are described in (Edwards and Spurgeon, 1998):

(i). Robust pole-placement (Ryan and Corless, 1984)

(ii). Quadratic minimization (Utkin and Young, 1978), and

(iii). Eigenstructure assignment (Zinober, 1990)

Another approach to design the regular form is to pay more attention to specific design of the matrix M. (Choi, 1997) describes an approach that defines $S = B^T X^{-1}$, together with the sliding surface function $\sigma(t) = B^T X^{-1} x(t)$. The new coordinate vector after transformation then follows as:

$$\dot{z}_1(t) = A_{11} z_1(t) + A_{12} \sigma(t) \tag{4-9}$$

$$\dot{\sigma}(t) = A_{21} z_1(t) + A_{22} \sigma(t) + B_2 u(t) \tag{4-10}$$

In this case, the associated vector $z_2 = \sigma$ and a LMI based sliding surface function designing approach can be applied.

As mentioned above, if there are some disturbances or uncertainties in the system, the sliding mode can compensate all the perturbations appear in (4-4). The reason is that if the system has the following form:

$$\dot{x}(t) = Ax(t) + Bu(t) + Df(x,t) \tag{4-11}$$

where $D = BR$, then the so called matching condition is satisfied. By using the sliding function $\sigma(t) = Sx(t)$, if the sliding surface is reached and can be maintained, then $\sigma(t) = 0$ and $\dot{\sigma}(t) = 0$. The control law is then equivalent to:

$$u_{eq}(t) = -(SB)^{-1} SAx(t) - (SB)^{-1} SDf(x,t) \tag{4-12}$$

One should note that SB must be non-singular is required. Then the ideal sliding mode is given by substituting (4-12) into the system (4-11):

$$\dot{x}(t) = (I - B(SB)^{-1} S)Ax(t) + (I - B(SB)^{-1} S)Df(x,t) \tag{4-13}$$

As for this case, $D = BR$, it follows that:

$$(I - B(SB)^{-1}S)D = (I - B(SB)^{-1}S)BR = 0 \tag{4-14}$$

Thus, by substituting (4-14) into (4-13), there is no perturbation, i.e. the controller rejected all the matched perturbations after the sliding surface is reached and maintained. This is the main property of sliding mode that the ideal sliding motion is totally insensitive to the uncertain function if $(D) \subset (B)$ (Ryan and Corless, 1984; Dorling and Zinober, 1986; DeCarlo, 1998; Zinober, 1990; Edwards and Spurgeon, 1998).

Now the essential design challenges as discussed in the following sections are to determine: (1). the system response before reaching the sliding surface (reachability); (2). The control law design; and (3) the nature of the unmatched perturbations.

4.2.2 Reachability Problem and Reaching Phase

Once the sliding surface function $\sigma(x, t)$ is designed, a control law should be carefully designed in order to drive the states trajectory to the sliding surface. This problem is the so called *"Reachability problem"*. From the description in Section 4.2.1, the system is stable and insensitive to the matched perturbations only if the sliding surface is reached, i.e. $\sigma(x, t) = 0$.

In both (Hung, 1993) and (Edwards and Spurgeon, 1998), the solution to the single input single output reachability problem is explained clearly. If a system can reach the sliding surface, the sliding surface should be "*at least locally attractive*". This can be expressed mathematically as:

$$\lim_{\sigma \to 0^+} \dot{\sigma} < 0 \quad \text{and} \quad \lim_{\sigma \to 0^-} \dot{\sigma} > 0 \tag{4-15}$$

for some domain $\Omega \in \mathbb{R}^n$.

For the MIMO system, Lyapunov theory is used. Consider the Lyapunov function for the sliding surface:

$$V = \sigma^T \sigma = \|\sigma\|^2 \tag{4-16}$$

The derivative of the Lyapunov function should satisfy the condition:

$$\dot{V} = 2\sigma^T \dot{\sigma} < 0 \tag{4-17}$$

Also, similar to the SISO case described by (Edwards and Spurgeon, 1998), define "η-reachability condition" in the MIMO case as:

$$\dot{V} \leq -\eta\|\sigma\| \qquad (4\text{-}18)$$

where, η is a positive design scalar.

To prove this, rewrite (4-18) as:

$$\frac{dV}{dt} \leq -\eta\sqrt{V}$$

Using chain rule, the inequality can be simplified to

$$\frac{1}{\sqrt{V}}\sqrt{V}\frac{d2\sqrt{V}}{dt} \leq -\eta$$

i.e.

$$\frac{d2\sqrt{V}}{dt} \leq -\eta$$

And by integrating both sides from 0 to t_s, it follows that:

$$2\sqrt{V(t_s)} - 2\sqrt{V(0)} \leq -\eta t_s$$

Thus, the time taken to reach $V(t_s) = 0$, represented by t_s, satisfies

$$t_s \leq 2\sqrt{V(0)}/\eta$$

Since $\sqrt{V(t_s)}$ is proportional to the sliding function $\sigma(t)$, we can conclude that the sliding surface can be reached in finite time.

Other reaching conditions can be found in (Hung, 1993), to specify the characteristics of the system during the reaching phase and guarantee the finite time reachability. In multi-state systems, one can design the sliding surface function using the so called "Reaching law approach". This is done by designing the derivative of the sliding surface function as:

a) $\dot{\sigma} = -Qsign(\sigma)$

b) $\dot{\sigma} = -Qsign(\sigma) - G\sigma$

c) $\dot{\sigma}_i = -q_i|\sigma|^\alpha sign(\sigma_i)$ $0 < \alpha < 1$

The system can then reach the sliding surface with specified characteristic time behaviour.

The reachability problem is one of the main disadvantages of the sliding mode. During the *reaching phase* the system does not have the benefit and properties of a sliding mode controller, e.g. during the reaching phase the system is sensitive to the matched perturbations. Hence, it is of interest to drive the system to the sliding surface as soon as possible.

(Utkin and Shi, 1996) proposed a new sliding surface function design approach named *"integral sliding mode control"*, in which the sliding surface is reached from initial time and maintained there during the entire system operation by adding an integral part in the sliding surface function. This method brings up a new concept that the sliding mode can be a control component to reject the matched perturbations and some other controllers can be designed to handle the unmatched perturbations. With this concept, numerous methods can be combined with sliding mode to achieve better performance. This Integral sliding mode control is discussed and extended to the output based approach in Chapter 5.

4.2.3 Control law design

As another important part of sliding mode theory, control law is mainly designed with two parts:

$$u = u_l + u_n \tag{4-19}$$

where u_l is the linear component and u_n is the discontinuous switching control component and usually has the form (Ryan and Corless, 1984):

$$u_n = \begin{cases} -\rho(x,u,t)\dfrac{\sigma}{\|\sigma\|} & \sigma \neq 0 \\ 0 & \sigma = 0 \end{cases} \tag{4-20}$$

These two components u_l and u_n form the sliding mode control law. In different sliding mode control strategies, these two parts have different functions. For example, if the sliding surface function is designed as $\sigma(t) = B^T X^{-1} x(t)$ as is described in Section 4.2.1, both of these two components are used to drive the system states to the sliding surface and the choice of sliding surface function helps stabilize the system after the sliding surface is reached. However, in the integral sliding mode, the switching component u_n is used to reject the matched perturbations whilst the linear part u_l is used to stabilize the system while the system is running in the sliding surface. This Section considers the former case in which both linear and nonlinear control laws are used to drive the system to the sliding surface with the sliding surface gain matrix used to stabilize the system after reaching the sliding surface.

Consider the system in the form of:

$$\dot{x}(t) = Ax(t) + B(u(x,t) + f(t)) \tag{4-21}$$

where $f(t)$ represents a generalized perturbation function. The sliding surface function is designed as:

$$\sigma(t) = Sx(t) \tag{4-22}$$

If both linear and discontinuous parts of the SMC are designed to ensure that the sliding surface is reached, with the Lyapunov function $V = \frac{1}{2}\sigma^T \sigma$, The time derivative of this Lyapunov function is given by:

$$\dot{V} = \sigma^T \dot{\sigma}$$
$$= \sigma^T (SAx + SB(u + f)) \tag{4-23}$$

If the linear controller is chosen as $u_l = -(SB)^{-1}SAx$ and the discontinuous controller is designed according to (4-20), (4-23) can be further rewritten as:

$$\dot{V} = \sigma^T (SAx + SB(u + f))$$
$$\leq \|\sigma\|(f - \rho(x,u,t)) \tag{4-24}$$

It is clear to see from (4-24) that if the sliding surface can be reached, the gain $\rho(x,u,t)$ has a lower bound given by:

$$\rho(x,u,t) \geq \|f\| + \eta \tag{4-25}$$

$\|f\|$ is the upper bound of the disturbance and η is a user selected positive scalar. Following this, the derivative of the Lyapunov function (4-25) satisfies $\dot{V} < -\eta\|\sigma\|$, which means the sliding surface is reached in finite time. Furthermore, the reaching time is given by integrating $\dot{V} < -\eta\|\sigma\|$ as proposed in Section 4.2.2. Moreover, by dividing the system into the matched part and unmatched part, Eq. (4-3) and (4-4) follow.

It can be assumed that in this coordinate system, the sliding gain matrix $S = [S_1 \quad S_2]$. Thus, with proper choice of S, the unmatched part of the system is stable, i.e. $\dot{z}_1 = (A_{11} - A_{12}S_2^{-1}S)z_1$ is stable and furthermore:

$$\lambda_{\max}\left((A_{11} - A_{12}S_2^{-1}S)\right) < 0 \tag{4-26}$$

Adaptive mechanism

Using the inequality (4-25), the derivative of the Lyapunov function (4-24) is negative. However, the bound of the unknown disturbance should be known. This is a very restrictive condition because the bounds of the disturbances or faults are not usually known in practice. Some research has been done to discuss this restriction. For example, (Yu and Kaynak, 2009) summarizes several soft-computing methods including neural networks and fuzzy systems which when combined with the sliding mode obtain partial information about the disturbance bounds. A typical use of this adaptive mechanism can be to estimate the bound of the disturbance automatically. With the adaptive mechanism, the controller gain is given by:

$$\rho(t) = \tau\hat{\beta}(t) + \delta \tag{4-27}$$

where, $\tau > 0$ is chosen by the designer to specify the reaching speed. Assume that there exist an unknown bound for the matched disturbance or uncertainties such that $\|f\| < \beta < \infty$, where β is a virtual constant which exists but is unknown Then $\hat{\beta}$ in Eq. (4-27) is assumed to be an estimate of β. The adaptive law can be proposed as:

$$\dot{\hat{\beta}}(t) = \kappa\|\sigma(t)\| \tag{4-28}$$

where $\kappa \geq 1$. With this adaptive gain, the sliding motion is insensitive to the matched disturbances/uncertainties.

The stability of this kind of adaptive mechanism can be proved using another Lyapunov function $V = \frac{1}{2}\left[\sigma^T \sigma + (\beta - \hat{\beta})^2\right]$, with time-derivative:

$$\begin{aligned}\dot{V} &\leq \|\sigma\|(f - \rho) - (\beta - \hat{\beta})\kappa\|\sigma\| \\ &\leq \left(\beta - \kappa\beta + (\kappa - \tau)\hat{\beta} - \delta\right)\|\sigma\|\end{aligned} \tag{4-29}$$

There is some design freedom to choose κ and η. The easiest way is to define $\kappa = \tau = 1$, for which $\dot{V} \leq -\delta\|\sigma\|$, satisfying (4-29). Thus, the sliding surface is reached in finite time as described above, and the known upper bound constraint is relaxed. Alternatively, κ and τ can be chosen as $\kappa > 1$ and $\tau > \kappa$ to decrease the reaching time.

The newest research on adaptive mechanism for first order sliding mode is given by (Plestan *et al*, 2010) in which the adaptive law is designed as:

$$\dot{\hat{\beta}}(t) = \begin{cases} \kappa\|\sigma(t)\|sign(\|\sigma(t)\| - \psi) & \text{if } \beta > \mu \\ \mu & \text{if } \beta \leq \mu \end{cases} \tag{4-30}$$

where ψ, μ are small positive constants facilitating the decrease of $\rho(t)$ when the sliding surface function remains within a small region $\|\sigma(t)\| < \psi$. In fact, if $\psi = 0$, $sign(\|\sigma(t)\| - \psi) \equiv 1$, (4-30) is equivalent to (4-28). The advantage of this algorithm (compared with the first algorithm (4-27) and (4-28)) is that it prevents $\rho(t)$ from increasing. An increase in the values of $\rho(t)$ may lead to serious "chattering" or rapid discontinuous motion around the switching boundary itself. In (Plestan *et al*, 2010), ψ can also be designed using adaptive mechanism. The parameter μ is used to keep the gain positive.

Boundary Layer

When the system is running exactly in the sliding surface, it is called the "*ideal sliding mode*", i.e. for which $\sigma = 0$ is satisfied exactly. However, in most situations, it is difficult to keep the system running in the sliding surface. Also the discontinuous control law might cause chattering motion due to high gain operation, since the gain $\rho(t)$ has a lower bound but no upper bound. To increase the reaching speed and to

compensate the unknown upper bound perturbation, the gain should be designed to be as large as possible. However, the larger the gain is, the larger the chattering comes. For many industrial applications, high frequency switching control is unacceptable due to hardware physical constraints (bandwidth of actuators and conversion ranges, etc) and indeed high frequency motion cannot actually result from band-limited systems. Hence, for real applications, the concept of the *boundary layer* is used to overcome this problem. This idea has been discussed for many years and systematically described in (Edwards and Spurgeon, 1998), although these authors do not provide a proof for the stability of a SMC system that incorporates a boundary layer. In the following a proof is proposed to give conditions under which the SMC system with boundary layer remains stable.

1. Non smooth boundary layer.

Instead of using the control law (4-20), the sliding mode control with boundary layer can be written as:

$$u_n = -\rho(x,u,t)sat\left(\frac{\sigma}{\Delta}\right), \quad sat(\chi) = \begin{cases} \chi & if\ |\chi| \leq 1 \\ sign(\chi) & if\ |\chi| > 1 \end{cases} \tag{4-31}$$

The boundary layer is $\|\sigma\| \leq \Delta$.
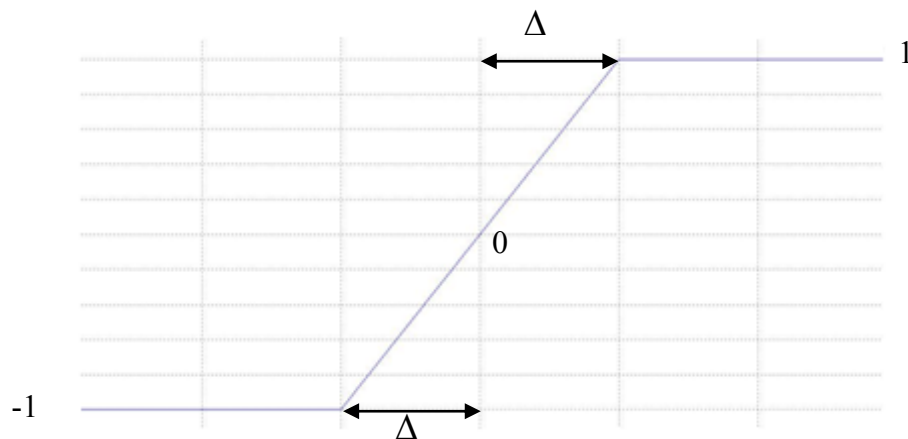
Figure 4-1. A nonlinear discontinuous boundary layer function

Figure 4-1 shows the boundary layer function (4-31) with a single-input case. To prove the reachability of the sliding region and the stability of the system, we have to consider two situations: 1) when the system running outside of the boundary layer, we have to

prove the system is running toward the sliding region and 2) when the system running inside of the boundary layer, the system is stable.

When the system operates outside the boundary layer, $\|\sigma\| > \Delta$, then by using the Lyapunov function:

$$V = \frac{1}{2}\sigma^T\sigma$$

$\dot{V} \leq -\delta\|\sigma\|$ with the gain (4-25). It follows that $\|\sigma\| > \Delta > 0$, $\|\sigma\|$ is strictly decreasing until the system reaches the boundary layer and stability is satisfied subject to this bound.

When the system trajectories are inside the boundary layer, $\|\sigma\| < \Delta$. Moreover, the control law becomes $u = -(SB)^{-1}SAx - \rho\frac{\sigma}{\Delta}$. With the constraint (4-25), it follows without loss of generality, that ρ can be chosen as $\rho = \|f\| + \pi$.

Then considering the separation of the system into matched and unmatched parts, it follows that:

$$\dot{z}_1(t) = A_{11}z_1(t) + A_{12}z_2(t)$$

$$\dot{z}_2(t) = A_{21}z_1(t) + A_{22}z_2(t) + B_2(u(t) + f(t))$$

The sliding surface matrix S in this new coordination is $S = [S_1 \quad S_2]$ with $\det(S_2) \neq 0$ (Edwards and Spurgeon, 1998). When the system is in the boundary layer, the motion is given by $S_1z_1 + S_2z_2 = \sigma$, and hence:

$$\dot{z}_1 = (A_{11} - A_{12}S_2^{-1}S_1)z_1 + A_{12}\sigma \tag{4-32}$$

Consider the Lyapunov function for system (4-32) $V_z = 0.5z_1^Tz_1$, with time derivative:

$$\begin{aligned}
\dot{V}_z &= z_1^T\left[(A_{11} - A_{12}S_2^{-1}S_1)z_1 + A_{12}\sigma\right] \\
&\leq \|z_1\|\left[\lambda_{\max}\left((A_{11} - A_{12}S_2^{-1}S_1)\right)\|z_1\| + \|A_{12}\|\|\sigma\|\right] \\
&\leq \|z_1\|\left[\lambda_{\max}\left((A_{11} - A_{12}S_2^{-1}S_1)\right)\|z_1\| + \Delta\|A_{12}\|\right]
\end{aligned} \tag{4-33}$$

It can now be proved by contradiction that the system state $\|z_1\|$ is bounded. If $\|z_1\|$ is unbounded, i.e. $\|z_1\| \to \infty$ as $t \to \infty$, from (4-26), we have that $\dot{V}_z < 0$ which implies

that $\|z_1\|$ is bounded and leads to a contradiction. Thus, $\|z_1\|$ is bounded and the original system is bounded. Moreover, by defining $\mu_0 = \lambda_{\max}\left(\left(A_{11} - A_{12}S_2^{-1}S_1\right)\right)$, $\mu_1 = \sqrt{\lambda_{\max}(A_{12})}$, the inequality (4-33) can be rewritten as:

$$
\begin{aligned}
\dot{V}_z &= z_1^T \left[(A_{11} - A_{12}S_2^{-1}S_1)z_1 + A_{12}\sigma\right] \\
&\leq \mu_0 \|z_1\|^2 + \Delta\mu_1 \|z_1\| \\
&\leq \|z_1\|(\mu_0 \|z_1\| + \Delta\mu_1)
\end{aligned}
$$

which implies that the sliding motion is ultimately bounded with respect to:

$$
\Omega = \left\{z_1 : \|z_1\| < -\Delta\mu_1/\mu_0 + \varepsilon\right\} \tag{4-34}
$$

where $\varepsilon > 0$ is an arbitrarily small positive scalar.

From (4-34) we know that the size of the set is dependent on the choices of sliding surface gain matrix S and the boundary layer Δ. i.e. smaller (more negative) largest eigenvalue of $(A_{11} - A_{12}S_2^{-1}S_1)$ and Δ lead to better regulation performance. Hence, if the boundary layer must be used, the eigenvalues of the matrix $(A_{11} - A_{12}S_2^{-1}S_1)$ should be chosen to be as small (more negative) as possible.

2.   Smooth boundary layer.

Another choice of boundary layer is make the control law a continuous function (Burton and Zinober, 1986):

$$
u_n = -\rho(x, u, t)\frac{\sigma}{\|\sigma\| + \Delta} \tag{4-35}
$$

where Δ is a small group and the size of boundary layer is approximately 20Δ. The advantage of this method is that the function (4-35) is smooth, i.e. there is no discontinuity in the derivative function of (4-35).

Chapter 6 describes the use of the boundary layer formulation of (4-35) as the most suitable choice for the fault estimation problem.

Figure 4-2 shows the smooth boundary layer function with a single input case. It is easy to verify this method using a proof similar to Non-smooth boundary layer. A formal

examination of the properties of this boundary layer function is given in (Burton and Zinober, 1986).
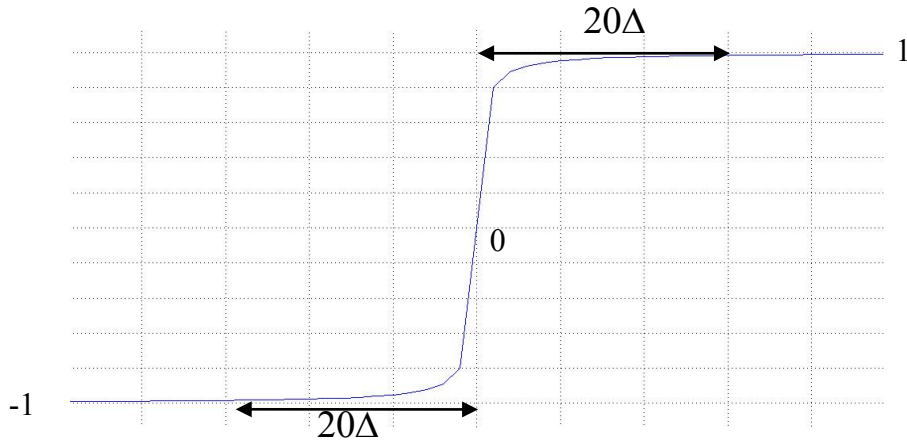
Figure 4-2. A smooth boundary layer function

When considering combining adaptive mechanism and boundary layer theory together, the control law can be designed as:

$$u_n = -\rho(x,u,t)\frac{\sigma}{\|\sigma\|+\Delta}, \ \rho(t) = \hat{\beta}(t) + \delta,$$

$$\dot{\hat{\beta}}(t) = \begin{cases} \kappa\|\sigma(t)\|sign(\|\sigma(t)\|-\psi) & if \ \beta > \mu \\ \mu & if \ \beta \le \mu \end{cases} \tag{4-36}$$

where, Δ, δ, κ, and ψ are chosen by the designer. Δ is the parameter chosen to determine the accuracy of the SMC; δ, κ determine the duration of the reaching phase and ψ restrict the magnitude of the gain. In fact, all of these parameters affect the chattering of the SMC. It should be noted that the original SMC control law $u = -\rho sign(\sigma(t))$ can be replaced by (4-36) with the stability of the system remaining unaffected.

4.3   Decentralized SMC design using LMI approach

This Section describes a novel design method for decentralized typical sliding mode control for LSSs. In this thesis, the method used for sliding surface function design is LMI approach based on the Lyapunov function. The regular form of this method for a single system was first proposed by (Choi, 1997) using the original system matrix.

Compared with the algorithm proposed by (Edwards & Spurgeon, 1998), there is no need to transfer the system into regular form in the sliding function design process. Moreover, even in the proof of this theorem, the regular form only requires one transformation. As discussed in Section 4.2.3, the control law in this method uses both linear and switching control parts to drive the system to the sliding surface. The stability of the unmatched part of the system is left to the choice of sliding surface function.

4.3.1 Control law design with LMI approach

Consider a large scale system contains N small subsystems after decomposition, the i-th ($i = 1, \ldots, N$) subsystem has the form:

$$\dot{x}_i(t) = A_i x_i(t) + B_i(u_i(t) + f_i(x_i, u_i, t)) + h_i(x, t) \tag{4-37}$$

where, $x_i \in \mathbb{R}^{n_i}$, $u_i \in \mathbb{R}^{n_i}$ are the states and inputs of this subsystem respectively. $A_i \in \mathbb{R}^{n_i \times n_i}$, $B_i \in \mathbb{R}^{n_i \times m_i}$ are the system matrices.

It must be assumed that the following are valid:

A1: the pairs (A_i, B_i) are controllable.

A2: the local states x_i are available.

A3: there are some known bounded positive constants for the matched disturbance:

$$\|f_i(x, u, t)\| \leq f_{i1}\|x\| + f_{i2}\|u\| + f_{i3}$$

All the matched uncertainties (multiplicative faults) and external disturbance (additive faults) should satisfy this constraint. They should be bounded but the constraint of known constants can be relaxed by the adaptive mechanism.

A4: the interactions of the subsystem satisfy the quadratic constraint (Šiljak and Stipanović, 2000):

$$h_i^T(x, t) h_i(x, t) \leq \alpha_i^2 x^T H_i^T H_i x$$

Where α_i is a bounding constant.

The overall system can be written in a compact form as:

77

$$\dot{x}(t) = Ax(t) + B(u(t) + f(x,u,t)) + h(x,t) \qquad (4\text{-}38)$$

where, $A = diag(A_1, \dots, A_N)$, $B = diag(B_1, \dots, B_N)$, $f(t) = [f_1^T(t), \dots, f_N^T(t)]^T$ and $h(x,t) = [h_1^T(x,t), \dots, h_N^T(x,t)]^T$. With the assumption A4, the interconnections $h(x,t)$ are bounded as follows:

$$h^T(x,t)h(x,t) \le x^T \left(\sum_{i=1}^N \alpha_i^2 H_i^T H_i \right) x = x^T H^T H x \qquad (4\text{-}39)$$

This quadratic constraint is first proposed by (Šiljak and Stipanović, 2000) in the framework of single system and extended to decentralized system using the S-procedure Lemma. This constraint could not only represent the nonlinear interactions but also the uncertainty of the i-th subsystem. The stabilization problem for LSS is also solved in Šiljak and Stipanović's work. They proposed that the decentralized control could be obtained by solving the following LMI:

Minimize $\sum_{i=1}^N \gamma_i$, subject to $P > 0$,

$$\begin{bmatrix} AP + PA^T + BL + L^T B^T & PH_1^T & \cdots & PH_N^T & I \\ H_1 P & -\gamma_1 I & \cdots & 0 & 0 \\ \vdots & \vdots & \ddots & \vdots & \vdots \\ H_N P & 0 & \cdots & -\gamma_N I & 0 \\ I & 0 & \cdots & 0 & -I \end{bmatrix} < 0 \qquad (4\text{-}40)$$

The decentralized control gain matrix K is obtained by $K = LP^{-1}$.

The objective of the method proposed in this Section is to design a totally decentralized SMC that robustly regulates the state of the overall system without any information exchange between the controllers. Different to (Šiljak and Stipanović, 2000), within control design procedure in this section, the overall (decentralised) system must be robust to all the uncertainties and insensitive to matched perturbations.

Theorem 4.1. For the overall system (4-38), the system is asymptotically stable after the sliding surface is reached if there exists an s.p.d. matrix $X = diag(X_1, \dots, X_N)$ satisfying the following LMIs:

Minimize $\sum_{i=1}^{N} \gamma_i$, subject to $X > 0$,

$$\begin{bmatrix} \tilde{B}^T(AX + XA^T + I)\tilde{B} & \tilde{B}^T XH_1^T & \cdots & \tilde{B}^T XH_N^T \\ H_1 X\tilde{B} & -\gamma_1 I & \cdots & 0 \\ \vdots & \vdots & \ddots & \vdots \\ H_N X\tilde{B} & 0 & \cdots & -\gamma_N I \end{bmatrix} < 0 \qquad (4\text{-}41)$$

where $\tilde{B}$ is the orthogonal complement of the input matrix B.

with sliding surface function in the form:

$$\sigma(x,t) = \left[\sigma_1^T(x_1,t),...,\sigma_N^T(x_N,t)\right]^T = B^T X^{-1} x(t) = diag(S_1,...,S_N)x(t)$$

Proof:

Define a transformation matrix for the overall system

$$T = \begin{bmatrix} \tilde{B}^T \\ S \end{bmatrix} = \begin{bmatrix} \tilde{B}^T \\ B^T X^{-1} \end{bmatrix} \qquad (4\text{-}42)$$

And the associated vector z:

$$z(t) = \begin{bmatrix} z_1(t) \\ z_2(t) \end{bmatrix} = Tx(t) \qquad (4\text{-}43)$$

where, $z_1 \in \mathbb{R}^{n-m}$, $z_2 \in \mathbb{R}^m$. It can be seen that the sliding surface function is $\sigma(x,t) = z_2(t)$.

As $\tilde{B}^T$ is the orthogonal matrix of B, i.e. $\tilde{B}^T B = 0$, $\tilde{B}^T \tilde{B} = I$, the transformation matrix T is non-singular and has full rank, i.e. it is invertible. The inverse matrix can easily be determined from:

$$T^{-1} = \left[X\tilde{B}(\tilde{B}^T X\tilde{B})^{-1} \quad B(SB)^{-1} \right] \qquad (4\text{-}44)$$

Then the associated vector is given as:

$$\dot{z}(t) = TAT^{-1}z(t) + TB(u(x,t) + f(x,u,t)) + Th(x,t) \qquad (4\text{-}45)$$

By substituting the transformation (4-42) and (4-44) into (4-45), the associated vector equation can be rewritten as:

$$\begin{bmatrix} \dot{z}_1 \\ \dot{z}_2 \end{bmatrix} = \begin{bmatrix} \widetilde{B}^T A X \widetilde{B} (\widetilde{B}^T X \widetilde{B})^{-1} & \widetilde{B}^T A B (SB)^{-1} \\ SAX\widetilde{B}(\widetilde{B}^T X \widetilde{B})^{-1} & SAB(SB)^{-1} \end{bmatrix} \begin{bmatrix} z_1 \\ z_2 \end{bmatrix} + \begin{bmatrix} 0 \\ SB \end{bmatrix} (f(x,u,t)+u(x,t)) + \begin{bmatrix} \widetilde{B}^T \\ S \end{bmatrix} h(x,t)$$

$$(4-46)$$

When the system is running in the sliding surface $\sigma = z_2 = 0$ and $\dot{\sigma} = \dot{z}_2 = 0$, it becomes

$$\dot{z}_1(t) = \widetilde{B}^T A X \widetilde{B}(\widetilde{B}^T X \widetilde{B})^{-1} z_1(t) + \widetilde{B}^T h(x,t) \qquad (4\text{-}47)$$

This is the so called "*sliding motion*". It contains the unmatched part of the systems. Since the sliding surface is reached, i.e. matched part of the system has been compensated, the remaining problem is to find the sliding surface matrix X which can stabilize the sliding motion (4-47).

Because X is an s.p.d matrix, $\widetilde{B}^T X \widetilde{B}$ is also an s.p.d. matrix. In this case, a suitable Lyapunov function can be defined as:

$$V(z_1) = z_1^T Y z_1 \qquad (4\text{-}48)$$

The time derivative of $V(z_1)$ is:

$$\begin{aligned} \dot{V}(z_1) = z_1^T & \left[(\widetilde{B}^T A X \widetilde{B}(\widetilde{B}^T X \widetilde{B})^{-1})^T Y + Y\widetilde{B}^T A X \widetilde{B}(\widetilde{B}^T X \widetilde{B})^{-1} \right] z_1 \\ & + z_1^T Y \widetilde{B}^T h + h^T \widetilde{B} Y z_1 \end{aligned} \qquad (4\text{-}49)$$

With a useful lemma that is introduced in (Boyd *et al*, 1993):

$$X^T Y + Y^T X \le X^T X + Y^T Y \qquad (4\text{-}50)$$

From (4-50) it follows that:

$$z_1^T Y \widetilde{B}^T h + h^T \widetilde{B} Y z_1 \le z_1^T Y \widetilde{B}^T \widetilde{B} Y z_1 + h^T h \qquad (4\text{-}51)$$

And from assumption A4:

$$h^T(x,t)h(x,t) \le x^T H^T H x = z^T (T^{-1})^T H^T H T^{-1} z$$
$$\le z_1^T (\widetilde{B}^T X \widetilde{B})^{-T} \widetilde{B}^T X H^T H X \widetilde{B} (\widetilde{B}^T X \widetilde{B})^{-1} z_1 \tag{4-52}$$

Substitute (4-51) and (4-52) into (4-49), then gives:

$$\dot{V}(z_1) \le z_1^T \begin{bmatrix} (\widetilde{B}^T A X \widetilde{B}(\widetilde{B}^T X \widetilde{B})^{-1})^T Y + Y \widetilde{B}^T A X \widetilde{B}(\widetilde{B}^T X \widetilde{B})^{-1} + Y \widetilde{B}^T \widetilde{B} Y \\ + (\widetilde{B}^T X \widetilde{B})^{-T} \widetilde{B}^T X H^T H X \widetilde{B}(\widetilde{B}^T X \widetilde{B})^{-1} \end{bmatrix} z_1$$

The stabilization of the system requires $\dot{V}(z_1) < 0$ for all $z_1 \ne 0$, which leads to

$$(\widetilde{B}^T A X \widetilde{B}(\widetilde{B}^T X \widetilde{B})^{-1})^T Y + Y \widetilde{B}^T A X \widetilde{B}(\widetilde{B}^T X \widetilde{B})^{-1} + Y \widetilde{B}^T \widetilde{B} Y$$
$$+ (\widetilde{B}^T X \widetilde{B})^{-T} \widetilde{B}^T X H^T H X \widetilde{B}(\widetilde{B}^T X \widetilde{B})^{-1} < 0 \tag{4-53}$$

Since it can be easily found that $(\widetilde{B}^T X \widetilde{B})$ and its inverse matrix are both s.p.d. matrices as long as X is a s.p.d. matrix, define $Y = (\widetilde{B}^T X \widetilde{B})^{-1}$ and pre- and post-multiply (4-53) by $Y^{-1} = (\widetilde{B}^T X \widetilde{B})$, it gives:

$$\widetilde{B}^T (AX + XA^T + I + XH^T H X) \widetilde{B} < 0 \tag{4-54}$$

Recalling Assumption A4, rewrite the inequality (4-54) as:

$$\widetilde{B}^T (AX + XA^T + I + \sum_{i=1}^{N} \alpha_i^2 X H_i^T H_i X) \widetilde{B} < 0$$

By defining $\gamma_i = 1/\alpha_i^2$ and using the well known Schur complement lemma, the above inequality can be rewritten in the form of inequality (4-41). Thus, if there exists a solution matrix X to (4-41), the derivative of the above Lyapunov function is negative: $\dot{V}(z_1) < 0$, i.e. the associated system is asymptotically stable after the system reaching sliding surface and hence the proof is complete. ∎

The proof for Theorem 4.1 shows that after reaching the sliding surface, the remaining system (sliding motion) is stable. As $z_2 = 0$ and $\dot{z}_2 = 0$, it can easily be seen that Theorem 4.1 concerns the unmatched part of the system.

Hence, the next step is to ensure the reachability of the sliding function (unmatched part of the system) which is given by Theorem 4.2.

Theorem 4.2. For the *i*-th LSS subsystem (4-37), if the sliding surface function $\sigma_i = B_i^T X_i^{-1} x_i$ could be obtained from Theorem 4.1, the control law (4-55) can drive each subsystem to the sliding surface and compensate the matched perturbations.

$$u_i(x_i,t) = \begin{cases} -(S_i B_i)^{-1} S_i A_i x_i(t) + \Psi_i sign(\sigma_i(x_i,t)), & \sigma_i(x_i,t) \neq 0 \\ -(S_i B_i)^{-1} S_i A_i x_i(t), & \sigma_i(x_i,t) = 0 \end{cases} \tag{4-55}$$

where,

$$\Psi_i = -\eta_i - \left\| (S_i B_i)^{-1} S_i \right\| \hat{\beta}_i(t), \quad \dot{\hat{\beta}}_i(t) = \|\sigma_i\| \tag{4-56}$$

$\eta_i = f_{i1}\|x_i\| + f_{i2}\|u_i\| + f_{i3} + \varepsilon$ with ε a positive constant chosen by the designer.

Proof:

From (4-47), the sliding motion is given by:

$$\widetilde{B}^T \dot{x}(t) = \widetilde{B}^T A X \widetilde{B} (\widetilde{B}^T X \widetilde{B})^{-1} \widetilde{B}^T x(t) + \widetilde{B}^T h(x,t) \tag{4-57}$$

The derivative of the sliding function for the *i-th* subsystem is:

$$\sigma_i(x_i,t) = S_i \dot{x}_i(t) = S_i A_i x_i(t) + S_i B_i(u_i(t) + f_i(x_i,u_i,t)) + S_i h_i(x,t) \tag{4-58}$$

Assume that there exists some constants large enough (i.e. $\beta_i \to \infty$) to satisfy $\|h_i(x,t)\| \leq \beta_i < \infty, i = 1,\dots,N$. The value of these unknown constants are estimated by the adaptive terms $\hat{\beta}_i(t)$. Define the estimation errors $\bar{\beta}_i(t) = \hat{\beta}_i(t) - \beta_i$, it is easy to verify that the derivative of these errors are $\dot{\bar{\beta}}_i(t) = \dot{\hat{\beta}}_i(t) = \|\sigma_i\|$.

Now, define the Lyapunov function for the sliding function as

$$V(\sigma) = \frac{1}{2} \sum_{i=1}^{N} \left[\left(\sigma_i^T (S_i B_i)^{-1} \sigma_i \right) + \left\| (S_i B_i)^{-1} S_i \right\| \bar{\beta}_i^2 \right] \tag{4-59}$$

It can be seen that $(S_i B_i)^{-1}$ is an s.p.d. matrix as $(S_i B_i)^{-1} = (B_i^T X B_i)^{-1} > 0$. The time derivative of the Lyapunov function (4-59) is given by:

$$\dot{V}(\sigma) = \frac{1}{2}\sum_{i=1}^{N}\left[\frac{d}{dt}\left(\sigma_i^T(S_iB_i)^{-1}\sigma_i\right)+2\left\|(S_iB_i)^{-1}S_i\right\|\overline{\beta}_i\dot{\overline{\beta}}_i\right]$$

$$\leq \sum_{i=1}^{N}\left\{\begin{array}{l}\sigma_i^T\left[(S_iB_i)^{-1}S_iA_ix_i(t)+u(x,t)+f(x,u,t)+(S_iB_i)^{-1}h_i(x,t)\right]\\ +\left\|\sigma_i\right\|\left\|(S_iB_i)^{-1}S_i\right\|(\hat{\beta}_i-\beta_i)\end{array}\right\} \qquad \text{(4-60)}$$

It can be verified that $\sigma_i^T\text{sign}(\sigma_i) = \|\sigma_i\|$, hence by substituting the control law (4-55) and (4-56) into (4-60):

$$\dot{V}(\sigma) \leq \sum_{i=1}^{N}\left\{\left\|\sigma_i\right\|\Psi_i+\left\|\sigma_i\right\|\left\|f_i(x_i,u_i,t)\right\|+\left\|\sigma_i\right\|\left\|(S_iB_i)^{-1}S_i\right\|\left\|h_i(x,t)\right\|+\left\|\sigma_i\right\|\left\|(S_iB_i)^{-1}S_i\right\|(\hat{\beta}_i-\beta_i)\right\}$$

$$\leq \sum_{i=1}^{N}\left\{\left\|\sigma_i\right\|\left\|(S_iB_i)^{-1}S_i\right\|(\beta_i-\hat{\beta}_i)-\varepsilon\left\|\sigma_i\right\|+\left\|\sigma_i\right\|\left\|(S_iB_i)^{-1}S_i\right\|(\hat{\beta}_i-\beta_i)\right\}$$

$$\leq -\sum_{i=1}^{N}\varepsilon\left\|\sigma_i\right\|$$

$$\text{(4-61)}$$

which implies that the sliding surface can be reached in finite time as proved in Section 4.2.3. Thus, the system trajectories can reach the sliding surface in finite time and remain on it with stable sliding motion. This completes the Proof. ∎

From the first part of the proof it can be found that, LMI (4-41) focuses on the unmatched part of the system. Thus, the transformation introduced in (Edwards and Spurgeon, 1998) is not necessary.

The adaptive part introduced in this method can relax the common bound constraint. Moreover, there is no need to assume the known bound of the matched perturbation $f_i(x_i, u_i, t)$, i.e. Assumption A3. The adaptive mechanism can estimate it as long as it is bounded. Thus, one of the main constraints of sliding mode is relaxed.

4.3.2 Feasibility discussion

Theorem 4.1 in Section 4.3.1 shows the sufficient condition for the SMC design. Although the assumptions A1-A4 are introduced, it is not enough to prove the feasibility of the LMIs (4-41). It is valuable to determine under what conditions solutions to the LMIs exist, as discussed in this Section.

The sliding surface invariance property guarantees insensitivity to matched faults. Hence, it is now feasible to consider an overall system without matched faults:

$$\dot{x}(t) = Ax(t) + Bu(t) + h(x,t) \qquad (4\text{-}62)$$

All the parameters of (4-62) are in the same form as (4-38). The well-known constraint for the system stability is: There exists a state feedback control law $u = Kx$ for the system $\dot{x}(t) = Ax(t) + Bu(t)$ if and only if there is an s.p.d. matrix X such that:

$$XA^T + AX + XK^TB + BKX < 0 \qquad (4\text{-}63)$$

Furthermore, (4-63) can be restricted to:

$$XA^T + AX + XK^TB + BKX + I + \sum_{i=1}^{N} \frac{1}{\gamma_i} XH_i^T H_i X < 0 \qquad (4\text{-}64)$$

The sufficient condition for the solvability of this inequality (4-64) in the decentralized system is that the overall system (4-62) is controllable. This can be ensured by the controllability of each subsystem. As a consequence of the system controllability, one can always find a gain matrix K and a p.s.d matrix X satisfying (4-64) with large enough γ_i. Using the projection lemma by (Gahinet and Apkarian, 1994), the following inequality is feasible with large enough γ_i:

$$\widetilde{B}^T \left(XA^T + AX + I + \sum_{i=1}^{N} \frac{1}{\gamma_i} XH_i^T H_i X \right) \widetilde{B} < 0 \qquad (4\text{-}65)$$

which implies that the LMIs (4-41) is feasible, i.e. if all the subsystems are controllable, one can always find a feasible solution to (4-41) and construct an SMC as discussed in Section 4.3.1.

If the interaction term of the overall system can be written in the form of $h(x,t) = DFEx(t)$, where $\|F\| \leq 1$, some existing results could be used to discuss the feasibility. If the system can be written in the form:

$$\dot{x}(t) = [A + DFE]x(t) + Bu(t)$$

The results from (Khargonekar Petersen and Zhou, 1990) show that the above system is quadratically stable via a constant linear state feedback control $u(t) = Kx(t)$ **if and**

only if there exists an s.p.d. matrix P such that for some $m \times n$ gain matrices K (Choi, 1998):

$$AP + PA^T + DD^T + PE^T EP + BKP + PK^T B^T < 0$$

Using the projection lemma and $P = X$, it gives:

$$\widetilde{B}^T(AX + XA^T + DD^T + PE^T EP)\widetilde{B} < 0$$

Choosing $D = I, E = H$, the above inequality is in the same form of (4-65).

4.3.3 Pole assignment, H_∞ and quadratic minimization Improvement

The LMI approach presented in section 4.3.1 can be easily extended. In this case, the SMCs are treated as matched perturbation components and can be combined with other robust methods. It is shows that the proposed LMI based decentralized SMC strategy has such good compatibility that it can be combined with other robust method and achieve specific robust performance. Although the methods proposed in this section are not illustrated in Section 4.4, it is still valuable to list some of the strategies, since this idea of combination with other robust control method is important in the rest of this thesis. This Section introduces several methods to extend the design features of the basic linear control outlined above. These extensions methods include eigenvalue assignment, H_∞ and quadratic minimization.

Eigenvalues assignment

The LMIs (4-41) provides some degrees of freedom. The eigenvalues assignment can be used with D-stability theory. Here two D stability regions are proposed:

1. $D_1 = \{s \in C : Re(s) < -\delta\}$

    It is well known that to assign all the eigenvalues of the unmatched overall system in the left hand side of the line $s = -\delta$ (Figure 4-3), it is necessary to find a solution to the following LMIs

    $$\text{Minimize } \sum_{i=1}^{N} \gamma_i, \text{ subject to } X = diag(X_1, ... X_N) > 0,$$

$$\begin{bmatrix} \tilde{B}^T(AX + XA^T + I + 2\delta X)\tilde{B} & \tilde{B}^T XH_1^T & \cdots & \tilde{B}^T XH_N^T \\ H_1 X\tilde{B} & -\gamma_1 I & \cdots & 0 \\ \vdots & \vdots & \ddots & \vdots \\ H_N X\tilde{B} & 0 & \cdots & -\gamma_N I \end{bmatrix} < 0 \qquad (4\text{-}66)$$
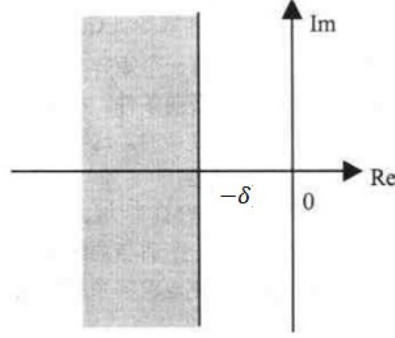
Figure 4-3. Eigenvalue clustering on the left hand side of $\square = -\square$

2. $D_2 = \{s \in C : Re(s) < -\delta\}$

To assign all the eigenvalues to lie in a disk of radius r and center $-q$. Consider the sliding motion (4-47):

$$\dot{z}_1(t) = \tilde{B}^T AX\tilde{B}(\tilde{B}^T X\tilde{B})^{-1} z_1(t) + \tilde{B}^T h(x,t)$$

Define $\bar{A} = \tilde{B}^T AX\tilde{B}(\tilde{B}^T X\tilde{B})^{-1}$. Assume that the interactions term satisfies

$$h(x,t) = \bar{H}(x,t)x(t) = \bar{H}(x,t)X\tilde{B}(\tilde{B}^T X\tilde{B})^{-1} z_1(t) = \bar{H}(x,t)\Gamma z_1(t)$$

and the assumption A4 is satisfied by $\bar{H}^T(x,t)\bar{H}(x,t) \leq \sum_{i=1}^N \alpha_i^2 H_i^T H_i$. According to the LMI region function, the following inequality should be feasible:

$$\begin{pmatrix} -r & q \\ q & -r \end{pmatrix} \otimes Y + \begin{pmatrix} 0 & 1 \\ 0 & 0 \end{pmatrix} \otimes (\bar{A}Y + \tilde{B}^T \bar{H}\Gamma Y) + \begin{pmatrix} 0 & 0 \\ 1 & 0 \end{pmatrix} \otimes (Y\bar{A}^T + Y\Gamma^T \bar{H}^T \tilde{B}) < 0$$

i.e.

$$\begin{bmatrix} -rY & qY + \bar{A}Y \\ qY + Y\bar{A}^T & -rY \end{bmatrix} + \begin{bmatrix} \tilde{B}^T \\ 0 \end{bmatrix} \begin{bmatrix} 0 & \bar{H}\Gamma Y \end{bmatrix} + \begin{bmatrix} 0 \\ \bar{H}^T \Gamma^T Y \end{bmatrix} \begin{bmatrix} \tilde{B} & 0 \end{bmatrix}$$

$$\leq \begin{bmatrix} -rY & qY + \bar{A}Y \\ qY + Y\bar{A}^T & -rY \end{bmatrix} + \begin{bmatrix} \tilde{B}^T \tilde{B} & 0 \\ 0 & Y\Gamma^T \bar{H}^T \bar{H}\Gamma Y \end{bmatrix}$$

$$= \begin{bmatrix} -rY + \widetilde{B}^T \widetilde{B} & qY + \overline{A}Y \\ qY + Y\overline{A}^T & -rY + Y\Gamma^T \overline{H}^T \overline{H}\Gamma Y \end{bmatrix} < 0$$

Define $Y = (\widetilde{B}^T X \widetilde{B})$, the above inequality can be rewritten as:

$$\begin{bmatrix} \widetilde{B}^T(-rX + I)\widetilde{B} & \widetilde{B}^T(qX + AX)\widetilde{B} \\ \widetilde{B}^T(qX + XA^T) & \widetilde{B}^T(-rX + XH^T HX)\widetilde{B} \end{bmatrix} < 0$$

Furthermore, using Shur Complement, the LMIs are given by:

Minimize $\sum_{i=1}^{N} \gamma_i$, subject to $X = diag(X_1, ... X_N) > 0$,

$$\begin{bmatrix} \widetilde{B}^T(-rX + I)\widetilde{B} & \widetilde{B}^T(qX + AX)\widetilde{B} & 0 & \cdots & 0 \\ \widetilde{B}^T(qX + XA^T) & -r\widetilde{B}^T X\widetilde{B} & \widetilde{B}^T XH_1^T & \cdots & \widetilde{B}^T XH_1^T \\ 0 & H_1 X\widetilde{B} & -\gamma_1 I & \cdots & 0 \\ \vdots & \vdots & \vdots & \ddots & \vdots \\ 0 & H_N X\widetilde{B} & 0 & \cdots & -\gamma_N I \end{bmatrix} < 0 \qquad (4\text{-}67)$$

If the above LMIs (4-67) have feasible solution, then the poles of the sliding motion are assigned in the disk D_2 as shown in Figure 4-4.
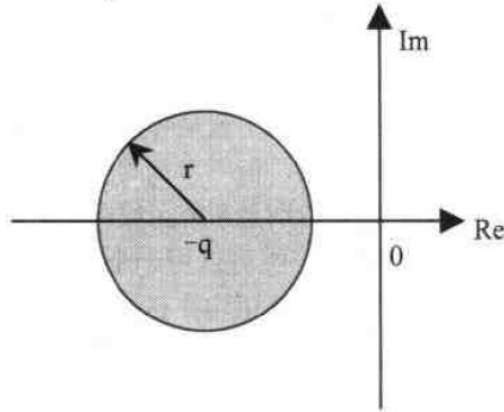
Figure 4-4. Eigenvalue clustering inside the disk D_2

H_∞ optimization

Consider the sliding motion:

$$\dot{z}_1(t) = \underbrace{\widetilde{B}^T A X \widetilde{B} (\widetilde{B}^T X \widetilde{B})^{-1}}_{\overline{A}} z_1(t) + \underbrace{\widetilde{B}^T}_{\overline{B}} h(x,t)$$

$$x = T^{-1}z = \underbrace{X\widetilde{B}(\widetilde{B}^T X \widetilde{B})^{-1}}_{\overline{C}} z_1$$

The well known bounded real lemma (Gahinet and Apkarian, 1994) can be written in the form of:

Minimize γ, subject to $Y > 0$,

$$\begin{bmatrix} Y\overline{A}^T + \overline{A}Y & \overline{B} & Y\overline{C}^T \\ \overline{B}^T & -\gamma I & 0 \\ \overline{C}Y & 0 & -\gamma I \end{bmatrix} < 0$$

By treating $h(x,t)$ as disturbance in the first equation and $x(t)$ as regulator in the second equation, it gives:

$$Y\left(\widetilde{B}^T(A+\overline{H})X\widetilde{B}(\widetilde{B}^T X\widetilde{B})^{-1}\right)^T + \widetilde{B}^T(A+\overline{H})X\widetilde{B}(\widetilde{B}^T X\widetilde{B})^{-1}Y + \frac{1}{\gamma}\widetilde{B}^T\widetilde{B}$$

$$+\frac{1}{\gamma}Y\left(X\widetilde{B}(\widetilde{B}^T X\widetilde{B})^{-1}\right)^T X\widetilde{B}(\widetilde{B}^T X\widetilde{B})^{-1}Y < 0$$

Thus, re-build the *bounded real lemma* by using $Y = (\widetilde{B}^T X \widetilde{B})$, it follows:

$$\widetilde{B}^T\left[XA^T + AX + X\overline{H}^T + \overline{H}X + \frac{1}{\gamma} + \frac{1}{\gamma}XX\right]\widetilde{B} < 0$$

Using Shur complement, the following LMIs are given:

Minimize $\gamma + \sum_{i=1}^{N}\gamma_i$, subject to $X = diag(X_1,...X_N) > 0$,

$$\begin{bmatrix} \widetilde{B}^T\left(XA^T + AX + I\right)\widetilde{B} & \widetilde{B}^T & \widetilde{B}^T X & \widetilde{B}^T XH_1 & \cdots & \widetilde{B}^T XH_N \\ \widetilde{B} & -\gamma I & 0 & 0 & \cdots & 0 \\ X\widetilde{B} & 0 & -\gamma I & 0 & \cdots & 0 \\ H_1^T X\widetilde{B} & 0 & 0 & -\gamma_1 I & \cdots & 0 \\ \vdots & \vdots & \vdots & \vdots & \ddots & \vdots \\ H_N^T X\widetilde{B} & 0 & 0 & 0 & \cdots & -\gamma_N I \end{bmatrix} < 0$$

(4-68)

It should be noted that there is no need to know the exact value of $\bar{H}(x,t)$ since this matrix is only used in the design procedure and can be replaced. Thus, one only need to assume that the structure of interaction of the overall system is in the form of $h(x,t) = \bar{H}(x,t)x(t)$.

Quadratic Minimization

For the system (4-62), consider the problem of minimizing the quadratic performance index

$$J = \int_{t_s}^{\infty} x(t)^T Q x(t) dt = \int_{t_s}^{\infty} x(t)^T \Xi^T \Xi x(t) dt \tag{4-69}$$

where $Q = \Xi^T \Xi$ is both symmetric and positive. t_s is the time at which the sliding motion commences. The aim is to minimize the cost function (4-69).

To minimise the cost function, consider the Lyapunov function for the system:

$$V(x) = x^T P x$$

The problem becomes that to find a feasible solution to the LMIs:

$$\left[\frac{d}{dt}V(x) + x^T \Xi^T \Xi x\right] < 0$$

The matrix Q from (4-69) is transformed and partitioned compatibly with z using (4-42) and (4-44):

$$T^{-T}QT^{-1} = \begin{bmatrix} \left(X\tilde{B}(\tilde{B}^T X\tilde{B})^{-1}\right)^T QX\tilde{B}(\tilde{B}^T X\tilde{B})^{-1} & \left(X\tilde{B}(\tilde{B}^T X\tilde{B})^{-1}\right)^T QB(SB)^{-1} \\ \left(B(SB)^{-1}\right)^T QX\tilde{B}(\tilde{B}^T X\tilde{B})^{-1} & \left(B(SB)^{-1}\right)^T QB(SB)^{-1} \end{bmatrix}$$

Because $z_2(t \geq t_s) = \sigma(t \geq t_s) = 0$ is the sliding surface. (4-69) can be written in term of the z coordinate system as

$$J = \int_{t_s}^{\infty} z(t)^T T^{-T} \Xi^T \Xi T^{-1} z(t) dt$$

$$= \int_{t_s}^{\infty} z_1(t)^T \left(X\widetilde{B}\left(\widetilde{B}^T X\widetilde{B}\right)^{-1} \right)^T \Xi^T \Xi X\widetilde{B}\left(\widetilde{B}^T X\widetilde{B}\right)^{-1} z_1(t) dt$$

Re-consider the Lyapunov function in the new coordinates z, as follows:

$$\left[\frac{d}{dt} V(z_1) + z_1(t)^T \left(X\widetilde{B}\left(\widetilde{B}^T X\widetilde{B}\right)^{-1} \right)^T \Xi^T \Xi X\widetilde{B}\left(\widetilde{B}^T X\widetilde{B}\right)^{-1} z_1(t) \right] < 0$$

where $V(z_1) = z_1^T Y z_1$.

The time derivative of $V(z_1)$ is given by:

$$V(z_1) \leq z_1^T \left\{ \begin{matrix} \left[\widetilde{B}^T A X\widetilde{B}\left(\widetilde{B}^T X\widetilde{B}\right)^{-1} \right]^T Y + Y\widetilde{B}^T A X\widetilde{B}\left(\widetilde{B}^T X\widetilde{B}\right)^{-1} + Y\widetilde{B}^T \widetilde{B}Y + \\ \left[X\widetilde{B}\left(\widetilde{B}^T X\widetilde{B}\right)^{-1} \right]^T H^T H X\widetilde{B}\left(\widetilde{B}^T X\widetilde{B}\right)^{-1} \end{matrix} \right\} z_1$$

Thus, if the system is quadratic stable, it gives the following inequality

$$z_1^T \left\{ \begin{matrix} \left[\widetilde{B}^T A X\widetilde{B}\left(\widetilde{B}^T X\widetilde{B}\right)^{-1} \right]^T Y + Y\widetilde{B}^T A X\widetilde{B}\left(\widetilde{B}^T X\widetilde{B}\right)^{-1} + Y\widetilde{B}^T \widetilde{B}Y + \\ \left[X\widetilde{B}\left(\widetilde{B}^T X\widetilde{B}\right)^{-1} \right]^T H^T H X\widetilde{B}\left(\widetilde{B}^T X\widetilde{B}\right)^{-1} + \left(X\widetilde{B}\left(\widetilde{B}^T X\widetilde{B}\right)^{-1} \right)^T \Xi^T \Xi X\widetilde{B}\left(\widetilde{B}^T X\widetilde{B}\right)^{-1} \end{matrix} \right\} z_1 < 0$$

which leads to:

$$\left[\widetilde{B}^T A X\widetilde{B}\left(\widetilde{B}^T X\widetilde{B}\right)^{-1} \right]^T Y + Y\widetilde{B}^T A X\widetilde{B}\left(\widetilde{B}^T X\widetilde{B}\right)^{-1} + Y\widetilde{B}^T \widetilde{B}Y +$$
$$\left[X\widetilde{B}\left(\widetilde{B}^T X\widetilde{B}\right)^{-1} \right]^T H^T H X\widetilde{B}\left(\widetilde{B}^T X\widetilde{B}\right)^{-1} + \left(X\widetilde{B}\left(\widetilde{B}^T X\widetilde{B}\right)^{-1} \right)^T \Xi^T \Xi X\widetilde{B}\left(\widetilde{B}^T X\widetilde{B}\right)^{-1} < 0$$

By pre-multiplying and post-multiplying by the matrix $Y^{-1} = (\widetilde{B}^T X\widetilde{B})$, it follows:

$$\widetilde{B}^T \left(XA^T + AX + I + XH^T HX + X\Xi^T \Xi X \right) \widetilde{B} < 0$$

Thus, the LMIs can be written as:

$$\text{Minimize} \sum_{i=1}^{N} \gamma_i \text{, subject to } X = diag(X_1, \dots X_N) > 0,$$

$$\begin{bmatrix} \tilde{B}^T(XA^T + AX + I)\tilde{B} & \tilde{B}^T X \Xi^T & \tilde{B}^T X H_1^T & \cdots & \tilde{B}^T X H_N^T \\ \Xi X \tilde{B} & -I & 0 & \cdots & 0 \\ H_1 X \tilde{B} & 0 & -\gamma_1 I & \cdots & 0 \\ \vdots & \vdots & \vdots & \ddots & \vdots \\ H_N X \tilde{B} & 0 & 0 & \cdots & -\gamma_N I \end{bmatrix} < 0 \qquad (4\text{-}70)$$

4.4   Simulation results

This Chapter has two purposes, (1) the review of SMC theory and (2) the proposal of a novel approach to decentralized SMC for LSSs. This Section introduces a numerical example to illustrate the SMC design strategy proposed in Section 4.3. The example is of an interconnected system model consisting of three subsystems with non-linear interconnection (Huang and Patton, 2012a). Similar examples can be found in other publications (Zhu and Pagilla, 2007; Kalsi Lian and Żak, 2009, 2010). The 1st subsystem is a second-order system and the 2nd and 3rd are third-order systems. Each subsystem is a linear system with a matched disturbance input comprising both an exogenous signal and a non-linear self-feedback.

$$\dot{x}_1 = \begin{bmatrix} 0 & 1 \\ 0 & 0 \end{bmatrix} x_1 + \begin{bmatrix} 0 \\ 1 \end{bmatrix} (u_1 + f_1(x_1, t)) + h_1(x, t)$$

$$\dot{x}_2 = \begin{bmatrix} 0 & 1 & 0 \\ 0 & 0 & 1 \\ 0 & 0 & 0 \end{bmatrix} x_2 + \begin{bmatrix} 0 \\ 0 \\ 1 \end{bmatrix} (u_2 + f_2(x_2, t)) + h_2(x, t)$$

$$\dot{x}_3 = \begin{bmatrix} -3 & 0 & 1 \\ 1 & 2 & 0 \\ 0 & 1 & -2 \end{bmatrix} x_3 + \begin{bmatrix} 0 \\ 1 \\ 0 \end{bmatrix} (u_3 + f_3(x_2, t)) + h_3(x, t)$$

where, $x_1 = [x_{11} \quad x_{12}]^T$, $x_2 = [x_{21} \quad x_{22} \quad x_{23}]^T$, $x_3 = [x_{31} \quad x_{32} \quad x_{33}]^T$ are the state vectors of the subsystems.

$$f_1(x_1, t) = 0.4\sin(x_{11}) + 0.5\sin(10t)$$

$$f_2(x_1, t) = 0.3\cos(x_{22}) + 0.6\sin(5t)$$

$$f_3(x_1, t) = 0.5\cos(x_{33}) + 0.6\sin(7t)$$

are the matched disturbance signals for subsystems.

The non-linear interactions between the subsystems are defined as follows:

$$h_1(x,t) = \alpha_1 \cos(x_{22}) H_1 x$$

$$h_2(x,t) = \alpha_2 \cos(x_{32}) H_2 x$$

$$h_3(x,t) = \alpha_3 \cos(x_{11}) H_3 x$$

with $\alpha_1 = \alpha_2 = \alpha_3 = 0.1$ and with

$$H_1 = \frac{1}{\sqrt{10}} \begin{bmatrix} 1 & 1 & 1 & 1 & 1 & 1 & 1 & 1 \\ 1 & 1 & 1 & 1 & 1 & 1 & 1 & 1 \end{bmatrix}$$

$$H_2 = \frac{1}{\sqrt{15}} \begin{bmatrix} 1 & 1 & 1 & 1 & 1 & 1 & 1 & 1 \\ 1 & 1 & 1 & 1 & 1 & 1 & 1 & 1 \\ 1 & 1 & 1 & 1 & 1 & 1 & 1 & 1 \end{bmatrix}$$

$$H_3 = \frac{1}{\sqrt{13}} \begin{bmatrix} 1 & 1 & 1 & 1 & 1 & 1 & 1 & 1 \\ 1 & 1 & 1 & 1 & 1 & 1 & 1 & 1 \\ 1 & 1 & 1 & 1 & 1 & 1 & 1 & 1 \end{bmatrix}$$

To have a general idea of the influence from interactions and disturbance, although using different method, it is still reasonable to design a linear controller. A suitable LMI based state feedback control approach to this type of system is described in (Šiljak and Stipanović, 2000). It is therefore useful to use their design method as a basis for comparison with the SMC approach derived in Section 4.3.

By solving the LMIs (4-40), the decentralized state feedback control gain matrix K is given:

$$K = \begin{bmatrix} -24.47 & -21.87 & 0 & 0 & 0 & 0 & 0 & 0 \\ 0 & 0 & -19.17 & -21.15 & -17.80 & 0 & 0 & 0 \\ 0 & 0 & 0 & 0 & 0 & -0.96 & -4.70 & -10.33 \end{bmatrix}$$

The result is shown in Figure 4-5.
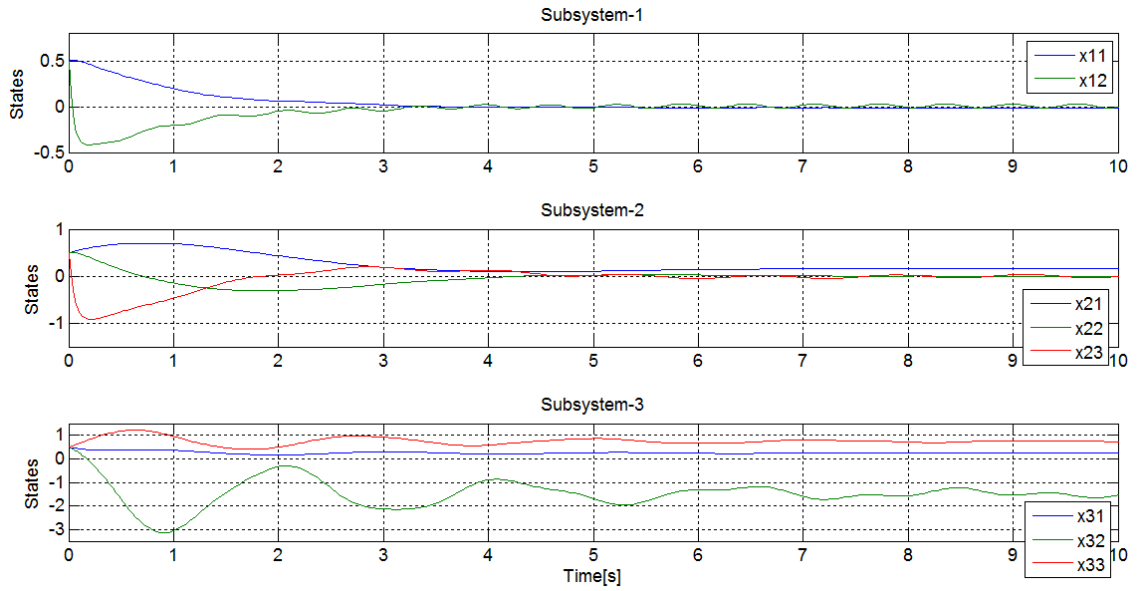
Figure 4-5. State responses with only linear control

It can be seen that the deviation in all of the subsystems because of the disturbance and interactions (unwanted signals). To solve this problem, solving the LMIs (4-41) and using the control law in Theorem 4.2, the X_i matrix for each subsystem is given by:

$$X_1 = \begin{bmatrix} 25 & -11.2 \\ -11.2 & 25 \end{bmatrix}, \ X_2 = \begin{bmatrix} 29.62 & -10.40 & -6.19 \\ -10.40 & 17.23 & -10.40 \\ -6.19 & -10.40 & 29.62 \end{bmatrix} X_3 = \begin{bmatrix} 30.84 & -0.54 & -0.10 \\ -0.54 & 36.19 & -8.28 \\ -0.10 & -8.27 & 2.87 \end{bmatrix}$$

Thus, the gain matrix S_i of the sliding function $\sigma_i = S_i x_i$ can be given by:

$$S_1 = \begin{bmatrix} 0.022 & 0.050 \end{bmatrix}, \ S_2 = \begin{bmatrix} 0.032 & 0.055 & 0.060 \end{bmatrix}, \ S_3 = \begin{bmatrix} 0.0007 & 0.081 & 0.234 \end{bmatrix}$$

The adaptive mechanism is chosen as $\Psi_i = -1 + 10\|(S_i B_i)^{-1} B_i\|\hat{\beta}$, with $\dot{\hat{\beta}} = 10\|\sigma_i\|$. And combine with the boundary layer method, the control law is designed as:

$$u_i(x_i, t) = \begin{cases} -(S_i B_i)^{-1} S_i A_i x_i(t) + \Psi_i \dfrac{\sigma_i(x_i, t)}{\|\sigma_i(x_i, t)\| + 0.01}, & \|\sigma_i(x_i, t)\| > 0.01 \\ -(S_i B_i)^{-1} S_i A_i x_i(t), & \|\sigma_i(x_i, t)\| \le 0.01 \end{cases}$$

The states response of using decentralized SMC is shown in Figure 4-6. It shows that disturbances and interactions are compensated by the SMC. Although the deviation is too small to be noticed (Figure 4-7), it is still worth discussing since it shows some of the properties of SMC.

93
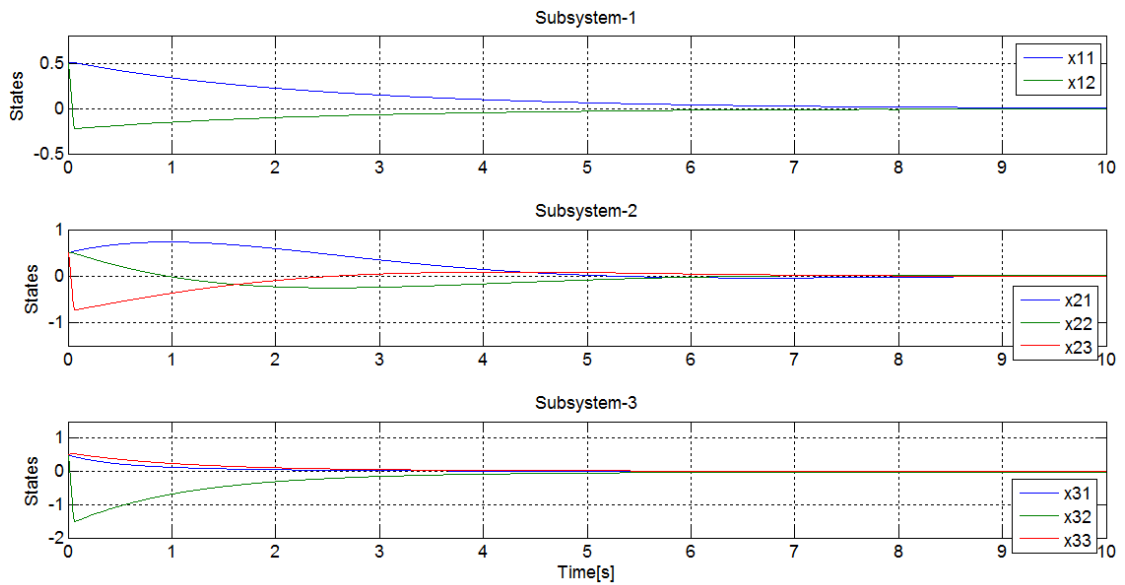
Figure 4-6. States responses with decentralized SMC
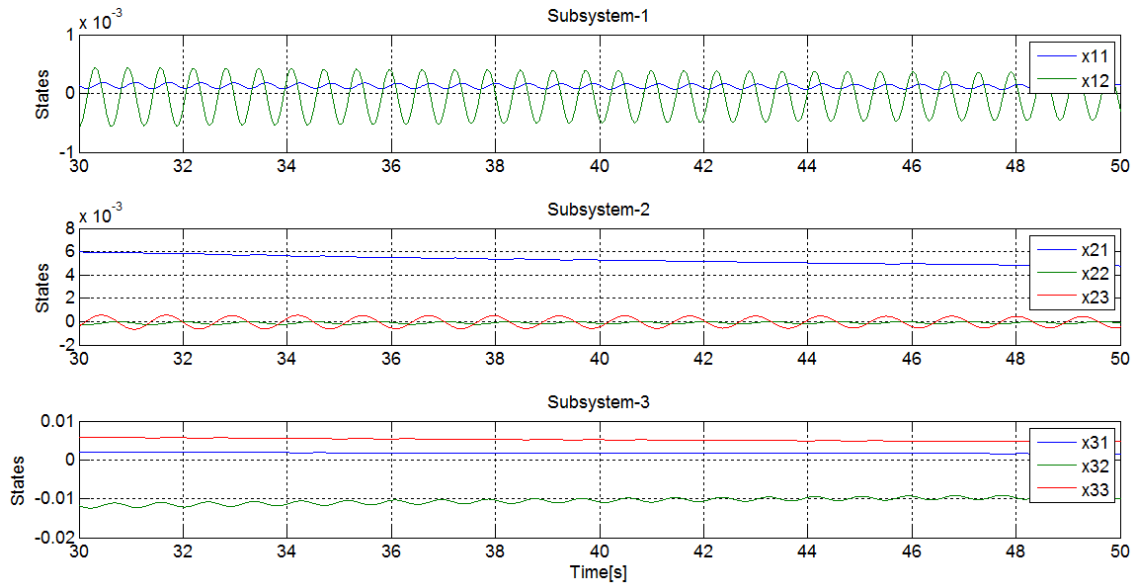
Figure 4-7. Influence from unwanted signals between *t=30s* and *t=50s*

Figure 4-7 shows the small perturbation in the states response after 30s. It can be seen that the perturbations are not fully compensated by the SMC because of the boundary layer. As discussed in Section 4.2.3, the boundary layer theory allows the perturbations exist in the sliding region. This explains why there are still disturbances in some of the states of subsystem-1 and subsystem-2. On the other hand, because of the adaptive mechanism, any state away from the sliding region is driven to the surface. Thus, it can be seen that states, e.g. $x32$, $x31$ and $x21$, are still in the process of convergence. The

speed of convergence can be increased by changing the adaptive mechanism Ψ_i (Figure 4-8). Use the same adaptive structure $\Psi_i = -\eta + 10\|(S_iB_i)^{-1}B_i\|\hat{\beta}$ with different η to see the value of the first state of subsystem-2 in the time period *t=30s* to *t=40s*.

In Figure 4-8, it is clear that with $\eta = 5$, better speed of convergence is given. It is well known that in sliding mode control, the larger the gain is, the more insensitive to faults and faster response the system has. However, high gain value might not available in practice (wind-up) and might cause chattering problem (even with boundary layer theory). Thus, finding an acceptable high gain is one of the main problems in SMC design.
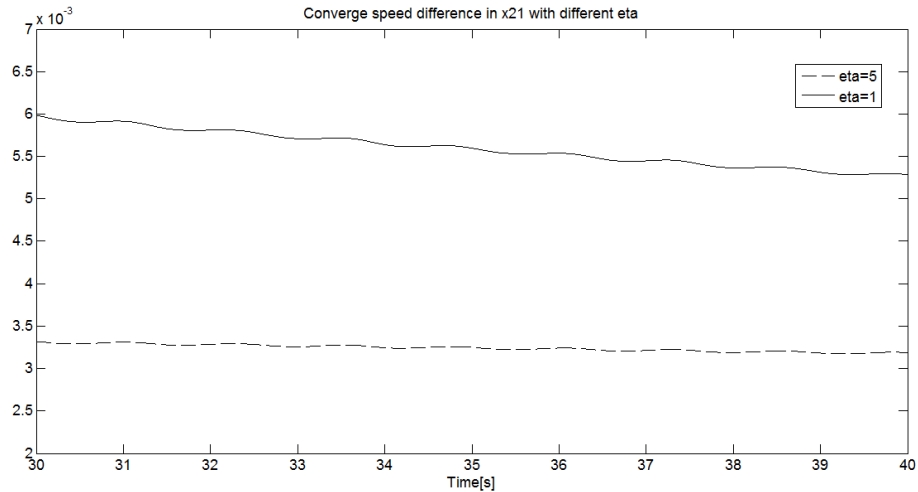
Figure 4-8. Convergence speed difference represented by state *x21* from *t=30s*.

4.5   Conclusion

In this Chapter, sliding mode control is carefully described. In the description of regular form, two types of regular form are introduced and it can be easily found that the perturbations are rejected by SMC if they are matched. The adaptive mechanism for relaxation of known upper bound of perturbation is discussed and proved, as well as the boundary layer method for chattering elimination. This section also proves the sliding surface reachability and system stability with boundary layer and the bound set of the sliding motion with boundary layer is calculated. With the set, one can design the sliding mode control systematically.

The second part of this Chapter introduces a novel SMC design procedure for LSSs using an LMI approach. The idea of this method is based on Choi's regular form for single system. Within a simple LMI approach, one can design the sliding mode state feedback controller without any *apriori* transformation. Both matched and unmatched perturbations (interactions) are discussed. The known bound constraints of matched perturbations can be relaxed by adaptive mechanism. When there are unmatched perturbations, the unmatched part of the system will be affected. In this case, some special sliding function design methods should be used to ensure the stability of the system. Furthermore, some improvements like eigenvalues assignment and H_∞ robust method can be easily added into this method, providing good compatibility. The knowledge introduced in this chapter is the basis to output feedback which is introduced in Chapter 5.

Chapter 5

Decentralized Output based Sliding Mode Control

5.1 Introduction

In most practical situations, complete state measurements are not available at each individual subsystem for decentralized control. In some circumstances, it is impossible or expensive to measure all of the system states. Alternatively, some systems may be nonlinear or too complex that an identification approach should be applied to obtain a simpler model. In this case, the states in the simpler model might have no physical meaning and are thus not measurable (Edwards and Spurgeon, 1998).

As discussed in Chapter 2, decentralized control uses local information available at the level of each subsystem in the controller implementation for large scale interconnected systems. Thus, decentralized controllers have the possibility of simpler architecture than their centralized control counterparts and can thus be more practical to realize on a real physical system.

It is well known that there are three ways to deal with the design of an output feedback control system: 1). Static output feedback (SOF) design; 2). Dynamic compensator based controller design and 3). Observer based controller design.

The assumption of the interactions (*quadratic constraint*) is the same as described in Chapter 4 so that the optimization problem is posed in a fashion that will result in selection of controller and observer gains that will not only stabilize the overall large-scale system but also simultaneously maximize the interconnection bounds (Šiljak and Stipanović, 2000; Zhu and Pagilla, 2007).

The objective of this Chapter is to describe a design framework for decentralized SMC of LSS where only local output information is available. Suitable control system architectures for this problem are: Static output feedback control, dynamic compensator based control and decentralized observer based control. The properties of these architectures are summarised as follows:

5.2 Static output feedback

Consider a LSS with N subsystems. Each of the i-th subsystems has the state space form:

$$\dot{x}_i(t) = A_i x_i(t) + B_i(u_i(t) + f_i(t, x_i, u_i)) + h_i(x, t)$$
$$y_i(t) = C_i x_i(t)$$

(5-1)

where the state vector $x_i \in \mathbb{R}^{n_i}$, the control signal $u_i \in \mathbb{R}^{m_i}$ the output signal $y_i \in \mathbb{R}^{p_i}$ and the condition $m \leq p < n$ is fulfilled. The system triple (A_i, B_i, C_i) is assumed to be known and the matrix pair (A_i, B_i, C_i) is assumed to be stabilizable and detectable. Further, it is assumed that any invariant zeros of the triple (A_i, B_i, C_i) lie in the left-half of the complex plane, the matrix product $C_i B_i$ has full rank and that all the plant inputs and output are independent.

The perturbation $f_i(x_i, u_i, t)$ for the i-th subsystem assumed unknown but bounded and furthermore it acts in the input channel of the system as a matched perturbation according to the definition of (Draženović, 1969). It can thus be assumed that $f_i: \mathbb{R}^n \times \mathbb{R}^m \times \mathbb{R}_+ \to \mathbb{R}^m$ is bounded by a known constant f_{iu} and a known function $\varphi_i(y, t)$, so that

$$\|f_i(x_i, u_i, t)\| < f_{iu}\|u_i\| + \varphi_i(y, t)$$

(5-2)

Furthermore, the interactions are assumed to satisfy the following quadratic constraint introduced by (Šiljak and Stipanović, 2000) (see description in Section 4.3):

$$h_i^T(x, t) h_i(x, t) \leq \alpha_i^2 x^T H_i^T H_i x$$

where α_i are bounding constants.

The overall system can be written in a compact form as:

$$\dot{x}(t) = Ax(t) + B(u(t) + f(x, u, t)) + h(x, t)$$
$$y = Cx$$

(5-3)

where:

$$A = diag(A_1, \ldots, A_N), B = diag(B_1, \ldots, B_N), C = diag(C_1, \ldots, C_N)$$

$$f(x, u, t) = [f_1^T(x_1, u_1, t), \ldots, f_N^T(x_N, u_N, t)]^T$$

98

$$h(x,t) = [h_1^T(x,t), \ldots, h_N^T(x,t)]^T$$

$x \in \mathbb{R}^n$, $u \in \mathbb{R}^m$, $y \in \mathbb{R}^p$ $n = n_1 + \cdots + n_N$, $m = m_1 + \cdots + m_N$ and $p = p_1 + \cdots + p_N$ are the numbers of the states, inputs and outputs, respectively. The interconnection $h(x,t)$ for the aggregate system is bounded as follows:

$$h^T(x,t)h(x,t) \leq x^T \left(\sum_{i=1}^{N} \alpha_i^2 H_i^T H_i \right) x = x^T H^T H x \tag{5-4}$$

In the output feedback case, the states are not fully available. Thus, the sliding surface function cannot be designed as a function of x but a function of y (e.g. $y = Cx$). Define an output based sliding surface function of the form:

$$\sigma = \begin{bmatrix} \sigma_1^T & \cdots & \sigma_N^T \end{bmatrix}^T = diag(F_1, \ldots, F_N) \begin{bmatrix} y_1 \\ \vdots \\ y_N \end{bmatrix} \tag{5-5}$$

$F = diag(F_1, \ldots, F_N) \in \mathbb{R}^{m \times p}$ a block diagonal matrix such that the $F_i C_i B_i, i = 1, \ldots, N$ are nonsingular and the reduced $(n - m)$ th-order equivalent system dynamics restricted to $Fy = FCx = 0$ are asymptotically stable. By defining the overall control law $= Ky = KCx$, the Lyapunov function for the overall system (5-3) can be constructed as:

$$V(x) = x^T P x \tag{5-6}$$

where $P = diag(P_1, \ldots, P_N) \in \mathbb{R}^{n \times n}$ is an s.p.d. matrix. First consider the system control without perturbations, i.e. $f(x,u,t) = 0$. Taking the time derivative along the system trajectory, it yields:

$$\begin{aligned}\dot{V}(x) &= x^T(PA + A^T P + PBKC + C^T K^T B^T P)x + x^T Ph + h^T Px \\ &\leq x^T(PA + A^T P + PBKC + C^T K^T B^T + PP + H^T H)x\end{aligned} \tag{5-7}$$

The aggregated system is globally stable in the Lyapunov sense if matrices K and P can be found to satisfy the bi-linear matrix inequality:

$$PA + A^T P + PP + H^T H + PBKC + C^T K^T B^T P < 0 \tag{5-8}$$

Or equivalently finding matrices K and X satisfying (Boyd *et al*, 1993):

$$AX + XA^T + BKCX + XC^T K^T B^T + I + XH^T HX < 0 \qquad (5\text{-}9)$$

It is well known that the inequalities (5-8) and (5-9) are not convex for P and K or X and K. Moreover, (5-8) and (5-9) are coupled since $X = P^{-1}$. It is hence impossible to solve these inequalities with conventional LMI tools. This is the main obstacle in designing static output feedback control.

This topic has been widely researched in single system level. For example, (Geromel, 1994) presented a min/max iteration algorithm for SOF. (Syrmos *et al*, 1997) proposed a comprehensive paper survey concerning the development of the SOF problem and pointed out that the dynamic output-feedback problem can be transformed into a static output-feedback problem. (Cao, James and Sun, 1998) proposed an approach to avoid the coupled inequalities using iteration based on LMI theory. (Benton and Smith, 1998) proposed a necessary and sufficient condition for SOF which contains two coupled LMIs. They also proposed an algorithm to solve the LMIs without iteration. The infeasibility of the LMIs considered do not give insight into the infeasibility of the SOF control designs, although the computational simplicity makes the approach attractive. (Edwards and Spurgeon, 2003) designed a sliding mode based SOF control for a single system based on Benton and Smith's method (Benton and Smith, 1998) which requires several state space transformations. In the following, a simpler method of SOF SMC is proposed that has two advantages:

- Simplicity. This method is designed without using any transformation, this simplifies the design procedure.

- Compatibility: As this method is based on the LMI approach, some other additional LMIs that introduce some performance requirements, for example using multi-objective optimization can easily be added.

Several Lemmas should be introduced since they play a central role in the proposed approach.

Lemma 5.1 (Gahinet and Apkarian, 1994): Consider a symmetric matrix $\Psi \in \mathbb{R}^{m \times m}$, and two matrices Γ, W of column dimension m, then consider the problem of finding some matrix Θ of compatible dimensions such that:

$$\Psi + \Gamma^T \Theta^T W + W^T \Theta \Gamma < 0 \qquad (5\text{-}10)$$

Denoted by $\tilde{\Gamma}$ and $\widetilde{W}$ any matrices whose columns form bases of the null spaces of Γ and W respectively. Then (5-10) is solvable for Θ if and only if:

$$\tilde{\Gamma}^T \Psi \tilde{\Gamma} < 0 \text{ and } \widetilde{W}^T \Psi \widetilde{W} < 0 \tag{5-11}$$

Lemma 5.1 is the so called "*Elimination Lemma*" or "*Projection Lemma*".

It is easy to find that the inequalities (5-8) and (5-9) are in the form of (5-10), which means matrix K can be eliminated by using Lemma 5.1, if and only if matrices P and X can be found that satisfy: $P > 0, X > 0$, together with:

$$\tilde{C}^T (PA + A^T P + PP + H^T H)\tilde{C} < 0, \tag{5-12}$$

$$\tilde{B}^T (AX + XA^T + I + XH^T HX)\tilde{B} < 0 \tag{5-13}$$

Hence, the inequalities (5-8) and (5-9) are solvable and thus the system is quadratically stable.

Lemma 5.2 (Finsler's Lemma, Boyd *et al*, 1993) Let $x \in \mathbb{R}^n$, $Q \in \mathbb{S}^n$, $B \in \mathbb{R}^{m \times n}$ such that $rank(B) < n$, the following statements are equivalent:

i). $x^T Q x < 0$, for all $Bx = 0, x \neq 0$

ii). $\tilde{B}^T Q \tilde{B} < 0$.

iii). $\exists \mu \in \mathbb{R}: Q - \mu B^T B < 0$

iv). $\exists \mathcal{X} \in \mathbb{R}^{n \times m}: Q + \mathcal{X}B + B^T \mathcal{X} < 0$

Hence, if combined with conditions ii) and iii), the inequalities (5-12) and (5-13) can further be written in the form (Benton and Smith, 1998):

$$PA + A^T P + PP + H^T H - PBB^T P < 0 \tag{5-14}$$

$$PA + A^T P + PP + H^T H - \tau C^T C < 0 \tag{5-15}$$

It should be noted that (5-14) and (5-15) are not convex and thus cannot be solved by conventional LMI methods, i.e. the Schur complement lemma cannot be applied to (5-14) since $PBB^T P > 0$. In this case, (Benton and Smith, 1998) advocate synthesising an s.p.d. matrix P such that the matrix inequalities:

$$P(A + BK_{sf}) + (A + BK_{sf})^T P < 0$$

$$PA + A^T P - \tau C^T C < 0$$

hold for some $\tau > 0$, where $K_{sf} = B^T P_{are}$ is a pre-calculated matrix. P_{are} is the solution to the algebraic Riccati equation:

$$P_{are} A + A^T P_{are} - P_{are} BB^T P_{are} = -Q$$

where $Q = -\varepsilon I$ and $\varepsilon > 0$ is a small design scalar.

The following algorithm is based on the algorithm of (Benton and Smith, 1998) extended to include the SMC computation for the decentralized output feedback control system problem defined by (5-1) to (5-5).

Algorithm 5.1

1) Define $A_\delta = A + \delta I$, where δ is the desired prescribed degree of stability (as described in Chapter 4).

2) Solve the algebraic Riccati equation:

$$P_{sf} A_\delta + A_\delta^T P_{sf} - P_{sf} BB^T P_{sf} + \varepsilon I = 0 \tag{5-16}$$

where $\varepsilon > 0$ is arbitrarily small.

3) Set $K_{sf} = -(1 + \kappa) B^T P_{sf}$ where $\kappa > 0$ is arbitrarily small.

4) Define $W_1 = diag(W_{11}, ..., W_{1N})$ and $W_2 = diag(W_{21}, ..., W_{2N})$, where $W_{1i} \in \mathbb{R}^{(n_i - m_i) \times (n_i - m_i)}$, $W_{2i} \in \mathbb{R}^{p_i \times p_i}$. Solve the following LMI minimization problem:

Minimize $\sum_{i=1}^{N} \gamma_i$, subject to $P = \tilde{B} W_1 \tilde{B}^T + C^T W_2 C > 0, \tau > 0$,

$$\begin{bmatrix} (A + BK_{sf})^T P + P(A + BK_{sf}) & P & H_1^T & \cdots & H_N^T \\ P & -I & 0 & \cdots & 0 \\ H_1 & 0 & -\gamma_1 I & \cdots & 0 \\ \vdots & \vdots & \vdots & \ddots & \vdots \\ H_N & 0 & 0 & \cdots & -\gamma_N I \end{bmatrix} < 0 \tag{5-17}$$

$$\begin{bmatrix} A^T P + PA - \tau C^T C & P & H_1^T & \cdots & H_N^T \\ P & -I & 0 & \cdots & 0 \\ H_1 & 0 & -\gamma_1 I & \cdots & 0 \\ \vdots & \vdots & \vdots & \ddots & \vdots \\ H_N & 0 & 0 & \cdots & -\gamma_N I \end{bmatrix} < 0 \qquad (5\text{-}18)$$

5) Fix $P = \tilde{B} W_1 \tilde{B}^T + C^T W_2 C, \gamma_i, i = 1, \ldots, N$ and solve the LMI minimization problem

Minimization λ, subject to

$$\begin{bmatrix} \lambda I & K^T \\ K & M \end{bmatrix} > 0, \qquad (5\text{-}19)$$

$$\Sigma = \begin{bmatrix} (A + BKC)^T P + P(A + BKC) & P & H_1^T & \cdots & H_N^T \\ P & -I & 0 & \cdots & 0 \\ H_1 & 0 & -\gamma_1 I & \cdots & 0 \\ \vdots & \vdots & \vdots & \ddots & \vdots \\ H_N & 0 & 0 & \cdots & -\gamma_N I \end{bmatrix} < 0 \qquad (5\text{-}20)$$

The inequality (5-19) is used to minimize the quadratic norm of the gain K and thereby produce a design with good numerical conditioning and practical control variations.

It can be clearly seen that the crucial idea of this algorithm is to find a matrix K_{sf}, to ensure that the condition (5-14) is satisfied. The feasibility of the LMIs (5-17) and (5-18) can then be ensured using the same idea as discussed in Section 4.3.2. If it is the case that the bounding parameters γ_i are not small enough, the parameters ε and κ can be increased in steps 2) & 3).

The design method for $P = \tilde{B} W_1 \tilde{B}^T + C^T W_2 C$ is to ensure that one can find a solution to the equation $B^T P = FC$. In this case, $F = B^T C^T W_2$.

As a consequence of the interactions terms, it is not enough to ensure the feasibility of this algorithm by assuming the triple (A_i, B_i, C_i) is stabilizable and detectable. Controllability and observability are joint sufficient conditions for the feasibility of LMIs (5-17) to (5-20) (Benton and Smith, 1998). Moreover, as Edwards and Spurgeon (1998) describe for single systems, the subsystems should also satisfy the conditions

that $rank(C_iB_i) = rank(B_i)$ and any invariant zeros of (A_i, B_i, C_i) lie in the open left half plane (automatically satisfied when the system is controllable and observable). To conclude, the conditions for the output feedback control are that the triple (A_i, B_i, C_i) for i-th subsystem ($i = 1, ..., N$) satisfy: 1). relative degree one, 2). controllability and 3). observability.

The proof of the quadratic stability of the system is now given.

Theorem 5.1. For the aggregate system of (5-3), the above algorithm can be used with the sliding surface function defined by

$$\sigma = \begin{bmatrix} \sigma_1^T & ... & \sigma_N^T \end{bmatrix}^T = diag(F_1, ..., F_N) \begin{bmatrix} y_1 \\ \vdots \\ y_N \end{bmatrix} \tag{5-5}$$

and with the following decentralized control law:

$$u_i = \begin{cases} K_i y_i - \rho_i \dfrac{\sigma_i}{\|\sigma_i\|}, & \sigma_i \neq 0 \\ K_i y_i, & \sigma_i = 0 \end{cases} \tag{5-21}$$

The aggregate system control vector is given by: $u = [u_1^T \quad ... \quad u_N^T]^T)$

This system is quadratically stable and insensitive to the matched uncertainties.

Proof:

Define the Lyapunov function for the aggregate system in terms of the addition of Lyapunov functions of each subsystem:

$$V(x) = \sum_{i=1}^{N} x_i^T P_i x_i \tag{5-22}$$

The time derivative of (5-22) is given by:

$$\dot{V}(x) \leq x^T (PA + A^T P + PBKC + C^T K^T B^T P + PP + H^T H)x$$

$$+ \sum_{i=1}^{N} \left(2x_i^T P_i B_i f_i - 2x_i^T P_i B_i \rho_i \frac{\sigma_i}{\|\sigma_i\|} \right)$$

$$\leq x^T \Theta x + 2 \sum_{i=1}^{N} \left[x_i^T C_i^T F_i^T \left(\|f_i\| - \rho_i \frac{\sigma_i}{\|\sigma_i\|} \right) \right] \qquad (5\text{-}23)$$

$$\leq x^T \Theta x + 2 \sum_{i=1}^{N} \left[\|\sigma_i\| (\|f_i\| - \rho_i) \right]$$

Since $\Theta < 0$ is already ensured by the LMI (5-20) in step 5), so that is $\rho_i > \|f_i\|, i = 1, \ldots, N$, it can be claimed that the system is quadratically stable as $\dot{V}(x) < 0$. In this case, ρ_i can be chosen as $\rho_i = f_{iu}\|u\| + \varphi_i(y, t) + \eta_i, i = 1, \ldots, N$ where $\eta_i, i = 1, \ldots, N$ are positive constants chosen by the designer. The adaptive mechanism described in Chapter 4 can also be used to relax the known upper bound assumption of the perturbations. It is also necessary to prove that the sliding surface can be reached.

Consider the time derivative of the sliding surface function given by:

$$\dot{\sigma}(t) = FC\dot{x}(t) = FCAx(t) + FCB(u(t) + f(t,x,u)) + FCh(x,t) \qquad (5\text{-}24)$$

Then the Lyapunov function for the sliding surface function of the aggregate system is given by:

$$V(\sigma) = \frac{1}{2} \sum_{i=1}^{N} \left[\sigma_i^T (F_i C_i B_i)^{-1} \sigma_i \right] \qquad (5\text{-}25)$$

The matrices $(F_i C_i B_i)$ satisfy the s.p.d constraint as $F_i C_i B_i = B_i^T P_i B_i$.

Hence, the time derivative of (5-25) is:

$$\dot{V} = \sigma_i^T \left[(F_i C_i B_i)^{-1} F_i C_i \left[(A_i + B_i K_i C_i)x_i + h_i \right] + f_i - \rho_i \frac{\sigma_i}{\|\sigma_i\|} \right]$$

$$\leq \|\sigma_i\| (F_i C_i B_i)^{-1} F_i C_i \left[(A_i + B_i K_i C_i)x_i + h_i \right] + \|\sigma_i\| (\|f_i\| - \rho_i) \qquad (5\text{-}26)$$

Using $\rho_i = f_{iu}\|u\| + \varphi_i(y, t) + \eta_i, i = 1, \ldots, N$, (5-26) can now be rewritten as:

$$\dot{V} \leq \sum_{i=1}^{N} \left\{ \|\sigma_i\| \left[(F_i C_i B_i)^{-1} F_i C_i \left[(A_i + B_i K_i C_i)x_i + h_i \right] - \eta_i \right] \right\} \qquad (5\text{-}27)$$

Let $0 < \tilde{\eta}_i < \eta_i$. As a consequence of quadratic stability of the closed-loop subsystems the subsystem trajectories will enter into their respective stability regions Ω_i in finite time. These regions are defined by:

$$\Omega_i = \left\{ x_i : \left\| (F_i C_i B_i)^{-1} F_i C_i \right\| \left\| (A_i + B_i K_i C_i) x_i + h_i \right\| < \eta_i - \tilde{\eta}_i \right\} \quad i = 1, \dots, N \quad (5\text{-}28)$$

in which $\dot{V} \leq \sum_{i=1}^{N}(-\tilde{\eta}_i \|\sigma_i\|)$ implies that all of the sliding surfaces $\sigma_i = 0$ can be reached in finite time and remained there subsequently. With this the proof is complete. ∎

It is important to note that the nonlinear control law is only used to compensate any unwanted matched perturbations. Thus, the most important part of designing an SOF SMC is to obtain the aggregated system sliding surface gain matrix F. In other words, there are some other methods available to derive the linear gain matrix K (for example, Shaked, 2003; Bara and Boutayeb, 2005; Peaucelle and Arzelier, 2005, Cao James and Sun, 1998). But whatever method is chosen, one can still use the LMI (5-17) with pre-structured matrix $P = \tilde{B} W_1 \tilde{B}^T + C^T W_2 C$ to get the sliding surface matrix F. The SOF SMC can then be applied as long as the following LMI is feasible for (W_1, W_2):

$$\text{Minimize } \sum_{i=1}^{N} \gamma_i, \text{ subject to } P = \tilde{B} W_1 \tilde{B}^T + C^T W_2 C > 0$$

$$\Sigma = \begin{bmatrix} (A+BKC)^T P + P(A+BKC) & P & H_1^T & \cdots & H_N^T \\ P & -I & 0 & \cdots & 0 \\ H_1 & 0 & -\gamma_1 I & \cdots & 0 \\ \vdots & \vdots & \vdots & \ddots & \vdots \\ H_N & 0 & 0 & \cdots & -\gamma_N I \end{bmatrix} < 0 \quad (5\text{-}29)$$

5.3   Dynamic compensator design approach

If the system does not satisfy the well-known Kimura Davison condition, there might be no available SOF control law. To overcome this problem and to provide additional degrees of freedom, some researchers introduce a dynamic compensator so that the augmented system satisfies the Kimura-Davison condition. The main idea of this method is to build an augmented system which satisfies the Kimura-Davison condition and then design the static output feedback based on it. Since the SOF SMC design approach has been introduced in Section 5.2, based on an extension of the method by Benton and Smith (1998), an alternative method is presented in this section.

Consider the *i*-th subsystem

$$\dot{x}_i(t) = A_i x_i(t) + B_i(u_i(t) + f_i(t, x_i, u_i)) + h_i(x, t)$$
$$y_i(t) = C_i x_i(t)$$

(5-1)

together with a compensator given by

$$\dot{x}_{ic}(t) = A_{ic} x_{ic}(t) + B_{ic} y_i(t), \quad x_{ic}(0) = x_{ic0}$$

(5-30)

The control using the compensator has the form:

$$u_i(t) = C_{ic} x_{ic} + D_{ic} y_i(t) + v_i(t)$$

(5-31)

where the matrices $A_{ic} \in \mathbb{R}^{q_i \times q_i}$, $B_{ic} \in \mathbb{R}^{q_i \times p_i}$, $C_{ic} \in \mathbb{R}^{m_i \times q_i}$, and $D_{ic} \in \mathbb{R}^{m_i \times p_i}$ are gain matrices to be determined. The nonlinear switching term $v_i(t)$ is used to reject any matched perturbations and is in the following form:

$$v_i = -\rho_i(t) \frac{\sigma_i}{\|\sigma_i\|}$$

(5-32)

where $\rho_i(t)$ is a positive scalar function and σ_i is the sliding surface function for the *i*-th subsystem (as described in Section 5.2). When combined with the state equation of the *i*-th subsystem (5-1) and the control law (5-31) and (5-32), the augmented system is then given by:

$$\begin{bmatrix} \dot{x}_i \\ \dot{x}_{ic} \end{bmatrix} = \begin{bmatrix} A_i & 0 \\ 0 & 0 \end{bmatrix} \begin{bmatrix} x_i \\ x_{ic} \end{bmatrix} + \begin{bmatrix} B_i & 0 \\ 0 & I_{q_i} \end{bmatrix} \begin{bmatrix} D_{ic} & C_{ic} \\ B_{ic} & A_{ic} \end{bmatrix} \begin{bmatrix} C_i & 0 \\ 0 & I_{q_i} \end{bmatrix} \begin{bmatrix} x_i \\ x_{ic} \end{bmatrix} + \begin{bmatrix} B_i \\ 0 \end{bmatrix} (v_i(t) + f_i(t, x_i, u_i))$$
$$+ \begin{bmatrix} h_i(x, t) \\ 0 \end{bmatrix}$$

$$\bar{y}_i = \begin{bmatrix} C_i & 0 \\ 0 & I_{q_i} \end{bmatrix} \begin{bmatrix} x_i \\ x_{ic} \end{bmatrix}$$

(5-33)

Define

$$\bar{x}_i = \begin{bmatrix} x_i^T & x_{ic}^T \end{bmatrix}^T, \quad \bar{A}_i = \begin{bmatrix} A_i & 0 \\ 0 & 0 \end{bmatrix}, \quad \bar{B}_i = \begin{bmatrix} B_i & 0 \\ 0 & I_{q_i} \end{bmatrix}, \quad K_i = \begin{bmatrix} D_{ic} & C_{ic} \\ B_{ic} & A_{ic} \end{bmatrix}, \quad \bar{C}_i = \begin{bmatrix} C_i & 0 \\ 0 & I_{q_i} \end{bmatrix},$$

$$B_{i0} = \begin{bmatrix} B_i \\ 0 \end{bmatrix}, \ G_i = \begin{bmatrix} I_{n_i} \\ 0 \end{bmatrix}$$

Then the augmented system (5-33) can be simplified as:

$$\dot{\bar{x}}_i = \overline{A}_i \bar{x}_i + \overline{B}_i K_i \overline{C}_i \bar{x}_i + B_{i0}\big(v_i(t) + f_i(t, x_i, u_i)\big) + G_i h_i(x, t)$$
$$\bar{y}_i = \overline{C}_i \bar{x}_i \tag{5-34}$$

Because of the augmentation, the structure of the quadratic constraint for interactions, as described in Section 5.2, should be changed to:

$$h_i^T(x,t) G^T G h_i(x,t) = \bar{h}_i^T(\bar{x},t) \bar{h}_i(\bar{x},t) \le \alpha_i^2 \bar{x}^T \begin{bmatrix} H_i & 0 \\ 0 & 0 \end{bmatrix}^T \begin{bmatrix} H_i & 0 \\ 0 & 0 \end{bmatrix} \bar{x}$$

In the augmented state space, (Choi, 2008) gives the linear sliding surface function as:

$$\sigma_i = F_i \bar{y}_i = [F_{i1}, F_{i2}] \overline{C}_i \bar{x}_i = F_{i1} y + F_{i2} x_c \tag{5-35}$$

where $F_{i1} \in \mathbb{R}^{m_i \times p_i}$, $F_{i2} \in \mathbb{R}^{m_i \times q_i}$

The augment subsystems satisfy the Kimura-Davison constraint. Combining all of the augmented subsystems into the aggregate system, it yields:

$$\dot{\bar{x}} = \overline{A}\bar{x} + \overline{B}K\overline{C}\bar{x} + B_0\big(v(t) + f(t, x, u)\big) + \bar{h}(x, t)$$
$$\bar{y} = \overline{C}\bar{x} \tag{5-36}$$

where,

$$\overline{A} = diag(\overline{A}_1, \dots, \overline{A}_N), \overline{B} = diag(\overline{B}_1, \dots, \overline{B}_N), \overline{C} = diag(\overline{C}_1, \dots, \overline{C}_N)$$

$$B_0 = diag(B_{10}, \dots, B_{N0}), f(x, u, t) = [f_1^T(x_1, u_1, t), \dots, f_N^T(x_N, u_N, t)]^T$$

$$G = diag(G_1, \dots, G_N), \bar{h}(x, t) = \left[\bar{h}_1^T(x, t), \dots, \bar{h}_N^T(x, t)\right]^T$$

$x \in \mathbb{R}^{\bar{n}}$, $y \in \mathbb{R}^{\bar{p}}$ where $\bar{n} = n_1 + \cdots + n_N + q_1 + \cdots + q_N$ and $p = p_1 + \cdots + p_N + q_1 + \cdots + q_N$ are the numbers of the states and outputs respectively. The interconnection $h(x, t)$ for overall system is bounded as follows:

$$\bar{h}^T(\bar{x},t)\bar{h}(\bar{x},t) \le \bar{x}^T \left(\sum_{i=1}^{N} \alpha_i^2 \begin{bmatrix} H_i^T & 0 \\ 0 & 0 \end{bmatrix} \begin{bmatrix} H_i & 0 \\ 0 & 0 \end{bmatrix} \right) \bar{x} = \bar{x}^T \bar{H}^T \bar{H} \bar{x} \qquad (5\text{-}37)$$

In this case, solve the following LMI for the augmented overall system:

$$\bar{P}\bar{A} + \bar{A}^T \bar{P} + \bar{P}\bar{B}K\bar{C} + \bar{C}^T K^T \bar{B}^T \bar{P} < 0, \quad B_0^T \bar{P} = F\bar{C} \qquad (5\text{-}38)$$

The structure of the inequality (5-38) is similar with the inequality (5-8):

$$PA + A^T P + PP + H^T H + PBKC + C^T K^T B^T P < 0 \qquad (5\text{-}8)$$

Thus, the same algorithm described in Section 5.2 can be used. Here, an alternative method first proposed by (Choi, 2008) is extended to provide the elements of $\bar{P}$ matrix for the compensator without recourse to iteration. Furthermore, the coupled matrix $\bar{P}^{-1}$ can be calculated manually.

Extending Choi's $\bar{P}$ matrix design structure into decentralized form, it follows that:

$$\bar{P}_i = \begin{bmatrix} \tilde{B}_i W_{i1} \tilde{B}_i^T + C_i^T W_{i2} C_i & V_i \bar{N}_i \\ \bar{N}_i^T V_i^T & I \end{bmatrix} \qquad (5\text{-}39)$$

For which V_i and $\bar{N}_i$ are defined below.

Theorem 5.2 Define $W_1 = diag(W_{11}, \ldots, W_{1N})$, $W_2 = diag(W_{21}, \ldots, W_{2N})$ $X \in \mathbb{R}^{n \times n}$ are s.p.d. matrices with $W_{1i} \in \mathbb{R}^{(n_i - m_i) \times (n_i - m_i)}$, $W_{2i} \in \mathbb{R}^{p_i \times p_i}$. Considering the overall system (5-3), the problem (5-38) is solvable if the following LMIs are feasible:

Minimize $\sum_{i=1}^{N} \gamma_i$, subject to $P = \tilde{B} W_1 \tilde{B}^T + C^T W_2 C > 0, X > 0$

$$\begin{bmatrix} \tilde{B}^T(AX + XA^T + I)\tilde{B} & \tilde{B}^T XH_1^T & \cdots & \tilde{B}^T XH_N^T \\ H_1 X\tilde{B} & -\gamma_i I & \cdots & 0 \\ \vdots & \vdots & \ddots & \vdots \\ H_N X\tilde{B} & 0 & \cdots & -\gamma_N I \end{bmatrix} < 0 \qquad (5\text{-}40)$$

$$\begin{bmatrix} \tilde{C}^T(PA+A^TP)\tilde{C} & \tilde{C}^T H_1^T & \cdots & \tilde{C}^T H_N^T & \tilde{C}^T P \\ H_1\tilde{C} & -\gamma_i I & \cdots & 0 & 0 \\ \vdots & \vdots & \ddots & \vdots & \vdots \\ H_N\tilde{C} & 0 & \cdots & -\gamma_N I & 0 \\ P\tilde{C} & 0 & \cdots & 0 & -I \end{bmatrix} < 0 \qquad (5\text{-}41)$$

$$\begin{bmatrix} \tilde{B}^T W_1 \tilde{B} + C^T W_2 C & I \\ I & X \end{bmatrix} \geq 0 \qquad (5\text{-}42)$$

Proof:

($\Rightarrow$) Assume that (5-38) is feasible, then $\bar{P} = diag(\bar{P}_i), i = 1, \dots, N$. Then partition every $\bar{P}_i$ and its inverse matrix $\bar{\Pi}_i$ as:

$$\bar{P}_i = \begin{bmatrix} P_{i1} & P_{i2} \\ P_{i2}^T & P_{i3} \end{bmatrix}, \quad \bar{\Pi}_i = \begin{bmatrix} \Pi_{i1} & \Pi_{i2} \\ \Pi_{i2}^T & \Pi_{i3} \end{bmatrix} \qquad (5\text{-}43)$$

Using the matrix inversion lemma:

$$\begin{bmatrix} P_{i1} & P_{i2} \\ P_{i2}^T & P_{i3} \end{bmatrix}^{-1} = \begin{bmatrix} \left(P_{i1} - P_{i2}P_{i3}P_{i2}^T\right)^{-1} & \left(P_{i1} - P_{i2}P_{i3}P_{i2}^T\right)^{-1} P_{i2}P_{i3}^{-1} \\ -\left(P_{i3} - P_{i2}^T P_{i1}^{-1} P_{i2}\right)^{-1} P_{i2}^T P_{i1}^{-1} & \left(P_{i3} - P_{i2}^T P_{i1}^{-1} P_{i2}\right)^{-1} \end{bmatrix} \qquad (5\text{-}44)$$

It follows that

$$\left(P_{i1} - P_{i2}P_{i3}P_{i2}^T\right)^{-1} = \Pi_{i1} \qquad (5\text{-}45)$$

It is easily determined that $(P_{i2}P_{i3}P_{i2}^T)^{-1} > 0$, and this leads to (Choi, 2008):

$$P_{i1} \geq \Pi_{i1}^{-1} \qquad (5\text{-}46)$$

Since $P_{i1} = \tilde{B}_i W_{1i} \tilde{B}_i^T + C_i^T W_{2i} C_i \in \mathbb{R}^{n_i \times n_i}$ and $\Pi_{i1} = X_i$, considering the overall system and using the Schur complement, (5-46) can be rewritten as:

$$\begin{bmatrix} \tilde{B} W_1 \tilde{B}^T + C^T W_2 C & I_n \\ I_n & X \end{bmatrix} \geq 0 \qquad (5\text{-}47)$$

Using the partition (5-43) and Elimination Lemma (Projection Lemma), the LMIs (5-40) and (5-41) are easily determined.

($\Leftarrow$) If one can find solutions to the LMIs (5-40) to (5-42), it implies that $\tilde{B}_i W_{1i} \tilde{B}_i^T + C_i^T W_{2i} C_i \geq X_i^{-1}$. Moreover, further define $P_{i3} = I_{p_i}$. From (5-45), it gives:

$$P_{i2} P_{i2}^T = P_{i1} - X_i^{-1}$$

i.e.

$$P_{i2} P_{i2}^T = \tilde{B}_i W_{1i} \tilde{B}_i^T + C_i^T W_{2i} C_i - X_i^{-1} = M_i \qquad (5\text{-}48)$$

Using the diagonal decomposition, the matrix M_i can be expressed as:

$$M_i = V_i \Theta_i V_i^T \qquad (5\text{-}49)$$

where V_i and $\Theta_i = diag(\lambda_{ij})$ are the eigenvector matrix and the eigenvalues diagonal matrix for matrix M_i . Since M_i is an s.p.d matrix, $V_i^{-1} = V_i^T$. By defining $\overline{\Theta} = diag(\sqrt{\lambda_{ij}})$, the matrix P_{i2} can be given by:

$$P_{i2} = V_i \overline{\Theta}_i \qquad (5\text{-}50)$$

Thus, the matrix $\overline{P}_i$ can be written as

$$\overline{P}_i = \begin{bmatrix} \tilde{B}_i W_{i1} \tilde{B}_i^T + C_i^T W_{i2} C_i & V_i \overline{\Theta}_i \\ \overline{\Theta}_i^T V_i^T & I \end{bmatrix}$$

(Choi, 2008) also gives the inverse matrix of this matrix as:

$$\overline{P}_i^{-1} = \begin{bmatrix} X_i & -X_i P_{i2} \\ -P_{i2}^T X_i & I + P_{i2}^T X_i P_{i2} \end{bmatrix}$$

Moreover, the sliding surface matrix $F = diag(F_i), i = 1, \dots, N$ can be given with

$$F_i = \begin{bmatrix} B_i^T C_i^T W_{2i}, B_i^T V_i \overline{N}_i \end{bmatrix} \qquad (5\text{-}51)$$

such that the equation $B_0^T \overline{P} = F \overline{C}$ holds. Using the Elimination Lemma, the feasibility of LMIs (5-40) to (5-42) implies the existence of the control gain matrix K satisfying (5-38) with a given P. The proof completed. ∎

The stability of the system and the reachability of the sliding surface can be ensured by using the same proof as in Theorem 5.1. The compensator design algorithm is given as follows:

Algorithm 5.2

1) Design the augmented system (5-34);

2) Solve the LMIs (5-40) to (5-42) to get W_1, W_2, X and $W_{1i}, W_{2i}, X_i, i = 1, \dots, N$.

3) Use (5-48)-(5-50) to get the matrix P_{i2}, then calculate the s.p.d matrix $\bar{P}_i, i = 1, \dots, N$ for each augmented subsystem.

4) Solve (5-38) with the solution matrix W_1, W_2, X from step (2) and $\bar{P}$ from step 3 to get the controller matrix $K = diag(K_i), i = 1, \dots, N$;

5) Decompose the controller matrix K_i with $K_i = \begin{bmatrix} D_{ic} & C_{ic} \\ B_{ic} & A_{ic} \end{bmatrix}$ to get the gain matrices of each compensator.

6) Design the sliding surface with (5-51) and design the controller with (5-30)-(5-32).

The advantage of this method is that it is not necessary to solve the SOF problem described in Section 5.2. This means that the space complexity of the LMI problem is reduced. One can note that the orders of the LMIs (5-40) and (5-41) are less than the LMIs in SOF problem.

5.4 Output Integral sliding mode control

As we known, besides static output feedback and dynamic compensation, another method can be used to deal with output feedback problem, i.e. observer-based output feedback control. The main idea of observer based output feedback control is to use the well known "separation principle" through which the observer and state feedback designs can be made separately if and only if the state space model used for design is a precise model of the system. However, the Separation Principle cannot be used for designing the decentralized system because of the uncertainty arising from interactions between the subsystems. The interaction terms appear in both the state and observer error dynamics of the system. Some recent research has been done by (Kalsi, Lian and Żak, 2010), but they assumed that the interactions satisfy the "matching condition" for

the sliding mode observer. Although it is possible to recover the Separation Principle with a linear sliding surface, but this detail is omitted here since in this work local controllers use integral sliding mode surfaces, rather than the conventional linear sliding surface approach.

The concept of integral sliding mode (ISM) was proposed by (Utkin and Shi, 1996). In comparison with the conventional sliding surface design, ISM uses the same order as the original system. This implies that ISM does not separate the system into matched and unmatched subsystems. Although the state space is not partitioned as in the conventional sliding case, the feedback still compensate for the matched perturbations, whilst the unmatched perturbations still affect the closed-loop system behaviour.

The main advantage of ISM is that the robustness of the system can be guaranteed throughout an entire response of the system starting from time $t = 0$ (Utkin and Shi, 1996). The ISM was developed further by (Cataños and Fridman, 2005, 2006). They clarify the choice of integral sliding surface gain matrix and make it simple enough to be designed.

It is worth outlining here the main disadvantages of classical linear sliding compared with ISM control. In the classical case, the sliding mode drives the system to the sliding surface and once the system reaches this surface, the structure of the feedback loop is adaptively altered to slide the system states along the sliding surface. As discussed in Section 4.2 there is a reaching phase during which the matched uncertainties actually affect the system response, i.e. during the reaching phase there is no robustness. As stated above for the ISM case there is no reaching phase and hence by definition the sliding commences immediately and the matched uncertainty is decoupled from the system response.

A second advantage of the ISM control is that for the state feedback case as the sliding surface dimension is the same as the order of the system, the interaction between the designs of the liner feedback and the non-linear (switched) feedback is removed. This has an important consequence that the linear part of the feedback design can, in principle, be designed using a wide range of linear design methods and this facilitates a way of comparing the robustness behaviour of an uncertain linear state feedback system

with its ISM control counterpart. However, this only applies in the state feedback case. For output feedback the situation is more complex.

A disadvantage of the original ISM control formulation is that full knowledge of the system states is required. In other words, the ISM control (in its original form) is limited to state feedback control. (Bajarano, Fridman and Poznyak, 2007) was the first to propose an output feedback approach to ISM control. However, they considered only the matched perturbations for a single (i.e. centralized) system. This section proposes a novel output feedback ISM control (OISMC) strategy which can deal with unmatched perturbations, i.e. subsystem interactions and modelling uncertainty.

To state the strategy, re-consider the overall system in the form of (5-3):

$$\dot{x}(t) = Ax(t) + B(u(t) + f(x,u,t)) + h(x,t)$$
$$y = Cx \tag{5-3}$$

Assume that the triple (A, B, C) are the system matrices with appropriate dimensions with which assume the system is controllable and observable. The appropriate bounds on the matched perturbations and the interactions are given by (5-2) and (5-4), respectively.

$$\left\| f_i(x_i, u_i, t) \right\| < f_{iu} \left\| u_i \right\| + \varphi_i(y, t) \tag{5-2}$$

$$h^T(x,t)h(x,t) \leq x^T \left(\sum_{i=1}^{N} \alpha_i^2 H_i^T H_i \right) x = x^T H^T H x \tag{5-4}$$

An extra bound condition for the interactions term should be satisfied as follows:

$$\left\| h(x,t) \right\| \leq \omega_1 \left\| Cx \right\| + \omega_2$$

where ω_1 and ω_2 are known constants.

(Castaños and Fridman, 2006) proposed that every perturbation can be divided into matched and unmatched parts. Thus, partition the interactions $h(x,t)$ as:

$$h(x,t) = BB^+ h(x,t) + \tilde{B}\tilde{B}^+ h(x,t) \tag{5-52}$$

Following the standard sliding mode control principle the control law is designed with a linear component $u_0(t)$ and a non-linear component $u_1(t)$, so that $u(t) = u_0(t) + u_1(t)$. The linear control component is designed to make the sliding motion stable and having desired transient and steady-state behaviour. $u_1(t)$ is the nonlinear (discontinuous) part which is designed to force the closed-loop system trajectories to remain within the sliding surface.

The observer used here is the typical linear full-order Luenberger observer:

$$\dot{\hat{x}}(t) = A\hat{x}(t) + Bu_0(t) + L(y - \hat{y})$$
$$\hat{y}(t) = C\hat{x}(t) \tag{5-53}$$

where L is the observer gain matrix to be designed. The sliding surface appropriate to the output feedback case is:

$$\sigma(y,\hat{x},t) = \underbrace{G(y(t) - y(t_0))}_{\{1\}} - \underbrace{G\int_{t_0}^{t} CA\hat{x}(s) + CBu_0(s)ds}_{\{2\}} \tag{5-54}$$

There are two main terms in the sliding surface eq. of (5-54). The first part {1} is a linear combination of the system outputs whilst the second part {2} contains an integral term which is used to reject some unwanted terms of {1} in the analysing later. $G \in \mathbb{R}^{m \times n}$ is a projection matrix in diagonal form which satisfies the invertibility of GCB. Note that at $t = t_0$, the sliding surface function is identically zero, i.e. $\sigma = 0$, and hence the system trajectories start within the sliding manifold. The time derivative of the sliding surface (5-54) is given by:

$$\dot{\sigma}(y,\hat{x},t) = GC[Ax(t) + B(u(t) + f) + d(y,t)] - GCA\hat{x}(t) - GCBu_0(t)$$
$$= GCAe(t) + GCB(u_1(t) + f) + GCd(y,t) \tag{5-55}$$

It should be noted that $\sigma(y,\hat{x},t) = [\sigma_1^T(y_1,\hat{x}_1,t) \quad \dots \quad \sigma_N^T(y_N,\hat{x}_N,t)]^T$ which is a consequence of using the diagonal form for the G matrix.

As described above, the nonlinear discontinuous control law of the local subsystem is designed to keep maintain the motion within the sliding surface. This is designed as follows:

$$u_{i1}(t) = -\rho_i \frac{\sigma_i(y_i,\hat{x}_i,t)}{\|\sigma_i(y,\hat{x}_i,t)\|} \tag{5-56}$$

where ρ_i a suitable gain to be designed. As the system motion starts from the sliding surface, it must be proved that the time derivative of the Lyapunov function for the sliding surface is less than or equal to zero. Consider the Lyapunov function for the sliding surface as $V = 0.5 \sum_{i=1}^{N} \sigma_i^T \sigma_i$

When combined with (5-55), the time derivative of the Lyapunov function is given by:

$$
\begin{aligned}
\dot{V} &= \sum_{i=1}^{N} \sigma_i^T \left(G_i C_i A_i e_i(t) + G_i C_i B_i (u_{i1}(t) + f_i(x_i,u_i,t)) + G_i C_i h_i(x,t) \right) \\
&= \sum_{i=1}^{N} \sigma_i^T \left(G_i C_i B_i \right) \left[(G_i C_i B_i)^{-1} (G_i C_i A_i e_i(t) + G_i C_i h_i(x,t)) + u_{i1}(t) + f_i(x_i,u_i,t) \right] \\
&\leq \sum_{i=1}^{N} \|\sigma_i\| \|G_i C_i B_i\| \left[\begin{array}{l} \left\| (G_i C_i B_i)^{-1} \right\| \left(\|G_i C_i A_i e_i\| + \|G_i C_i\| (\omega_1 \|y\| + \omega_2) \right) - \rho_i \\ + f_{iu} \|u_i\| + \varphi_i(y,t) \end{array} \right]
\end{aligned}
$$

$$\tag{5-57}$$

Then by choosing

$$\rho_i \geq \left\| (G_i C_i B_i)^{-1} \right\| \left(\|G_i C_i A_i e_i\| + \|G_i C_i\| (\omega_1 \|y\| + \omega_2) \right) + f_{iu} \|u_i\| + \varphi_i(y,t) + \eta \tag{5-58}$$

where η is a positive scalar, it follows:

$$\dot{V} \leq -\|\sigma\| \|GCB\| \eta \leq 0$$

From Chapter 4, it can be understood that the system trajectories will stay within the sliding surface. Since there is an unmeasured varying parameter $e_i(t)$ in (5-58), the gain ρ_i cannot be easily chosen. However, if one can assume that the Euclidean norm of the initial estimation error $\|e_i(t)\|$ is bounded by a realistic value e_{init} then (5-58) can be changed to:

$$\rho_i \geq \left\| (G_i C_i B_i)^{-1} \right\| \left(\|G_i C_i A_i\| e_{init} + \|G_i C_i\| (\omega_1 \|y\| + \omega_2) \right) + f_{iu} \|u_i\| + \varphi_i(y,t) + \eta_i \tag{5-59}$$

To ensure that the sliding motion is maintained, it is also necessary to assume a large enough value for the scalar η_i. Moreover, it is necessary to prove that the system

estimation error is decreasing in order to make sure that the inequality (5-58) is always guaranteed. This proof involves the design of a linear control law and linear observer gain matrix.

When the overall system is running in the sliding surface, i.e. $\sigma(y, \hat{x}, t) = 0$ and $\dot{\sigma}(y, \hat{x}, t) = 0$, using the equivalent control method, it gives:

$$u_{eq}(t) = -(GCB)^{-1} GC(Ae(t) + h(x,t)) - f(x,u,t) \qquad (5\text{-}60)$$

Using the equivalent control (5-60), the sliding motion is then given by:

$$\dot{x}(t) = Ax(t) + Bu_0(t) + (I - B(GCB)^{-1}GC)h(x,t) - B(GCB)^{-1}GCAe(t)$$

According to (Castaños and Fridman, 2006), using the projection lemma, the best way to design the sliding gain matrix is $GC = B^T$ or $GC = B^+$, in this case, the magnitude of unmatched uncertainties would not be amplified. Hence, choose:

$$G = B^T C^+ \text{ and } (I - B(GCB)^{-1}GC) = I - BB^+$$

where $G = diag(G_1, ..., G_2)$ and $G_i = B_i^T C_i^+, i = 1, ..., N$.

By defining $M = (I - BB^+)$ and $\Lambda = BB^+A$, the sliding motion can then be rewritten as:

$$\dot{x}(t) = Ax(t) + Bu_0(t) + Mh(x,t) - \Lambda e(t) \qquad (5\text{-}61)$$

From (5-61), it can be seen that the matched perturbations $f_i(x_i, u_i, t)$ have been rejected completely. Also it is possible to attempt to minimize the effect of the unmatched component with the linear control law $u_0(t)$. This provides some additional design freedoms that can be used for example to improve the robustness to the unmatched perturbations. However, the order of the sliding dynamics is equal to the order of system states and this itself may be a slight disadvantage.

The design of the linear control law $u_0(t) = K\hat{x}(t)$ is discussed in the rest of this Section.

Since the system is running in the sliding surface, and from the sliding motion defined by (5-61), the error system in the sliding surface is given by:

$$\dot{e}(t) = (A - LC)e(t) + Mh(x,t) - \Lambda e(t) \tag{5-62}$$

By combining (5-61) and (5-62) the augmented system is derived as:

$$\bar{\dot{x}}(t) = \begin{bmatrix} \dot{x}(t) \\ \dot{e}(t) \end{bmatrix} = \begin{bmatrix} A + BK & -BK - \Lambda \\ 0 & A - LC - \Lambda \end{bmatrix} \begin{bmatrix} x(t) \\ e(t) \end{bmatrix} + \begin{bmatrix} M \\ M \end{bmatrix} h(x,t) \tag{5-63}$$

then considering the Lyapunov function for the augment system:

$$V(x,t) = \bar{x}^T(t) P \bar{x}(t)$$

where $P = diag(P_1, P_2)$, $P_1 = diag(P_{1i})$, $P_2 = diag(P_{2i}), i = 1, \dots, N$ are s.p.d. matrices, along with their matrix components. The time derivative of the Lyapunov function is:

$$\dot{V}(x,t) = \bar{x}^T(t) P \dot{\bar{x}}(t) + \dot{\bar{x}}^T(t) P \bar{x}(t) \tag{5-64}$$

$$\dot{V}(x,e,t) = \begin{bmatrix} x \\ e \end{bmatrix}^T \begin{bmatrix} P_1 A + A^T P_1 + P_1 BK + K^T B^T P_1 & -P_1 BK - P_1 \Lambda \\ -K^T B^T P_1 - \Lambda^T P_1 & \Sigma \end{bmatrix} \begin{bmatrix} x \\ e \end{bmatrix}$$
$$+ \begin{bmatrix} x \\ e \end{bmatrix}^T \begin{bmatrix} P_1 M \\ P_2 M \end{bmatrix} h + h^T \begin{bmatrix} M^T P_1 & M^T P_2 \end{bmatrix} \begin{bmatrix} x \\ e \end{bmatrix}$$

where: $\Sigma = P_2 A + A^T P_2 - P_2 LC - C^T L^T P_2 - P_2 \Lambda - \Lambda^T P_2$

i.e.

$$\dot{V}(x,t) = \begin{bmatrix} x \\ e \\ h \end{bmatrix}^T \Pi \begin{bmatrix} x \\ e \\ h \end{bmatrix} \tag{5-65}$$

where:

$$\Pi = \begin{bmatrix} \Pi_1 & -P_1 BK - P_1 \Lambda & P_1 M \\ -K^T B^T P_1 - \Lambda^T P_1 & \Pi_2 & P_2 M \\ M^T P_1 & M^T P_2 & 0 \end{bmatrix}$$

with:

$$\Pi_1 = P_1 A + A^T P_1 + P_1 BK + K^T B^T P_1$$

$$\Pi_2 = P_2 A + A^T P_2 - P_2 LC - C^T L^T P_2 - P_2 \Lambda - \Lambda^T P_2$$

The objective is to make the time derivative of the Lyapunov function (5-65) negative. However, the inequality $\Pi < 0$ is difficult to achieve because of the structure of Π.

To solve this, the quadratic constraint:

$$h^T(x,t)h(x,t) \leq x^T \left(\sum_{i=1}^{N} \alpha_i^2 H_i^T H_i \right) x = x^T H^T H x \tag{5-4}$$

 is used to achieve a quadratic form:

$$\begin{bmatrix} x \\ e \\ d \end{bmatrix}^T \begin{bmatrix} H^T H & 0 & 0 \\ 0 & 0 & 0 \\ 0 & 0 & I \end{bmatrix} \begin{bmatrix} x \\ e \\ d \end{bmatrix} \leq 0 \tag{5-66}$$

Then by using the S-procedure of (Boyd *et al*, 1993), combine (5-65) and (5-66) into one inequality with a positive scalar τ:

$$\begin{bmatrix} \Pi_1 + \tau H^T H & -P_1 BK - P_1 \Lambda & P_1 M \\ -K^T B^T P_1 - \Lambda^T P_1 & \Pi_2 & P_2 M \\ M^T P_1 & M^T P_2 & -\tau I \end{bmatrix} < 0 \tag{5-67}$$

where $\Pi_1 = P_1 A + A^T P_1 + P_1 BK + K^T B^T P_1$

$$\Pi_2 = P_2 A + A^T P_2 - P_2 LC - C^T L^T P_2 - P_2 \Lambda - \Lambda^T P_2$$

Now the problem becomes:

Find $P_1 > 0$, $P_2 > 0$, K, L such that (5-67) is satisfied (5-68)

In this case, the time derivative of Lyapunov function $\dot{V}(x,e,t) < 0$, which implies asymptotic stability of both the error and the original systems. Two strategies can be applied to solve the problem (5-68).

Strategy 1:

The scalar parameter τ can be eliminated by defining $F_1 = 1/\tau\, P_1$ and $F_2 = 1/\tau\, P_2$. Moreover, define $Y = F_1^{-1}$, $W_1 = KY$, $W_2 = F_2 L$ and pre- and post- multiply the block diagonal matrix $\begin{bmatrix} Y & 0 & 0 \\ 0 & I & 0 \\ 0 & 0 & I \end{bmatrix}$. The inequality (5-67) can be rewritten as:

$$
\begin{bmatrix}
\Pi_1^* + YH^T HY & -BK - \Lambda & M \\
-K^T B^T - \Lambda^T & \Pi_2^* & F_2 M \\
YM^T & M^T F_2 & -I
\end{bmatrix} < 0
\tag{5-69}
$$

where:

$$\Pi_1^* = AY + YA^T + BW_1 + W_1^T B^T$$

$$\Pi_2^* = F_2 A + A^T F_2 - W_2 C - C^T W_2^T - F_2 \Lambda - \Lambda^T F_2$$

It should be noted that the both W_1 and W_2 are in block diagonal form, i.e. $W_1 = diag(W_{1i})$, $W_2 = diag(W_{2i})$, $i = 1, \dots, N$.

Since there are coupled matrices Y, W_1 and K in the inequality (5-69), it cannot be solved with conventional LMI approach. However, this problem is similar to the linear observer based decentralized linear control problem of (Zhu and Pagilla, 2007) which can be solved by the following algorithm

Algorithm 5.3:

Step 1. Solve the LMIs problem:

Minimize $\sum_{i=1}^{N} \gamma_i + \kappa_Y + \kappa_{W1}$, subject to $Y = diag(Y_i) > 0, \kappa_Y, \kappa_{W1} > 0$

$$
Q = \begin{bmatrix}
AY + YA^T + BW_1 + W_1^T B^T & YH_1^T & \cdots & YH_N^T \\
H_1 Y & -\gamma_1 I & \cdots & 0 \\
\vdots & \vdots & \ddots & \vdots \\
H_N Y & 0 & \cdots & -\gamma_N I
\end{bmatrix} < 0
$$

$$\begin{bmatrix} Y & I \\ I & \kappa_Y I \end{bmatrix} > 0, \quad \begin{bmatrix} -\kappa_{W1}I & W_1 \\ W_1^T & -I \end{bmatrix} < 0 \tag{5-70}$$

Step 2. Get the control gain matrix $K = W_1 Y^{-1}$ from the solution to (5-70).

Step 3. Fix K, Y, and W_1 and solve the following LMIs

Minimize $\sum_{i=1}^{N} \beta_i + \kappa_F + \kappa_{W2}$, subject to $F_2 > 0, \kappa_F, \kappa_{W2} > 0$

$$\begin{bmatrix} \Phi Q & -BK - \Lambda & M \\ -K^T B^T - \Lambda^T & F_2 A + A^T F_2 - W_2 C - C^T W_2^T - F_2 \Lambda - \Lambda^T F_2 & F_2 M \\ Y M^T & M^T F_2 & -I \end{bmatrix} < 0$$

$$\begin{bmatrix} F_2 & I \\ I & \kappa_F I \end{bmatrix} > 0, \quad \begin{bmatrix} -\kappa_{W2}I & W_2 \\ W_2^T & -I \end{bmatrix} < 0 \tag{5-71}$$

where $\Phi = diag(\beta_1 I_{n_1}, \dots, \beta_N I_{n_N}, \beta_1 I_{n_1}, \dots, \beta_N I_{n_N})$

Step 4. Get the observer gain matrix $L = F_2^{-1} W_2$

Remark: The LMIs involving $\kappa_Y, \kappa_{W1}, \kappa_F, \kappa_{W2}$ are considered as optimization constraints. These constraints were first proposed by (Šiljak and Stipanović, 2000), for the purpose of choosing the appropriate size of the gain matrices K and L.

The feasibility of (5-70) has been proved in Chapter 4. Moreover, with large enough β_i, the feasibility of (5-71) can be ensured. The sufficient condition for the feasibilities of LMIs (5-70) and (5-71) is that the controllability and observability of each subsystem triple (A_i, B_i, C_i) is ensured. This algorithm is similar to the one given in (Zhu and Pagilla, 2007)., although in this work the output feedback problem involves the ISM control system (rather than purely linear system).

Strategy 2

Eliminate τ by defining $F_1 = 1/\tau P_1$ and $F_2 = 1/\tau P_2$. And defining $Y = F_1^{-1}$, $W_1 = KY$, $W_2 = F_2 L$. Then the inequality (5-67) can be re-written as:

$$\begin{bmatrix} \Sigma_{11} & \Sigma_{12} \\ \Sigma_{12}^T & \Sigma_{22} \end{bmatrix} < 0 \tag{5-72}$$

where:

$$\Sigma_{11} = F_1 A + A^T F_1^T + F_1 BK + K^T B^T F + H^T H$$

$$\Sigma_{12} = \begin{bmatrix} -F_1 BK - F_1 \Lambda & F_1 M \end{bmatrix}$$

$$\Sigma_{22} = \begin{bmatrix} F_2 A + A^T F_2 - W_2 C - C^T W_2^T - F_2 \Lambda - \Lambda^T F_2 & F_2 M \\ M^T F_2 & -I \end{bmatrix}$$

Pre- and post- multiplying the inequality (5-72) by the matrix $\mathcal{W} = diag(Y, \mathcal{V})$ where $\mathcal{V} = diag(Y, I)$, it gives:

$$\begin{bmatrix} Y\Sigma_{11}Y & Y\Sigma_{12}\mathcal{V} \\ \mathcal{V}\Sigma_{12}^T Y & \mathcal{V}\Sigma_{22}\mathcal{V} \end{bmatrix} < 0$$

From (Ichalal *et al*, 2010) that:

$$\mathcal{V}\Sigma_{22}\mathcal{V} \le -\mu(\mathcal{V} + \mathcal{V}^T) - \mu^2 \Sigma_{22}$$

Thus, using the Schur complement lemma, rewrite the inequality (5-72) as:

$$\begin{bmatrix} Y\Sigma_{11}Y & Y\Sigma_{12}\mathcal{V} & 0 \\ \mathcal{V}\Sigma_{12}^T Y & -2\mu\mathcal{V} & \mu I \\ 0 & \mu I & \Sigma_{22} \end{bmatrix} < 0$$

Then the LMI can be further written as:

$$\begin{bmatrix}
\Pi_1^* & -BW_1 - \Lambda Y & M & 0 & 0 & YH_1^T & \cdots & YH_N^T \\
-W_1^T B^T - Y\Lambda^T & -2\mu Y & 0 & \mu I & 0 & 0 & \cdots & 0 \\
M^T & 0 & -2\mu I & 0 & \mu I & 0 & \cdots & 0 \\
0 & \mu I & 0 & \Pi_2^* & F_2 M & 0 & \cdots & 0 \\
0 & 0 & \mu I & M^T F_2 & -I & 0 & \cdots & 0 \\
H_1 Y & 0 & 0 & 0 & 0 & -\lambda_1 I & \cdots & 0 \\
\vdots & \vdots & \vdots & \vdots & \vdots & \vdots & \ddots & \vdots \\
H_N Y & 0 & 0 & 0 & 0 & 0 & \cdots & -\lambda_N I
\end{bmatrix} < 0$$

(5-73)

where

$$\Pi_1^* = AY + YA^T + BW_1 + W_1^T B$$

$$\Pi_2 = F_2 A + A^T F_2 - W_2 C - C^T W_2^T - F_2 \Lambda - \Lambda^T F_2$$

Moreover, when combined with the restriction matrices for Y, F_2, K and L in Strategy 1, the solution to the problem (5-68) is given by solving an appropriate set of LMIs as follows:

$$\text{Minimize } \sum_{i=1}^{N} \gamma_i + \kappa_F + \kappa_Y + \kappa_{W1} + \kappa_{W2}, \text{ subject to} \qquad \text{(5-73) and}$$

$$F_2, Y > 0, \kappa_Y, \kappa_{W1}, \kappa_F, \kappa_{W2} > 0,$$

$$\begin{bmatrix} F_2 & I \\ I & \kappa_F I \end{bmatrix} > 0, \begin{bmatrix} -\kappa_{W2} I & W_2 \\ W_2^T & -I \end{bmatrix} < 0, \begin{bmatrix} Y & I \\ I & \kappa_Y I \end{bmatrix} > 0, \begin{bmatrix} -\kappa_{W1} I & W_1 \\ W_1^T & -I \end{bmatrix} < 0 \quad \text{(5-74)}$$

By using either Strategy 1 or Strategy 2 the main results can be derived as stated by the following Theorem:

Theorem 5.3. For the overall system (5-3), design the observer:

$$\dot{\hat{x}}(t) = A\hat{x}(t) + Bu_0(t) + L(y - \hat{y})$$
$$\hat{y}(t) = C\hat{x}(t) \qquad \qquad \text{(5-53)}$$

and the sliding surface:

$$\sigma(y, \hat{x}, t) = G(y(t) - y(t_0)) - G \int_{t_0}^{t} CA\hat{x}(s) + CBu_0(s)ds \qquad \text{(5-54)}$$

The system is asymptotically stable with the control law:

$$u_i(t) = K_i \hat{x}_i - \rho_i \frac{\sigma_i(y_i, \hat{x}_i, t)}{\|\sigma_i(y, \hat{x}_i, t)\|}$$

where ρ_i satisfies the constraint:

$$\rho \geq \left\| (G_i C_i B_i)^{-1} \right\| \left(\|G_i C_i A_i\| e_{init} + \|G_i C_i\| (\omega_1 \|y\| + \omega_2) \right) + f_{iu} \|u_i\| + \varphi_i(y, t) + \eta_i \quad \text{(5-59)}$$

if the problem (5-68) can be solved by **Strategy 1** or **Strategy 2**.

The matrices Y and F_2 solved by both algorithms are s.p.d. matrices. Moreover, the matrices Y, F_2, W_1, W_2 are in the block diagonal form such that $Y = diag(Y_i)$, $F_2 =$

$diag(F_{2i})$, $W_1 = diag(W_{1i})$, $W_2 = diag(W_{2i}), i = 1, ..., N$ and $Y_i, F_{2i} \in \mathbb{R}^{n_i \times n_i}$
$W_{1i} \in \mathbb{R}^{m_i \times n_i}, W_{2i} \in \mathbb{R}^{n_i \times p_i}$.

The control gain matrix K_i and the observer gain matrix L_i can be given by: $K = W_{1i} Y_i^{-1}$ and $L = F_{2i}^{-1} W_{2i}$.

The proof can be easily obtained from the discussion in this Section.

Note that if the problem (5-68) is solvable, $\dot{V}(x, e, t) < 0$, which also implies that the errors states $e(t)$ keep decreasing during the system operation. Thus, the inequality (5-58) is ensured with the gain ρ_i designed from (5-59).

The adaptive mechanism cannot normally be applied in this OISMC method. The reason is that this method requires that the sliding surface should be reached from the beginning. To achieve this, a large enough gain to keep the system running in the sliding surface from initial time should be given initially. However, the adaptive mechanism introduced in Chapter 4 has the property that the gain increases if the sliding surface is not reached. Hence, by defining a sufficiently large values of ρ_i, the adaptive mechanism is not necessary.

5.5   Multi-machine power system case study

The multi-machine power system has been widely used to illustrate the decentralized methods. The interactions of this system are nonlinear which makes the development of a suitable decentralized output feedback control system more challenging. Various papers have described this problem (Guo Hill and Wang, 2000; Šiljak, Stipanović and Zečević, 2002; Zecivic and Šiljak, 2004; Zhu and Pagilla, 2007; Tlili and Braiek, 2009; Kalsi Lian and Żak, 2009, etc). One of the important reasons why this system is used as a case study is to illustrate how to construct the quadratic constraint for the interactions.

5.5.1 System description

An *N*-machine power system with steam valve control can be described by the interconnection of *N* subsystems, under the form of (5-1). Let $x_i = [\Delta\delta_i(t) \quad \omega_i(t) \quad \Delta P_{m_i}(t) \quad \Delta X_{e_i}(t)]^T$ denote the state vector of each machine. The dynamics of *i*-th machine, $i = 1, ..., N$, can be represented as follows (Tlili and Braiek, 2009):

$$\dot{x}_i(t) = A_i x_i(t) + B_i u_i(t) + h_i(x, t)$$
$$y_i(t) = C_i x_i(t)$$

<div align="right">(5-75)</div>

where $h_i(x, t) = \sum_{j=1, j \neq i}^{N} p_{ij} G_{ij} g_{ij}(x_i, x_j)$ is a nonlinear vector function characterizing the interactions between the subsystems. The subsystem state space parameters are given as:

$$A_i = \begin{bmatrix} 0 & 1 & 0 & 0 \\ 0 & -\dfrac{D_i}{2H_i} & \dfrac{\omega_o}{2H_i} & 0 \\ 0 & 0 & -\dfrac{1}{T_{mi}} & \dfrac{K_{mi}}{T_{mi}} \\ 0 & \dfrac{-K_{ei}}{T_{ei}R_i\omega_o} & 0 & -\dfrac{1}{T_{ei}} \end{bmatrix}, \ B_i = \begin{bmatrix} 0 \\ 0 \\ 0 \\ \dfrac{1}{T_{ei}} \end{bmatrix}, \ C_i^T = \begin{bmatrix} 1 \\ 0 \\ 0 \\ 0 \end{bmatrix}, \ G_{ij} = \begin{bmatrix} 0 \\ -\dfrac{\omega_o E_{qi}' E_{qj}' B_{ij}}{2H_i} \\ 0 \\ 0 \end{bmatrix}$$

The interactions between the subsystems are defined as $g_{ij}(x_i, x_j) = \sin\left(\delta_i(t) - \delta j t - \sin\left(\delta i 0 - \delta j 0\right)\right)$

The physical meanings of the parameters of system (5-75) are defined by the following:

- $\Delta\delta_i(t) = \delta_i(t) - \delta_{i0};$

- $\Delta P_{m_i}(t) = P_{m_i}(t) - P_{m_{i0}}$

- $\Delta X_{e_i}(t) = X_{e_i}(t) - X_{e_{i0}}$

- $u_i(t)$ is the control vector of i-th subsystem;

- $y_i(t)$ is the output vector of the i-th subsystem;

- $\delta_i(t)$ is the rotor angle for the i-th machine, in radians;

- $\omega_i(t)$ is the relative speed for the i-th machine, in radians;

- $P_{m_i}(t)$ is the per unit mechanical power for i-th machine;

- $X_{e_i}(t)$ is the per unit steam valve aperture for i-th machine;

- p_{ij} is a constant of either 1 or 0 ($p_{ij} = 0$ means there is no connection between the i-th and j-th machines);

- H_i is the inertia time constant for the i-th machine, in seconds;

- D_i is per unit damping coefficient for i-th machine;

- T_{m_i} is time constant for i-th machine's turbine, in seconds;

- K_{m_i} is the gain of i-th machine's turbine;

- T_{e_i} is time constant for the i-th machine's speed governor, in seconds;

- K_{e_i} is the gain of the i-th machine's speed governor;

- R_i is per unit regulation constant for the i-th machine;;

- B_{ij} is per unit nodal susceptance between the i-th and j-th machines;

- ω_o is the synchronous machine speed, $\omega_o = 2\pi f_0$, in radians·s^{-1};

- E'_{qi} is the per unit internal transient voltage for the i-th machine (assumed constant);

- $\delta_{i0}, P_{m_{io}}, X_{e_{io}}$ are the nominal values of $\delta_i(t), P_{m_i}(t), X_{e_i}(t)$.

In this study a 3-machine system is used and the structure of this system is shown in Figure 5-1.
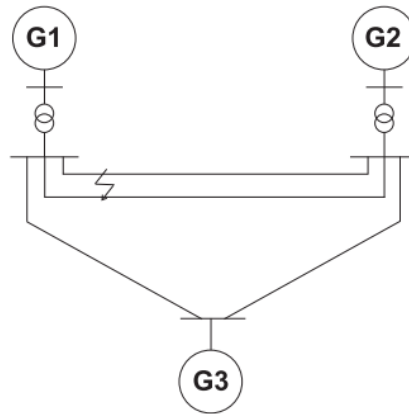
Figure 5-1. Three-machine power system

Before designing an output feedback decentralized control in this model, the quadratic constraint for interactions should be determined first. (Kalsi, Lian and Żak, 2009).

Define $\alpha_{ij} = -\frac{\omega_o E'_{qi} E'_{qj} B_{ij}}{2H_i}$ and $p_{ij} = 1, i, j = 1,2,3, i \neq j$ for each of the interconnected machines. The interaction terms can be written as $h_i(x,t) = \sum_{j=1,j\neq i}^{N} p_{ij} G_{ij} g_{ij}(x_i, x_j) = \sum_{j=1,j\neq i}^{N} \alpha_{ij} g_{ij}(x_i, x_j)$. Applying standard trigonometric identities, interaction terms can be represented as:

$$h_i(x,t) = [0 \quad 1 \quad 0 \quad 0]^T \sum_{j=1, j \neq i}^{N} \alpha_{ij} \gamma_{ij} sin\omega_{ij}$$

where $\gamma_{ij} = 2\cos(0.5(\delta_i(t) - \delta_j(t) + \delta_{i0} - \delta_{j0}))$ and

$$\omega_{ij} = 0.5(\Delta\delta_i - \Delta\delta_j) = 0.5(x_{i1} - x_{j1}), j \neq i$$

Define:

$$\gamma_i = [\gamma_{i1} \quad \cdots \quad \gamma_{i(i-1)} \quad \gamma_{i(i+1)} \quad \cdots \quad \gamma_{iN}]^T$$

$$\mathcal{U}_i = diag(\alpha_{i1}, \dots, \alpha_{i(i-1)}, \alpha_{i(i+1)}, \dots, \alpha_{iN})$$

$$z_i = [sin\omega_{i1} \quad \cdots \quad sin\omega_{i(i-1)} \quad sin\omega_{i(i+1)} \quad \cdots \quad sin\omega_{iN}]^T$$

It then follows that $h_i^T(x,t) h_i(x,t) = z_i^T \Theta_i z_i$, where $\Theta_i = \mathcal{U}_i \gamma_i \gamma_i^T \mathcal{U}_i^T$. Assuming that $\alpha_{ij}, i,j = 1, \dots, N, i \neq j$ are constants, the elements of Θ_i, θ_{kj} can be easily obtained which satisfy $|\theta_{kj}| \leq 4\alpha_{ik_{max}}\alpha_{ij_{max}}$. On the other hand, applying the inequality:

$$|\sin \omega_{ij}||\sin \omega_{ik}| \leq \frac{\omega_{ij}^2 + \omega_{ik}^2}{2}$$

leads to the quadratic form $h_i^T(x,t) h_i(x,t) \leq \bar{\omega}_i^T \mathcal{D}_i \bar{\omega}_i$, where:

$$\bar{\omega}_i = [\omega_{i1} \quad \cdots \quad \omega_{i(i-1)} \quad \omega_{i(i+1)} \quad \cdots \quad \omega_{iN}]^T$$

$$\mathcal{D}_i = diag(d_{i1}, \dots, d_{i(i-1)}, d_{i(i+1)}, \dots, d_{iN})$$

with $d_{ik} = 4\alpha_{ik_{max}} \sum_{j=1, j \neq i}^{N} \alpha_{ij_{max}} > 0$

For an N-machine system, see (Kalsi Lian and Żak, 2009) the interactions can be derived in a systematic way. As a special case for the three-machine power system, the quadratic constraints can be written manually as:

$$\mathcal{D}_1^{1/2} \bar{\omega}_1 = 0.5 \begin{bmatrix} d_{12}^{1/2} & 0_3^T & -d_{12}^{1/2} & 0_3^T & 0 & 0_3^T \\ d_{13}^{1/2} & 0_3^T & 0 & 0_3^T & -d_{13}^{1/2} & 0_3^T \end{bmatrix} x = H_1 x$$

$$\mathcal{D}_2^{1/2} \bar{\omega}_2 = 0.5 \begin{bmatrix} -d_{21}^{1/2} & 0_3^T & d_{21}^{1/2} & 0_3^T & 0 & 0_3^T \\ 0 & 0_3^T & d_{23}^{1/2} & 0_3^T & -d_{23}^{1/2} & 0_3^T \end{bmatrix} x = H_2 x$$

$$\mathcal{D}_3^{1/2}\bar{\omega}_3 = 0.5 \begin{bmatrix} -d_{31}^{1/2} & 0_3^T & 0 & 0_3^T & d_{31}^{1/2} & 0_3^T \\ 0 & 0_3^T & -d_{32}^{1/2} & 0_3^T & d_{32}^{1/2} & 0_3^T \end{bmatrix} x = H_3 x$$

The parameters are the same as given in (Tlili and Braiek, 2009)

Table 5-1. The parameters of the power system with three interconnected machines

Parameter	Machine 1	Machine 2	Machine 3
H(s)	4	5.1	5.1
D(pu)	5	3	3
T_m(s)	0.35	0.35	0.35
T_e(s)	0.1	0.1	0.1
R	0.05	0.05	0.05
K_m	1	1	1
K_e	1	1	1
ω_o $(rad \cdot s^{-1})$	314.159	314.159	314.159

Moreover, the parameters $\alpha_{ij_{max}}$ are given by (Wang, Hill and Guo, 1998; Kalsi Lian and Żak, 2009; Tlili and Braiek, 2009) as follows:

$$\alpha_{12_{max}} = \alpha_{13_{max}} = 27.49, \alpha_{21_{max}} = \alpha_{23_{max}} = \alpha_{32_{max}} = \alpha_{31_{max}} = 23.10$$

Some work on static output feedback control on multi-machine power systems has been reported (Yan *et al*, 2004). However, the model they used is a simplified system (the order of their subsystem is 3 instead of 4). To illustrate the static output feedback method proposed in this Chapter it is assumed that the steam valve opening variations can be measured. In this case, the condition $rank(CB) = rank(B)$ is satisfied. Moreover, to use static output feedback, assume that the relative speed is measured in order to make the static output feedback method available. The output matrix can be written as:

$$C_i = \begin{bmatrix} 1 & 0 & 0 & 0 \\ 0 & 1 & 0 & 0 \\ 0 & 0 & 0 & 1 \end{bmatrix}$$

5.5.2 Static output feedback sliding mode control

Using Algorithm 5.1, solve the K_i matrix for each subsystem such that:

$$K_1 = [-133.02 \quad -89.793 \quad -149.44]$$

$$K_2 = [-159.59 \quad -113.22 \quad -174.87]$$

$$K_3 = [-70.738 \quad -79.694 \quad -124.66]$$

The sliding surface gain matrices F_i are also given by:

$$F_1 = [-0.587 \quad -0.406 \quad -0.689], \quad F_2 = [-0.564 \quad -0.408 \quad -0.639]$$

$$F_3 = [-0.504 \quad -0.577 \quad -0.917]$$

Using the control law aims structure given in section 5.2, the time responses of the states of this multi-machine system are shown in Figure 5-2 to Figure 5-5. These show that with this static output feedback control, the system is stabilized. If consider an actuator fault in Subsystem 1, for which a step signal is applied to the steam valve aperture variation, the system is shown to be insensitive to this fault with SOF SMC.
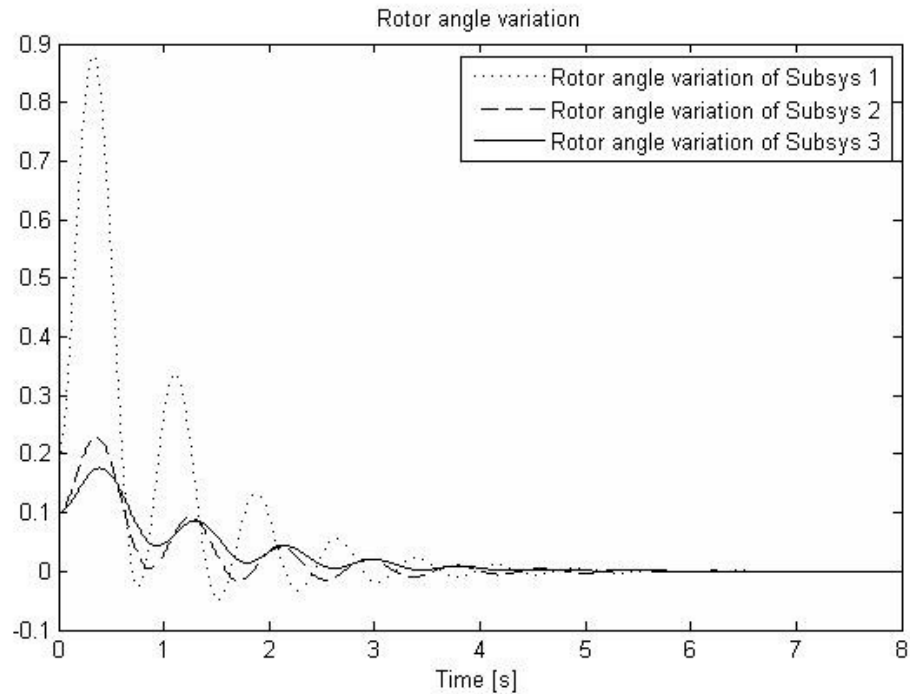
Figure 5-2. Stabilized power system states $\Delta\delta_i, i = 1,2,3$ for 3 interconnected systems
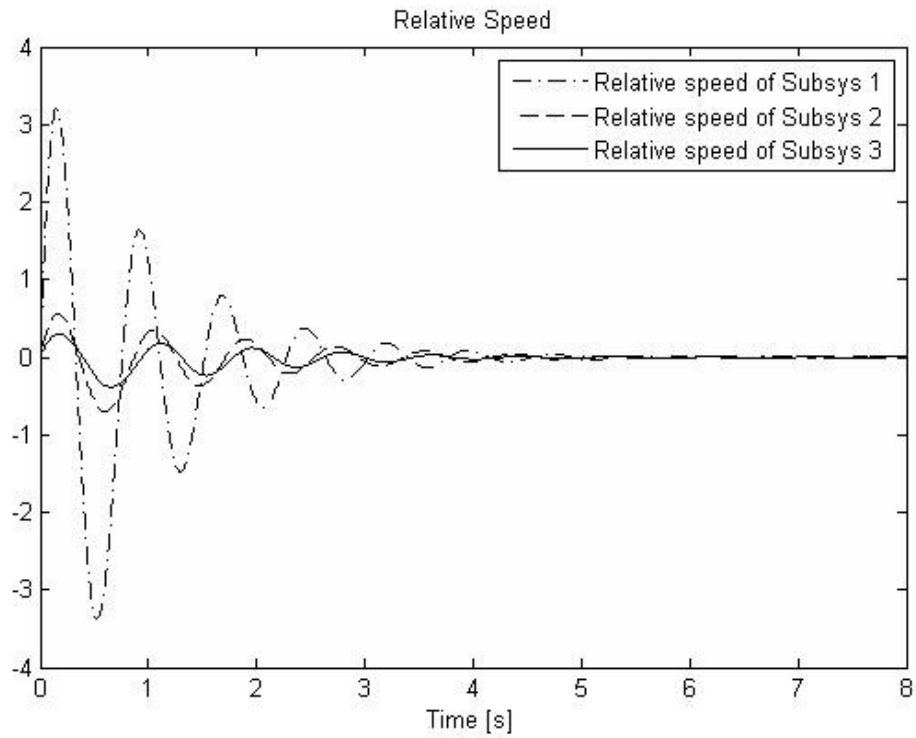
Figure 5-3. Stabilized power system states $\omega_i, i = 1,2,3$ for 3 interconnected systems
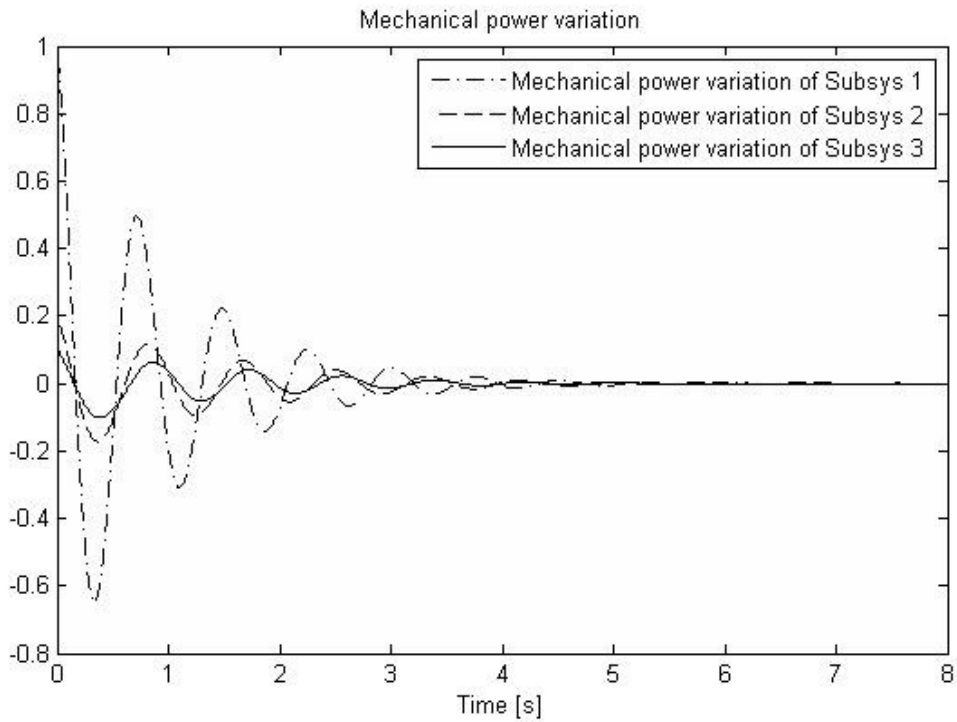
Figure 5-4. Stabilized power system states $\Delta P_{m_i}, i = 1,2,3$ for 3 interconnected systems
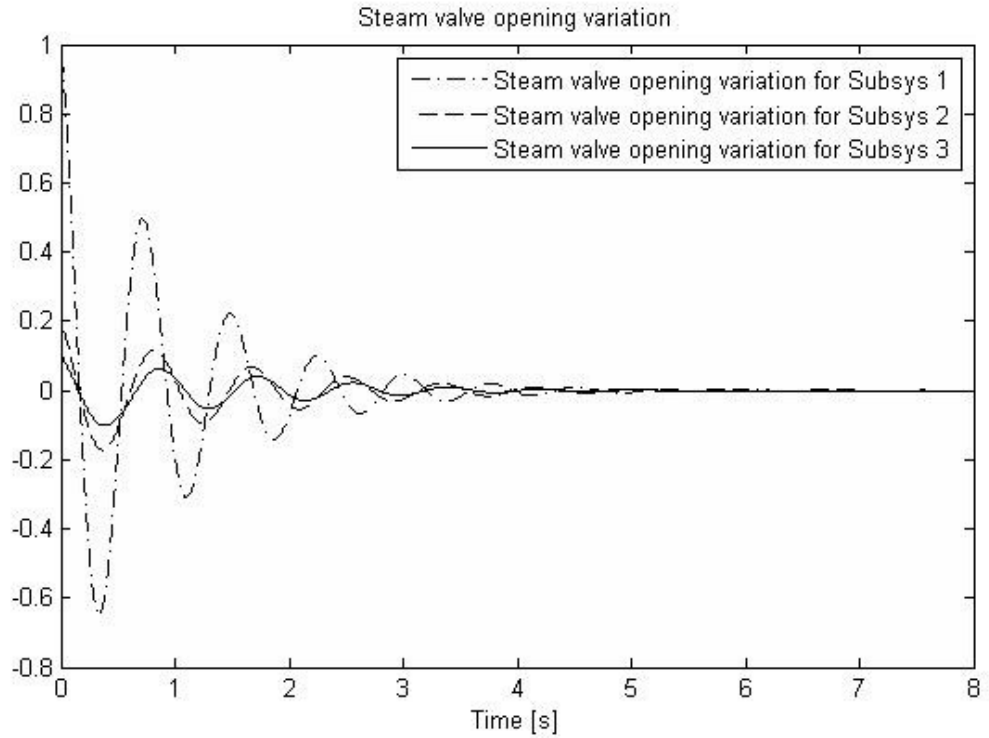
Figure 5-5. Stabilized power system states $\Delta X_{e_i}, i = 1,2,3$ for 3 interconnected systems

Setting the magnitude of the step signal $U(t) = 0.5, t \geq 15$ and add this signal to steam valve aperture variation. The results are given in Figure 5-6. The result of system with only linear SOF control is compared with the system with SOF SMC control.

From Figure 5-6, it is clear that the subsystems still respond to the faults even with the SMC because that boundary layer is used to avoid the chattering problem. The insensitivity can be improved by increasing the gain. But it is still necessary to find a trade-off balance between avoiding chattering and improving insensitivity.
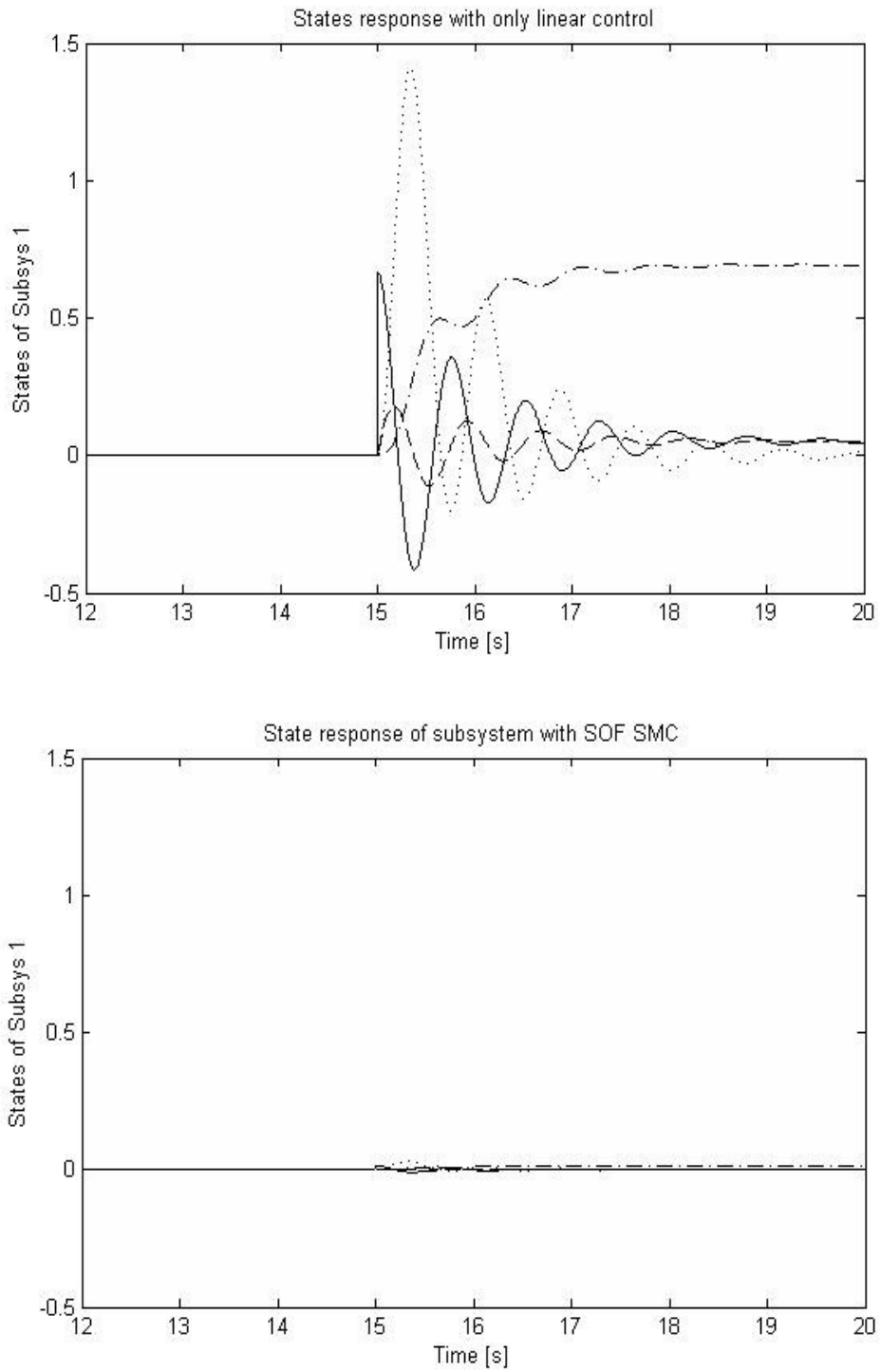
Figure 5-6. States responses with (lower) and without (upper) the sliding mode non-linear gain, for a step fault of U(t) = 0.5 at $\tau = 15s$

5.5.3 Observer based integral sliding mode control

Following the theoretical discussion in Section 5.4, it is interesting to apply the observer based ISM control to the interconnected system model. In contrast to the static output feedback case, 2 measurable states can be used successfully instead of requiring that 3 measurable states are available. Hence, to reduce the cost of requiring additional measurements, the output matrices C_i can be modified as:

$$C_i = \begin{bmatrix} 1 & 0 & 0 & 0 \\ 0 & 0 & 0 & 1 \end{bmatrix}$$

Figure 5-7 shows that the system is stabilized by this method. Moreover, it can be observed that the error system is asymptotically stable as shown in Figure 5-8.
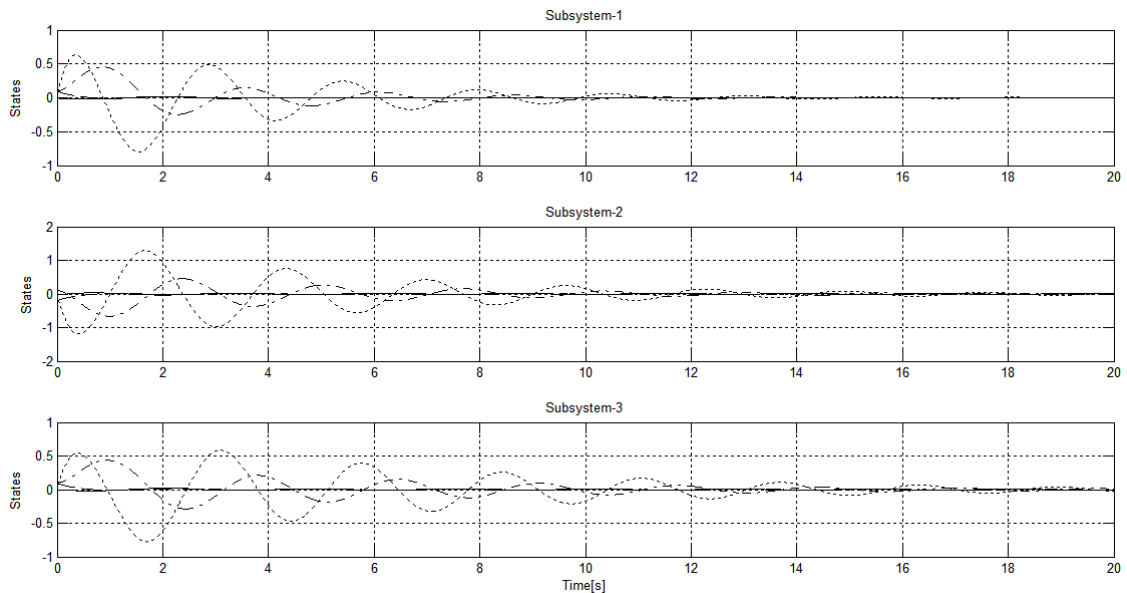
Figure 5-7. State responses of all three subsystems using the observer based ISMC
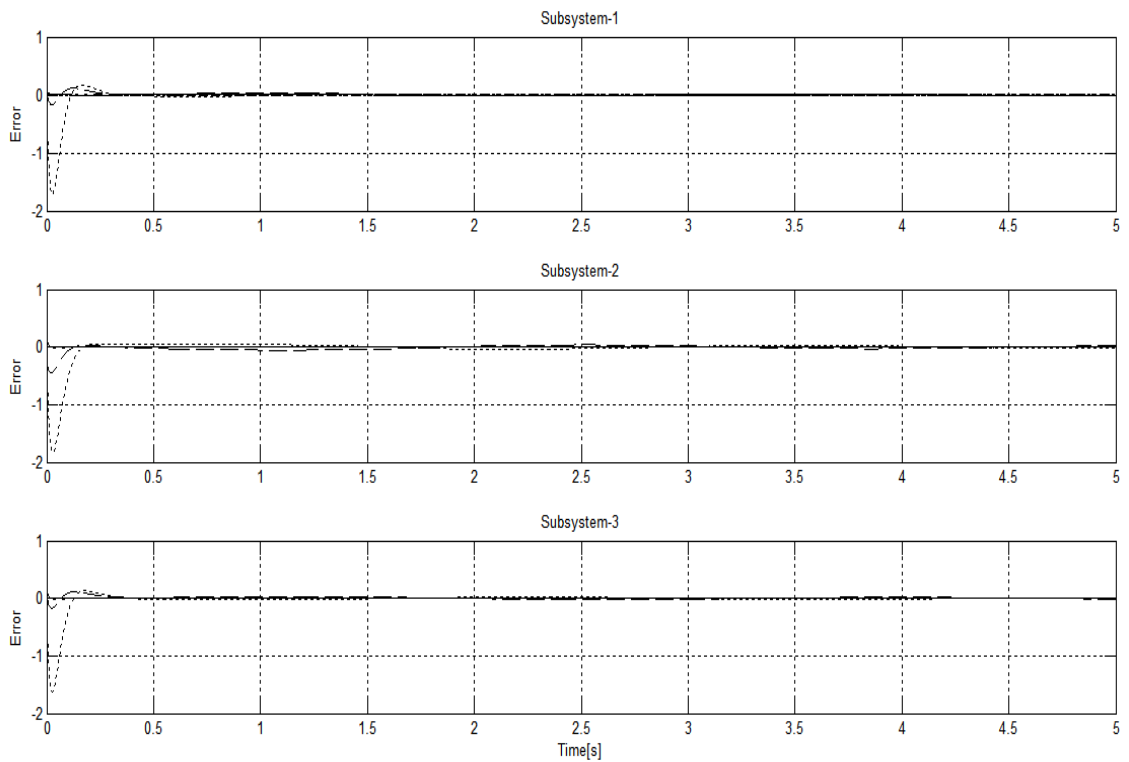
Figure 5-8. Errors between original subsystems and local observers

On the other hand, using this method, the matched fault (the same step signal as given in Section 5.5.2) can also be compensated.

For Figure 5-9, the upper diagram shows the state response when there is a step fault in subsystem 1. It can be seen that the linear output feedback control no longer stabilizes the system since the effect of the fault is transferred from the first subsystem to the others. However, by adding an integral sliding mode controller to the linear observer based control in each subsystem all the subsystems are stabilized and can be made insensitive to this fault, as shown in the lower diagram of Figure 5-9.
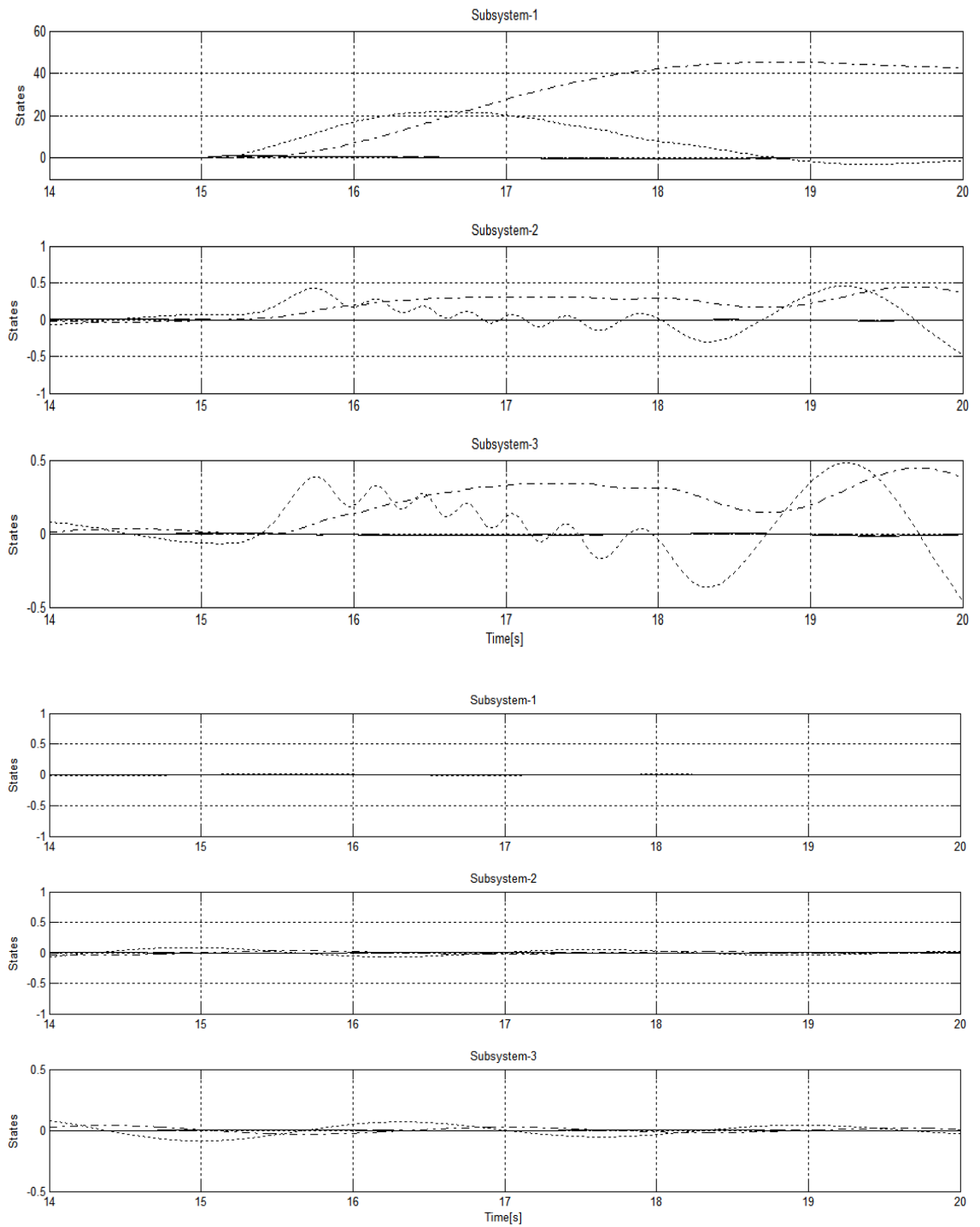
Figure 5-9. State responses with (lower) and without (upper) the OISMC non-linear gain term for a step fault of U(t) = 0.5 at $t = 15s$

5.6   Conclusion

This Chapter focuses on novel approaches to SMC based on output feedback designs for LSSs with (a) static output feedback, (b) dynamic compensation feedback, and (c) observer-based output feedback. New contributions of both decentralized static output feedback and decentralized dynamic compensator SMC are introduced. As a consequence of this study, combining with decentralized state feedback SMC, a more complete contribution to the theory of LMI-based decentralized output feedback SMC has been established.

As distinct from most publications, all the output feedback SMC methods in this Chapter are concerned with both the matched and unmatched cases of faults and perturbations. This is the most challenging scenario in decentralized control.

Moreover, this Chapter also proposes a novel observer-based ISM. In fact, a linear observer-based SMC with linear sliding surface can also be constructed using a similar algorithm. It is well known that the original state feedback ISM control by (Utkin and Shi, 1996) asks for full knowledge of the system and states. However, as a main contribution, the observer-based ISM control proposed in this Chapter can overcome this disadvantage. Furthermore, the observer based output feedback ISM control approach eliminates the reaching phase which is also one of the main disadvantages of classical linear sliding surface SMC theory.

A multi-machine model is used then to illustrate both static output feedback and observer based ISMC methods proposed in this Chapter. In this case study, the approach to construct quadratic constraint for interactions is also illustrated. Both SOF SMC and observer based ISM shows satisfactory results.

Chapter 6

Decentralized Sliding Mode Observer and Fault Estimation

6.1 Introduction

For LSSs, as discussed in Section 5.4, if the system cannot be controlled by static output feedback due to a problem of infeasibility of the appropriate coupled LMIs problem, one of the best ways is to use observer based control. In this case, a state feedback method can be used to construct the local controllers based on state estimate feedback (Bakule, 1996; Pagilla and Zhu, 2004; Tlili and Braiek, 2009; Benigni *et al*, 2010; Kalsi, 2009, 2010; Shafai Ghadami and Saif, 2011).

Another observer function can be based on fault estimation and there are several powerful approaches in the literature for robust fault estimation using specialised observers (Hassan Sultan and Attia, 1992; Chung and Speyer, 1998; Shankar Darbha and Datta, 2002; Yan and Edwards, 2008, etc.), for example proportional multi integral observers, unknown input observers, adaptive observers, sliding mode observers (SMO), etc. Please refer to Chapter 2 for a brief review of some of these methods. In this study the SMO has been chosen as this is in keeping with the mathematical developments given elsewhere in the thesis, i.e. based on sliding mode.

There is a significant possibility that faults can occur in a LSS due to the wide distribution of interconnected subsystems. Because of the interconnections, a fault occurring in a subsystem might lead to a failure in the overall system. The main challenge of fault monitoring and fault estimation in LSS is to understand and take into account the separate effects and influences from interactions and uncertainties. This is actually an extension of the now classical problem of robustness of FDI which is defined in terms of sensitivity to faults and minimization of the effects of uncertainty. Hence, the motivation of this Chapter is to extend the classical concepts into the domain of application of decentralized systems as a realistic approach to robust estimation, based on the use of the SMO.

The Chapter first reviews some typical SMO methods applicable to a single (centralized) system. The Walcott-Żak form of SMO is applied to a decentralized system problem to simultaneously estimate the states and actuator/sensor faults.

6.2   Sliding mode observer

By analogy with the SMC, by introducing a nonlinear control component, the error system trajectories reach the sliding surface in finite time such that the error system is insensitive to faults and perturbations satisfying certain conditions. To provide useful background this Section provides an outline of two SMO methods: the Walcott-Żak observer and the Edwards and Spurgeon observer. The main differences between these two observers are: the former type has simpler structure and it is easier to understand while the latter requires a triple state transformation but on the other hand gives more system information. However, both of these SMO strategies follow the same basic sliding concepts that of design of a sliding surface with respect to the output error. Once the sliding surface is reached, the state estimation error will be asymptotically stable.

6.2.1 Walcott-Żak observer

The Walcott-Żak observer is first developed by Walcott and Żak (1987), it is also referred to as a "Lyapunov-based" observer because the observer design is based directly on a Lyapunov function. However, the Walcott-Żak observer includes, in addition to the Lyapunov function formulation, an additional matrix equation constraint. It could be argued that this adds some complexity to the derivation and solution approach. It is certainly complicated to solve using algebraic methods, details could be found in (Hui and Żak, 2005). Both (Xiang, Su and Chu, 2005) and (Choi, 2005) propose a structured LMI approach which by pre-structuring the s.p.d. matrix in a Lyapunov function, leads to a effective solution to the Walcott-Żak observer problem. In this section, the idea of Walcott-Żak observer is reviewed and a new contribution by way of an improved structure for this type of SMO is given.

Consider a system has the following form:

$$\dot{x}(t) = Ax(t) + Bu(t) + Gf(y,u,t)$$
$$y(t) = Cx(t)$$

$$(6\text{-}1)$$

where $x \in \mathbb{R}^n$ is the system states, $y \in \mathbb{R}^m$ is the output of the system, $f(t)$ represent all the disturbance and uncertainties in the system. A, B, C, G are the system matrices of appropriate dimensions. Also assume that $q \le p < n$ and the matrices B, C and G are of full rank. The perturbation is assumed unknown but bounded by

$$\|f(y,u,t)\| \le \alpha(y,u,t) \tag{6-2}$$

where $\alpha(y, u, t)$ is a known continuous function.

Moreover, assume that zeros of the system model given by the triple (A, G, C) are in the left-hand complex plane and $rank(CG) = q$.

Consider the following observer structure:

$$\dot{\hat{x}}(t) = A\hat{x}(t) + Bu(t) + LCe(t) + K_n v$$
$$\hat{y} = C\hat{x} \tag{6-3}$$

where L and K_n are the matrices to be determined. v is the switching part of the SMO. In a similar way to the SMC problem the SMO switching function has the following form:

$$v = -\rho(y,u,t)\frac{\sigma}{\|\sigma\|} \tag{6-4}$$

where $\rho(y, u, t)$ is chosen such that $\rho(y, u, t) \ge \|F\|\alpha(y, u, t) + \eta$, $\eta > 0$ is positive scalar designed by the designer, where F is the sliding gain matrix to be designed later. The sliding surface is defined as:

$$\sigma = Ce = (y - C\hat{x}) \tag{6-5}$$

One might note that the sliding surface is different from the original Walcott-Żak observer given by $\sigma = FCe = Fe_y$. This will be discussed at the end of this Section.

Thus, combined with (6-1) and (6-3), the error system can be constructed as:

$$e(t) = x(t) - \hat{x}(t) \tag{6-6}$$

$$\dot{e}(t) = (A - LC)e(t) + Gf(t) - K_n v \tag{6-7}$$

The basic idea of the Walcott-Żak observer is to calculate L, P and F so that $(A - LC)$ is stable and satisfies the following condition:

$$G^T P = FC \qquad (6\text{-}8)$$

$$P(A-LC)+(A-LC)^T P = -Q \qquad (6\text{-}9)$$

where P and Q are s.p.d. matrices. The main problem of the Walcott-Żak observer is how to develop the most effective solution approach for Eqs. (6-8) and (6-9). In the original paper by (Walcott and Żak, 1987), the solution to (6-8) is assumed to be known. (Corless and Tu, 1998) point out that the solvability of (6-8) and (6-9) equivalent to the conditions outlined in the following Lemma:

Lemma 6.1 (Corless and Tu, 1988): If there exist s.p.d. matrices P and Q, the solution to (6-8) and (6-9) could be found if and only if $rank(CG) = rank(G)$ and the zeros of the system model given by the triple (A, G, C) are in the left-hand complex plane.

In this case, the switching gain matrix K_n of the observer (6-3) can be given by:

$$K_n = P^{-1} C^T \qquad (6\text{-}10)$$

Theorem 6.1 For the system (6-1), design an observer of the form (6-3) with (6-4), (6-5) and (6-10). If the conditions (6-8) are (6-9) are satisfied, the observer (6-3) will track the state trajectories of the system robustly and become insensitive to the system perturbations.

Proof:

Following the derivation of the classical sliding mode system theory two steps are required to prove this Theorem: 1). Ensure that the sliding surface can be reached and 2). Prove that the error system is stable after the sliding surface is reached. In this case, the state error system can be proved to be asymptotically stable. Following this the reachability of the sliding surface is obtained

Consider the derivative of the error system (6-7):

$$\dot{e}(t) = (A-LC)e(t)+Gf(t)-K_n v \qquad (6\text{-}7)$$

Construct the Lyapunov function $\dot{V}_e = e^T P e$ and its time derivative:

$$
\begin{aligned}
\dot{V}_e &= e^T \left[P(A-LC)+(A-LC)^T P \right] e + 2e^T PGf - 2e^T PK_n v \\
&= -e^T Qe + 2e^T C^T F^T f - 2e^T C^T v \\
&\leq -e^T Qe + 2\|\sigma\|\|F\|f - 2\|\sigma\|\rho(y,u,t)\frac{\sigma}{\|\sigma\|} \\
&\leq -e^T Qe - 2\|\sigma\|\eta \\
&\leq -e^T Qe
\end{aligned}
\tag{6-11}
$$

(6-11) implies that the estimation error system is quadratically stable. This also explains the reason why the solution to equation (6-8), i.e. $G^T P = FC$, is required.

From condition (6-9), $\dot{V}_e < 0$. Thus, the error system is quadratically stable. Next, consider the Lyapunov function for the sliding surface:

$$
V_y = e_y^T \frac{1}{2}(CP^{-1}C^T)^{-1} e_y
\tag{6-12}
$$

The time derivative of (6-12) along the error system (6-7) is:

$$
\dot{V}_y = e_y^T (CP^{-1}C^T)^{-1} C(A-LC)e + e_y^T (CP^{-1}C^T)^{-1}CGf - e_y^T (CP^{-1}C^T)^{-1}CK_n v
$$

Note that $G = CP^{-1}C^T F^T$, it follows that:

$$
\begin{aligned}
\dot{V}_y &= e_y^T (CP^{-1}C^T)^{-1} C(A-LC)e + e_y^T F^T f - e_y^T v \\
&\leq e_y^T (CP^{-1}C^T)^{-1} C(A-LC)e + \|e_y\|\|F\|\left[\alpha(y,u,t)-\rho(y,u,t)\right] \\
&< \|e_y\|(CP^{-1}C^T)^{-1} C(A-LC)e - \|e_y\|\eta \\
&< \|e_y\|\left[(CP^{-1}C^T)^{-1} C(A-LC)e - \eta\right]
\end{aligned}
\tag{6-13}
$$

Define $0 < \tilde{\eta} \leq \|\sigma\|\eta$, because of the asymptotic stability of the closed-loop estimation error system (6-7), the trajectory of this system will enter the following domain in finite time:

$$
\Omega = \{e \mid \|(CP^{-1}C^T)^{-1} C(A-LC)\|\|e\| < (\eta - \tilde{\eta})\}
\tag{6-14}
$$

Thus, $\dot{V}_y < -\|e_y\|\tilde{\eta} < 0$, which implies that the sliding surface $e_y = 0$ can be reached in finite time and remain there subsequently. With this the proof is complete. ∎

(Edwards and Spurgeon, 1998) state that the null space of the sliding surface gain matrix F spanned by e_y in the original formulation of the Walcott-Żak observer is non-empty, i.e. $Fe_y = 0$ for some $e_y \neq 0$ (the trivial solution). Hence, if the sliding surface is designed by $\sigma = Fe_y$, the observer does not necessarily track the system outputs perfectly. Actually, this statement is not complete, as the system will still track the output perfectly in finite time. But, when the sliding surface is reached, the output error e_y might not be identically zero. However, in the method proposed in this Section, instead of using $K_n = G = P^{-1}C^T F^T$, the gain matrix $K_n = P^{-1}C^T$ is chosen. In this case, the sliding surface can be designed so that $\sigma = e_y$. This modification does not change the essential properties of the Walcott-Żak observer whilst guaranteeing that the output error becomes zero after reaching the sliding surface.

In the Section 6.2.2, the well-known Edwards & Spurgeon observer is reviewed. It is shown in particular how the calculation of $G^T P = FC$ is obviated by way of developing an alternative approach.

6.2.2 Edwards & Spurgeon observer

In this Section, the Edwards & Spurgeon observer is described. This type of observer is an extension to the Uktin observer, which requires a triple state transformation during the design procedure (Edwards and Spurgeon, 1998). A consequence of the use of transformation is that after designing the observer gain matrices the state system must be transferred back into the original coordinates. It is shown in this study that the complexity of the triple transformation gives enhanced accuracy and a better understanding of the observer structure (Edwards and Spurgeon, 1998).

Consider the system of the same form of (6-1) and use similar assumptions to those given in Section 4.2.1, as follows:

1) The pair (A, C) is observable
2) $q \leq p < n$ and the matrices B, C and G are of full rank.
3) The perturbation is assumed be unknown but bounded by:

$$\|f(y,u,t)\| \leq \alpha(y,u,t) \tag{6-2}$$

where $\alpha(y, u, t)$ is a known function.
4) $rank(CG) = rank(G) = q$ and the zeros of the system model given by the

142

triple (A, G, C) are in the left-hand complex plan, that is:

$$\begin{bmatrix} sI - A & G \\ C & 0 \end{bmatrix} = n + q$$

for all s such that $\Re(s) \geq 0$.

Suppose that there exist a linear change of coordinates which transfer the system into *observer canonical form*: $x| \rightarrow T_0 x$, and the output distribution matrix becomes:

$$CT_0^{-1} = \begin{bmatrix} 0 & I_p \end{bmatrix}$$

Therefore, the new coordinate system can be written as:

$$\begin{aligned} \dot{x}_1(t) &= A_{11} x_1(t) + A_{12} y(t) + B_1 u(t) \\ \dot{y}(t) &= A_{21} x_1(t) + A_{22} y(t) + B_2 u(t) + G_2 f(t) \end{aligned} \tag{6-15}$$

where $x_1 \in \mathbb{R}^{n-p}$, $y \in \mathbb{R}^p$ and the matrix A_{11} has stable eigenvalues. (Edwards and Spurgeon, 1998).

Consider an observer of the form:

$$\begin{aligned} \dot{\hat{x}}_1(t) &= A_{11} \hat{x}_1(t) + A_{12} \hat{y}(t) + B_1 u(t) - A_{12} e_y(t) \\ \dot{\hat{y}}(t) &= A_{21} \hat{x}_1(t) + A_{22} \hat{y}(t) + B_2 u(t) - (A_{22} - A_{22}^s) e_y(t) + v \end{aligned} \tag{6-16}$$

where A_{22}^s is a stable design matrix and $e_y = \hat{y}(t) - y(t)$. The switching part of observer v is designed as:

$$v = \begin{cases} -\rho(t, y, u) \|G\| \dfrac{P_2 e_y}{\|P_2 e_y\|} & \text{if } e_y \neq 0 \\ 0 & \text{otherwise} \end{cases} \tag{6-17}$$

where: P_2 is an s.p.d matrix and satisfies the following Lyapunov equation:

$$A_{22}^{s\,T} P_2 + P_2 A_{22}^s = -I \tag{6-18}$$

where Q' is an s.p.d matrix. The scalar function $\rho(y, u, t)$, like the one given in the original formulation of the Walcott-Żak observer, should be chosen so that it is larger than the upper boundary of the fault:

$$\rho(y,u,t) \geq \alpha(y,u,t) + \eta \tag{6-19}$$

where η is a positive scalar.

Although (6-18) is similar to (6-9), however it reduces the order of the problem.

Thus, the error system can be written as:

$$e_1(t) = A_{11}e_1(t) \tag{6-20}$$

$$e_y(t) = A_{21}e_1(t) + A_{22}^s e_y(t) + v - G_2 f \tag{6-21}$$

In (Edwards and Spurgeon, 1998), it has been proved that if the observer system has the form (6-16), then the error system (6-20) and (6-21) is quadratically stable. Thus, the Edwards and Spurgeon observer structure is summarized as:

$$\dot{\hat{x}}(t) = A\hat{x}(t) + Bu(t) - G_l Ce(t) + G_n v \tag{6-22}$$

where the linear gain is:

$$G_l = T_0^{-1} \begin{bmatrix} A_{12} \\ A_{22} - A_{22}^s \end{bmatrix} \tag{6-23}$$

The switching non-linear gain is:

$$G_n = \|G_2\| T_0^{-1} \begin{bmatrix} 0 \\ I_p \end{bmatrix} \tag{6-24}$$

and

$$v = \begin{cases} -\rho(t,y,u) \dfrac{P_2 Ce}{\|P_2 Ce\|} & if \ Ce \neq 0 \\ 0 & otherwise \end{cases} \tag{6-25}$$

Since it is a review of Edwards and Spurgeon observer, the details of this observer are omitted. For more details, see (Edwards and Spurgeon, 1998). The main difference between the Edwards & Spurgeon and Walcott-Żak observers is the choice of the gain matrix in the sliding surface. In the Edwards and Spurgeon observer, when the sliding surface is reached, it follows that $e_y = 0$ since P_2 is an s.p.d. matrix (invertible and full

rank). However, as $F \in \mathbb{R}^{q \times p}$ in the conventional Walcott-Żak observer, F is not required to be full rank. Hence, once the sliding surface is reached, $e_y = 0$ cannot be guaranteed when the system reaches sliding surface. For this reason, Edwards & Spurgeon point out that in their view the Walcott-Żak observer does not necessarily track the system outputs perfectly. Compared with the Walcott-Żak observer, the Edwards & Spurgeon observer does not require the solution of Eq. (6-8). It does however require the rather complicated transformation matrix T_0. The system in the new coordinates should satisfy the following conditions:

(i).   The matrix A_{11} has stable eigenvalues. Moreover, (Edwards and Spurgeon, 1998) states that the system matrix can be written as:

$$\overline{A} = \begin{bmatrix} A_{11} & A_{12} \\ A_{211} & \\ A_{212} & A_{22} \end{bmatrix}, \quad A_{211} = \begin{bmatrix} 0 & A_{21}^o \end{bmatrix}, \quad A_{11} = \begin{bmatrix} A_{11}^o & A_{12}^o \\ 0 & A_{22}^o \end{bmatrix}, \tag{6-26}$$

where $A_{11}^o \in \mathbb{R}^{r \times r}$ and $A_{21}^o \in \mathbb{R}^{(p-q) \times (n-q-r)}$ for some $r \geq 0$ and the pair (A_{22}^o, A_{21}^o) is observable, Furthermore, the eigenvalues of A_{11}^o are the invariant zeros of (A, D, C).

(ii).   The disturbance distribution matrix has the following form:

$$\overline{G} = \begin{bmatrix} 0 \\ G_2 \end{bmatrix} \tag{6-27}$$

where $G_2 \in \mathbb{R}^{q \times q}$ is non-singular matrix

(iii).   The output distribution matrix has the form

$$\overline{C} = \begin{bmatrix} 0 & T \end{bmatrix} \tag{6-28}$$

where $T \in \mathbb{R}^{q \times q}$ is an orthogonal matrix.

This system in the new coordination is the so called *"canonical form"* for the SMO. For more details see (Edwards and Spurgeon, 1998).

(Tan and Edwards, 2001) then realized that the gain matrix (6-24) does not exploit all the degrees of freedom available. The new method suggests that the gain matrix for the nonlinear part should be given by:

$$G_n = \|G_2\| T_0^{-1} \begin{bmatrix} -\bar{L}T^T \\ T^T \end{bmatrix} \tag{6-29}$$

where $\bar{L} \in \mathbb{R}^{(n-p)\times p}$ and $\bar{L} = [L \quad 0]$ with $\bar{L} \in \mathbb{R}^{(n-p)\times(n-p)}$. The gain L is also to be determined but the orthogonal matrix T is part of the $\bar{C}$ matrix of (6-28) in the new coordinate system (Tan and Edwards, 2001).

Compared with the gain matrix (6-24), all of the design freedom is exploited in (6-29). (Tan and Edwards, 2001) also gave the LMI based algorithm for the observer:

Suppose that after transformation, the system is in the *canonical form* and satisfies the condition (i)-(iii) and can be written as:

$$\dot{\bar{x}}(t) = \bar{A}\bar{x}(t) + \bar{B}u(t) + \bar{G}f(t,x,u)$$
$$\bar{y} = \bar{C}\bar{x} \tag{6-30}$$

Step 1. Check that $rank(CD) = q$ and the eigenvalues of A_{11}^o have negative real parts. If not, the approach is not applicable.

Step 2. Define two symmetric matrices $\bar{P} \in \mathbb{R}^{n\times n}$ and $\bar{X} \in \mathbb{R}^{n\times n}$. And an extra matrix $\bar{Y} \in \mathbb{R}^{n\times p}$ for the linear gain matrix design.

Step 3. Form the LMIs:

Minimize $trace$ $(\bar{X})$, subject to

$$\bar{P} = \begin{bmatrix} P_{11} & P_{12} \\ P_{12}^T & P_{22} \end{bmatrix} > 0, \quad \begin{bmatrix} -\bar{P} & I \\ I & -\bar{X} \end{bmatrix} < 0 \tag{6-31}$$

$$\begin{bmatrix} \bar{P}\bar{A} + \bar{A}^T\bar{P} - \bar{Y}\bar{C} - (\bar{Y}\bar{C})^T & \bar{P} & \bar{Y} \\ \bar{P} & -W^{-1} & 0 \\ \bar{Y} & 0 & -V^{-1} \end{bmatrix} < 0 \tag{6-32}$$

where W and V are assumed to be s.p.d..

Step 4. Partition the resulting matrix $\bar{P}$ to obtain P_{11}, P_{12} and P_{22} as defined in (35). Compute $\bar{L} = P_{11}^{-1}P_{12}$, $\bar{P}_2 = P_{22} - P_{12}^T P_{11}^{-1} P_{12}$ and $P_2 = T\bar{P}_2 T^T$ where T is the orthogonal matrix from (6-28).

Step 5. The observer gain matrices (in the co-ordinates of the canonical form from Step 1) can be calculated as

$$G_l = T_0^{-1} \bar{P}^{-1} \bar{Y} \text{ and } G_n = \|G_2\| T_0^{-1} \begin{bmatrix} -\bar{L} T^T \\ T^T \end{bmatrix} \tag{6-33}$$

The nonlinear switching part is the same as (6-25).

6.2.3 LMI approach for decentralized Walcott-Żak observer

Compared with the Edwards & Spurgeon observer, the advantages of the Walcott-Żak observer are that it requires less transformations and has simpler structure if the Eqs. (6-8), i.e. $G^T P = FC$, can be solved. However, the only remaining problem in the design of the Walcott-Żak observer lies in the determination of P and F satisfying (6-8), although (Xiang, 2005; Choi, 2005) point out that the problem has a direct solution approach via the use of LMIs. It can be shown that the observer parameters are determined by solving only one LMI problem. However, the disadvantage of this method is that there is less freedom when compared with the SMO of Edwards and Spurgeon. As it can be seen the essential idea of the Walcott-Żak observer is try to calculate two matrices with which the perturbation distribution matrix of the original system can be reconstructed, i.e. $G = P^{-1} C^T F^T$. This further limits the design freedom of the sliding surface in the Walcott-.Żak case.

No matter whether the observer is designed for control design or fault estimation, the decentralized structure with only local output information is the way to build observers for large scale system.

Theorem 6.2 The problem (6-8) and (6-9) can be solved by finding s.p.d. matrices $W_1 \in \mathbb{R}^{(n-m)\times(n-m)}$, $W_2 \in \mathbb{R}^{p\times p}$ and a general matrix $Y \in \mathbb{R}^{n\times p}$ such that:

$$\widetilde{G} W_1 \widetilde{G}^T + C^T W_2 C > 0 \tag{6-34}$$

$$\left(\widetilde{G} W_1 \widetilde{G}^T + C^T W_2 C\right) A + A^T \left(\widetilde{G} W_1 \widetilde{G}^T + C^T W_2 C\right) - YC - C^T Y^T < 0 \tag{6-35}$$

One can get the solution that

$$P = \widetilde{G} W_1 \widetilde{G}^T + C^T W_2 C$$
$$L = P^{-1} Y, \quad F = G^T C^T W_2 \tag{6-36}$$

where $\tilde{G}$ is the orthogonal matrix for G, i.e. $\tilde{G}^T G = 0$. One can solve the LMIs (6-34) and (6-35) directly by using MATLAB LMI tools. Compared with (Tan and Edwards, 2001), Theorem 6.2 simplifies the design algorithm significantly.

A similar algorithm has been used in the static output feedback sliding mode control part in Chapter 4. The only difference is that the controller can only deal with matched perturbations, i.e. $R(G) \subset R(B)$. However, in the SMO design, the perturbation gain matrix G does not need to satisfy this matching condition, and the SMO *matching condition* is $rank(CG) = rank(G)$. Another advantage of this method is that the design of matrices L and P can be separated. From Theorem 6.2, it can be noted that the LMI (6-35) contains two variables. If there exists a matrix L which makes $(A - LC)$ stable, P can be obtained by solving:

$$\left(\tilde{G}W_1\tilde{G}^T + C^T W_2 C\right)(A - LC) + (A - LC)^T\left(\tilde{G}W_1\tilde{G}^T + C^T W_2 C\right) < 0$$

This means that the linear part of the SMO and the discontinuous nonlinear part of the SMO can be designed separately. However, although the design of L does not affect the solvability of the LMIs (6-34) and (6-35), it does affect the feasible solution region of (6-35).

When considering the LSS problem, in contrast to the single (centralized) system structure assumed in (6-1), there always exist interaction terms. However, as discussed in Chapter 1, for the overall system, the interaction terms can always be considered as bounded uncertainties if the overall system has proper local controllers. The influence of the interactions in the estimation error of each local observer is unavoidable unless each interaction satisfies the corresponding (local) rather restrictive observer matching condition $rank(CG) = rank(G)$. This Section considers an extension of the Walcott-Żak method where the overall system contains uncertainties/interactions which do not satisfy the "matching condition" $rank(CG) = rank(G)$. Also, the constraint of the known upper bound of the perturbations can be relaxed by an adaptive mechanism which is described in Chapter 4.

Now, assuming that for a LSS, the local controllers are well designed such that the overall system is stable and the interactions are bounded. Consider the *i*-th subsystem in the form of:

$$\dot{x}_i(t) = A_i x_i(t) + B_i u_i(t) + G_i f_i(x_i, u_i, t) + M_i h_i(u, x, t)$$
$$y_i(t) = C_i x_i(t) \tag{6-37}$$

where the state vector $x_i \in \mathbb{R}^{n_i}$, the output signal $y_i \in \mathbb{R}^{p_i}$. $G_i \in \mathbb{R}^{n_i \times q_i}$. The system zeros given by the triples (A_i, G_i, C_i) are in the left-hand complex plane for all the subsystems and $q_i \leq p_i < n_i$, $rank(C_i G_i) = rank(G_i)$. $f_i(x_i, u_i, t)$ represents the system faults. Here $h_i(u, x, t)$ represents the uncertainties and interactions between subsystems, which do not satisfy the observer matching condition, i.e. $rank(C_i M_i) \neq rank(M_i)$. However, due to the formulation of stable local controllers, assume that the term $h_i(u, x, t)$ is bounded by unknown constants $\|h_i(u, x, t)\| \leq \varpi_i$

The overall system can be written as:

$$\dot{x}(t) = Ax(t) + Bu(t) + Gf(x, u, t) + Mh(u, x, t)$$
$$y(t) = Cx(t) \tag{6-38}$$

where, $x(t) = [x_1^T(t) \quad \cdots \quad x_N^T(t)]^T$, $y(t) = [y_1^T(t) \quad \cdots \quad y_N^T(t)]^T$

$$A = diag(A_1, \dots, A_N), B = diag(B_1, \dots, B_N), C = diag(C_1, \dots, C_N)$$

$$M = diag(M_1, \dots, M_N)$$

$$f(x, u, t) = [f_1^T(x_1, u_1, t), \dots, f_N^T(x_N, u_N, t)]^T$$

$$h(x, t) = [h_1^T(x, t), \dots, h_N^T(x, t)]^T \text{ and } \|h(u, x, t)\| \leq \varpi$$

$x \in \mathbb{R}^n$, $u \in \mathbb{R}^m$, $y \in \mathbb{R}^p$ $n = n_1 + \cdots + n_N$, $m = m_1 + \cdots + m_N$ and $p = p_1 + \cdots + p_N$ are the numbers of the states, inputs and outputs, respectively.

The local observer for the subsystem (6-37) can be written as:

$$\dot{\hat{x}}_i(t) = A_i \hat{x}_i(t) + B_i u_i(t) + L_i C_i(y(t) - \hat{y}(t)) + K_{ni} v_i(t)$$
$$\hat{y}_i(t) = C_i \hat{x}_i(t) \tag{6-39}$$

Thus, the observer system based on the overall system is given by:

$$\dot{\hat{x}}(t) = A\hat{x}(t) + Bu(t) + LCe(t) + K_n v(t)$$
$$\hat{y}(t) = C\hat{x}(t) \tag{6-40}$$

where $L = diag(L_i), K_n = diag(K_{ni}), i = 1, \dots, N$.

The error system is of the form:

$$\dot{e}(t) = (A - LC)e(t) + Gf(x,u,t) - K_n v(t) + Mh(u,x,t)$$
$$e_y(t) = Ce(t)$$
(6-41)

The LMI approach for the robust sliding mode observer (6-40) is designed using the following theorem:

Theorem 6.3. The aggregated state estimation error $e(t) = x(t) - \hat{x}(t)$ is ultimately bounded if the observer is in the form of (6-40), where the gain matrices are given by solving the following LMIs:

Define matrices $W_1 = diag(W_{1i})$, $W_2 = diag(W_{2i})$, $Y = diag(Y_i)$, $W_{1i} \in \mathbb{R}^{(n_i-m_i)\times(n_i-m_i)}$, $W_{2i} \in \mathbb{R}^{p_i \times p_i}$ and $Y_i \in \mathbb{R}^{n_i \times p_i}$ such that:

$$\widetilde{G}W_1\widetilde{G}^T + C^T W_2 C > 0$$

$$\left(\widetilde{G}W_1\widetilde{G}^T + C^T W_2 C\right)A + A^T\left(\widetilde{G}W_1\widetilde{G}^T + C^T W_2 C\right) - YC - C^T Y^T < 0$$
(6-42)

One can derive observer gain matrices that are calculated from:
$$P_i = \widetilde{G}_i W_{1i}\widetilde{G}_i^T + C_i^T W_{2i} C_i$$
$$L_i = P_i^{-1}Y_i, \quad F_i = G_i^T C_i^T W_{2i}, \quad K_n = P_i^{-1}C_i^T$$
(6-43)

The sliding mode switching term for the local observer is designed in the form of:

$$v_i(t) = \left(\|F_i\|\Psi_i(t) + \eta_i\right)\frac{e_y(t)}{\|e_y(t)\|}, \quad \dot{\Psi}_i(t) = \|e_{yi}(t)\|, \quad \eta_i > 0, \quad \Psi_i(0) \geq 0$$
(6-44)

Proof (by contradiction):

The state estimation error has the form of:

$$\dot{e}(t) = (A - LC)e(t) + Gf(x,u,t) - K_n v(t) + Mh(u,y,t)$$

We assume that the fault are bounded by large enough unknown constants, i.e. $\|f_i(x_i,u_i,t)\| \leq \psi_i < \infty$, $\|f(x,u,t)\| \leq \psi < \infty$. Then the designs of the Lyapunov function $\dot{V}_e = \sum_{i=1}^{N} e_i^T P_i e_i$ for the aggregate system and it's time derivatives along the estimation error state trajectory is:

$$\dot{V}_e = \sum_{i=1}^{N} \left\{ e_i^T \left[P_i(A_i - L_i C_i) + (A_i - L_i C_i)^T P_i \right] e_i + 2 e_i^T P_i G_i f - 2 e_i^T C_i^T v_i + 2 e_i^T P_i M_i h_i \right\}$$

$$= \sum_{i=1}^{N} \left[e_i^T Q_i e_i + 2 e_{yi}^T F_i^T f - 2 e_{yi}^T v + 2 e_i^T P_i M_i h_i \right]$$

$$\leq \sum_{i=1}^{N} \left[e_i^T Q_i e_i + 2 e_i^T P_i M_i \varpi_i + 2 \left\| e_{yi} \right\| \left(\left\| F_i \right\| \psi_i - \left\| F_i \right\| \Psi_i(t) - \eta_i \right) \right]$$

$$(6\text{-}45)$$

where $- Q_i = P_i(A_i - L_i C_i) + (A_i - L_i C_i)^T P_i$ and according to (6-42), $Q_i > 0$.

It is to be proved that the sliding gain $\Psi_i(t)$ is not unbounded, using contradiction. Since $\dot{\Psi}_i(t) = \left\| e_y \right\| > 0$ and $\Psi_i(0) > 0$, the adaptive gain $\Psi_i(t)$ is positive and increasing. Assume that $\Psi_i(t)$ is unbounded and $\Psi_i(t) \to \infty$ asymptotically. Thus, there exists a time $t = T_1$ such that for all $t > T_1$, the adaptive gain:

$$\left\| F_i \right\| \Psi_i(t) \geq \left\| F_i \right\| \psi_i - \eta, \qquad (6\text{-}46)$$

which implies that:

$$\dot{V}_e \leq \sum_{i=1}^{N} \left(- e_i^T Q_i e_i + 2 e_i^T P_i M_i \varpi_i \right)$$

$$\leq \sum_{i=1}^{N} \left[- \lambda_{\max}(Q_i) \left\| e_i \right\|^2 + 2 \left\| e_i \right\| \left\| P_i M_i \right\| \varpi_i \right] \qquad (6\text{-}47)$$

$$\leq \sum_{i=1}^{N} \left\| e_i \right\| \left[- \lambda_{\max}(Q_i) \left\| e_i \right\| + 2 \left\| P_i M_i \right\| \varpi_i \right]$$

Note that since the interactions terms ϖ_i are bounded and $\lambda_{min}(Q_i) > 0$, if $\left\| e_i \right\|$ is unbounded, i.e. $\left\| e_i \right\| \to \infty$, it follows that $\dot{V}_e < 0$ (i.e. $\left\| e_i \right\|$ is bounded) which leads to a contradiction. Thus, $\left\| e_i \right\|$ is bounded.

Moreover, defining, $\mu_{0i} = - \lambda_{\max}(Q_i)$, $\mu_{1i} = \sqrt{\lambda_{\max}(M_i^T P_i M_i)}$, it follows:

$$\dot{V}_e \leq \sum_{i=1}^{N} \left\| e_i \right\| \left(- \mu_{0i} \left\| e_i \right\| + 2 \mu_{1i} \varpi_i \right) \qquad (6\text{-}48)$$

Following from (Tan and Edwards, 2003), the state estimation error $e(t)$ is ultimately bounded with respect to the set:

$$\Omega_{\varepsilon} = \left\{ e_i : \|e_i\| < 2\mu_{1i}\varpi_i / \mu_{0i} + \varepsilon_i \right\}$$

where $\varepsilon_i > 0$ is an arbitrarily small positive scalar.

The reachability of the sliding surface is described as follows:

$$\sigma_i(t) = C_i e_i(t) = C_i(A_i - L_i C_i)e_i(t) + C_i G_i f_i(x_i, u_i, t) - C_i K_{ni} v_i(t) + C_i M_i h_i(u, x, t)$$

By defining an unknown positive scalar $\varphi_i \geq \left\|(G_i^T P_i G_i)^{-1} F_i C_i M_i\right\|\varpi_i + \psi_i > 0$, the computation of the adaptive gain $\Psi_i(t)$ is equivalent to the computation of the estimate of φ_i. Consider the Lyapunov function for the sliding surface:

$$V_\sigma = \frac{1}{2}\sum_{i=1}^{N}\left[\sigma_i^T \left(C_i P_i^{-1} C_i^T\right)^{-1}\sigma_i + \|F_i\|(\varphi_i - \Psi_i(t))^2\right] \tag{6-49}$$

Differentiating (6-49) with respect to time yields:

$$\begin{aligned}
\dot{V}_\sigma &= \sum_{i=1}^{N}\left[\begin{array}{l} e_{yi}^T \left(C_i^T P_i^{-1} C_i\right)^{-1} C_i (A_i - L_i C_i) e_i(t) + e_{yi}^T F_i^T f(t) - e_{yi}^T v(t) \\ + e_{yi}^T \left(C_i^T P_i^{-1} C_i\right)^{-1} C_i M_i h_i(u, x, t) - \|F_i\|(\varphi_i - \Psi_i(t))\|e_{yi}\| \end{array}\right] \\
&\leq \sum_{i=1}^{N}\left[\begin{array}{l} \|e_{yi}\|\left\|\left(C_i^T P_i^{-1} C_i\right)^{-1} C_i\right\|\|(A_i - L_i C_i)e_i + M_i h_i\| + \|e_{yi}\|(\|F_i\|\varphi_i - \|F_i\|\Psi_i(t) - \eta_i) \\ - \|e_{yi}\|\|F_i\|(\varphi_i - \Psi_i(t)) \end{array}\right] \\
&\leq \sum_{i=1}^{N}\left\{\|e_{yi}\|\left[\left\|\left(C_i^T P_i^{-1} C_i\right)^{-1} C_i\right\|(\|(A_i - L_i C_i)e_i\| + \|M_i h_i\|) - \eta_i\right]\right\}
\end{aligned}$$

If define the gain

$$\eta_i \geq \left\|\left(C_i^T P_i^{-1} C_i\right)^{-1} C_i\right\|\left[(A_i - L_i C_i)(2\mu_{1i}\varpi_i / \mu_{0i} + \varepsilon_i) + \|M_i\|\varpi_i\right] + \eta_{0i}$$

with η_{0i} a positive scalar, in finite time $e_i(t) \in \Omega_\varepsilon$, which implies that $\|e_i(t)\| < 2\mu_{1i}\varpi_i / u_{0i} + \varepsilon_i$, and it thus follows that:

$$\dot{V}_\sigma \leq \sum_{i=1}^{N} -\eta_{0i}\|\sigma_i\| \leq 0 \tag{6-50}$$

Integrating (6-50) from 0 to t yields:

$$V_\sigma(0) \geq V_\sigma(t) + \int_0^t \sum_{i=1}^N \eta_{0i} \|\sigma_i(s)\| ds \geq \int_0^t \sum_{i=1}^N \eta_{0i} \|\sigma_i(s)\| ds \qquad (6\text{-}51)$$

As $t \to \infty$, $\int_0^t \sum_{i=1}^N \eta_{0i} \|\sigma_i(s)\| ds$ is always less or equal to $V_\sigma(0)$. However, since $V_\sigma(0)$ is positive and bounded, using Barbalat lemma, it follows:

$$\lim_{t \to \infty} \eta_{0i} \|\sigma_i(t)\| = 0$$

i.e. the sliding surface function is reachable. The error system trajectory converges to the sliding manifold $\sigma_i(t) = e_{yi} = 0$. Furthermore, it should be noted that because of (6-51), $V_\sigma(t) \leq V_\sigma(0)$, i.e. $V_\sigma(t)$ is bounded. This also implies that $\|\sigma_i(t)\|$ and $\Psi_i(t)$ are bounded for all $t > 0$. This leads to a contradiction to the assumption that $\Psi_i(t)$ is unbounded. Thus, $\Psi_i(t), i = 1, \ldots, N$ are bounded. We assume that there is a semi-positive scalar such that $\Psi_{is} \geq 2\|C_i\|(\|F_i\|\psi_i - \|F_i\|\Psi_i(t) - \eta_i)$, $\Psi_{is} = 0$ when the right-hand side of this inequality less than zero, the inequality (6-47) can be rewritten as:

$$\dot{V}_e \leq \sum_{i=1}^N \left\{ \|e_i\| \left[-\lambda_{\max}(Q_i)\|e_i\| + 2\|P_iM_i\|\varpi_i + \Psi_{is} \right] \right\}$$

Note that $\|e_i(t)\|$ is still bounded and the set becomes:

$$\overline{\Omega}_\varepsilon = \left\{ e_i : \|e_i\| < \left(2\mu_{1i}\varpi_i + \Psi_{is} \right) / \mu_{0i} + \varepsilon_i \right\} \qquad (6\text{-}52)$$

Following the same proof as given for the algorithm (6-49) to (6-50), if define:

$$\eta_i \geq \left\| \left(C_i^T P_i^{-1} C_i \right)^{-1} C_i \right\| \left[(A_i - L_iC_i)(2\mu_{1i}\varpi_i/\mu_{0i} + \Psi_{is} + \varepsilon_i) + \|M_i\|\varpi_i \right] + \eta_{0i}$$

the (6-50) still holds, leading to $e_{yi} = 0$ in finite time. Thus, the proof is complete. ∎

Remark 6.1 From the above proof, it can be seen that the bounds for the uncertainty and the fault are not required. This highlights the benefit of using the adaptive mechanism.

Remark 6.2 The set (6-52) shows that the tracking accuracy is affected by 1). The eigenvalues of Q_i, i.e. the choice of linear gain matrix L and s.p.d matrix P; 2). The norm bound of the interactions ϖ_i and 3). The values of the sliding gain functions $\Psi_i(t)$

and the parameters η_i. Thus, one can adjust the design strategy based on these relationships.

In this case, if the constraint $q \leq p$ can be extended to $q = p$, SMO cannot only deal with the faults but some parts of the interactions/uncertainties. Thus, consider the following two conditions:

1). Find $\mathcal{G}_i \in \mathbb{R}^{n_i \times p_i}, i = 1, \dots, N$ such that for i-th subsystem, the system zeros given by the triple $(A_i, \mathcal{G}_i, C_i)$ are in the left-hand complex plane.

2). $rank(C_i \mathcal{G}_i) = rank(\mathcal{G}_i) = p_i$

The objective of finding the $\mathcal{G}_i$ is to use the maximum capability of the nonlinear term of SMO such. In this case, give $G_i = \mathcal{G}_i \bar{G}_i$ and $M_i = \mathcal{G}_i \bar{M}_{1i} + \tilde{\mathcal{G}}_i \bar{M}_{2i} = M_{1i} + M_{2i}$. And according to (Xiang, 2005), it can always be found matrices $\mathcal{P}_i$ and $\mathcal{F}_i$ such that $\mathcal{G}_i^T \mathcal{P}_i = \mathcal{F}_i C_i$. Thus, building an SMO based on $\mathcal{P}_i$ and $\mathcal{F}_i$, it is easy to verify that the nonlinear terms of SMO can compensate both faults and interactions, i.e. $G_i f_i(x_i, u_i, t)$ and $M_{1i} h(x, u, t)$. Therefore, the error domain is contracted because only parts of the interactions $M_{2i} h(x, u, t)$ need to be handled.

The discontinuous part of SMO plays a special role in rejecting the fault or disturbance in the error system. In this case, if both the discontinuous part and the "matched" fault (disturbances) are taken off. The problem becomes to design an observer that can deal with the remaining uncertainties. Thus, the H_∞ method can be applied. Considering the overall system (6-38) and the observer (6-40), by solving the following LMIs (6-53), the observer gain matrix L is given and it is robust to the uncertainties.

Minimize γ, subject to $P > 0$,

$$\begin{bmatrix} A^T P + PA - WC - C^T W^T & PM_2 & I \\ M_2^T P & -\gamma I & 0 \\ I & 0 & -\gamma I \end{bmatrix} < 0 \qquad (6\text{-}53)$$

where $M_2 = diag(M_{2i}), i = 1, \dots, N$.

The observer gain matrix is determined as $L = P^{-1} W$.

Since the main problem of building Walcott-Żak observer is to find the matrices P and F satisfying $G^T P = FC$, if defining $P = \tilde{G} W_1 \tilde{G}^T + C^T W_2 C$ and solving the above LMIs with respect to $W_1 = diag(W_{1i})$, $W_2 = diag(W_{2i})$, $W = diag(W_i)$, where $W_{1i} \in \mathbb{R}^{(n_i - p_i) \times (n_i - p_i)}$, $W_{2i} \in \mathbb{R}^{p_i \times p_i}$ are s.p.d matrices, and $W_i \in \mathbb{R}^{n_i \times p_i}$, the SMO can then be designed using (6-40) and (6-44), with the norm bound of the error system given by $\|T_{eh}\| < \gamma$. This approach can attenuate the worst case influence from interactions and uncertainties acting in the state estimation error system. This can be proved using a similar procedure as given for Theorem 6.2.

Optimization of the gain matrices

By solving the LMIs (6-53), a γ with small magnitude could be obtained together with a L of large magnitude. For practical application of an SMO the size of the norm of the gain matrix L should be minimized, e.g. using LMIs. The idea to do this is to restrict the norms of W_1, W_2, W. In this case, set:

$$W^T W < \beta_W I, \beta_W > 0$$

and

$$\left(\tilde{G} W_1 \tilde{G}^T + C^T W_2 C \right)^{-1} < \beta_p I, \beta_p > 0$$

Both of these inequalities can be written in the LMI form:

$$\begin{bmatrix} \beta_w I & W \\ W^T & I \end{bmatrix} > 0, \begin{bmatrix} \beta_p I & I \\ I & \tilde{G} W_1 \tilde{G}^T + C^T W_2 C \end{bmatrix} > 0$$

From these constraints, the desired bound could be given by:

$$LL^T = P^{-1} W W^T P^{-1} < \beta_W \beta_p^2 I$$

And with these modifications, the H_∞ optimization problem with respect to minimizing the effects (in the estimation error) of the unmatched uncertainties and unmatched interactions in the SMO becomes:

$$\text{Minimize } \gamma + \beta_w + \beta_p, \text{ subject to } P = \widetilde{G}W_1\widetilde{G}^T + C^T W_2 C > 0,$$

$$\begin{bmatrix} A^T P + PA - WC - C^T W^T & PM_2 & I \\ M_2^T P & -\gamma I & 0 \\ I & 0 & -\gamma I \end{bmatrix} < 0$$

$$\begin{bmatrix} \beta_w I & W \\ W^T & I \end{bmatrix} > 0, \quad \begin{bmatrix} \beta_p I & I \\ I & \widetilde{G}W_1\widetilde{G}^T + C^T W_2 C \end{bmatrix} > 0 \tag{6-54}$$

6.3   Decentralized SMO fault estimation

Since the SMO can track the state trajectories and be insensitive to the perturbations, from this result it is also possible to provide robust estimation or reconstruction of faults.

Fault reconstruction (fault estimation) is an aspect of fault detection and isolation (FDI) which has the purpose of raising an alarm when faults occur. One well known approach to FDI is to make use of an observer to generate residual signals which are a form of estimation error (Patton, Frank and Clarke, 1989). This approach can then be used to detect the onset of faults and even determine the location of faults (fault isolation).When the residual magnitude or norm exceeds a given threshold it can be declared that a fault has occurred. However, if the residual threshold is exceeded because of disturbances or modelling uncertainty there is a potential for a false alarm to be raised. There is thus a robustness problem of FDI which relates to the degree to which the residual can be made correctly sensitive to one or more faults but insensitive or robust to uncertainties, disturbance or perturbations.

However, in most case, the fault cannot be reconstructed in FDI residual schemes and this is a significant advantage of this approach. If a fault signal can be reconstructed then there is also a possibility of making direct use the fault estimate in a control scheme that compensates for the fault. Hence, it turns out that the estimation of faults is a more powerful way to perform FDI since the alternative use of FDI residuals gives complexity which is not really required.

The development of FDI in terms of the estimation/reconstruction of faults using SMO is provided by (Edwards and Spurgeon, 1998), using the idea of "equivalent injection signals". Their work was further developed by (Tan and Edwards, 2002) who

considered the sensor faults. Also the minimization the influences from uncertainties in fault reconstruction is also researched by (Tan and Edwards, 2003).

The ideas for fault reconstruction in single (centralized) systems carry over well to LSS based on decentralized structure. Recent research about decentralized sliding mode fault estimation can be found in (Yan and Edwards, 2008). They successfully estimate the faults acting in local subsystems of a decentralized system using the Edwards & Spurgeon SMO. In their work they also discuss the relationship between the effects of interactions and faults in the estimation. However, as mentioned in the Section 6.2.3, the method requires several state transformations which make the algorithm complicated and not easy to understand. This Section describes an important development of sliding mode fault estimation which does not suffer from the transformations problem of the Edwards and Spurgeon approach but also makes use of the extension to the Walcott and Żak SMO described in Section 6.2.3. In fact the approach for decentralized SMO is applied to fault reconstruction for both actuator and sensor faults. The mathematical representation of this LSS for the nominal linear case is given as follows:

$$\dot{x}_i(t) = A_i x_i(t) + B_i u_i(t) + G_i f_{ai}(x_i, u_i, t) + M_i h_i(u, x, t)$$
$$y_i(t) = C_i x_i(t) + f_{oi}(t)$$

(6-55)

where the state vector $x_i \in \mathbb{R}^{n_i}$, the output signal $y_i \in \mathbb{R}^{p_i}$. The $f_{ai}(x_i, u_i, t)$ represent the actuator faults with distribution matrix G_i and the $f_{oi}(t)$ represent the sensor faults acting in the i-th subsystem. $h_i(u, x, t)$ is the interactions term for the i-th subsystem which might also includes the subsystem modelling uncertainties.

If the system contains both actuator and sensor faults, e.g. acting simultaneously, the approach for reconstruction of both faults is inevitable complex. This is still an open problem since the actuator faults and sensor faults might have interacting effects on the system and the state estimation. In the description given in the following Sections, it is assumed that one fault is to be reconstructed whilst the other is absent.

6.3.1 Actuator fault reconstruction

When systems contain only actuator faults, i.e. $f_{ai} \neq 0$ and $f_{oi} = 0$, the SMO method proposed in Section 6.2.3 can be used to reconstruct the fault signals very effectively. According to the description in Section 6.2.3, the local SMOs are designed in the form of (6-39):

$$
\begin{aligned}
\dot{\hat{x}}_i(t) &= A_i \hat{x}_i(t) + B_i u_i(t) + L_i C_i (y(t) - \hat{y}(t)) + K_{ni} v_i(t) \\
\hat{y}_i(t) &= C_i \hat{x}_i(t)
\end{aligned}
\tag{6-39}
$$

The local state estimation error system is given in the form of (6-6):

$$
\begin{aligned}
\dot{e}_i(t) &= (A_i - L_i C_i) e_i(t) + G_i f_i(x,u,t) - K_{ni} v_i(t)) + M_i h_i(u,x,t) \\
e_{yi}(t) &= C_i e_i(t)
\end{aligned}
\tag{6-41}
$$

Using the expansion matrix $\mathcal{G}_i$ introduced in Section 6.2.3, it is possible to attenuate the influence from interactions. Thus, assuming that the reachability is ensured and the state estimation error is bounded:

i). In finite time, the sliding surface is reached and maintained, i.e.

$$
C_i e_i = 0, \quad C \dot{e}_i = 0
$$

ii). After reaching the sliding surface, the state estimation errors are bounded. For simplicity, assume that after finite time, the sate estimation error will enter the domain:

$$
\overline{\Omega}_\varepsilon = \left\{ e_i : \| e_i \| < \| e_{Bi} \| \right\}
$$

where $\| e_{Bi} \|, i = 1, \dots, N$ are the estimation boundary constants assumed which might be calculated following the proof procedure in Section 6.2.3.

Since the expansion matrix $\mathcal{G}_i$ for the i-th subsystem is used, the rank condition is satisfied, i.e. $rank(C_i \mathcal{G}_i) = rank(\mathcal{G}_i) = p_i$. Moreover, $G_i = \mathcal{G}_i \bar{G}_i$ and $M_i = \mathcal{G}_i \bar{M}_{1i} + \tilde{\mathcal{G}}_i \bar{M}_{2i} = M_{1i} + M_{2i}$ can be constructed. This means that all the information about the f_{ai} and some of the information about interactions, i.e. $M_{1i} h(x, u, t)$, are preserved in the output. In this case, using the equivalent output error injection signal, after sliding motion take place, yields:

$$0 = C_i(A_i - L_iC_i)e_i(t) + C_iG_if - C_iK_{ni}v_{eq,i} + C_iM_ih_i \qquad (6\text{-}56)$$

where $v_{eq,i}$ is the equivalent output error injection signal which plays the same role as the "equivalent control" in sliding mode control (Edwards and Spurgeon, 1998). The equivalent output injection signal is represented by the values of the nonlinear switching terms v_i defined by (6-44), which is necessary to maintain the sliding motion.

Note that since $C_iG_i = C_i\mathcal{P}_i^{-1}C_i^T\mathcal{F}_i^T\bar{G}_i$, $C_iK_{ni} = C_i\mathcal{P}_i^{-1}C_i^T$ and $C_iM_i = C_i\mathcal{P}_i^{-1}C_i^T\mathcal{F}_i^T\bar{M}_{1i} + C_iM_{2i}$, by multiplying each side by $(C_i\mathcal{P}_i^{-1}C_i^T)^{-1}$, it follows:

$$v_{eq,i} = \mathcal{F}_i^T(\bar{G}_if_i + \bar{M}_{1i}h_i) + (C_i\mathcal{P}_i^{-1}C_i^T)^{-1}C_i[(A_i - L_iC_i)e_i + M_{2i}h_i]$$

Thus, the fault estimation is given by:

$$f_i = \bar{G}_i^+(F_i^+)^Tv_{eq,i} - \bar{G}_i^+\bar{M}_{1i}h_i + \mathcal{X}[(A_i - L_iC_i)e_i + M_{2i}h_i] \qquad (6\text{-}57)$$

where $\mathcal{X} = \bar{G}_i^+(F_i^+)^T(C_i\mathcal{P}_i^{-1}C_i^T)^{-1}C_i$.

By using the equivalent output injection, our estimation of faults is $\hat{f} = \bar{G}_i^+(F_i^+)^Tv_{eq,i}$. Then consider the following two cases:

Case 1. If $\bar{G}_i^+\bar{M}_{1i} = 0$ and $M_{2i} = 0$

In this case, the interactions satisfy $rank(C_iM_i) = rank(M_i)$. The interactions act within a different channel of the system compared with the faults, and their distribution matrices are therefore orthogonal. It is easy to verify that the sliding mode switching term can completely compensate the interactions. Thus, the error $e(t)$ is quadratically stable. (6-57) can then be rewritten as:

$$f_i = \bar{G}_i^+(F_i^+)^Tv_{eq,i} + \mathcal{X}(A_i - L_iC_i)e_i$$

As $t \to \infty$, $\lim_{t\to\infty}e_i(t) = 0$, thus,

$$\hat{f}_{ai} = \bar{G}_i^+(F_i^+)^Tv_{eq,i} = f_{ai}$$

which means that the faults can be estimated precisely.

Case 2. If $\bar{G}_i^+ \bar{M}_{1i} \neq 0$ and $M_{2i} \neq 0$

According to (6-57),

$$\|f_{ai} - \hat{f}_{ai}\| = \bar{G}_i^+ \bar{M}_{1i} h_i + \mathcal{X}[(A_i - L_i C_i)e_i + M_{2i}h_i]$$

Following a similar procedure to Theorem 6.2, according to ii), the local state estimation error system reaches the following domain in finite time:

$$\overline{\Omega}_\varepsilon = \left\{ e_i : \|e_i\| < \|e_{Bi}\| \right\}$$

Meanwhile, as assumed in Section 6.2.3, $\|h_i(u, x, t)\| \leq \varpi_i$, it follows that:

$$\|f_{ai} - \hat{f}_{ai}\| \leq (\|\bar{G}_i^+ \bar{M}_{1i}\| + \|\mathcal{X}_i M_{2i}\|)\varpi_i + \|\mathcal{X}_i (A_i - L_i C_i)\|\|e_{Bi}\| \qquad (6\text{-}58)$$

As long as the matrices M_i pre-multiplying the interactions are not satisfying as in Case 1, the fault estimation cannot track the actual faults precisely. But from (6-58), it can be seen that the fault estimation errors are bounded.

Moreover, recalling the discontinuous part in (6-44), $sign(e_y) = e_y / \|e_y\|$ is either 0 or 1, which means that the fault estimation could not be constructed by this discontinuous *sign* function. (Edwards and Spurgeon, 1998) propose that by adding a small positive scalar in the denominator, as described in Section 4.2.3, a continuous fault estimation signal will result. Thus, the nonlinear part for the SMO (6-44) is modified to:

$$v_i(t) = (\|F_i\|\Psi_i(t) + \eta_i)\frac{e_y(t)}{\|e_y(t)\| + \Delta}, \quad \dot{\Psi}_i(t) = \|e_{yi}(t)\|, \quad \eta_i > 0, \quad \Psi_i(0) \geq 0 \quad (6\text{-}59)$$

where Δ is a small positive scalar.

For Case 1, the fault reconstruction can be written as:

$$\hat{f}_{ai} \approx \bar{G}_i^+ (F_i^+)^T \|F_i\|\Psi_i(t) + \eta_i)\frac{e_y(t)}{\|e_y(t)\|} \qquad (6\text{-}60)$$

Reconsider now the SMC described in Chapters 4 and 5. Note that SMC is such a robust control method that it can compensate any matched perturbations (completely compensation in ideal case). Since most of the actuator faults are matched, if the system can tolerate the actuator faults with SMC, is it still valuable to do the actuator fault

estimation using SMO? It seems that the functions of the actuator fault tolerance using SMC and the actuator fault estimation using SMO somehow overlap. However, looking at the problem form an industrial system point of view, the answer to this question is positive due to the following reasons:

a) If the actuator fault is an actuator *outage* or the actuator is *stuck*, the actuator is no longer able to function. Thus, even with powerful SMC, the fault cannot be tolerated. The only solution to this problem is to replace the actuator. This is the reason why practical plants must use redundant actuators. This is the case, for example in aircraft where wing actuators are duplicated. Hence, the actuator fault estimation using SMO is necessary to determine when the fault is significant for the second actuator to be brought into action to replace the assumed faulty one.

b) If the actuator loses *effectiveness*, with SMC, the control input required by the system stabilization or tracking makes the actuator overload. Thus, although the actuator faults can be tolerated with SMC, it is still valuable to detect these faults so one can decide whether the actuator should be replaced.

c) If the actuator faults are considered as external disturbances (uncertainties), and the compensation signal produced by SMC does not exceed the saturation of the actuator, then there is no need to estimate the disturbance.

From the above discussion, it can be seen that for the case of actuator faults that might lead to actuator failures, the best way is to detect (estimate) them instead of attempting to compensate them with SMC. This deduction leads to another discussion about the capability of the SMC. In practical problems, the actuator operates within practical bounds of $\pm\omega$. When applying SMC, since the choice of the gain ρ should be larger than the norm bound of disturbances/uncertainties $\rho > \|f\|$, the bound values of the actuator $\pm\omega$ limit the capability of the SMC $\rho < \|\omega\|$. Thus, if a actuator fault occurs and the bound of this fault exceed $\pm\omega$, the SMC cannot tolerate it. Thus, a fault detection component should be considered to raise the alarm. Thus, when consider the combination of SMC and SMO, the SMC is designed to tolerate the disturbances and uncertainties and SMO is used to estimate the actuator faults in order to provide fault information to the engineer.

6.3.2 Sensor fault reconstruction

In contrast to actuator fault reconstruction, the equivalent control method is not suitable to be used alone to reconstruct the sensor fault. The work by (Edwards and Spurgeon, 1998) proposed a case when the sensor fault varies slowly, i.e. $\dot{f}_{oi} \approx 0$, the equivalent control method can still be applied to get the approximate fault reconstruction. However, this constraint is rather restrictive for sensor faults.

Thus, an output filter is proposed by (Tan and Edwards, 2002) as a compensator to reconstruct the output signals based on use of the Edwards and Spurgeon observer. The idea of this strategy is to use a filter to filter the outputs so that the augmented system (combination of original system and filters) has reliable measurements. Thus, the sensor faults can be treated as actuator faults. This Section proposes a sensor fault reconstruction algorithm using the Walcott-Żak observer applicable to a decentralized system (as described in Section 6.2.3).

Consider the local subsystem state variables $z_{fi} \in \mathbb{R}^p$ for the filter:

$$\dot{z}_{fi}(t) = -A_{fi}z_{fi}(t) + A_{fi}y_i(t) \tag{6-61}$$

where $(-A_{fi})$ is a stable and invertible matrix, usually selected as $A_{fi} = aI$.

Substituting the system output equation (6-55) into the filter (6-61), yields:

$$\dot{z}_{fi}(t) = -A_{fi}z_{fi}(t) + A_{fi}C_ix_i(t) + A_{fi}E_if_{oi} \tag{6-62}$$

Then combine the filter and the state equation into a new augmented system:

$$\begin{bmatrix} \dot{x}_i(t) \\ \dot{z}_{fi}(t) \end{bmatrix} = \begin{bmatrix} A_i & 0 \\ A_{fi}C_i & -A_{fi} \end{bmatrix} \begin{bmatrix} x_i(t) \\ z_{fi}(t) \end{bmatrix} + \begin{bmatrix} B_i \\ 0 \end{bmatrix} u_i(t) + \begin{bmatrix} M_i \\ 0 \end{bmatrix} h_i(x,u,t) + \begin{bmatrix} 0 \\ A_{fi}E_i \end{bmatrix} f_{oi}$$

$$y_{fi} = \begin{bmatrix} 0 & I_{p_i} \end{bmatrix} \begin{bmatrix} x_i(t) \\ z_{fi}(t) \end{bmatrix} \tag{6-63}$$

The new system can be written in the form of a system containing the actuator fault as:

$$\dot{z}_i(t) = A_{oi}z_i(t) + B_{oi}u_i(t) + M_{oi}h_i(t) + G_{oi}f_{oi}$$
$$y_{fi} = C_{oi}z_i(t) \tag{6-64}$$

where $A_{oi} \in \mathbb{R}^{(n_i+p_i)\times(n_i+p_i)}$, $B_{oi} \in \mathbb{R}^{(n_i+p_i)\times m_i}$, $M_{oi} \in \mathbb{R}^{(n_i+p_i)\times n_i}$ $G_o \in \mathbb{R}^{(n_i+p_i)\times p_i}$, $C_{oi} \in \mathbb{R}^{p_i\times(n_i+p_i)}$.The sensor faults become actuator faults in the augmented system (6-64). The same algorithm described in Section 6.2.3 can be used estimate the sensor fault. However, within this method, two crucial conditions still need to be satisfied:

1). $rank(C_{oi}G_{oi}) = rank(G_{oi})$

2). any invariant zero of (A_{oi}, G_{oi}, C_{oi}) must lie in $\mathbb{C}_-$

For the first condition, it is easy to verify that:

$$rank(C_o G_{oi}) = rank\left(\begin{bmatrix} 0 & I_{p_i} \end{bmatrix}\begin{bmatrix} 0 \\ A_{fi}E_i \end{bmatrix}\right) = rank\left(\begin{bmatrix} 0 \\ A_{fi}E_i \end{bmatrix}\right) = rank(G_{oi})$$

For the second condition, construct the Rosenbrock system matrix $P(z)$ based on the matrices (A_{oi}, G_{oi}, C_{oi}). (Tan and Edwards, 2003):

$$P(z) = \begin{bmatrix} sI - A_{oi} & G_{oi} \\ C_{oi} & 0 \end{bmatrix} = \begin{bmatrix} sI - A_i & 0 & 0 \\ -A_{fi}C_i & sI + A_{fi} & A_{fi}E_i \\ 0 & I & 0 \end{bmatrix}$$

Since the invariant zeros of (A_{oi}, G_{oi}, C_{oi}) are the values of s which make the matrix $P(z)$ lose rank. In this case, the matrix $P(z)$ loses rank if and only if $\tilde{P}(z)$ loses rank:

$$\tilde{P}(z) = \begin{bmatrix} sI - A_i & 0 \\ -A_{fi}C_i & A_{fi}E_i \end{bmatrix} = \begin{bmatrix} I & 0 \\ 0 & A_{fi} \end{bmatrix}\begin{bmatrix} sI - A_i & 0 \\ -C_i & E_i \end{bmatrix}$$

Since A_{fi} is invertible, the values of s which make $\tilde{P}(z)$ lose rank are the eigenvalues of A_i. As the observer is designed to estimate the faults, the original system is expected to be asymptotically stable. . This means that if one can build an SMO based on the original system, an SMO based on the augmented system can also be constructed.

(Tan and Edwards, 2002) state that the choice of A_f does not affect the reconstruction signal but affects the observer gains. However, the choice of A_f affects the accuracy of the sensor fault estimation. As can be seen from the SMO structure, the SMO for the augmented system estimates the filter outputs. The filtered outputs may not retain a good sensitivity to the faults, e.g. if a low-pass filter is used in the presence of a high

frequency sensor fault, then the SMO cannot estimate the fault properly since the fault effects appearing in the outputs of the filter are not the original sensor faults. For this first order filter, larger diagonal elements of A_f give better estimation accuracy. However, large elements of A_f might lead to high observer gain and further lead to significant chattering effect on the SMO state estimates. Thus, the value of the diagonal elements should be chosen carefully so that the numerical conditioning of the augmented system (6-63) can be maintained/established.

The purpose of sensor fault estimation is to monitor the effects of faults such as sensor deterioration. However, if the sensor fault signal can be precisely estimated, it can also be used to compensate the actual sensor fault appearing in the output feedback control input. The idea is quite straightforward: if the sensor faults are additive faults (added directly to the measurements), and the control law is designed as $u = f(y, t)$, sensor faults are estimated by $\hat{f}_o$, so that the control law after compensation is $u = f(y - \hat{f}_o, t)$. The idea of sensor fault compensation (sensor fault hidden in the control) is illustrated in Chapter 7.

6.4   Simulation result

To illustrate the observer and fault estimation algorithms, an example system comprising two interconnected linear subsystems with non-linear interconnections is given as follows.

$$\dot{x}_1 = \begin{bmatrix} 0 & 1 \\ 0 & 0 \end{bmatrix} x_1 + \begin{bmatrix} 0 \\ 1 \end{bmatrix} u_1 + \begin{bmatrix} 1 & 0 \\ 0 & 1 \end{bmatrix} h_1(x, t) + G_1 f_{a1}$$

$$y_1 = \begin{bmatrix} 1 & 1 \end{bmatrix} x_1 + E_1 f_{o1}$$

$$\dot{x}_2 = \begin{bmatrix} -1 & 0 & 1 \\ 1 & 2 & 0 \\ 0 & 1 & -1 \end{bmatrix} x_2 + \begin{bmatrix} 0 \\ 1 \\ 0 \end{bmatrix} u_2 + \begin{bmatrix} 1 & 0 & 0 \\ 0 & 1 & 0 \\ 0 & 0 & 1 \end{bmatrix} h_2(x, t) + G_2 f_{a2}$$

$$y_2 = \begin{bmatrix} 0 & 1 & 0 \\ 1 & 1 & 0 \end{bmatrix} x_2 + E_2 f_{o2}$$

$$h_1(x, t) = \alpha_1 \cos(x_{22}) H_1 x$$

$$h_2(x, t) = \alpha_2 \cos(x_{11}) H_2 x$$

with $\alpha_1 = \alpha_2 = 0.5$ represent the nonlinear interactions, where:

$$H_1 = \frac{1}{\sqrt{10}} \begin{bmatrix} 1 & 1 & 1 & 1 & 1 \\ 1 & 1 & 1 & 1 & 1 \end{bmatrix}$$

$$H_2 = \frac{1}{\sqrt{15}} \begin{bmatrix} 1 & 1 & 1 & 1 & 1 \\ 1 & 1 & 1 & 1 & 1 \\ 1 & 1 & 1 & 1 & 1 \end{bmatrix}$$

Assume that the system is already stabilized by the state feedback controller $u_i = K_i x_i$. Consider the actuator and sensor faults in turn using the fault estimation method proposed in section 6.3.

Actuator faults reconstruction

Assume that there are no sensor faults, i.e. $f_{oi} = 0, i = 1,2$.

Applying sinusoidal and step signals (to model actuator faults) to subsystems 1 and 2 respectively, the faults can be written as:

$$G_1 f_{a1} = \begin{bmatrix} 0 \\ 1 \end{bmatrix} \sin(t)$$

$$G_2 f_{a2} = \begin{bmatrix} 0 \\ 1 \\ 0 \end{bmatrix} u_c(t)$$

The fault for the first subsystem f_{a1} is given at time $t = 5s$ and the fault f_{a2} for the second subsystem is given at time $t = 8s$. Defining an expansion matrix for the aggregated system:

$$\mathcal{G} = \begin{bmatrix} 0 & 0 & 0 \\ 1 & 0 & 0 \\ 0 & 1 & 0 \\ 0 & 0 & 1 \\ 0 & 0 & 0 \end{bmatrix}$$

A feasible solution of the LMIs in (6-54), is $\gamma = 2.1$, with:

$$L_1 = \begin{bmatrix} -0.16 \\ 2.13 \end{bmatrix}, L_2 = \begin{bmatrix} -3.82 & 0.49 \\ -0.05 & 3.71 \\ -0.32 & 1.23 \end{bmatrix}$$

If only linear observers are used, the estimation error cannot be robust to both the faults and the interactions, as shown in Figure 6-1.
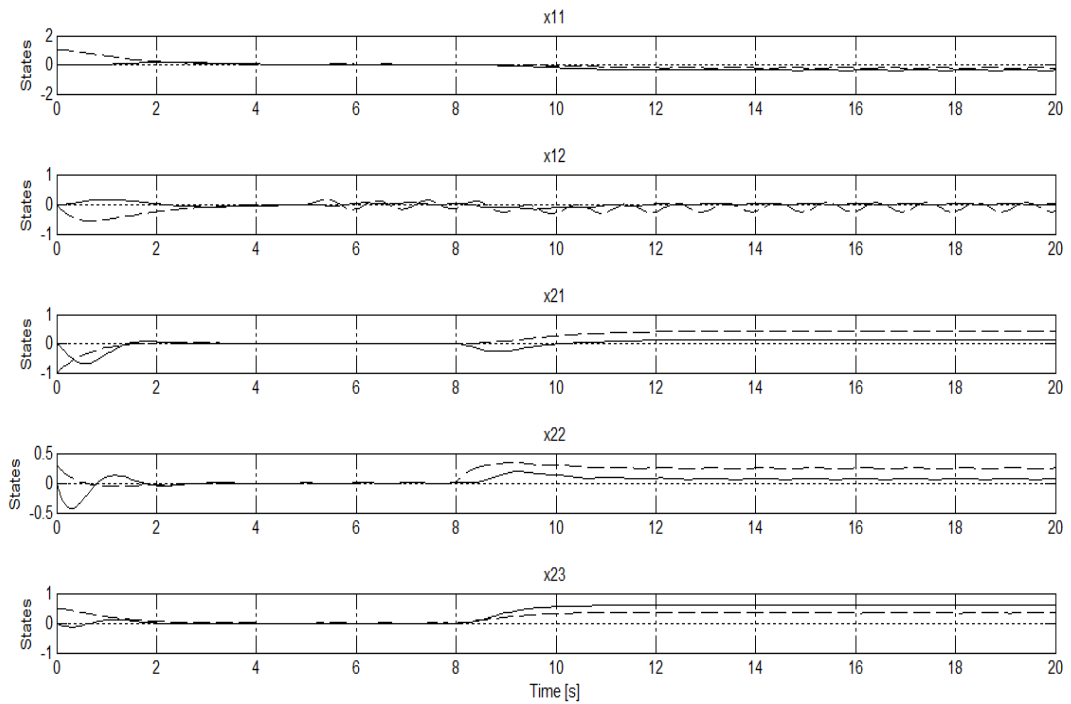
Figure 6-1. Linear observer case of state responses for both the system (dash) and observer (solid) when faults occur

To construct a Walcott-Żak observer, a switching term (6-44) is added to the feedback of the linear observer, the results is shown in Figure 6-2.

Figure 6-2 implies that the accuracy of sliding mode observer is much better than the accuracy with only linear observer. The error between the decentralized sliding mode observer and the original system is derived from "unmatched" interactions which cannot be avoided by using only sliding mode observer. The actuator faults can be estimated by the equivalent output injection
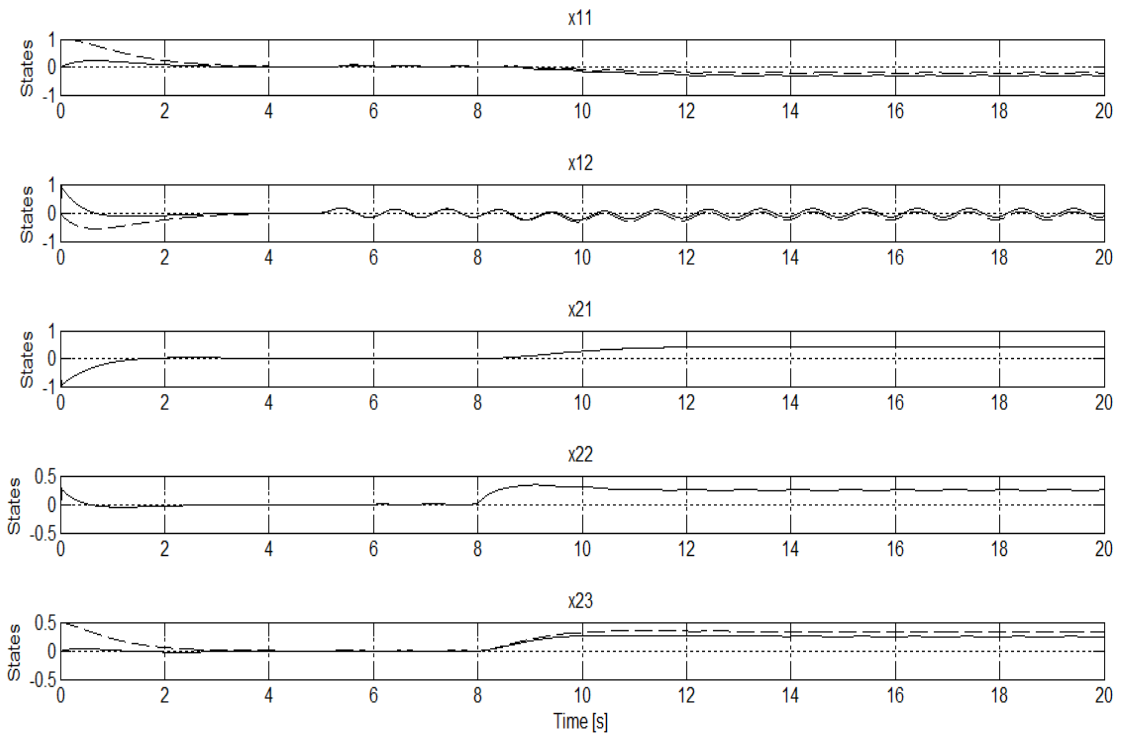
Figure 6-2. SMO case of state responses for both the system (dash) and observer (solid) when faults occur

From Figure 6-3, it should be noted that the fault estimation can estimate the faults properly. However, because of the influence from interactions, the estimation is not accuracy. To get accurate estimations, there should be some restriction for the interactions, as described in section 6.3:

$$M_1 = \begin{bmatrix} 0 & 0 \\ 0 & 0 \end{bmatrix}, \qquad M_2 = \begin{bmatrix} 1 & 0 & 0 \\ 0 & 0 & 0 \\ 0 & 0 & 0 \end{bmatrix}$$

The estimation is shown in Figure 6-4. It shows that the faults can be precisely estimated.
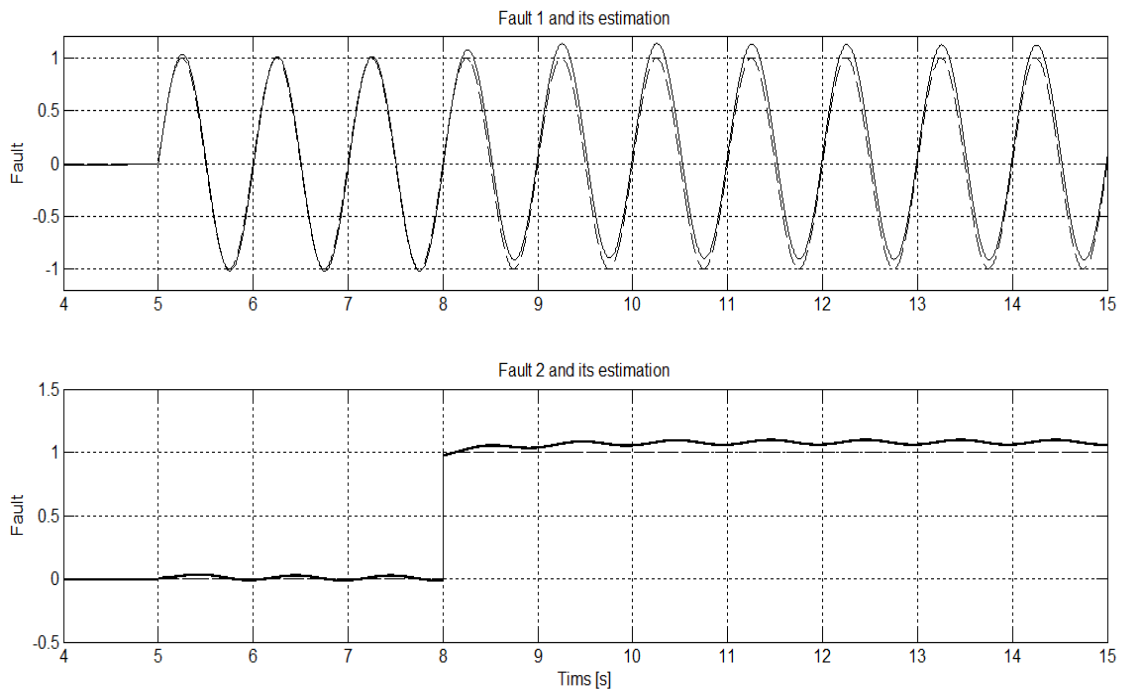
Figure 6-3. Faults (dash) and their estimations (solid) using equivalent output injection
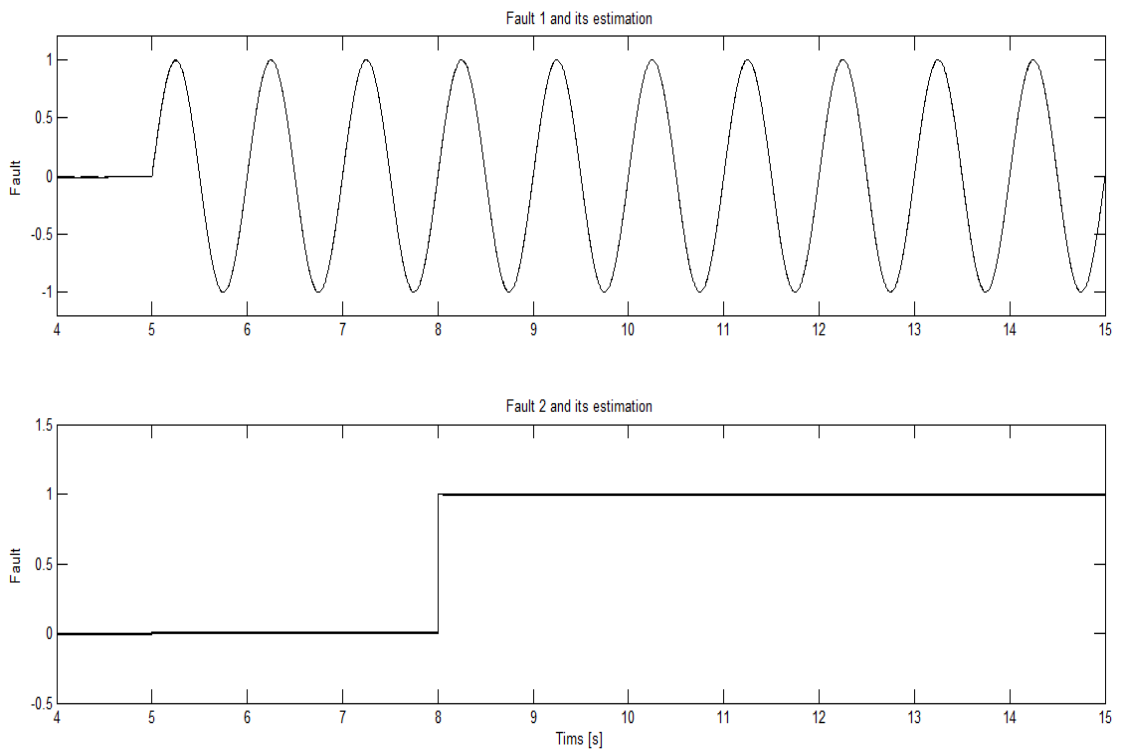

Figure 6-4. Faults (solid) and their estimations (dashed) with restricted interactions

168

Sensor fault reconstruction

As described in Section 6.3.2, by choosing the filter matrix $A_{f_i} = 20I_{p_i}$, the new augmented subsystem is in the form:

$$\begin{bmatrix} \dot{x}_i(t) \\ \dot{z}_{fi}(t) \end{bmatrix} = \begin{bmatrix} A_i & 0 \\ A_{fi}C_i & -A_{fi} \end{bmatrix} \begin{bmatrix} x_i(t) \\ z_{fi}(t) \end{bmatrix} + \begin{bmatrix} B_i \\ 0 \end{bmatrix} u_i(t) + \begin{bmatrix} M_i \\ 0 \end{bmatrix} h_i(x,u,t) + \begin{bmatrix} 0 \\ A_{fi}E_i \end{bmatrix} f_{oi}$$

$$y_{fi} = \begin{bmatrix} 0 & I_{p_i} \end{bmatrix} \begin{bmatrix} x_i(t) \\ z_{fi}(t) \end{bmatrix}$$

where, $E_1 = 0$, $E_2 = \begin{bmatrix} 0 \\ 1 \end{bmatrix}$. Here use a Gaussian noise signal as the sensor fault for subsystem 2. The new matrix A_{oi} for the augment system is given by:

$$\begin{bmatrix} A_1 & 0 \\ A_{f1}C_1 & -A_{f1} \end{bmatrix} = \begin{bmatrix} 0 & 1 & 0 \\ 0 & 0 & 0 \\ 20 & 20 & -20 \end{bmatrix}$$

$$\begin{bmatrix} A_2 & 0 \\ A_{f2}C_2 & -A_{f2} \end{bmatrix} = \begin{bmatrix} -1 & 0 & 2 & 0 & 0 \\ 1 & 2 & 0 & 0 & 0 \\ 0 & 1 & -1 & 0 & 0 \\ 0 & 20 & 0 & -20 & 0 \\ 20 & 20 & 0 & 0 & -20 \end{bmatrix}$$

It should also be noted that, the new output matrices C_{oi} have the same ranks as their counterparts C_i. However, the influence from the interactions cannot be compensated in the sensor fault SMO since whatever the structure of M_{oi} the $rank(C_{oi}M_{oi}) = 0$. This follows since the sensor fault problem is transformed into an actuator fault problem in which the actuator faults cannot be compensated. However, since this system is a regulator problem and a state feedback control is applied, the influence from interactions is not clear in this sensor fault estimation case as $h(x,t) \rightarrow 0$ when $x \rightarrow 0$.
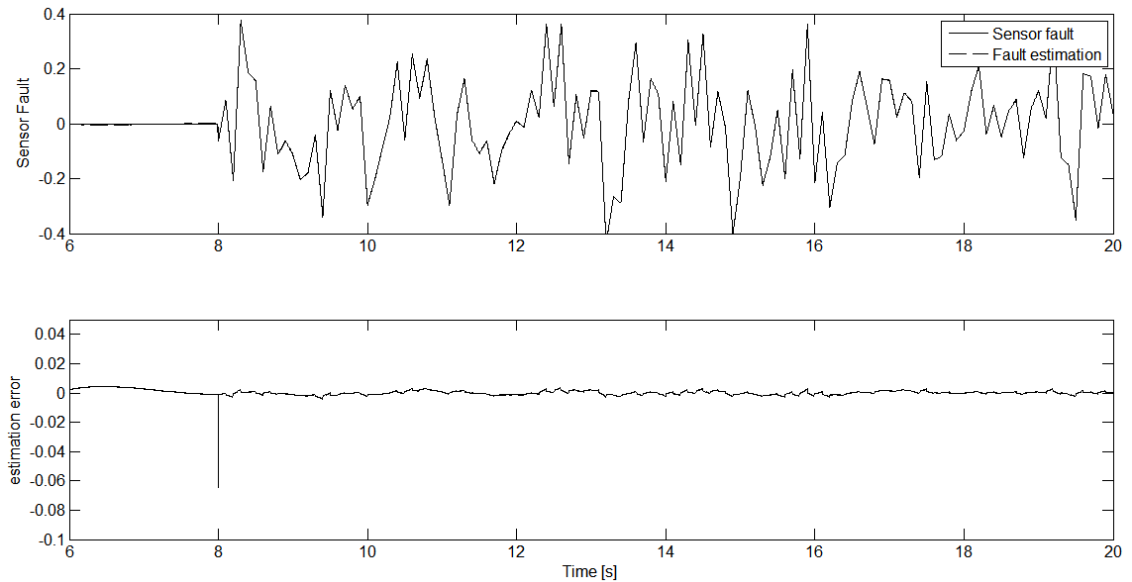
Figure 6-5. Sensor fault estimation (upper) and the fault estimation error (lower)

Figure 6-5 shows the SMO estimation of the sensor fault which has satisfactory accuracy. Thus, the method proposed in Section 6.3.2 can faithfully reconstruct the sensor fault.

6.5   Conclusion

The purpose of this Chapter is to develop a suitable framework for observer design for decentralized systems based on the sliding mode observer. Both the Walcott-Żak and Edwards & Spurgeon SMOs are reviewed. To avoid the complicated transformations of the latter observer, the Walcott-Żak SMO has been selected as the most appropriate state and fault estimation approach for decentralized systems. To not have to require state transformations is a big advantage for a complex LSS. Furthermore, to simplify the design procedure, the LMI method proposed recently has been used in order to de-couple the s.p.d. structure of the matrix P of constraint equation $G^T P = FC$ for the inequalities arise from Lyapunv function. On the other hand, as a further contribution in this work, the sliding surface of the Walcott-Żak SMO is modified to avoid the inaccurate output estimation when the sliding surface has been reached.

According to the output injection property of the SMO, the feedback switching term can approximate the "matched" unwanted signal in the system. The so-called "equivalent output injection" can then be used to estimate the actuator fault. Although the Edwards & Spurgeon observer has been researched extensively in the literature for the fault

estimation problem, a main contribution of this Chapter is a discussion of the capability of the Walcott-Żak observer for LSS systems. The difference between the single system and the LSS is the presence of interactions which lead to inevitable error in the actuator fault estimation. It is proposed in this Chapter that for a certain type of interactions, the influence of the interactions can be neglected in the actuator fault estimation.

For the sensor fault estimation problem to keep to the standard form of SMO (based on actuator faults), a filter is used to construct a suitable augmented system. The sensor fault problem is thus transferred to an equivalent actuator fault problem. The synthesised actuator fault estimation in this augmented system can then be treated as an actuator fault in the normal way in the SMO system. It should be noted that, with state feedback regulation, the output error will not be affected by any uncertainties/interactions. However, in the case of output feedback the presence of sensor faults leads to a difficult fault estimation problem which is currently still an open problem.

Finally, a simple example is used to illustrate the proposed extension to the Walcott-Żak SMO method. Both actuator fault and sensor fault estimation algorithms are applied in turn in this model to illustrate the validity of using this approach.

Chapter 7

Sliding Mode Control and Estimation for Furnace System Model

7.1 Introduction

From Chapter3, the nonlinear state space furnace system model is established, simulated and validated. Since the main objective of this thesis is the application of decentralized sliding mode, this Chapter focuses on robust decentralized control for this furnace model system. As a consequence of the strong non-linearities (heat source q and thermal properties of strip λ_s and c_s), the system must be linearized and simplified. When this has been done the model based control strategies can then be designed based on this linear model. However, in order to justify these methods, the local controllers should be implemented on the nonlinear system. The sliding mode fault estimation methods are also applied to this furnace model.

7.2 Linearization and controller design issues

As described in Chapter 3, the furnace model contains strong nonlinearities which make controller design very complicated. This nonlinear model has to be linearized before suitable advanced control methods can be used to design the decentralized controller. The nonlinearities arise from: 1). Radiation heat transfer and 2). The change of both thermal conductivity and heat capacity of the steel strip during the heating process. These nonlinearities in the linearization cannot be ignored otherwise the system model will not represent the true system dynamics closely enough.

Section 7.2.1 considers the linearization of the furnace model.

7.2.1 Linearization

The standard linear identification techniques using MATLAB Toolbox Linearization Tools are applied to derive the linear model of the furnace system. However, the linearized system only considered valid for one operating temperature. This temperature should lie within the linear range of the furnace operation. If the operating point lies outside or on the boundary of the operating region, then it would not be possible to

identify a linear model with high enough fidelity to the furnace system. Linearized models outside or on the operating boundary will result in unacceptable large modelling uncertainties and bad controller design.

The operating points for the three zones are determined as $T_{op} = T_{ref} = [480°C \quad 580°C \quad 680°C]^T$, as used in Chapter 3. Since the system cannot reach this operating point without suitable power input, three simple PID controllers (corresponding to these three heating zones) are used to drive the system to the reference temperatures.

Consider the modelling uncertainties in this furnace problem. Since the furnace model is a tracking problem, the uncertainties cannot be zero even though the system is stable ($f(x,t) \neq 0$ since $x \neq 0$). To improve the performance, an integral state is added to each subsystem.

To conclude, after linearization and the modification described above, the i-th linear subsystem can be considered to be of the form:

$$\dot{x}_i = \begin{bmatrix} \dot{x}_{i,a} \\ \dot{x}_{i,s} \\ \dot{x}_{i,w} \end{bmatrix} = \begin{bmatrix} 0 & \mathbf{0}_{(n_i-1)\times 1} & 1 & \mathbf{0}_{N_w \times 1} \\ \mathbf{0}_{1\times n_i} & \bar{A}_{i,11} & & \bar{A}_{i,12} \\ \mathbf{0}_{1\times N_w} & \bar{A}_{i,21} & & \bar{A}_{i,22} \end{bmatrix} x_i + \begin{bmatrix} 0 \\ B_i \end{bmatrix} u_i$$

where $x_{i,a} \in \mathbb{R}$ is the additive integral states to improve the system performance, $x_{i,s} = \Delta T_{i,s} = T_{i,s} - T_{i,ref} \in \mathbb{R}^{n_i}$. $x_{i,w} = \Delta T_{i,w} = T_{i,w} - T_{i,op} \in \mathbb{R}^{N_w}$ and:

$$\bar{A}_i = \begin{bmatrix} \bar{A}_{i,11} & \bar{A}_{i,12} \\ \bar{A}_{i,21} & \bar{A}_{i,22} \end{bmatrix}$$

is the system matrix after linearization, $\bar{B}_i$ is the input matrix after linearization. Because of the Stefan-Boltzmann constant, the elements of $\bar{B}_i$ are relatively small which can be slightly enlarged by choose kW as the unit of power input. Then, since the system is a 4.6 MW radiant furnace, the input bound (represented as a saturation) should be defined lower than 4600 kW. With the data from (McGuinness and Taylor, 2004), the input power boundary for each heating zone is 150kW.

7.2.2 Furnace controller design issues

The problems encountered during the furnace controller design are outlined briefly in this Section.

1. Saturation control

    As stated previously the power inputs are considered to have saturated behaviours. However, the detail as to whether the power inputs make use of gas or electrical power supply is not included in the modeling and hence the implications need not be discussed further other than to point out that the saturation is a strong non-linearity that has most effect in the beginning of the heating phase.

2. Uncertainties in the furnace

    The uncertainties of the furnace are the main problems in this Chapter. As described in Chapter 3, the thickness of the steel, the velocity variation, and power supply uncertainty are the main uncertainties in this furnace. According to the fault classification, the power supply uncertainty is matched actuator fault, whilst the thickness and velocity variations are component faults which can be separated into matched and unmatched components. To attenuate or remove the influence from uncertainties, sliding mode control is a proper choice for this furnace problem. As this is a tracking problem, in which the component faults are no-zero. Thus, the error is unavoidable but should be bounded in an acceptable range. According to data from the report by (McGuinness and Taylor, 2004), the acceptable temperature error range may be considered as $\pm 10°C$. The static error should not exceed this range.

3. Overshoot and Time Response

    The temperature overshoot is highly undesirable in the furnace, especially for the temperature at the output position. The high temperature overshoots might lead to different annealing results. Also it means wastage of energy and time, as one has to stop or lower the power supply to cool the strip down after the overshoot. This problem can be handled by using the input saturation. A related problem is the time response of the furnace which does not cause difficulties because the speed of the response is not the main issue in industrial furnace

4. Minimizing Chattering

The chattering of the input voltage can be removed by increasing the SMC boundary layer. This problem might becomes more serious in the SMO case if observer is used for control feedback, as the speed of observer should be faster than that of the closed-loop system characteristics.

The controller is firstly designed based on the linearized model. Then it is implemented and tested on the nonlinear simulation code.

7.3   Nonlinear closed-loop simulation

This Section shows results corresponding to the application of the different controllers. The most commonly applied PID controller is implemented first of all. It has been shown that there are some difficulties when designing a PID controller due to the difficulty in choosing a suitable gain. Moreover, it is clearly the case that when a PID controller alone is used the system is not robust to the uncertainties. It is then necessary to apply an advanced control strategy. The state feedback SMC is then applied to show the efficiency of this type of controller.

Since it would be very hard or expensive to measure all the temperatures at different grids, the static output feedback SMC structure is chosen as described in Chapter 5. With both of these SMC strategies, the matched faults can be rejected, which provides better performance than conventional PID controller.

7.3.1 PID controller performance and faults description

It is reasonable to compare the SMC methods with a conventional PID controller. As shown in Figure 3-8, without any faults the system runs smoothly and the strip exit temperatures meet the requirement, see Figure 7-1.

However, one of the main disadvantages of the PID controller is that it is very hard to choose the gains manually. An inappropriate choice of proportional or integral gain parameters leads to overshoot or slow time response.
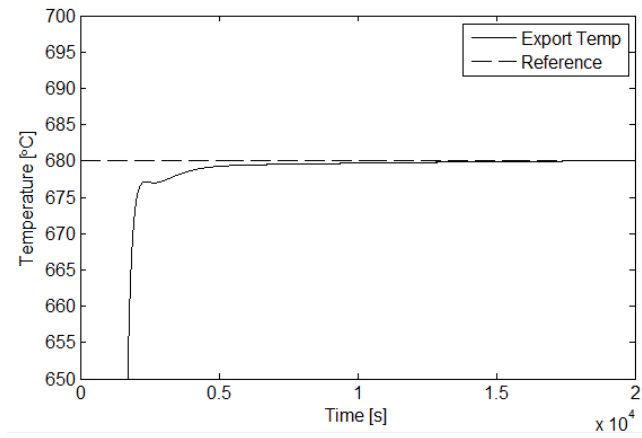
Figure 7-1. Furnace exit temperature tracking performance with PID controller

The control input is shown in Figure 7-2, showing that the gain choice of PID control leads to a slight overshoot problem in the second heating zone.
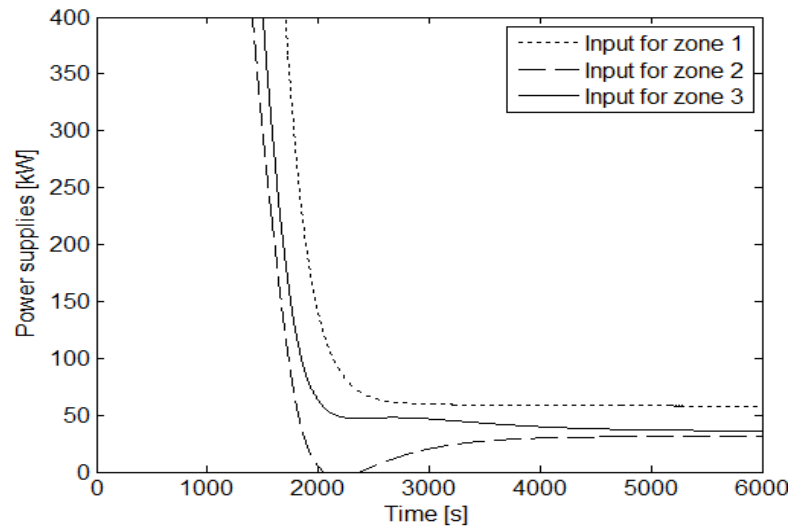
Figure 7-2. Power input for each heating zone with PID controller

When the faults occur, the PID controller cannot tolerate the faults. The system is sensitive to thickness and velocity changes, as well as sensitive to the power disturbance. The faults used in this system are shown in Figure 7-3.
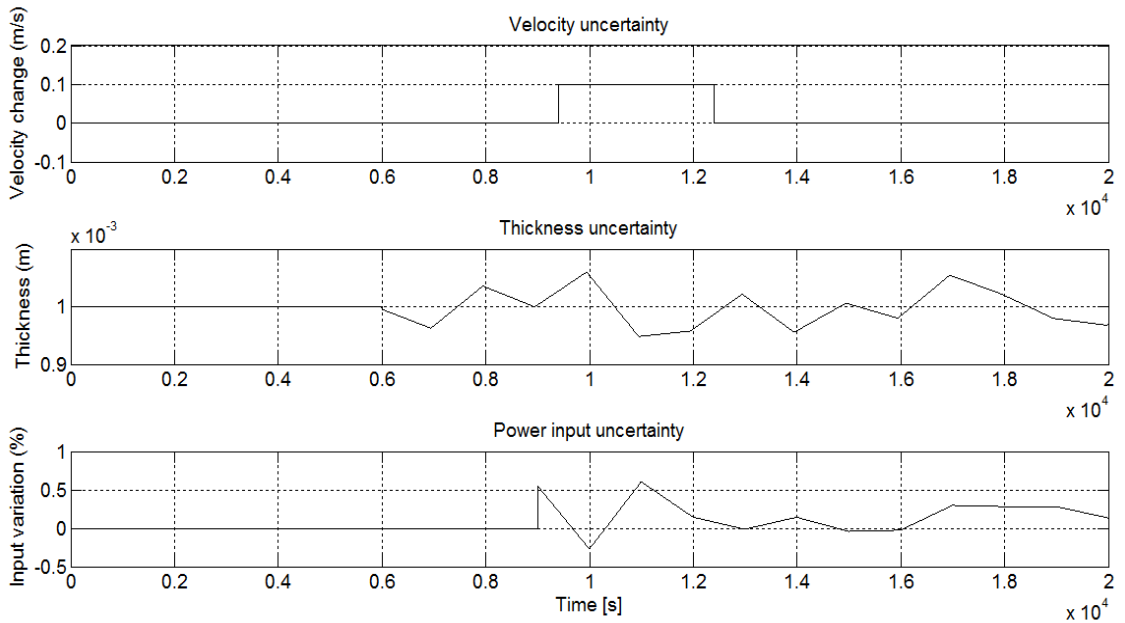
Figure 7-3. Faults (uncertainties) in furnace model system
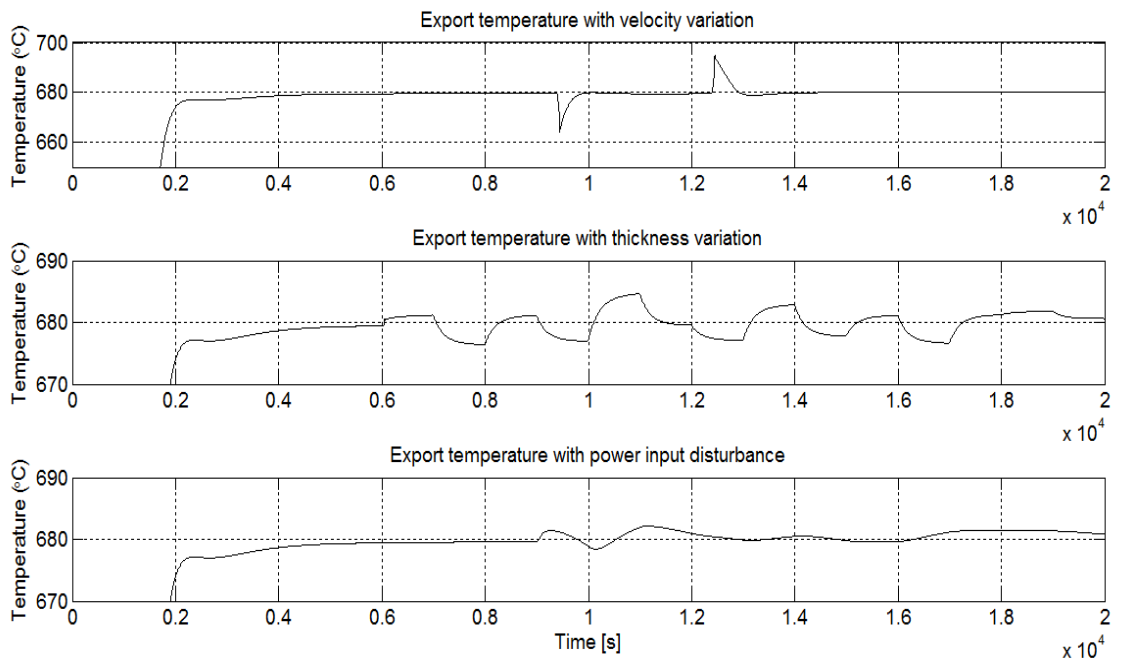
Figure 7-4. Furnace exit temperature with different types of faults using PID controller

Figure 7-4 shows the time responses of thee strip exit temperatures for three types of faults shown in Figure 7-3. It is easy to note that the increasing the strip velocity, strip thickness or decreasing the power input lead to the decline of the strip exit temperatures and vice versa.

According to the model description in Section 7.2.2, these three types of faults are 1). Unmatched (velocity variation), 2). Containing unmatched and matched components (thickness variation) and 3). Matched (power input disturbance). From the description of the sliding mode theory in Chapter 4, it is clear that the SMC can compensate the power input disturbance and a part (the matched component) of the thickness variation. But for the velocity variation, it is necessary to combine other methods to deal with this fault. Section 7.3.2 describes the furnace system model performance with state feedback SMC

7.3.2 State feedback sliding mode performance

It is feasible to use state feedback control in this furnace model system since all the temperature can be measured by either thermocouples or non-contact pyrometers. The latter are very expensive, whilst the thermocouples are cheap but unreliable. However, in this Section, the state feedback method, as described in Chapter 4, can give a very good overview of what the SMC can achieve. In Section 7.4.3 describes the performance of the output based SMC for the furnace model system.

The model-based state feedback SMC used in this Section is based on the model described in Section 7.2.1. The SMC robustness implies that with this controller, any matched unwanted signals can be compensated. Without considering the unmatched fault, Figure 7-5 shows the absolute value of the tracking error of the strip exit temperatures with each case of PID controller and SMC.
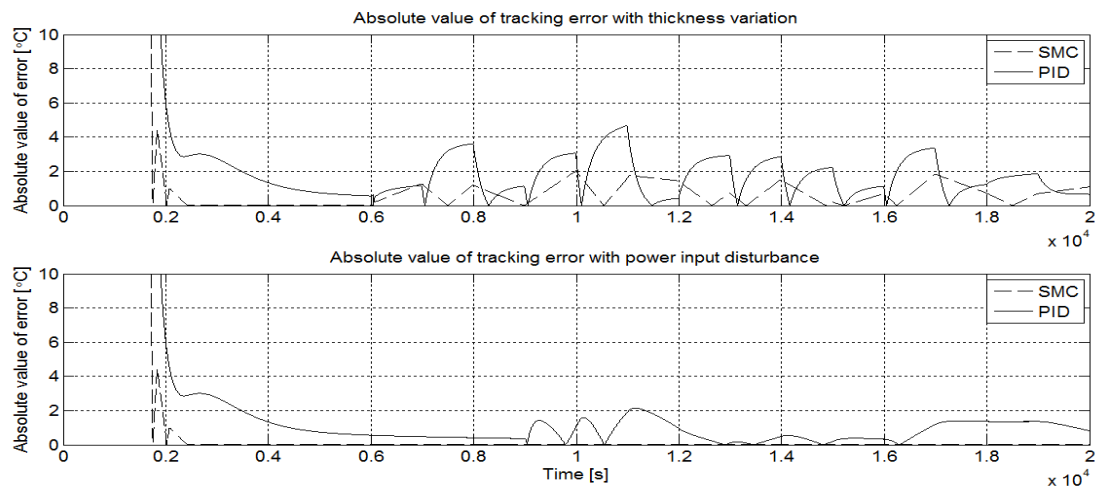

Figure 7-5. Absolute values of the strip exit temperature tracking error with thickness variation faults

From Figure 7-5, it shows that the SMC suppresses the disturbance from the thickness variation and rejects the matched power input disturbance completely. Since the thickness variation uncertainty contains both matched and unmatched parts in the linear model, the remaining unmatched parts still affect the system performance. However, by comparing the maximal value of tracking error between these two method, SMC ($max = 2$ at $t = 10000s$) shows better robustness than the PID controller ($max = 4.5$ at $t = 15000s$). Also the SMC gives improved time response.

The power input of both the SMC and PID controllers can be found in Figure 7-6. The SMC provides faster response in the input when faults occur. It gives better robustness but as a down side requires faster power input variations. The maximum levels of input power are seen to vary along the zones for both controller types.
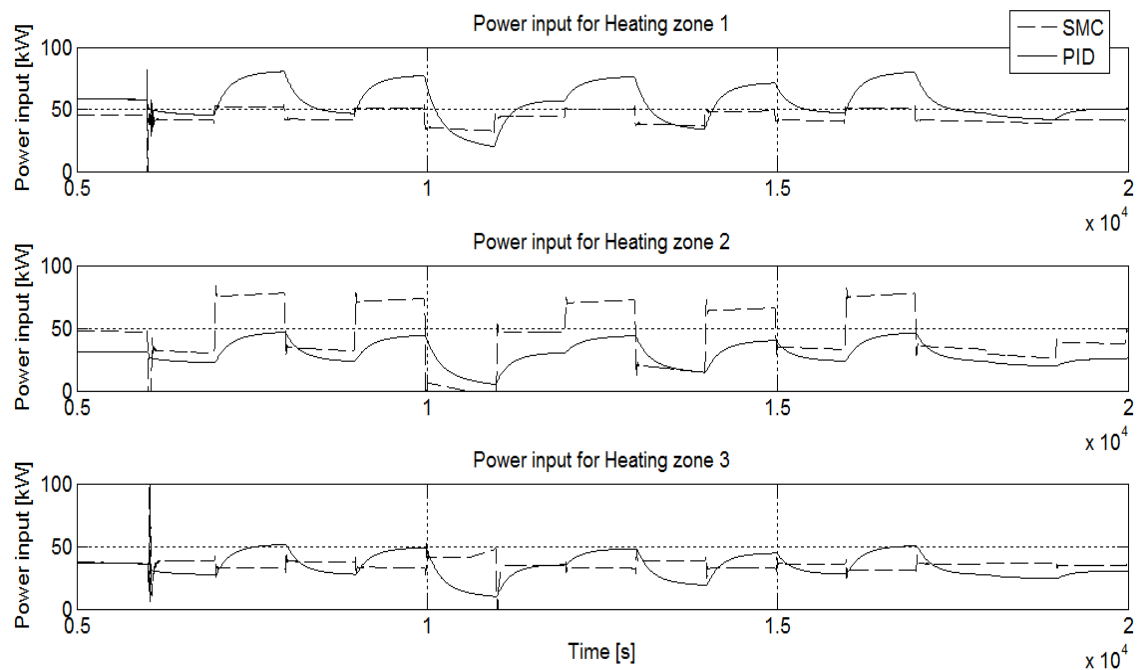
Figure 7-6. Power input for each heating zone when thickness uncertainty occurs

Since SMC can only reject the matched faults, the best way of using sliding mode is to combine SMC with another control method to deal with unmatched faults. Here state feedback is used with the H_∞ robustness optimization, as described in Section 4.3.3. The system outputs are defined as the strip exit temperatures. With only velocity variations, the minimal robustness criterion γ can be calculated. From Figure 7-7, it can

be noted that the tracking error when the velocity variation fault occurs is reduced compared with the equivalent tracking error for PID controller.
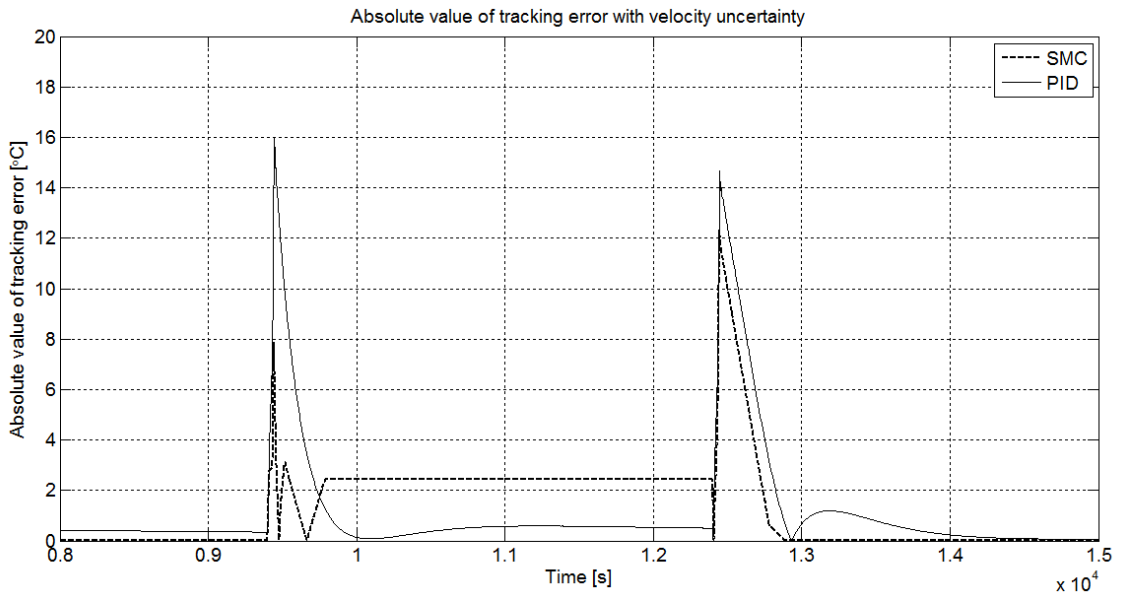
Figure 7-7. Absolute values of tracking error of strip exit temperatures with velocity uncertainty for PID and SMC, respectively

It is also worth to noting that the static error of PID when the fault occurs is smaller than it is in the SMC case. This is due to the integral term that is more effective in the PID control strategy. However, the idea of first order SMC is more like a proportional term which cannot remove the static output error. However, with all three types of faults, Figure 7-8 shows that SMC has better performance than PID controller.
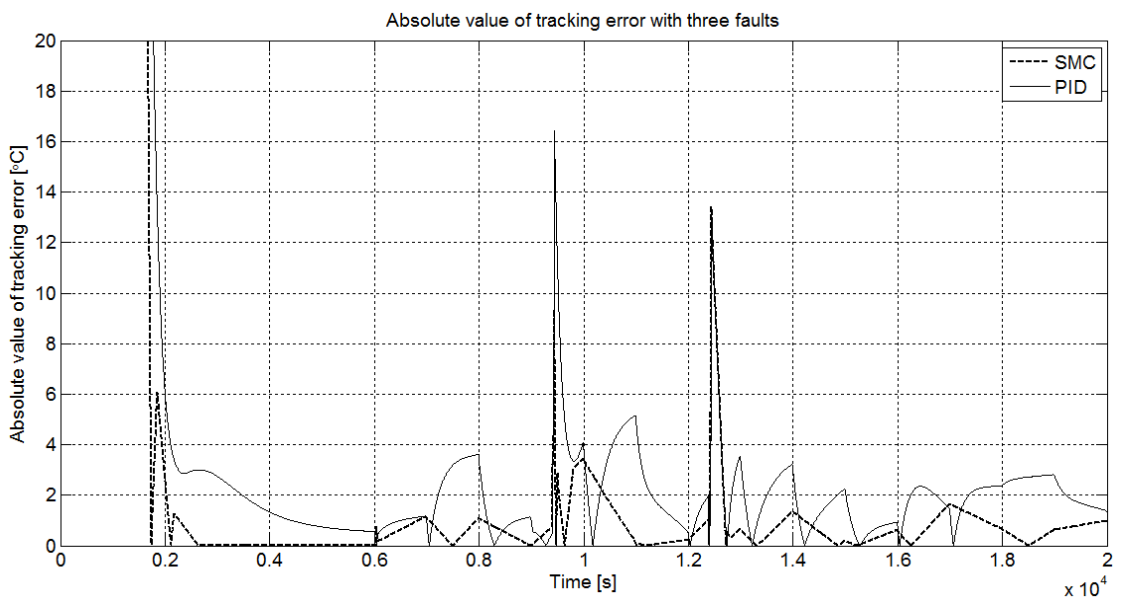
Figure 7-8. Absolute value of strip exit temperature tracking error with faults

7.3.3 Output feedback sliding mode control

If some of the furnace temperatures cannot be measured, output feedback control must be used. Actually, PID control is a static output feedback method which only requires the strip exit temperatures of the three heating zones. Moreover, since the system is already stable, it is still possible to design a suitable static output feedback controller with only PI control. Thus, although the Kimura-Davison condition is not satisfied (see Section 5.2), it is possible to design a static output feedback SMC which contains combined properties of both PI control and SMC. The reason that the derivate term of this model-based control is not used is because it is hard to achieve in state space when there are system uncertainties. Assume that for each heating zone, only strip exit temperatures (using pyrometers), the inner and outer wall temperatures (using thermocouples) and the integral term can be measured. Moreover, it is easy to verify that $rank(C_i) = 4, rank(C_iB_i) = rank(B_i) = 1$.

Following the algorithm proposed in Section 5.2, the sliding surface gain matrix for each heating zone is given by:

$$F_1 = [0.012049 \quad -0.002182 \quad 0.30798 \quad -7.928 \times 10^{-5}]$$

$$F_2 = [0.005661 \quad -0.011038 \quad -0.20632 \quad -3.8072 \times 10^{-5}]$$

$$F_3 = [0.007646 \quad -0.020364 \quad 0.029016 \quad -6.4661 \times 10^{-5}]$$

The gain matrices show that the sliding surfaces do not concern the outer wall temperature. These matrices can be tuned by choosing the Q matrix in step 2 of Algorithm 5.1. From a suitable choice of Q the output feedback gain matrices K_i are given by:

$$K_1 = [-0.4774 \times 10^{-3} \quad -91.274 \quad -110.57 \quad 0.2531]$$

$$K_2 = [-0.34905 \times 10^{-3} \quad -66.957 \quad -116.13 \quad 0.19321]$$

$$K_3 = [-2.292 \times 10^{-3} \quad -134.26 \quad -112.18 \quad 0.25374]$$

Thus, with the above local control gains:

$$u_i = K_i\Delta y_i - \rho_i \frac{F_i\Delta y_i}{\|F_i\Delta y_i\| + \Delta_i}$$

where $\Delta y_i = y_i - y_{op}$, $\rho_i = -50$ and $\Delta_i = 0.01$ are the SMCs parameters to be chosen by the designer. The furnace system is stable and shows robustness to the all three types of faults. It is predictable that with this SOF SMC strategy, the robustness of this system is not as good as for state feedback SMC method but it is better than PID controller. This prediction can be proved from the strip exit temperature response with only thickness uncertainty that contains both matched and unmatched faults. See Figure 7-9.
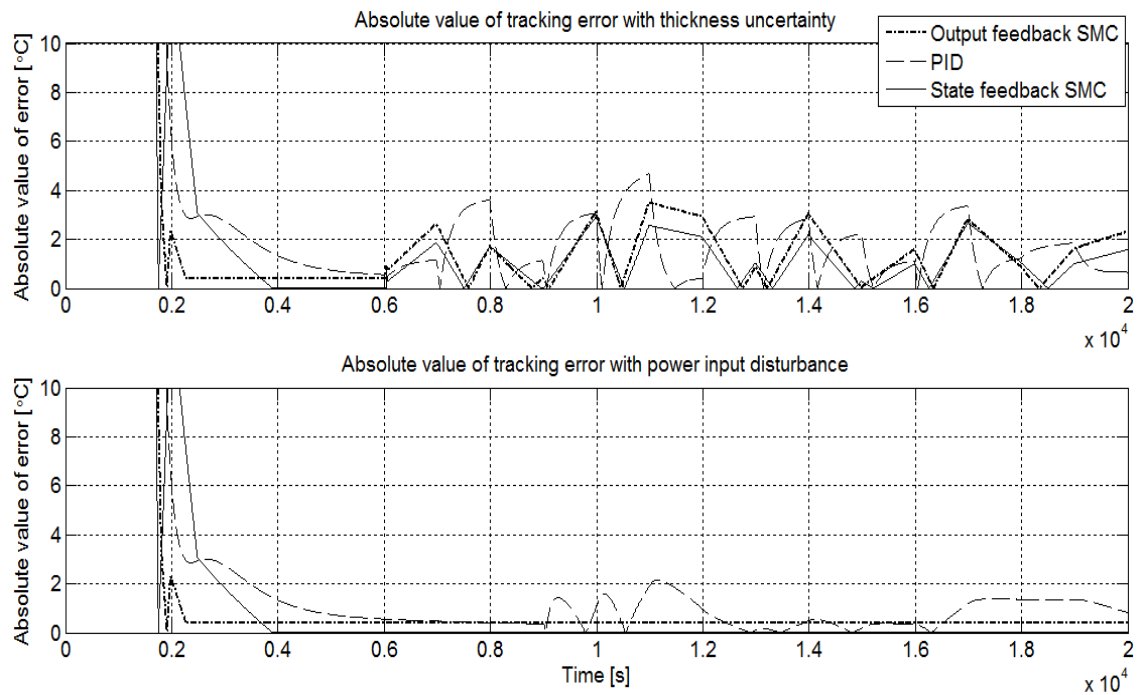
Figure 7-9. Absolute values of strip exit temperature tracking error with 3 methods

The reason for the static error of the SMC output feedback is that the integral gain is reduced for the purpose of decreasing the transient overshoot. From Figure 7-9, it can be found that the output feedback SMC can compensate the matched fault completely. Also when the thickness uncertainty occurs, although it reduces the value of the maximum tracking error, it is hard to tell which method is better. When there is velocity uncertainty, since the gain of the integral term is relatively small, there might be a larger static error. In this case, reducing the peak value of the tracking error seems to not be useful. To improve the robustness of this strategy, the initial Q matrix should be designed carefully.

Another valid local control design method is combining the pre-determined PI controller with output feedback sliding mode. The linear controllers are designed with the following gain structure:

$$K_i = [K_{i,I} \quad K_{i,P} \quad 0 \quad 0]$$

where $K_{i,I}$ and $K_{i,P}$ are the integral and proportional gain for the local PI controller of the i-th subsystem. If the pre-determined PI controller can stabilize the system, the sliding surface can be obtained by solving the LMIs (5-29). Hence, using the pre-determined PI controller gains:

$$K_1 = [0.0001 \quad 10 \quad 0 \quad 0]$$

$$K_2 = [0.0003 \quad 5 \quad 0 \quad 0]$$

$$K_3 = [0.0003 \quad 5 \quad 0 \quad 0]$$

The subsystem sliding surface gain matrices F_i are then given by:

$$F_1 = 10^{-5} \times [0.009441 \quad -0.0009 \quad 2.2901 \quad 2.0243]$$

$$F_2 = 10^{-4} \times [0.009486 \quad -0.0002 \quad 4.7641 \quad 4.9141]$$

$$F_3 = 10^{-3} \times [0.002585 \quad -0.00006 \quad 2.1044 \quad 3.7509]$$

For this subsystem controller structure the PI and output based SMC (PI-OSMC) are combined. There are no static tracking errors and the local subsystems are insensitive to the matched faults. The result is shown in Figure 7-10.
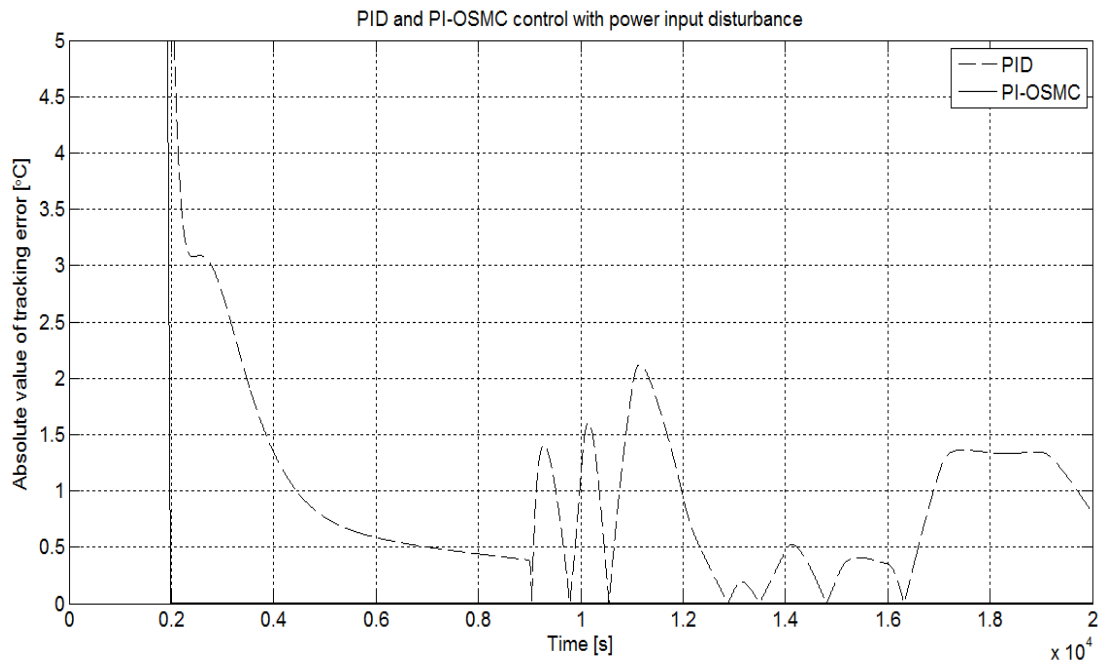
Figure 7-10. Absolute values of export temperature tracking error with PI controller and PI-OSMC controller

With this idea, the SMC can be applied to this furnace system as a matched fault compensator that does not affect the design of the PI control, i.e. these controllers are designed separately for each subsystem. This idea can be found in (Utkin and Shi, 1996; Castaños and Fridman, 2005, 2006), although these authors apply this idea to the ISMC the same idea is valid here because the OSMC structure (see Section 5.2) can be combined with a linear controller design (e.g. PI control) as is the case in the ISMC. The advantages of this method are 1). Reduction of the computation complexity, 2). Good compatibility with other robust methods, and 3). Matched fault compensation.

If the velocity uncertainty is known (measured by a velocity meter), the influence from this known uncertainty can be attenuated by changing the operating temperatures during the process, i.e. the new sliding surface becomes $\sigma = F(y - y_{op,new})$ as a consequence of the velocity changes. The absolute value of the strip exit temperature error (corresponding to subsystem 3) for this system is shown in Figure 7-11.
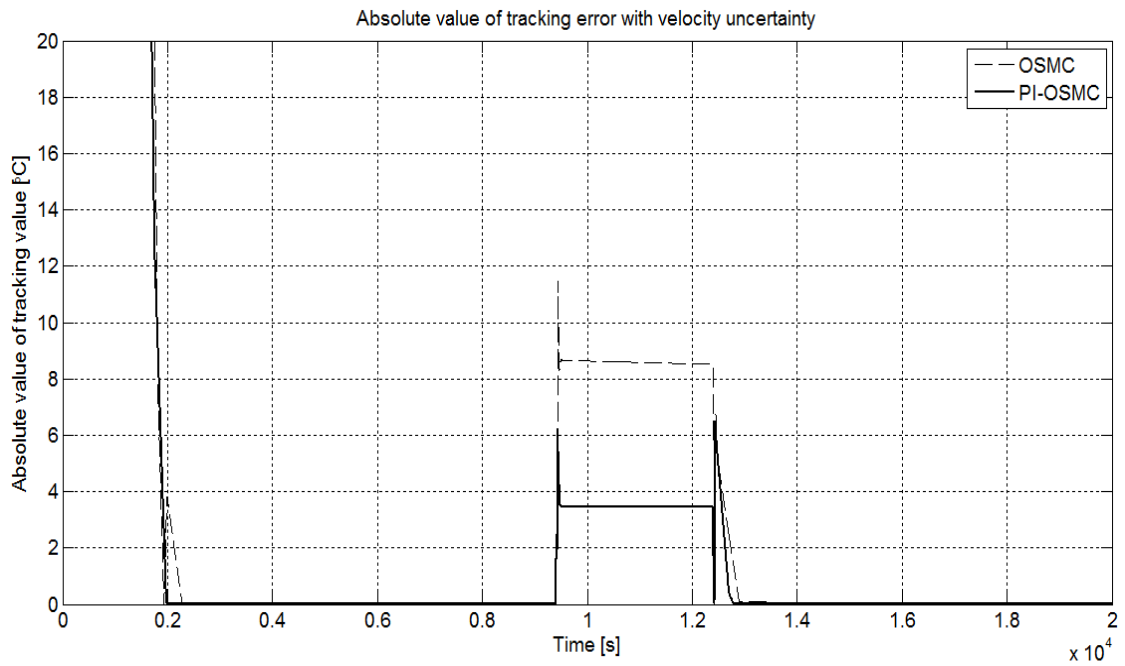
Figure 7-11. Absolute values of strip exit temperature tracking error with output feedback SMC and PI-OSMC controller

Compared with the output feedback control described at the beginning of this Section, this PI-OSMC provides better results.

Besides static output feedback, observer based control is another choice. However, the observer based ISMC method proposed in Chapter 5 is not applied to the furnace system described in this Chapter. From Section 5.4, it can be seen that to achieve sliding, the integral part of the sliding surface requires a sufficiently large enough gain function from initial time. To achieve this, the parameters $\rho_i, i = 1, \dots, N$ must be chosen to satisfy the inequality REF _Ref335134963 \h (5-59)

$$\rho_i \geq \left\| (G_i C_i B_i)^{-1} \right\| \left(\left\| G_i C_i A_i \right\| e_{init} + \left\| G_i C_i \right\| \left(\omega_1 \|y\| + \omega_2 \right) \right) + f_{iu} \|u_i\| + \varphi_i(y,t) + \eta_i \text{ REF \_Ref33513496}$$

the switching gains are not sufficiently large enough to satisfy REF _Ref335134963 \h (5-59) the reaching phase in each subsystem is unavoidable. Thus, there is no point in using a more complicated and expensive observer-based controller. Another reason is that the large switching gains result in large control inputs which might lead to the so called "wind-up" problem (input saturation) and reduce the robustness given by using SMC.

185

7.4　Fault estimation and sensor fault hidden for furnace model

As discussed in the Section 7.4, there are three types of faults that need to be handled in the controller design. However, with the application of SMC, the power input disturbance can be compensated. Normally, the conveyor system has its own subsystem and the velocity of this system is measured and controlled. For the thickness uncertainty, there is nothing that can be done whether or not this fault can be detected or not! This fault effect can only be tolerated, i.e. minimized. The remaining problem of fault estimation in the thermal furnace is to detect and isolate the sensor faults by means of fault estimation.

Chapter 3 has described the measurement methods applicable to this annealing furnace system. The exit strip temperatures are measured by non-contact pyrometers since the strip keeps moving during the heating process. The thermocouples, as simple and generally inexpensive sensors, are used to measure the inner and outer wall temperature. Compared with the much more expensive non-contact pyrometers, thermocouples have higher risk of failing. They are mostly due to metal fatigue wear and tear. Thermocouple deterioration until the sensors fail cannot easily be detected and often cause expensive process interruption. Removing a thermocouple from a furnace when at operating temperature can be difficult and dangerous. In fact the thermocouple can cause inaccurate readings for some time before any errors are detected. The errors usually cause low readings due to the thermocouple wires becoming thinner. The common method to avoid the thermocouple failure is to regularly measure the thermocouple loop and replace thermocouples during a planned maintenance period. In this section, a couple of SMOs is used to estimate the thermocouple failure and hide the fault in the controllers.

The SMO sensor fault estimation method has been proposed in Chapter 6. Choose the filter matrix $A_{fi} = 10 I_{n_i}, i = 1,2,3$. The augmented subsystem is established as (6-63):

$$
\begin{bmatrix} \dot{x}_i(t) \\ \dot{z}_{fi}(t) \end{bmatrix} = \begin{bmatrix} A_i & 0 \\ A_{fi} C_i & -A_{fi} \end{bmatrix} \begin{bmatrix} x_i(t) \\ z_{fi}(t) \end{bmatrix} + \begin{bmatrix} B_i \\ 0 \end{bmatrix} u_i(t) + \begin{bmatrix} M_i \\ 0 \end{bmatrix} h_i(x,u,t) + \begin{bmatrix} 0 \\ A_{fi} E_i \end{bmatrix} f_{oi}
$$

$$
y_{fi} = \begin{bmatrix} 0 & I_{p_i} \end{bmatrix} \begin{bmatrix} x_i(t) \\ z_{fi}(t) \end{bmatrix}
$$

The sensor faults of the system occur in the inner wall and outer wall thermocouples. If it is assumed that PID control is used within which inner wall surface temperatures are not required. The subsystem temperature measurements are the strip exit temperatures, as well as the inner wall surface and outer wall surface temperatures (for each zone). Since the thermocouples for the inner wall temperature measurements are of higher risk, it can be assumed that the sensor fault distribution matrices are $E_i = \begin{bmatrix} 0 & 1 & 0 \end{bmatrix}^T$. According to the thermo-electrical property of thermocouples, the decrease in temperature (due to the error) leads to the lower reading, i.e. $y_{i,2} = (1 - \vartheta_i)y_{i,2}$. Hence, the sensor fault can be written as multiplicative faults as follows:

$$f_{oi} = -\vartheta_i y_{i,2}$$

Using the observer proposed in Chapter 6, the sensor faults can be estimated with the augmented observer after the sliding surface is reached. Figure 7-12 shows the fault estimation for all the three heating zones when there are sensor faults in the first and second subsystems. As the sensor faults are multiplicative, by dividing the fault estimates by the operating inner wall temperatures (measured by redundant thermocouples), the approximate sensor output $\hat{\vartheta}_i \approx \vartheta_i$ is obtained i.e. the severity of the fault (or damage) to the thermocouple can be estimated.

From Figure 7-12, it can be seen that, when there are sensor faults in the first and second heating zones, they do not affect the estimated temperature signal for the third heating zone. Thus, with several observers, the sensor faults for every heating zone can be estimated effectively.
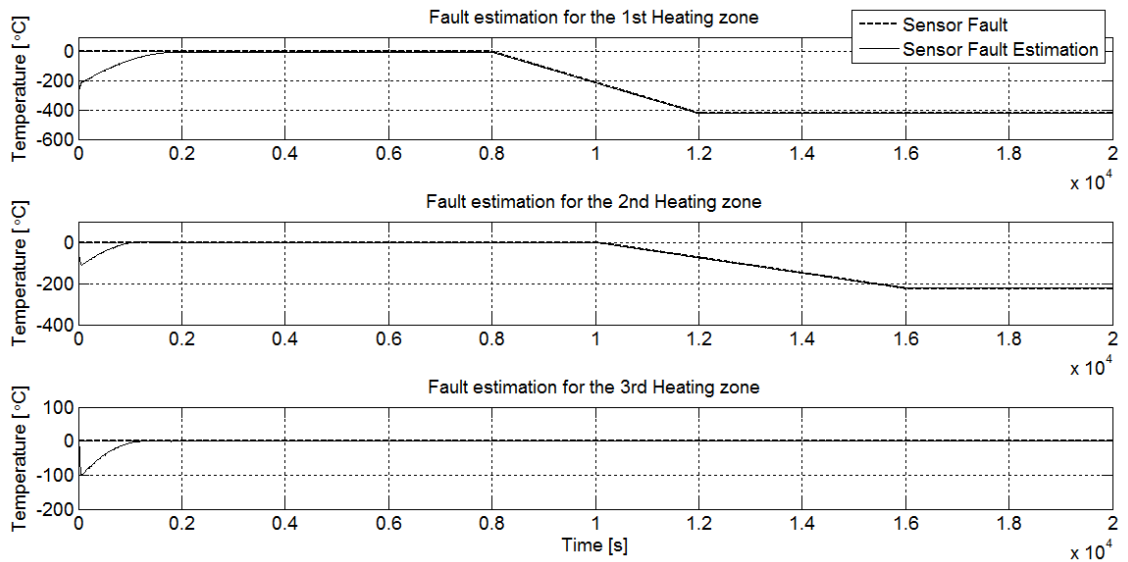
Figure 7-12. Sensor fault estimation for all the heating zones

The sensor fault estimation can be used to compensate the sensor faults when using the PI-OSMC controller. Compared with the use of PID control, the PI-OSMC requires the measurements of inner wall temperature to reject the matched power input disturbance. If there is any sensor fault, the PI-OSMC will drive the system away from the operating point. See Figure 7-13.
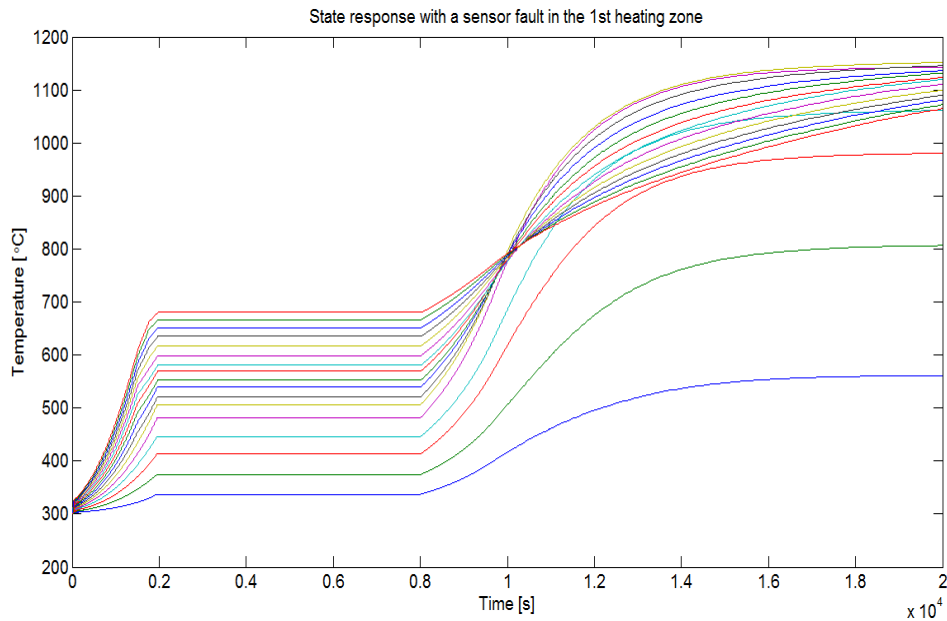
Figure 7-13. State responses with PI-OSMC when there is a sensor fault $\vartheta_i = 0.5$ in the 1st heating zone, fault occurs at $t = 8 \times 10^3 s$

The structure of the sensor fault compensation is shown in the Figure 7-14. The estimation of the sensor fault is used to compensate the actual sensor fault in the temperature measurement. The compensated output signal is then used in the PI-OSMC. This is an example of active FTC.
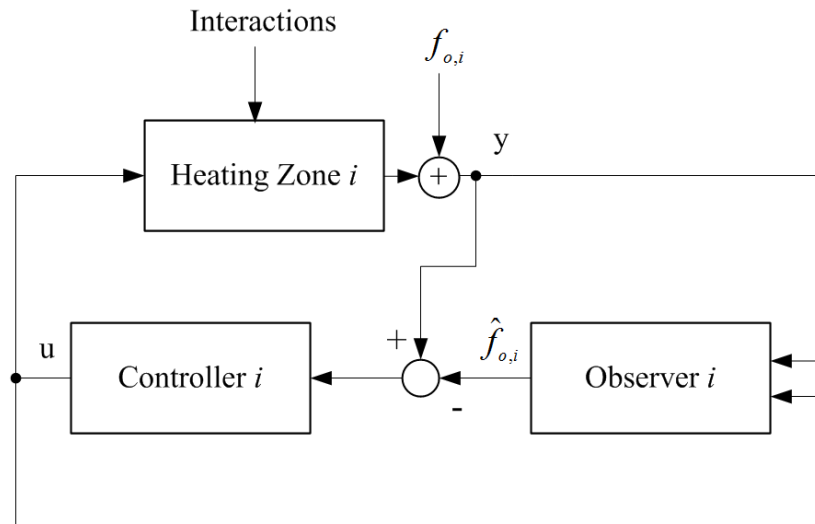
Figure 7-14. Sensor fault compensation structure for a single heating zone

Before using the sensor fault estimation, there must be a check as to whether the sliding surface of the SMO has been reached. In the reaching phase, the fault estimation is not zero-valued (since the robustness is reduced outside of the sliding surface) even when there are no sensor faults. The fault compensation can now be applied with the same fault as in Figure 7-13.
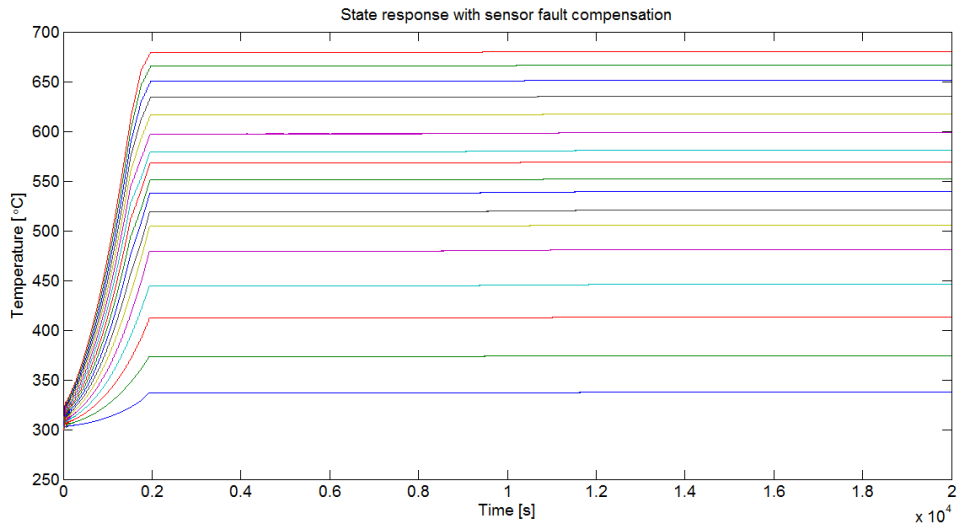
Figure 7-15. State response with sensor fault compensation, fault occurs at $t = 8 \times 10^3 s$
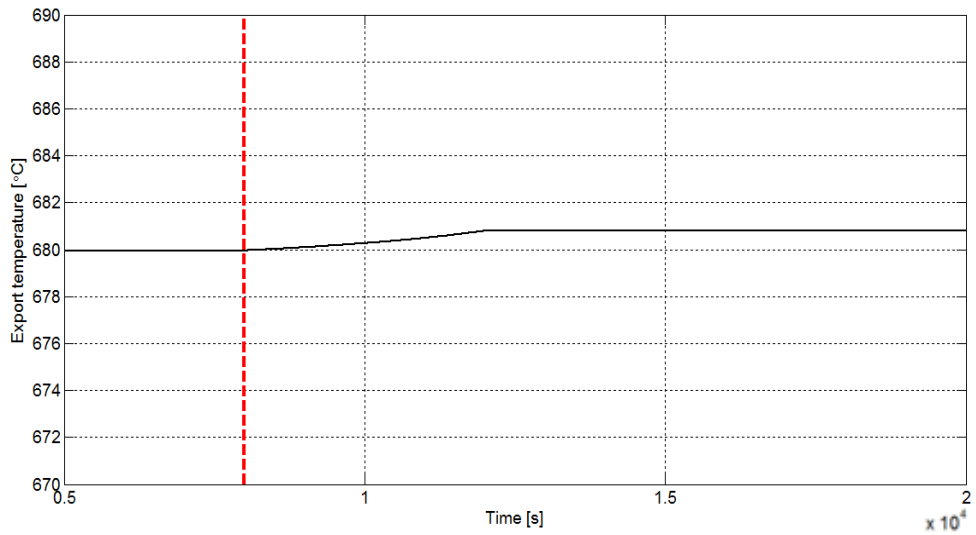
Figure 7-16. Strip exit temperature of the 3rd heating zone with sensor fault compensation, fault occurs at $t = 8 \times 10^3 s$

Figure 7-15 and Figure 7-16 show the effectiveness of this sensor fault estimation method. It can be found in Figure 7-12 that the sensor faults can be estimated precisely. Thus, using the faults estimation derived in SMO, and compensated the sensor faults in SMC, the sensor faults are hidden so that there is no need to disrupt the heating process. Thus, this approach allows enough time to finish the heating process and replace the thermocouples in the furnace wall.

This method also brings value to the idea of combination of SMC and SMO. In Chapter6, it has been argued that when there are actuator faults, the combination of SMC and SMO is valuable. However, for the sensor fault case, as shown in this example, the combination of SMC and SMO has better value since SMC do not have the ability to deal with sensor faults. Faults have to be estimated and hidden in the SMC using SMO so that the fault tolerance is achieved.

7.5   Conclusion

This Chapter shows the application of the proposed strategies described in Chapter 4, 5 and 6 to control the furnace problem represented in Chapter 3. Compared with traditional PID control, the proposed state feedback SMC and PI-OSMC controllers provide better robustness to the matched power input disturbance. These methods give new ideas about how to deal with furnace heating problems based on modern control theory.

The OSMC can be designed as a part of the robust PI control not using complicated observer based ISM theory. This idea combines the advantages of both PI control and SMC.

A sensor fault SMO strategy is also proposed in this Chapter to deal with thermocouple deterioration. The SMO provides accurate estimation of the sensor fault which can be used to form an active sensor FTC to combine with the PI-OSMC. In this case, when there are sensor faults, the controller can still control the temperature effectively.

Chapter 8

Conclusion and Future Work

8.1   Conclusion and Summary

This thesis focuses on the control and estimation methods for LSSs. The main work is to propose a systematic and novel LMI approach to sliding mode theory applied to LSS control and estimation problems. According to the literature review of the subject, decentralized control is still an attractive topic even after three decades of development. With the introduction of LMI tools into sliding mode design, the calculation approach is simplified and the interactions can be weakened. Based on the idea of designing the decentralized sliding mode with LMI tools, the work presented has made some contribution within not only state output feedback but also output feedback based control strategies for LSSs. However, the unmatched uncertainties/interactions of the LSSs affect the performance of systems both in the reaching phase and after reaching sliding surface. To attenuate the influences from the unmatched unwanted signals, the idea of combining other robust methods with sliding mode theory is also discussed in this thesis.

The work represented in this thesis deals with the well-known difficulties of LSSs: dimensionality, uncertainty and information constraint. These difficulties are outlined in Chapter 1 where the definition of faults in LSSs is defined as well. As pointed out in Chapter 1, since the large dimensionality can be dealt with by decomposing the system into several small subsystems with proper decomposition method, uncertainty and information constraints are the main topics in this thesis. Chapter 1 also includes the classification of faults according to their positions in an LSS (actuator, sensor, component faults e.g. subsystem parametric faults or faults in the interactions). In this case, FTC and FDI are necessary for LSSs. Thus, decentralized SMC and SMO theory, as powerful approaches to FTC and FDI, are chosen as the main approaches to solving LSS control and estimation problem in this thesis.

As discussed in Chapter 1, the information constraint and dimensionality are two main difficulties in LSSs. Chapter 2 reviews several approaches to handle these problems.

First of all, multi-level control structure is reviewed as a strategy to deal with information constraint in LSSs. Although it requires centralization (using coordinator), it provides better performance than decentralized single-level control strategy. On the other hand, single-level control strategy, as another strategy for information constraint problem, is introduced and chosen as the main strategy for this thesis. Then two main LSS decomposition structures based on single-level structure: disjoint decomposition and overlapping decomposition are reviewed to deal with dimensionality problem as well as to provide better system structure for control design. Although the strategies represented in this thesis are based on the disjoint structure, it is interesting to consider the overlapping structure due to the possibility of using the overlapping control to weaken the influence from interconnections as illustrated in (Huang and Patton, 2012b).

Since observer-based control design and fault estimation are the two main objectives of decentralized observer based estimation, Chapter 2 also reviews some of the decentralized observer design strategies for decentralized observer based control. However, finding that there is very little publication on fault estimation for LSSs using SMO theory motivates the proposed decentralized fault estimation SMO strategy in Chapter 6.

In Chapter 3, a furnace model is introduced, following a project report from the New Zealand Steel Company. The assumptions and simplifications form the New Zealand study are outlined. Since the model equations are partial differential equations which can hardly be controlled using model based control strategy. Two interpolation methods are introduced to approximate the partial differential equations to ordinary differential equations. With these methods, the thermal PDEs can be approximated by a set of ODEs which is available for state space modelling. Several simplifications and identifications procedure are described then in order to establish a nonlinear furnace state space model. Moreover, the established model are simulated and validated in this Chapter. This model is built as an example of LSS which is used to illustrate some of the ideas proposed in this thesis.

Chapter 4 starts from introduction of sliding mode theory. Several important elements in sliding mode theory are discussed: Regular forms, Reachability, Control law design. In this Chapter, adaptive mechanism and boundary layer as performance improvement accessories for SMC are also proposed. With the adaptive mechanism, the sliding mode

can deal with the faults with unknown bound whilst the chattering problem for SMC can be relieved by boundary layer. As the main topic of this Chapter, decentralized state feedback sliding mode control is then proposed. The idea of this method is to reject any matched faults with SMC and stabilize the sliding mode by carefully design of sliding surface using LMI approach. This method provides good compatibility to combine with other robust control strategy in the sliding surface design procedure. Eigenvalue assignment, H_∞ and quadratic optimization SMC are all discussed in this Chapter. A tutorial example with nonlinear interactions and uncertainties is used to illustrate the idea. And it shows that decentralized SMC strategy gives good regulation performance compare with linear control. The robust of SMC using boundary layer is also discussed at the end of this Chapter.

Some LSSs might not have all the states measured. To solve this problem, output feedback control strategies should be considered. In Chapter 5, three types of decentralized output based SMC approaches are proposed: Static output feedback, Dynamic compensation method and Observer based control. All of these methods have the same assumption for interactions, the so called "quadratic constraint". Thus, these methods combine with state feedback SMC give a systematic theory of decentralized SMC. The observer based control proposed in Chapter 5 use the idea of ISM theory and overcome the traditional constraint of ISM control which requires the full knowledge of system states. In the end of this Chapter, a multi machine power system is used as an example to illustrate the static output feedback control and observer based control method. Both of these methods show good fault tolerant control capability in this application study.

Different to SMC, sliding mode observer (SMO) introduced in Chapter 6 has the property that the observer state estimation errors are insensitive to some faults satisfying certain conditions. Both Walcott-Żak and Edwards & Spurgeon SMO are reviewed. A novel modification to the Walcott-Żak observer control law overcomes the inaccurate output estimation problem of this type of SMO. Both actuator faults and sensor faults estimation using SMO are proposed with the combination of equivalent output injection theory. This method gives less computation complexity than Edwards & Spurgeon SMO and provides accurate fault estimation. However, when there are both uncertainties/interactions and faults, it would be extremely hard to separate the fault

estimation from output injection. Chapter 6 also discusses the influence from uncertainties/interactions to the actuator fault estimation and points out that only if the uncertainties/interactions satisfying certain conditions, SMO can provide precisely fault estimation. This Chapter ends with a tutorial example which is similar with the one in Chapter 4. The statements made in Chapter 6 are illustrated using this example.

The strategies proposed in Chapter 4, 5 and 6 are demonstrated in Chapter 7 on the furnace model system based on Chapter 3. Since the SMC and SMO strategies proposed in this thesis are designed based on the linear model, linearization procedure is proposed to linearize the furnace model on a pre-decided operating point. Then the SMC and SMO approaches designing based on linearization model are applied to nonlinear system. Three types of faults are used to test the robust performance of the control strategy. Compare with the conventional PID control, state feedback decentralized SMC shows better robust performance. However, the static output feedback SMC has static error when uncertainties occur. To relief this problem, a PI-OSMC method is proposed based on the discussion in Chapter 5. For the fault estimation using SMO, the deterioration of thermocouples is considered. Using the SMO method proposed in Chapter 6, the deterioration could be estimated accurately and the estimation signal is sent back to the controllers (PI-OSMC) to hide the sensor fault. This combination gives a powerful way for the furnace model as an active FTC case.

8.2   Future work
The future work is listed below:

- SMC and SMO design for the Overlapping structure. To build up a novel decentralized sliding mode theory using overlapping structure is quite interesting since the unmatched interactions can be further attenuated by this structure. Although the structure is more complicated than disjoint decomposition, it might give better performance.
- Model reference decentralized SMC using the proposed LMI framework. The model reference control is more suitable than regulating control in modern industrial though the design algorithm should be similar.
- The maximum capability of linear sliding mode control is to reject the matched faults based on linear system. Further research can be how to deal with faults in

the nonlinear system. Higher order sliding mode is a possible choice. Decentralized multi model control is another interesting choice for nonlinear system.

- In the real industrial application, most of the systems are controller by a discrete time controller. Thus, how to achieve our methods in discrete time can be an interesting topic.

- Improve the accuracy of the furnace model using less restrictive interpolation method (instead of CS).

- Instead of using constant references, time varying references tracking problem for furnace should be considered using nonlinear control strategy or multi-model strategy.

Reference

Akar, M. & Özgüner, Ü. 2002. Decentralized sliding mode control design using overlapping decompositions. *Automatica,* 38**,** 1713-1718.

Aoki, M. 1972. On feedback stabilizability of decentralized dynamic systems. *Automatica,* 8**,** 163-173.

Bakule, L. 2008. Decentralized control: An overview. *Annual Reviews in Control,* 32**,** 87-98.

Bakule, L., Crainiceanu, F. P., Rodellar, J. & Rossell, J. M. 2005. Overlapping Reliable Control for a Cable-Stayed Bridge Benchmark. *IEEE Trans. on Control Systems Technology,* 13.

Bakule, L. & Lunze, J. 1988. Decentralized design of feedback control for large-scale system. *Kybernetika,* 24**,** 1-100.

Bakule, L. & Rodellar, J. 1996. Decentralised control design of uncertain nominally linear symmetric composite systems. *IEEE Proceeding - Control Theory and Applications,* 143**,** 530-536.

Bakule, L., Rodellar, J. & Rossell, J. M. 2001. Overlapping Quadratic Optimal Control of Linear Time-Varying Commutative Systems. *SIAM J. Control Optim.,* 40**,** 1611-1627.

Bakule, L. & Rossell, J. M. 2008. Overlapping controllers for uncertain delay continuous-time systems. *Kybernetika,* 44**,** 17-34.

Bejarano, F. J., Fridman, L. & Poznyak, A. 2007. Output integral sliding mode control based on algebraic hierarchical observer. *International Journal of Control,* 80**,** 443-453.

Bellman, R., Kashef, B. G. & Casti, J. 1972. Differential quadrature: A technique for the rapid solution of nonlinear partial differential equations. *Journal of Computational Physics,* 10**,** 40-52.

Benigni, A., D'antona, G., Ghisla, U., Monti, A. & Ponci, F. 2010. A Decentralized Observer for Ship Power System Applications: Implementation and Experimental Validation. *IEEE Trans. on Instrumentation and Measurement,* 59**,** 440-449.

Benton, R. E., Jr. & Smith, D. 1998. Static output feedback stabilization with prescribed degree of stability. *Automatic Control, IEEE Transactions on,* 43**,** 1493-1496.

Blanke, M., Kinnaert, M., Lunze, J. & Staroswiecki, M. 2006. *Diagnosis and Fault-Tolerant Control*, Springer.

Burton, J. A. & Zinober, A. S. I. 1986. Continuous approximation of variable structure control. *International Journal of Systems Science,* 17**,** 875-885.

Cao, Y., James, L. & Sun, Y. 1998. Static Output Feedback Stabilization: An ILMI Approach. *Automatica,* 34**,** 1641-1645.

Castaños, F. & Fridman, L. 2005. Integral Sliding Surface Design Using An H-infinite Criterion For Decentralized Control. *Proceedings of the 16th IFAC World Congress.* Czech Republic.

Castaños, F. & Fridman, L. 2006. Analysis and Design of Integral Sliding Manifolds for Systems With Unmatched Perturbations. *IEEE Trans. on Automatic Control,* 51.

Chao, P. C. P. & Chien-Yu, S. 2009. Sensorless Tilt Compensation for a Three-Axis Optical Pickup Using a Sliding-Mode Controller Equipped With a Sliding-Mode Observer. *IEEE Trans. on Control Systems Technology,* 17**,** 267-282.

Chen, J. & Patton, R. J. 1999. *Robust Model Based Fault Diagnosis for Dynamic Systems*, Kluwer Academic Publishers.

Chen, N., Gui, W. & Zhai, G. 2006. Design of robust decentralized H∞ control for interconnected descriptor systems with norm-bounded parametric uncertainties. *Proceedings of the 2006 IEEE International Symposium on Intelligent Control*, Munich, Germany, 3070-3075, 4-6 Oct.

Chen, N., Ikeda, M. & Gui, W. 2005. Design of Robust H∞ Control for Interconnected Systems: A Homotopy Method. *International Journal of Control, Automation, and Systems,* 3**,** 143-151.

Chen, P. 2012. Two-Level Hierarchical Approach to Unit Commitment Using Expert System and Elite PSO. *IEEE Trans. on Power Systems,* 27**,** 780-789.

Chen, X. B. & Stankovi, S. S. 2005. Decomposition and decentralized control of systems with multi-overlapping structure. *Automatica,* 41**,** 1765-1772.

Chen, X. B. & Stankovic, S. S. 2007. Overlapping decentralized approach to automation generation control of multi-area power systems. *International Journal of Control,* 80**,** 386-402.

Cheng, C.-C. & Chang, Y. 2008. Design of decentralised adaptive sliding mode controllers for large-scale systems with mismatched perturbations. *International Journal of Conrtol,* 81**,** 1507-1518.

Choi, H. H. 1997. A new method for variable structure control system design: A linear matrix inequality approach. *Automatica,* 33**,** 2089-2092.

Choi, H. H. 1998. An Explicit Formula of Linear Sliding Surfaces for a Class of Uncertain Dynamic Systems with Mismatched Uncertainties. *Automatica,* 34**,** 1015-1020.

Choi, H. H. 2008. Output feedback variable structure control design with an performance bound constraint. *Automatica,* 44**,** 2403-2408.

Choi, H. H. & Ro, K. S. 2005. LMI-based sliding-mode observer design method. *Control Theory and Applications, IEE Proceedings -,* 152**,** 113-115.

Chow, E. & Willsky, A. 1984. Analytical redundancy and the design of robust failure detection systems. *IEEE Trans. on Automatic Control,* 29**,** 603-614.

Chu, D. & Šiljak, D. D. 2005. A Canonical Form for the Inclusion Principle of Dynamic Systems. *SIAM J. Control Optim.,* 44**,** 969-990.

Chung, W. H. & Speyer, J. L. 1998. A decentralized fault detection filter. *Proceedings of the American Control Conference*, Philadelphia, Pennsylvania, 2017-2021, 21-26 Jun.

Clark, R. N. 1978. Instrument Fault Detection. *Aerospace and Electronic Systems, IEEE Transactions on,* AES-14**,** 456-465.

Corless, M. & Tu, J. a. Y. 1998. State and Input Estimation for a Class of Uncertain Systems. *Automatica,* 34**,** 757-764.

Date, R. A. & Chow, J. H. 1989. A reliable coordinated decentralized control system design. *Proceedings of the 28th IEEE Conference on Decision and Control*, Tampa, Florida, 1295-1300, 13-15 Dec.

Decarlo, R. A., Żak, S. H. & Matthews, G. P. 1988. Variable structure control of nonlinear multivariable systems: a tutorial. *Proceedings of the IEEE,* 76**,** 212-232.

Dorling, C. M. & Zinober, A. S. I. 1986. Two approaches to hyperplane design in multivariable variable structure control systems. *International Journal of Control,* 44**,** 65-82.

Drakunov, S. V. & Utkin, V. I. 1992. Sliding mode control in dynamic systems. *International Journal of Control,* 55**,** 1029-1037.

Draženović, B. 1969. The invariance conditions in variable structure systems. *Automatica,* 5**,** 287-295.

Edwards, C. & Menon, P. P. 2008. State reconstruction in complex networks using sliding mode observers. *Proceeding of the 47th IEEE Conference on Decision and Control*, Cancun, Mexico, 2832-2837, 9-11 Dec.

Edwards, C. & Spurgeon, S. K. 1998. *Sliding Mode Control: Theory and Applications*, Taylor and Francis, London, UK.

Edwards, C. & Spurgeon, S. K. 2000. On the limitations of some variable structure output feedback controller designs. *Automatica,* 36**,** 743-748.

Edwards, C., Spurgeon, S. K. & Patton, R. J. 2000. Sliding mode observers for fault detection and isolation. *Automatica,* 36**,** 541-553.

Feng, G. & Jiang, Y. A. 1995. Variable structure based decentralised adaptive control. *IEEE Proceeding - Control Theory and Applications,* 142**,** 439-443.

Feng, Y., Zheng, J., Yu, X. & Truong, N. V. 2009. Hybrid Terminal Sliding-Mode Observer Design Method for a Permanent-Magnet Synchronous Motor Control System. *Industrial Electronics, IEEE Transactions on,* 56**,** 3424-3431.

Ferrari, R., Parisini, T. & Polycarpou, M. M. 2009. Distributed Fault Diagnosis With Overlapping Decompositions: An Adaptive Approximation Approach. *IEEE Trans. on Automatic Control,* 54**,** 794-799.

Furuta, K. 1990. Sliding mode control of a discrete system. *Systems & Control Letters,* 14**,** 145-152.

Gahinet, P. & Apkarian, P. 1994. A Linear Matrix Inequality Approach to H∞ Control. *International Journal of Robust and Nonlinear Control, 4*, 421-448.

Gavel, D. T. & Šiljak, D. D. 1989. Decentralized Adaptive Control: Structural Conditions for Stability. *IEEE Trans. on Automatic Control, 34.*

Geromel, J. C., Bernussou, J. & Peres, P. L. D. 1994. Decentralized control through parameter space optimization. *Automatica, 30*, 1565-1578.

Gertler, J. J. 1988. Survey of model-based failure detection and isolation in complex plants. *IEEE Control Systems Magazine, 8*, 3-11.

Gomez-Exposito, A. & De La Villa Jaen, A. 2009. Two-Level State Estimation With Local Measurement Pre-Processing. *IEEE Trans. on Power Systems, 24*, 676-684.

Guo, Y., Hill, D. J. & Wang, Y. 2000. Nonlinear decentralized control of large-scale power systems. *Automatica, 36*, 1275-1289.

Hansheng, W. 2002. Decentralized adaptive robust control for a class of large-scale systems including delayed state perturbations in the interconnections. *IEEE Trans. on Automatic Control, 47*, 1745-1751.

Hassan, M. F., Sultan, M. A. & Attia, M. S. 1992. Fault detection in large-scale stochastic dynamic systems. *IEEE Proceeding - Control Theory and Applications, 139*, 119-124.

Himmelblau, D. M. 1978. *Fault Detection and Diagnosis in Chemical and Petrochemical Process*, Elsevier, Amsterdam.

Hsu, K. C. 1997. Decentralized variable-structure control design for uncertain large-scale systems with series nonlinearities. *International Journal of Conrtol, 68*, 1231-1240.

Hsu, M. H. 2009. Differential Quadrature Method for Solving Hyperbolic Heat Conduction Problems. *Tamkang Journal of Science and Engineering, 12*, 331-338.

Hu, Y. & Zhang, Y. 2002. Robust decentralized control for a class of large-scale systems with mismatched uncertainties. *Proceedings of the 4th World Congress on Intelligent Control and Automation*, Shanghai, China, 927-930, 10-14 Jun.

Hu, Z. 1994. Decentralized Stabilization of Large Scale Interconnected Systems with Delays. *IEEE Trans. on Automatic Control,* 39**,** 180-182.

Huang, Z. & Patton, R. J. 2012a. An adaptive sliding mode approach to decentralized control of uncertain systems. *UKACC International Conference on Control*, Cardiff, UK, 70-75, 3-5 Sep.

Huang, Z. & Patton, R. J. 2012b. Decentralized Control of Uncertain Systems Via Adaptive Sliding and Overlapping Decomposition. *7th IFAC Symposium on Robust Control Design*, Aalborg, Denmark, 784-789, 20-23 Jun.

Hung, J. Y., Gao, W. & Hung, J. C. 1993. Variable Structure Control: A Survey. *IEEE Trans. on Industrial Electronics,* 40**,** 2-22.

Hung, M. L. & Yang, J. J. 2007. Decentralized model-reference adaptive control for a class of uncertain large-scale time-varying delayed systems with series nonlinearities. *Chaos, Solitons and Fractals,* 33**,** 1558-1568.

Ichalal, D., Marx, B., Ragot, J. & Maquin, D. 2010. Observer based actuator fault tolerant control for nonlinear Takagi-Sugeno systems : an LMI approach. *Control & Automation (MED), 2010 18th Mediterranean Conference on*, 1278-1283, 23-25 June 2010.

İftar, A. 1991. Decentralized optimal control with overlapping decompositions. *IEEE International Conference on Systems Engineering*, Dayton, OH, USA, 299-302, 1-3 Aug.

İftar, A. 1993. Decentralized Estimation and Control with Overlapping Input, State, and Output Decomposition. *Automatica,* 29**,** 511-516.

Ikeda, M. 1989. Decentralized control of large scale systems. Nijmeijer, H. & Schumacher, J. (eds.) *Three Decades of Mathematical System Theory.* Springer Berlin Heidelberg.

Ikeda, M. & Siljak, D. D. 1980. Overlapping decompositions, expansions and contractions of dynamic systems. *Large Scale Systems,* 1**,** 29-38.

Ikeda, M. & Siljak, D. D. 1986. Overlapping decentralized control with input, state and output inclusion. *Control Theory and Advanced Technology,* 2**,** 155-172.

Ikeda, M., Šiljak, D. D. & White, D. E. 1981. Decentralized Control with Overlapping Information Sets. *Journal of optimization theory and applications,* 34**,** 279-310.

Ikeda, M., Šiljak, D. D. & Yasuda, K. 1983. Optimality of decentralized control for large-scale systems. *Automatica,* 19**,** 309-316.

Isermann, R. 1984. Process fault detection based on modeling and estimation methods—A survey. *Automatica,* 20**,** 387-404.

Isermann, R. 2006. *Fault-Diagnosis Systems An Introduction from Fault Detection to Fault Tolerance*, Springer-Verlag.

Itkis, U. 1976. *Control Systems of Variable Structure*, Wiley, New York.

Jain, S., Khorrami, F. & Fardanesh, B. 1994. Adaptive nonlinear excitation control of power systems with unknown interconnections. *IEEE Trans. on Control Systems Technology,* 2**,** 436-446.

Jiang, G., Wang, S. & Song, W. 2000. Design of observer with integrators for linear systems with unknown input disturbances. *Electronics Letters,* 36**,** 1168-1169.

Kalsi, K., Lian, J. & Żak, S. H. 2009. Decentralized control of multimachine power systems. *American Control Conference*, St. Louis, MO, USA, 2122-2127, 10-12 Jun.

Kalsi, K., Lian, J. & Żak, S. H. 2010. Decentralized Dynamic Output Feedback Control of Nonlinear Interconnected Systems. *IEEE Trans. on Automatic Control,* 55**,** 1964-1970.

Koan-Yuh, C. & Wen-June, W. 1999. H∞ norm constraint and variance control for stochastic uncertain large-scale systems via the sliding mode concept. *IEEE Trans. on Circuits and Systems I: Fundamental Theory and Applications,* 46**,** 1275-1280.

Labibi, B., Lohmann, B., Sedigh, A. K. & Maralani, P. J. 2003. Decentralized stabilization of large-scale systems via State-feedback and using descriptor systems. *IEEE Trans. on Systems, Man and Cybernetics, Part A: Systems and Humans,* 33**,** 771-776.

Larbah, E. & Patton, R. J. 2010. Fault tolerant plug and play vibration control in building structures. *49th IEEE Conference on Decision and Control*, Atlanta, GA, USA, 2462-2467, 15-17 Dec.

Lavaei, J., Momeni, A. & Aghdam, A. G. 2008. A Model Predictive Decentralized Control Scheme With Reduced Communication Requirement for Spacecraft Formation. *IEEE Trans. on Control Systems Technology,* 16**,** 268-278.

Lee, H. & Kim, Y. 2010. Fault-tolerant control scheme for satellite attitude control system. *Control Theory & Applications, IET,* 4**,** 1436-1450.

Levent, A. 1998. Robust exact differentiation via sliding mode technique. *Automatica,* 34**,** 379-384.

Lin, C., Patton, R. J. & Zong, Q. 2010. Integral hierarchical SMC of uncertain interconnected systems. *49th IEEE Conference on Decision and Control*, Atlanta, GA, USA, 4517-4522, 15-17 Dec.

Looze, D., Houpt, P., Sandell, N., Jr. & Athans, M. 1978. On decentralized estimation and control with application to freeway ramp metering. *IEEE Trans. on Automatic Control,* 23**,** 268-275.

Lu, L., Lin, Z. & Beteman, A. 2009. Decentralized control design for large-scale linear systems in the presence of multi-layer nested saturation. *IEEE International Symposium on Intelligent Control*, Saint Petersburg, Russia, 695-700, 8-10 Jul.

Lunze, J. 1989. Stability analysis of large-scale systems composed of strongly coupled similar subsystems. *Automatica,* 25**,** 561-570.

Mahmoud, M. S. 1977. Multilevel Systems Control and Applications: A Survey. *IEEE Trans. on Systems, Man and Cybernetics,* 7**,** 125-143.

Mahmoud, M. S. 2011. Design of control strategies for robust dynamic routing in traffic networks. *Control Theory & Applications, IET,* 5**,** 1716-1728.

Martynyuk, A. A. 1998. *Stability by Liapunov's Matrix Function Method with Applications*, New York: Marcel Dekker.

Mcguinness, M. & Taylor, S. W. 2004. Strip temperature in a metal coating line annealing furnace. *Proceeding of the 2004 Mathematics-in-Industry Study Group*, Massey University, Albany, NZ.

Meisel, J. 1980. Transient Stability Augmentation using A Hierarchical Control Structure. *IEEE Trans. on Power Apparatus and Systems,* PAS-99**,** 256-267.

Mukaidani, H. 2011. Local feedback pareto strategy for weakly coupled large-scale discrete-time stochastic systems. *Control Theory & Applications, IET,* 5, 2005-2014.

Nersesov, S. G. & Haddad, W. M. 2006. On the stability and control of nonlinear dynamical systems via vector Lyapunov functions. *IEEE Trans. on Automatic Control,* 51, 203-215.

Ocampo Martinez, C., Barcelli, D., Puig, V. & Bemporad, A. 2012. Hierarchical and decentralised model predictive control of drinking water networks: Application to Barcelona case study. *Control Theory & Applications, IET,* 6, 62-71.

Okou, F., Dessaint, L. A. & Akhrif, O. 2005. Power Systems Stability Enhancement Using a Wide-Area Signals Based Hierarchical Controller. *IEEE Trans. on Power Systems,* 20, 1465-1477.

Özgüner, Ü., Khorrami, F. & İftar, A. 1988. Two controller design approaches for decentralized systems. *AIAA Guidance, Navigation and Control Conference,* Minneapolis, MN, 237-244.

Pagilla, P. R. & Zhu, Y. 2004. A decentralized output feedback controller for a class of large-scale interconnected nonlinear systems. *Proceedings of the 2004 American Control Conference,* Boston, Massachusetts, 3711-3716, 30 Jun-2 Jul.

Pagilla, P. R. & Zhu, Y. 2005. A Decentralized Output Feedback Controller for a Class of Large-Scale Interconnected Nonlinear Systems. *Journal of Dynamic Systems, Measurement, and Control,* 127, 167-172.

Parutka, K. 2010. A Survey of Decentralized Adaptive Control. Meng Joo Er (Ed.) *New Trends in Technologies: Control, Management, Computational Intelligence and Network Systems.*

Patton, R., Kambhampati, C., Casavola, A., Zhang, P., Ding, S. & Sauter, D. 2007. A Generic Strategy for Fault-Tolerance in Control Systems Distributed Over a Network. *European Journal of Control,* 13, 280-296.

Patton, R. J. 1997. Fault tolerant control: The 1997 situation. *IFAC Safeprocess '97.* Hull, United Kingdom.

Patton, R. J., Frank, P. M. & Clark, R. N. 1989. *Fault diagnosis in dynamic System, Theory and Application, Control Engineering Series,* New York: Prentice Hall.

Patton, R. J., Putra, D. & Klinkhieo, S. 2010. Friction compensation as a fault-tolerant control problem. *International Journal of Systems Science,* 41**,** 987-1001.

Plestan, F., Shtessel, Y., Brégeault, V. & Poznyak, A. 2010. New methodologies for adaptive sliding mode control. *International Journal of Control,* 83**,** 1907-1919.

Pukdeboon, C., Zinober, A. S. I. & Thein, M. W. L. 2010. Quasi-Continuous Higher Order Sliding-Mode Controllers for Spacecraft-Attitude-Tracking Maneuvers. *IEEE Trans. on Industrial Electronics,* 57**,** 1436-1444.

Richter, S., Lefebvre, S. & Decarlo, R. 1982. Control of a class of nonlinear systems by decentralized control. *IEEE Trans. on Automatic Control,* 27**,** 492-494.

Rosinová, D. & Veselý, V. 2007. Robust PID Decentralized Controller Design Using LMI. *International Journal of Computers, Communications & Control,* II**,** 195-204.

Rosinová, D. & Veselý, V. 2012. Decentralized Robust Control of Linear Uncertain Systems. *7th IFAC Symposium on Robust Control Design*, Aalborg, Denmark, 412-417, 20-23 Jun.

Rubaai, A. 1991. Transient stability control: a multi-level hierarchical approach. *IEEE Trans. on Power Systems,* 6**,** 262-268.

Ryan, E. P. & Corless, M. 1984. Ultimate Boundedness and Asymptotic Stability of a Class of Uncertain Dynamical Systems via Continuous and Discontinuous Feedback Control. *IMA Journal of Mathematical Control and Information,* 1**,** 223-242.

Sandell, N., Varaiya, P., Athans, M. & Safonov, M. 1978. Survey of decentralized control methods for large scale systems. *IEEE Trans. on Automatic Control,* 23**,** 108-128.

Shafai, B., Ghadami, R. & Saif, M. 2011. Robust decentralized PI observer for linear interconnected systems. *IEEE International Symposium on Computer-Aided Control System Design*, Denver, CO, USA, 650-655, 28-30 Sep.

Shampine, L. F. & Allen, R. C. 1973. *Numerical computing: An introduction*, Saunders (Philadelphia).

Shankar, S., Darbha, S. & Datta, A. 2002. Design of a decentralized detection filter for a large collection of interacting LTI systems. *Mathematical Problems in Engineering,* 8**,** 233-248.

Shi, L. & Singh, S. K. 1992. Decentralized Adaptive Controller Design for Large-Scale Systems with Higher Order Interconnections. *IEEE Trans. on Automatic Control,* 37**,** 1106-1118

Shields, D. N. & Du, S. 2003. Fault detection observers for continuous non-linear polynomial systems of general degree. *International Journal of Control,* 76**,** 437-452.

Shyu, K.-K., Liu, W.-J. & Hsu, K.-C. 2005. Design of large-scale time-delayed systems with dead-zone input via variable structure control. *Automatica,* 41**,** 1239-1246.

Shyu, K. K., Liu, W. J. & Hsu, K. C. 2003. Decentralised variable structure control of uncertain large-scale systems containing a dead-zone. *IEEE Proceeding - Control Theory and Applications,* 150**,** 467-75.

Šiljak, D. D. 1978. *Large scale dynamic systems: Stability and structure*, New York: North Holland.

Šiljak, D. D. 1991. *Decentralized Control of Complex Systems*, Academic Press.

Šiljak, D. D. 1996. Decentralized control and computations: status and prospects. *Annual Reviews in Control,* 20**,** 131-141.

Šiljak, D. D. & Stipanović, D. M. 2000. Robust Stabilization of Nonlinear Systems: The LMI Approach. *Mathematical Problems in Engineering,* 6**,** 33.

Šiljak, D. D., Stipanović, D. M. & Zečević, A. I. 2002. Robust decentralized turbine/governor control using linear matrix inequalities. *IEEE Trans. on Power Systems,* 17**,** 715-722.

Šiljak, D. D. & Vukcevic, M. 1976. Decentralization, stabilization, and estimation of large-scale linear systems. *IEEE Trans. on Automatic Control,* 21**,** 363-366.

Šiljak, D. D. & Zečević, A. I. 2005. Control of large-scale systems: Beyond decentralized feedback. *Annual Reviews in Control,* 29**,** 169-179.

Singh, M. G., Hassan, M. F. & Titli, A. 1976. Multilevel Feedback Control for Interconnected Dynamical Systems Using the Prediction Principle. *Systems, Man and Cybernetics, IEEE Transactions on,* SMC-6**,** 233-239.

Singh, M. G. & Tamura, H. 1974. Modelling and hierarchical optimization for oversaturated urban road traffic networks. *International Journal of Control,* 20**,** 913-934.

Singh, M. G. & Titli, A. 1978. *Systems Decomposition, Optimization and Control*, Pergamon Press.

Smith, N. J. & Sage, A. P. 1973. An introduction to hierarchical systems theory. *Computers & Electrical Engineering,* 1**,** 55-71.

Stanković, S. S. & Šiljak, D. D. 2001. Contractibility of overlapping decentralized control. *Systems & Control Letters,* 44**,** 189-200.

Stanković, S. S. & Šiljak, D. D. 2003. Inclusion Principle for Linear Time-Varying Systems. *SIAM J. Control Optim.,* 42**,** 321-341.

Stanković, S. S., Stanković, M. S. & Stipanović, D. M. 2009. Consensus based overlapping decentralized estimation with missing observations and communication faults. *Automatica,* 45**,** 1397-1406.

Stanković, S. S., Stanojevic, M. J. & Šiljak, D. D. 2000. Decentralized overlapping control of a platoon of vehicles. *IEEE Trans. on Control Systems Technology,* 8**,** 816-832.

Stipanović, D. M., İnalhan, G., Teo, R. & Tomlin, C. J. 2004. Decentralized overlapping control of a formation of unmanned aerial vehicles. *Automatica,* 40**,** 1285-1296.

Sundareshan, M. & Huang, P. 1984. On the design of a decentralized observation scheme for large-scale systems. *IEEE Trans. on Automatic Control,* 29**,** 274-276.

Swarnakar, A., Marquez, H. J. & Tongwen, C. 2007. A New Scheme on Robust Observer Based Control Design for Nonlinear Interconnected Systems with Application to an Industrial Utility Boiler. *Proceedings of the 2007 American Control Conference*, New York City, USA, 5601-5606, 9-13 Jul.

Syrmos, V. L., Abdallah, C. T., Dorato, P. & Grigoriadis, K. 1997. Static output feedback—A survey. *Automatica,* 33**,** 125-137.

Tan, C. P. & Edwards, C. 2001. An LMI approach for designing sliding mode observers. *International Journal of Control,* 74**,** 1559-1568.

Tan, C. P. & Edwards, C. 2002. Sliding mode observers for detection and reconstruction of sensor faults. *Automatica,* 38**,** 1815-1821.

Tan, C. P. & Edwards, C. 2003. Sliding mode observers for robust detection and reconstruction of actuator and sensor faults. *International Journal of Robust and Nonlinear control,* 13**,** 443-463.

Titli, A., Lefevre, T. & Richetin, M. 1973. Multilevel optimization methods for non-separable problems and application. *International Journal of Systems Science,* 4**,** 865-880.

Tlili, A. S. & Braiek, N. B. 2009. Decentralized observer based guaranteed cost control for nonlinear interconnected systems. *International Journal of Conrtol and Automation,* 2**,** 29-45.

Uang, H. & Chen, B. 2000. Fuzzy decentralized controller and observer design for nonlinear interconnected systems. *The Ninth IEEE International Conference on Fuzzy Systems*, San Antonio, TX, 945-948, 7-10 May.

Utkin, V. 1977. Variable structure systems with sliding modes. *Automatic Control, IEEE Transactions on,* 22**,** 212-222.

Utkin, V. & Shi, J. 1996. Integral Sliding Mode in Systems Operating under Uncertainty Conditions. *Proceedings of the 35th Conference on Decision and Control*, Kobe, Japan, 4591-4596, 11-13 Dec.

Utkin, V. I. 1993. Sliding mode control design principles and applications to electric drives. *Industrial Electronics, IEEE Transactions on,* 40**,** 23-36.

Utkin, V. I. & Young, K. D. 1978. Methods for constructing discontinuity planes in multidimensional variable structure systems. *Automation and Remote Control,* 39**,** 1466-1470

Van Cutsem, T., Horward, J. L. & Ribbens-Pavella, M. 1981. A Two-Level Static State Estimator for Electric Power Systems. *IEEE Trans. on Power Apparatus and Systems,* PAS-100**,** 3722-3732.

Walcott, B. & Żak, S. H. 1987. State observation of nonlinear uncertain dynamical systems. *Automatic Control, IEEE Transactions on,* 32**,** 166-170.

Wang, W.-J. & Lee, J.-L. 1993. Decentralized Variable Structure Control Design in Perturbed Nonlinear Systems. *Journal of Dynamic Systems, Measurement, and Control,* 115**,** 551-554.

Wang, Y., Hill, D. J. & Guo, G. 1998. Robust decentralized control for multimachine power systems. *IEEE Trans. on Circuits and Systems I: Fundamental Theory and Applications,* 45**,** 271-279.

Wei, G. & Jin, X. 2012. Robust adaptive distributed large-scale system designs against loss effectiveness actuators. *24th Chinese Control and Decision Conference*, Taiyuan, China, 369-374, 23-25 May.

Wu, H. 2002. Decentralized adaptive robust control for a class of large-scale systems including delayed state perturbations in the interconnections. *IEEE Trans. on Automatic Control,* 47**,** 1745-1751.

Wu, H. 2003. Decentralized adaptive robust control for a class of large scale systems with uncertainties in the interconnections. *International Journal of Control,* 76**,** 253-265.

Wu, H. 2012. Decentralised adaptive robust control of uncertain large-scale non-linear dynamical systems with time-varying delays. *Control Theory & Applications IET,* 6**,** 629-640.

Xiang, J., Su, H. & Chu, J. 2005. On the design of Walcott-Zak sliding mode observer. *Proceedings of the 2005 American Control Conference*, Portland, OR, USA, 2451-2456, 8-10 Jun.

Xu, A. & Zhang, Q. 2004. Residual generation for fault diagnosis in linear time-varying systems. *IEEE Trans. on Automatic Control,* 49**,** 767-772.

Yan, J.-J., Tsai, J. S.-H. & Kung, F.-C. 1997. Robust Decentralized Stabilization of Large-Scale Delay Systems Via Sliding Mode Control. *Journal of Dynamic Systems, Measurement, and Control,* 119**,** 307-312.

Yan, X.-G. & Edwards, C. 2008. Robust decentralized actuator fault detection and estimation for large-scale systems using a sliding mode observer. *International Journal of Control,* 81**,** 591-606.

Yan, X.-G., Spurgeon, S. K. & Edwards, C. 2009. Global time-delay dependent decentralised sliding mode control using only output information. *Joint 48th*

IEEE Conference on Decision and Control and 28th Chinese Control Conference, Shanghai, China, 6709-6714, 15-18 Dec.

Yan, X. G., Edwards, C. & Spurgeon, S. K. 2004a. Decentralised robust sliding mode control for a class of nonlinear interconnected systems by static output feedback. *Automatica,* 40**,** 613-620.

Yan, X. G., Edwards, C., Spurgeon, S. K. & Bleijs, J. a. M. 2004b. Decentralised sliding-mode control for multimachine power systems using only output information. *IEEE Proceeding - Control Theory and Applications,* 151**,** 627-635.

Yan, X. G., Spurgeon, S. K. & Edwards, C. 2003. Decentralized Output Feedback Sliding Mode Control of Nonlinear Large-Scale Systems with Uncertainties. *Journal of optimization theory and applications,* 119**,** 597-614.

Yau, H.-T. & Yan, J.-J. 2009. Robust decentralized adaptive control for uncertain large-scale delayed systems with input nonlinearities. *Chaos, Solitons & Fractals,* 39**,** 1515-1521.

Young, K. D., Utkin, V. I. & Özgüner, Ü. 1999. A control engineer's guide to sliding mode control. *IEEE Trans. on Control Systems Technology,* 7**,** 328-342.

Yu, X. & Kaynak, O. 2009. Sliding-Mode Control With Soft Computing: A Survey. *IEEE Trans. on Industrial Electronics,* 56**,** 3275-3285.

Zečević, A. I. & Šiljak, D. D. 2004. Design of robust static output feedback for large-scale systems. *IEEE Trans. on Automatic Control,* 49**,** 2040-2044.

Zečević, A. I. & Šiljak, D. D. 2005. A new approach to control design with overlapping information structure constraints. *Automatica,* 41**,** 265-272.

Zhang, X., Polycarpou, M. M. & Parisini, T. 2010. Fault diagnosis of a class of nonlinear uncertain systems with Lipschitz nonlinearities using adaptive estimation. *Automatica,* 46**,** 290-299.

Zhu, M. & Li, Y. 2010. Decentralized adaptive fuzzy sliding mode control for reconfigurable modular manipulators. *International Journal of Robust and Nonlinear control,* 20**,** 472-488.

Zhu, Y. & Pagilla, P. R. 2007. Decentralized output feedback control of a class of large-scale interconnected systems. *IMA Journal of Mathematical Control and Information,* 24**,** 57-69.

Zinober, A. S. I. 1990. An introduction to variable structure control. Zinober, A. S. I. (Ed.) *Deterministic Control of Uncertain Systems*. Peter Peregrinus, Stevenage, UK.